SPR 396-6 OCTOBER 2013

Performance Evaluation of Arizona's LTPP SPS-6 Project:

Strategic Study of Rehabilitation Techniques

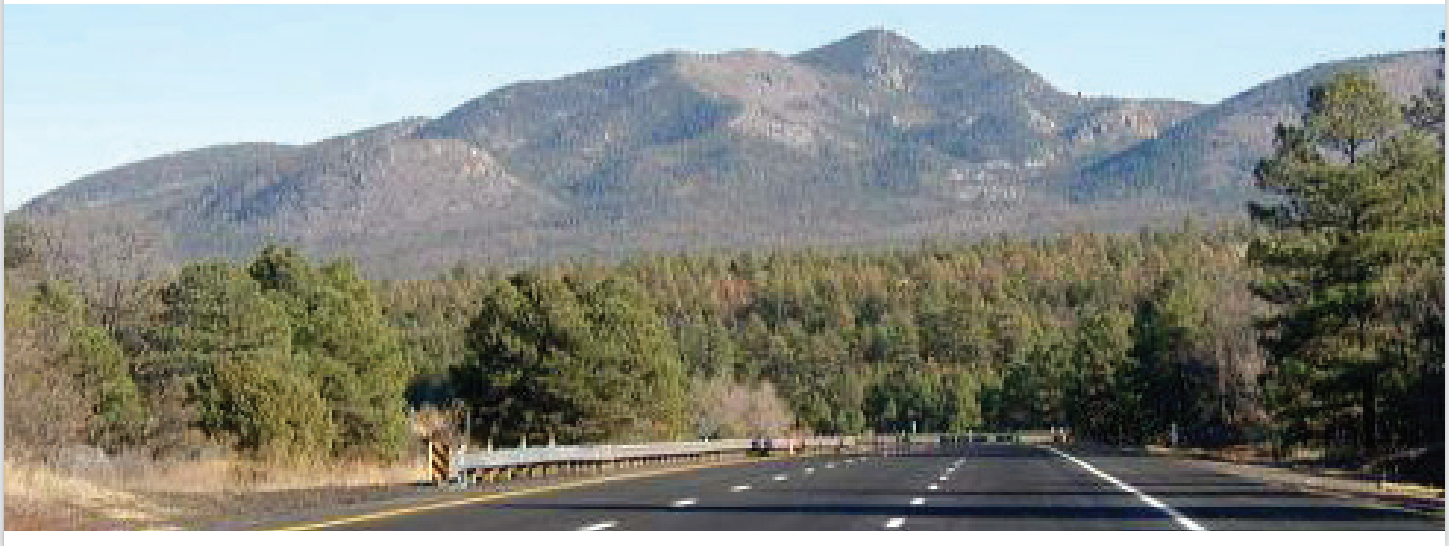

Arizona Department of Transportation Research Center

ADOT

Performance Evaluation of Arizona's LTPP SPS-6 Project: Strategic Study of Rehabilitation Techniques

Final Report 396-6
October 2013

Prepared by:
Jason Puccinelli
Nichols Consulting Engineers
1885 S. Arlington Avenue, Suite 111
Reno, NV 89509-3370

Steven M. Karamihas
The University of Michigan Transportation Research Institute
2901 Baxter Road
Ann Arbor, MI 48109

Kathleen T. Hall
Kathleen T. Hall Consulting
1271 Huntington Drive South
Mundeleine, IL 60060

Kevin Senn
Nichols Consulting Engineers
1885 S. Arlington Avenue, Suite 111
Reno, NV 89509-3370

Prepared for:
Arizona Department of Transportation
206 S. 17th Avenue
Phoenix, AZ 85007
in cooperation with
U.S. Department of Transportation
Federal Highway Administration

This report was funded in part through grants from the Federal Highway Administration, U.S. Department of Transportation. The contents of this report reflect the views of the authors, who are responsible for the facts and the accuracy of the data, and for the use or adaptation of previously published material, presented herein. The contents do not necessarily reflect the official views or policies of the Arizona Department of Transportation or the Federal Highway Administration, U.S. Department of Transportation. This report does not constitute a standard, specification, or regulation. Trade or manufacturers' names that may appear herein are cited only because they are considered essential to the objectives of the report. The U.S. government and the State of Arizona do not endorse products or manufacturers.

Technical Report Documentation Page

1. Report No. FHWA-AZ-13-396(6)	2. Government Accession No.	3. Recipient's Catalog No.
4. Title and Subtitle Performance Evaluation of Arizona's LTPP SPS-6 Project: Strategic Study of Rehabilitation Techniques		5. Report Date October 2013 6. Performing Organization Code
7. Author(s) Jason Puccinelli, Steven M. Karamihas, Kathleen T. Hall, Kevin Senn		8. Performing Organization Report No.
9. Performing Organization Name and Address Nichols Consulting Engineers 1885 S. Arlington Avenue Suite 111 Reno, NV 89509-3370 The University of Michigan Transportation Research Institute 2901 Baxter Road Ann Arbor, MI 48109		10. Work Unit No. (TRAIS) 11. Contract or Grant No. SPR 000-1(147) 396
12. Sponsoring Agency Name and Address Arizona Department of Transportation 206 S. 17th Avenue Phoenix, AZ 85007		13. Type of Report and Period Covered 14. Sponsoring Agency Code
15. Supplementary Notes Prepared in cooperation with the U.S. Department of Transportation, Federal Highway Administration		

16. Abstract

As part of the Long Term Pavement Performance (LTPP) Program, the Arizona Department of Transportation (ADOT) constructed 19 Specific Pavement Studies 6 (SPS-6) test sections on Interstate 40 near Flagstaff. The SPS-6 project studied the effect of specific rehabilitation treatments on jointed portland cement concrete pavement (JPCP) performance. The test sections had various JPCP surface preparations, including crack and seat, minimum and maximum restoration, rubblization, asphalt concrete (AC) with fabric, and asphalt rubber with conventional AC. Opened to traffic in 1991, the project was monitored at regular intervals until 2002. Surface distress, profile, and deflection data collected throughout the life of the pavement were used to evaluate the performance of various flexible pavement design features, layer configurations, and thickness. This report documents the analyses conducted as well as practical findings and lessons learned that will be of interest to ADOT.

17. Key Words LTPP, pavement performance, profile, distress, FWD, flexible, AC, deflections, roughness, back-calculation		18. Distribution Statement Document is available to the U.S. public through the National Technical Information Service, Springfield, VA, 22161		23. Registrant's Seal
19. Security Classification Unclassified	20. Security Classification Unclassified	21. No. of Pages 184	22. Price	

SI* (MODERN METRIC) CONVERSION FACTORS

APPROXIMATE CONVERSIONS TO SI UNITS

Symbol	When You Know	Multiply By	To Find	Symbol
		LENGTH		
in	inches	25.4	millimeters	mm
ft	feet	0.305	meters	m
yd	yards	0.914	meters	m
mi	miles	1.61	kilometers	km
		AREA		
in^2	square inches	645.2	square millimeters	mm^2
ft^2	square feet	0.093	square meters	m^2
yd^2	square yard	0.836	square meters	m^2
ac	acres	0.405	hectares	ha
mi^2	square miles	2.59	square kilometers	km^2
		VOLUME		
fl oz	fluid ounces	29.57	milliliters	mL
gal	gallons	3.785	liters	L
ft^3	cubic feet	0.028	cubic meters	m^3
yd^3	cubic yards	0.765	cubic meters	m^3
		NOTE: volumes greater than 1000 L shall be shown in m^3		
		MASS		
oz	ounces	28.35	grams	g
lb	pounds	0.454	kilograms	kg
T	short tons (2000 lb)	0.907	megagrams (or "metric ton")	Mg (or "t")
		TEMPERATURE (exact degrees)		
^oF	Fahrenheit	5 (F-32)/9 or (F-32)/1.8	Celsius	^oC
		ILLUMINATION		
fc	foot-candles	10.76	lux	lx
fl	foot-Lamberts	3.426	$candela/m^2$	cd/m^2
		FORCE and PRESSURE or STRESS		
lbf	poundforce	4.45	newtons	N
lbf/in^2	poundforce per square inch	6.89	kilopascals	kPa

APPROXIMATE CONVERSIONS FROM SI UNITS

Symbol	When You Know	Multiply By	To Find	Symbol
		LENGTH		
mm	millimeters	0.039	inches	in
m	meters	3.28	feet	ft
m	meters	1.09	yards	yd
km	kilometers	0.621	miles	mi
		AREA		
mm^2	square millimeters	0.0016	square inches	in^2
m^2	square meters	10.764	square feet	ft^2
m^2	square meters	1.195	square yards	yd^2
ha	hectares	2.47	acres	ac
km^2	square kilometers	0.386	square miles	mi^2
		VOLUME		
mL	milliliters	0.034	fluid ounces	fl oz
L	liters	0.264	gallons	gal
m^3	cubic meters	35.314	cubic feet	ft^3
m^3	cubic meters	1.307	cubic yards	yd^3
		MASS		
g	grams	0.035	ounces	oz
kg	kilograms	2.202	pounds	lb
Mg (or "t")	megagrams (or "metric ton")	1.103	short tons (2000 lb)	T
		TEMPERATURE (exact degrees)		
^oC	Celsius	1.8C+32	Fahrenheit	^oF
		ILLUMINATION		
lx	lux	0.0929	foot-candles	fc
cd/m^2	$candela/m^2$	0.2919	foot-Lamberts	fl
		FORCE and PRESSURE or STRESS		
N	newtons	0.225	poundforce	lbf
kPa	kilopascals	0.145	poundforce per square inch	lbf/in^2

*SI is the symbol for the International System of Units. Appropriate rounding should be made to comply with Section 4 of ASTM E380.
(Revised March 2003)

Contents

List of Figures

List of Tables

List of Acronyms

AASHTO	American Association of State Highway and Transportation Officials
AC	asphalt concrete
ACFC	asphalt concrete friction course
ADOT	Arizona Department of Transportation
AR	asphalt rubber
AR-ACFC	asphalt rubber asphalt concrete friction course
ARAC	asphalt rubber asphalt concrete
CBR	California Bearing Ratio
ESAL	equivalent single axle loads
FWD	falling weight deflectometer
HRI	Half-car Roughness Index
IRI	International Roughness Index
JPCP	jointed portland cement concrete pavement
LTPP	Long Term Pavement Performance
MP	milepost
MRI	Mean Roughness Index
OGFC	open-graded friction course
PCCP	portland cement concrete pavement
PSD	power spectral density
RN	Ride Number
SHRP	Strategic Highway Research Program
SPS	Specific Pavement Studies
WIM	weigh-in-motion

EXECUTIVE SUMMARY

As part of the Long Term Pavement Performance (LTPP) Program, the Arizona Department of Transportation (ADOT) constructed 19 Specific Pavement Studies (SPS-6) test sections on Interstate 40 (I-40) near Flagstaff, Arizona. The SPS-6 project studied the effect of specific maintenance and rehabilitation treatments on jointed portland cement concrete pavement (JPCP) performance. The SPS-6 project (040600) consisted of 19 test sections: eight core sections and 11 supplemental sections. The eight core sections comprised the standard experimental matrix for the Strategic Highway Research Program (SHRP) requirements and included three types of surface preparation of the existing JPCP: crack and seat, minimum restoration, and maximum restoration. Five sections had asphalt overlays (4 inches and 8 inches), two sections had no overlay, and one control section received only routine ADOT maintenance. ADOT added the 11 supplemental test sections to evaluate features that were not included in the SHRP experiment design and included rubblizing existing JPCP, an unbonded JPCP overlay, an asphalt overlay with fabric, various thickness combinations of asphalt rubber and conventional asphalt overlays, and an asphalt concrete friction course (ACFC). Construction of all 19 test sections occurred between June 1990 and October 1990; most sections were placed out-of-study in November 2002 with the exception of two sections that were removed in 1992 and one section that was removed in 1993.

This report provides general information about the project location, including climate, traffic, and subgrade conditions, as well as details about the layer configurations of each test section. All 19 of the SPS-6 test sections were constructed consecutively and so were exposed to the same traffic-loading, climate, and subgrade conditions. This allows direct comparisons between layer configurations and design features without the confounding effects introduced by different in situ conditions.

Six of the test sections were constructed with an asphalt rubber asphalt concrete friction course (AR-ACFC). These sections consisted of a 2 inch asphalt concrete (AC) layer overlaid with 3 inches of asphalt rubber asphalt concrete (ARAC). These sections experienced a significantly higher resistance to longitudinal and transverse reflective cracking than the other sections.

The most effective rehabilitation treatments, in terms of long-term increase in effective pavement thickness, were the 4.3 inch asphalt overlay of the replaced outer lane concrete, the 10 inch unbonded concrete overlay of the cracked and seated concrete, and the 8.4 inch asphalt overlay of the cracked and seated concrete. Differences in slab cracking patterns may be responsible for some of the differences in effectiveness among the crack and seat sections of comparable overlay thickness.

CHAPTER 1. INTRODUCTION

Understanding the contribution of maintenance and rehabilitation procedures on long-term performance can be extremely valuable to pavement managers looking to optimize resources and improve overall pavement performance. The research objectives were to document the overall performance trends of the SPS-6 project, identify key differences in performance among the various rehabilitation techniques, and document key findings that would be useful to ADOT.

This report provides the results of surface distress, deflection, and profile analyses for the LTPP SPS-6 site near Flagstaff, Arizona. The SPS-6 project (040600) studied the effect of specific maintenance and rehabilitation treatments on JPCP performance. The project had 19 test sections: eight core sections represented the standard experimental matrix that SHRP required; ADOT added 11 supplemental test sections to evaluate features that were not included in the SHRP experiment design.

In the eight core SPS-6 test sections, three types of surface preparation were used:

- Minimum restoration, which included joint and crack sealing, partial and full-depth patching, and full surface diamond grinding.
- Maximum restoration, which included removing and replacing existing joint and crack sealing, performing additional joint and crack sealing, removing and replacing existing partial and full-depth patching, performing additional partial and full-depth patching, correcting poor load transfer at joints, performing full surface diamond grinding, retrofitting subsurface edge drains, and undersealing.
- Crack and seat, which was intended to produce a nominal crack spacing of 3 × 3 ft for the majority of the SPS-6 sections. The pavement was then rolled until the broken pieces were seated.

The control section received only minimum routine maintenance. Five of the SHRP test sections received either a 4 or 8 inch thick asphalt overlay, which is commonly used in pavement design. The other three sections (including the control section) did not receive an overlay.

In the ADOT supplemental sections, the surface preparation techniques included rubblization of existing JPCP, unbonded JPCP overlays, asphalt overlays with fabric, various thickness combinations of asphalt rubber (AR) and conventional asphalt overlays, and the utilization of an asphalt rubber asphalt concrete friction course (AR-ACFC).

- Rubblization: The rubblizing procedure broke the pavement into nominal 1 to 2 inch pieces that were then compacted with a vibratory roller and primed before being overlaid with AC.
- Crack and seat: In the majority of the supplemental sections, this procedure produced a nominal crack spacing of 3 × 3 ft. The pavement was then rolled until the broken pieces

were seated. However, in two ADOT supplemental sections this procedure created a 4 × 6 ft cracking pattern. A tack coat was applied before the overlay.

The SPS-6 project was constructed on eastbound I-40 in Coconino County (Figure 1) and was incorporated in the ADOT rehabilitation project IR-40-4(123), which spanned from U.S. 89A at milepost (MP) 195 to the Walnut Canyon Interchange (MP 205).

Figure 1. Location of SPS-6 040600 Test Sections.

Prior to the construction of the SPS-6 project, the roadway was 38 ft wide with two travel lanes that were each 12 ft wide bounded by a 10 ft outside shoulder and a 4 ft inside shoulder. The lanes had an 8 to 9 inch thick portland cement concrete (PCC) pavement layer, and the shoulders had 2.5 to 3 inches of AC. Figure 2 shows a typical cross section of the road prior to construction.

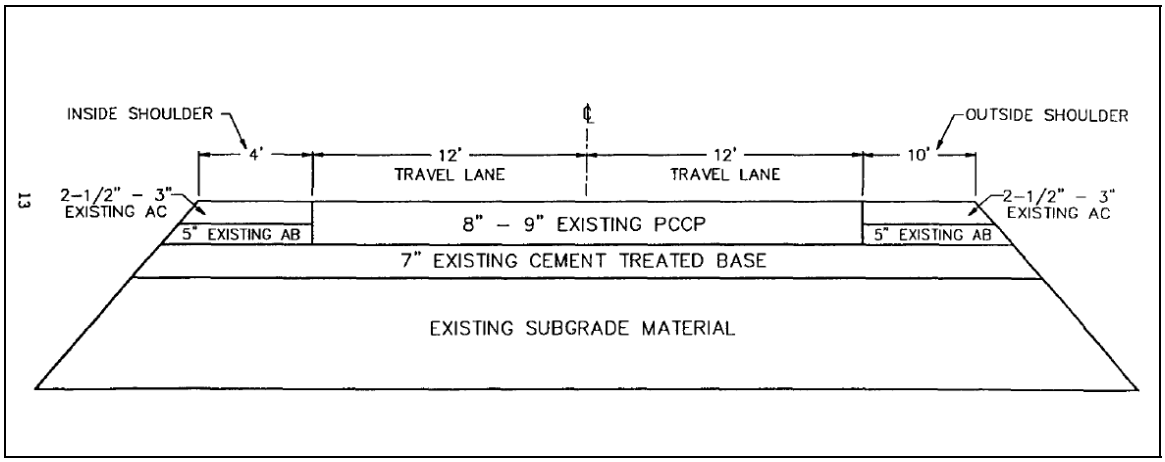

Figure 2. Existing Concrete Pavement Section Before SPS-6 Project Construction.

Before the SPS-6 project was constructed, the roadway was in very poor condition with extensive cracking after only five years of service (Way 1999). The deterioration first appeared as large corner cracks that later progressed to transverse cracks and high severity spalling at transverse joints. When ADOT determined that maintaining the road would be too costly, this site was selected for rehabilitation.

The SPS-6 project was constructed in a 2.7 mi segment of this 10 mi rehabilitation project and extends from MP 202.16 to MP 204.86 (Figure 3). The site is located in a forested, mountainous area on a longitudinal grade that varies from shallow fill to sandstone cut, to deep fill over a culvert, and back to an increasingly deep sandstone cut. The average length of each test section is approximately 500 ft, which does not include transitional segments between sections. The average elevation of the project is 6900 ft, with a latitude of 35° 13’ and longitude of -111°34’. The location and layout of the SPS-6 project are shown in Figures 2 and 3. The test section properties are shown in Table 1.

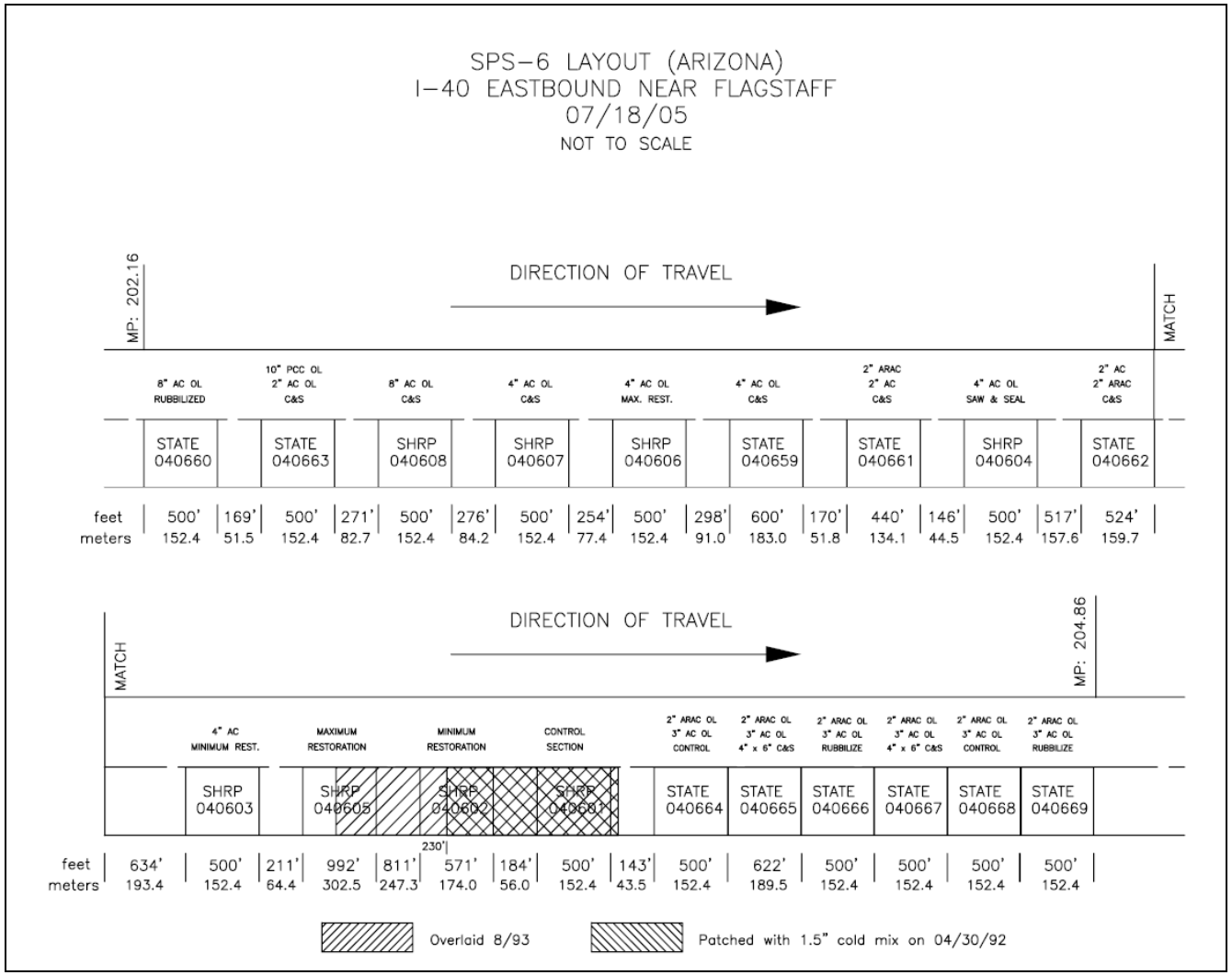

Figure 3. Layout of the SPS-6 Project.

Table 1. Arizona SPS-6 Project Layout.

Station (ft)	Station (m)	SHRP ID	ADOT ID	Original Construction						
				PCC		Base and Subbase			Subgrade	
				Thick (in)	Type	Thick (in)	Type	Code	Type	Code
0	0	040660	1	8.3	JPCP	3.5 7.7	cement-agg mix uncrushed gravel	331 302	silty sand with gravel	215
499	152									
669	204	040663	2	8.3	JPCP	3.4 7.4	cement-agg mix uncrushed gravel	331 302	silty sand with gravel	215
1,168	356									
1,440	439	040608	3	8.2	JPCP	3.9 8.1 6.2	cement-agg mix uncrushed gravel fine soil-agg mix	331 302 307	gravelly lean clay with sand	117
1,939	591									
2,215	675	040607	4	8.5*	JPCP	4.1 7.5 6.2	cement-agg mix uncrushed gravel fine soil-agg mix	331 302 307	sandstone bedrock	287
2,717	828									
2,969	905	040606	5	8.5	JPCP	3.9 7.6	cement-agg mix uncrushed gravel	331 302	silty sand with gravel	215
3,471	1,058									
3,770	1,149	040659	6	8.4	JPCP	2.7	cement-agg mix	331	silty sand with gravel	215
4,370	1,332									
4,541	1,384	040661	7	8.4	JPCP	4.2 6.8	cement-agg mix uncrushed gravel	331 302	sandstone bedrock	287
4,980	1,518									
5,125	1,562	040604	8	8.2	JPCP	4.9 6.8	cement-agg mix uncrushed gravel	331 302	clayey sand with gravel	217
5,627	1,715									
6,142	1,872	040662	9	8.1*	JPCP	3.9 9.0 17.1	cement-agg mix uncrushed gravel fine soil-agg mix	331 302 307	silty sand with gravel	215
6,667	2,032									

*For Section 040607, the LTPP database shows the PCC thickness as 8.5 inches before rehabilitation and 8.4 inches after rehabilitation. For Section 040662, the LTPP database shows the PCC thickness as 9.1 inches before rehabilitation and 9.0 inches after rehabilitation.

Table 1. Arizona SPS-6 Project Layout (Continued).

Station (ft)	Station (m)	SHRP ID	ADOT ID	Original Construction: PCC Thick (in)	PCC Type	Base and Subbase Thick (in)	Base and Subbase Type	Base and Subbase Code	Subgrade Type	Subgrade Code
7,300	2,225	040603	10	8.3	JPCP	4.2 7.9	cement-agg mix uncrushed gravel	331 302	clayey gravel with sand	267
7,799	2,377									
8,012	2,442	040605	11	8.3	JPCP	3.9 8.0 21.6	cement-agg mix uncrushed gravel fine-soil agg mix	331 302 307	sandstone bedrock	287
9,003	2,744									
9,587	2,922	040602	12	8.0	JPCP	3.6 8.4 21.6	cement-agg mix uncrushed gravel fine soil-agg mix	331 302 307	sandstone bedrock	287
10,157	3,096									
10,341	3,152	040601	13	7.9	JPCP	3.1 9.7	cement-agg mix uncrushed gravel	331 302	sandstone bedrock	287
10,840	3,304									
11,198	3,413	040664	14	7.9	JPCP	2.7 9.7	cement-agg mix uncrushed gravel	331 302	sandstone bedrock	287
11,696	3,565	040665	15	7.9	JPCP	2.7 9.7	cement-agg mix uncrushed gravel	331 302	sandstone bedrock	287
12,320	3,755	040666	16	7.9	JPCP	2.7 9.7	cement-agg mix uncrushed gravel	331 302	sandstone bedrock	287
12,818	3,907	040667	17	7.9	JPCP	2.7 9.7	cement-agg mix uncrushed gravel	331 302	sandstone bedrock	287
13,317	4,059	040668	18	7.9	JPCP	2.7 9.7	cement-agg mix uncrushed gravel	331 302	sandstone bedrock	287
13,819	4,212	040669	19	7.9	JPCP	2.7 9.7	cement-agg mix uncrushed gravel	331 302	sandstone bedrock	287
14,318	4,364									

The photographs in Figures 4 through 8 show the terrain of the SPS-6 project site. Figure 4 shows a box culvert in Section 040660, the first test section on the west end of the project site. Fill material is on both sides of the culvert, and the grade transitions from fill to cut near the end of the test section (as shown in the right side of the photo).

Figure 4. Box Culvert in Section 040660.

Figure 5 shows the unbonded overlay section (040663), the next test section at the west end of the site, in a shallow cut. As the photo indicates, the sandstone is not solid rock, but rather considerably weathered material. The LTPP database does not report that bedrock was encountered within the depth to which borings were obtained. Figure 6 is a photograph taken in Section 040662, the ninth test section along the project length, located over a substantial fill.

Figure 5. Shallow Sandstone Cut in Unbonded Overlay Section 040663.

Figure 6. Section 040662 Constructed Over Fill.

Figure 7 shows the depth of fill and uphill grade in Section 040605, the 11th test section along the project length.

Figure 7. Cut and Grade in Section 040605.

The photograph in Figure 8 was taken in Section 040602, the 12th test section along the project length, and shows the depth of cut and the weathering of the sandstone.

Figure 8. Cut in Section 040602.

Table 2 summarizes the features of each of the 19 test sections (Austin Research Engineers 1992). Table 2 also shows the actual thickness of the overlay layers based on LTPP Data (accessed from DataPave Online at www.ltpp-products.com). As can be seen, actual thicknesses of the overlay vary somewhat from the nominal design thickness provided in the ARE report.

Table 2. Summary of SPS-6 Test Sections.

SHRP ID	Location		Length (ft)	Surface Preparation	Overlay Material	Nominal Overlay Thickness (inches)	Actual Overlay Thickness (inches)
	From	To					
040660	0+00	5+00	500	Rubblize	AC	8	8.0
040663	6+69	11+69	500	Crack and seat	PCC/AC	10/2	10.0/2.0
040608	14+40	19+40	500	Crack and seat	AC[1]	8	8.4
040607	22+16	27+16	500	Crack and seat	AC[1]	4	4.3
040606	29+70	34+70	500	Maximum	AC[1]	4	4.3
040659	37+68	43+68	600	Fabric/crack and seat	AC[1]	4	4.0
040661	45+38	49+78	440	Crack and seat	ARAC/AC[1]	2/2	2.0/2.0
040604	51+24	56+24	500	Saw and seal/minimum	AC[1]	4	3.6
040662	61+41	66+65	524	Crack and seat	ARAC/AC[1]	2/2	2.0/2.0
040603	72+96	77+96	500	Minimum	AC[1]	4	3.5
040605	80+07	89+99	992	Maximum	None	None	None
040602	98+10	103+81	571	Minimum	None	None	None
040601	105+65	110+65	500	Routine maintenance	None	None (Control)	None (Control)
040664	112+08	117+08	500	None	AR-ACFC ARAC/AC	0.50 2/3	0.5 2.5/3.0
040665	117+08	123+30	622	Crack and seat[2]	AR-ACFC ARAC/AC	0.50 2/3	0.5 2.5/3.0
040666	123+30	128+30	500	Rubblize	AR-ACFC ARAC/AC	0.50 2/3	0.5 2.5/3.0
040667	128+30	133+30	500	Crack and seat[2]	AR-ACFC ARAC/AC	0.50 2/3	0.5 2.5/3.0
040668	133+30	138+30	500	None	AR-ACFC ARAC/AC	0.50 2/3	0.5 2.5/3.0
040669	138+30	143+30	500	Rubblize	AR-ACFC ARAC/AC	0.50 2/3	0.5 2.5/3.0

[1]Approximately one month after construction of Sections 040601 through 040604, 040606 through 040608, and 040659 through 040663, a 5/8 inch thick ACFC was placed on Sections 040603 through 040604, 040606 through 040608, 040659, and 040661 through 040662 to reduce concern about potential raveling and skid characteristics of the AC surface.

[2]The crack and seat procedure produced a 4 × 6 ft cracking pattern for Sections 040665 and 040667, while the rest of the sections had crack and seat operations producing 3 × 3 ft cracking patterns.

ACFC asphalt concrete friction course
ARAC asphalt rubber asphalt concrete
AR-ACFC asphalt rubber asphalt concrete friction course
PCCP portland cement concrete pavement

Researchers encountered some construction issues during the rubblization of Sections 0660 and 0666. The vibrations from the rubblization process caused the subgrade's fines to liquefy, resulting in upward water migration. As a result, the newly placed AC cracked severely and temporarily closed I-40 eastbound. To mitigate this issue, field workers applied a 3 inch overlay to both sections on August 5. Additionally, they excavated 4 to 7 ft of the subgrade in roughly one-third (150 ft) of the length of Section 040660, replaced it with graded crushed rock and then overlaid. This excavated section occurred 49 ft into the section. The remaining 350 ft of the section was not excavated or repaired, and therefore complied with the requirements of the experiment. Appendix A provides a more complete list of construction deviations.

Prior to the construction of the SPS-6 experiment, the distress located in the travel lane of the SHRP test sections was reviewed. Most of the slabs in each section experienced significant spalling and longitudinal/transverse cracking. In fact, the three sections that did not receive an overlay—0601, 0602, and 0605—and that utilized minimum or maximum restoration quickly deteriorated and were placed out-of-study within two to three years because they required reconstruction. Table 3 is a summary of the findings from this review, which shows the pavement's overall poor condition (Austin Research Engineers 1992).

The climate for this SPS-6 project location is considered to be a dry, no-freeze environment by LTPP definitions. Table 4 provides environmental details about the area. The temperature and precipitation information was derived from data collected at nearby weather stations and represents 40 years of recorded data. The humidity data was summarized from 22 years of virtual weather station data. These data can be accessed from DataPave Online (available at www.ltpp-products.com).

Table 3. Summary of Preconstruction Distress in Travel Lane.

SHRP ID	No. of Slabs	Total Slabs with Distress (%)	Joints with Spalling or Cracking (%)	Slabs with Longitudinal/Transverse Cracking[1] (%)	Shattered Slabs[2] (%)
040601	34	82	59	38	6
040602	33	79	39	33	9
040603	34	94	74	35	15
040604	32	84	50	38	19
040605	33	94	70	33	3
040606	33	94	52	48	6
040607	34	64	35	32	6
040608	34	62	24	18	15

[1]Slabs broken into two or less pieces.
[2]Slabs broken into three or more pieces.

Table 4. Climatic Information for SPS-6.

	44-year Average	44-year Maximum	44-year Minimum
Annual average daily mean temperature (°F)	45	47	43
Annual average daily maximum temperature (°F)	62	64	60
Annual average daily minimum temperature (°F)	29	32	26
Absolute maximum annual temperature (°F)	92	96	87
Absolute minimum annual temperature (°F)	-10	3	-27
Number of days per year above 32 °F	4	13	0
Number of days per year below 32 °F	219	245	198
Annual average freezing index (°F-days)	469	824	131
Annual average precipitation (inches)	20.7	30.9	11.3
Annual average daily maximum relative humidity (%)	77	87	69
Annual average daily minimum relative humidity (%)	31	36	24

N/A: Data not available.

Table 5 provides a summary of the total equivalent single axle loads (ESALs) computed from traffic loading information collected at the SPS-6 site. For 1990, no monitoring data were available and the ESALs reported were based on a separate report (Way 1999) that mentioned the traffic conditions of this site. In 1993 and from 2000–2002, no monitoring traffic data were available. The ESAL values given in Table 5 for these years were derived from estimates provided by ADOT. These data can be accessed from DataPave Online (available at www.ltpp-products.com).

To evaluate pavement performance of the SPS-6 project, three analyses were conducted: distress, deflection, and profile. The following chapters of this report address these analyses. Each chapter provides a description of the research approach along with performance comparisons between test sections, overall trends, a summary of the results, and key findings.

Table 5. Traffic Loading Summary.

Year	040600 ESALs
1990	1,600,000[1]
1991	N/A
1992	N/A
1993	1,400,000[2]
1994	1,214,260
1995	1,177,768
1996	1,234,130
1997	N/A
1998	1,326,856
1999	1,391,841
2000	2,123,000[2]
2001	2,482,000[2]
2002	2,902,000[2]
2003	N/A
2004	1,146,629
2005	1,021,430

[1]Way 1999.

[2]ADOT traffic estimate.

N/A: Data incomplete for these calendar years

CHAPTER 2. SPS-6 DEFLECTION ANALYSIS

This chapter describes the structural analysis of the SPS-6 test sections, based primarily on deflections measured before and at various times after rehabilitation. This structural analysis is a companion to other analyses being conducted of the test sections' distress history, longitudinal profile measurements, and elastic modulus measurements obtained using ground-penetrating radar.

ANALYSIS OF DEFLECTIONS MEASURED BEFORE REHABILITATION

The first 13 sections (ADOT ID numbers 1 through 13) were deflection tested June 7–10, 1990, before the rehabilitation work began. The last six sections at the site (supplemental sections 040664 through 040669, ADOT ID numbers 14 through 19) were not tested in June 1990.

Joint Load Transfer

Deflection load transfer is typically among the first concerns in a structural analysis of concrete pavements with intact slabs because the deflections used in the backcalculation must be adjusted for the effects of load transfer. The k-value of the foundation will be underestimated and the elastic modulus of the concrete pavement will be overestimated unless the appropriate adjustments are made to account for the finite size of the slabs and the degree of load transfer at the slab edges. However, an assessment of the prerehabilitation pavement condition of the Arizona SPS-6 site (Austin Research Engineers 1992) made measuring load transfer unnecessary:

> Pavement distress in the outside lane of the existing JCP consists of joint and crack spalling, longitudinal, transverse, and random direction cracking, and shattered slabs. Approximately 80%-90% of the slabs exhibit some kind of distress. Approximately 50% of the joints have spalling, 35%-40% have longitudinal/transverse cracking, and 5% to 15% of the slabs are shattered (broken into 3 or more pieces).

For a concrete pavement in such condition, it hardly makes sense to even measure load transfer at the transverse joints, without measuring load transfer at cracks as well. It is likely that the load transfer at transverse and diagonal cracks was at least as poor as at transverse joints and probably worse, given the absence of dowels at the cracks. It is also possible that some of the transverse joints were not even working, given the prevalence of transverse and diagonal cracks. The lack of mention in the construction report of joint faulting among the distresses observed also suggests that at least some of the joints might not have been working.

Table 6 shows the dates when the midslab deflections and approach load transfer and leave load transfer deflections were measured in June 1990 at each of the sections. In only five of the 13 tested sections were the midlane and load transfer deflections measured on the same day.

Table 6. Arizona SPS-6 Midslab and Joint Load Transfer Deflection Testing Dates.

Test Section	Midslab (J1)	Approach Joint (J4)	Leave Joint (J5)
040660	June 7, 1990		
040663	June 9, 1990		
040608	June 9, 1990	June 10, 1990	
040607	June 9, 1990	June 10, 1990	
040606	June 9, 1990	June 10, 1990	
040659	June 8, 1990		
040661	June 8, 1990		
040604	June 9, 1990	June 10, 1990	
040662	June 8, 1990	June 10, 1990	
040603	June 9, 1990	June 10, 1990	
040605	June 9, 1990	June 10, 1990	
040602	June 10, 1990		
040601	June 9, 1990	June 10, 1990	

The difficulty that this poses is that the adjustments made to the backcalculated foundation and pavement stiffnesses (obtained from the midslab, J1, deflections) for the effect of load transfer should be done using the load transfers measured at the same time, or at least at the same temperature. An added difficulty is that load transfer efficiencies at midslab cracks were not measured at all.

In-pavement temperatures (at various depths in the concrete slab) were apparently not measured during the June 1990 testing or at least are not in the LTPP database. Air temperatures and pavement surface temperatures were measured with the falling weight deflectometer (FWD), and the latter give an approximate indication of the concrete slab temperatures. Figure 9 shows how the air and surface temperature measurements from the four days of testing in June 1990 compared. There is a strong correlation between the two sets of temperature measurements.

Figure 9 suggests, and Figure 10 further illustrates, that most of the joint load transfer measurements were made at fairly high temperatures. Over the four days of testing, only 21 percent of the joints were tested when the air temperature was at or below 70 °F.

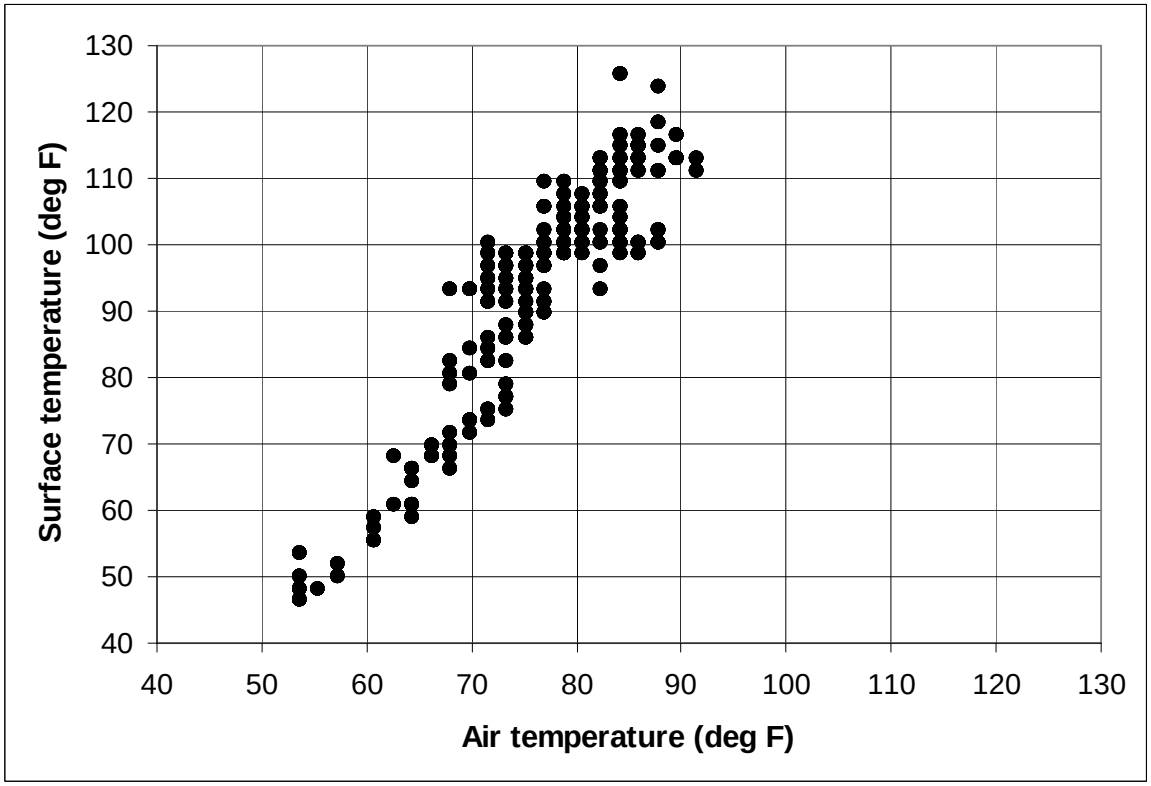

Figure 9. Air and Concrete Surface Temperatures, June 1990.

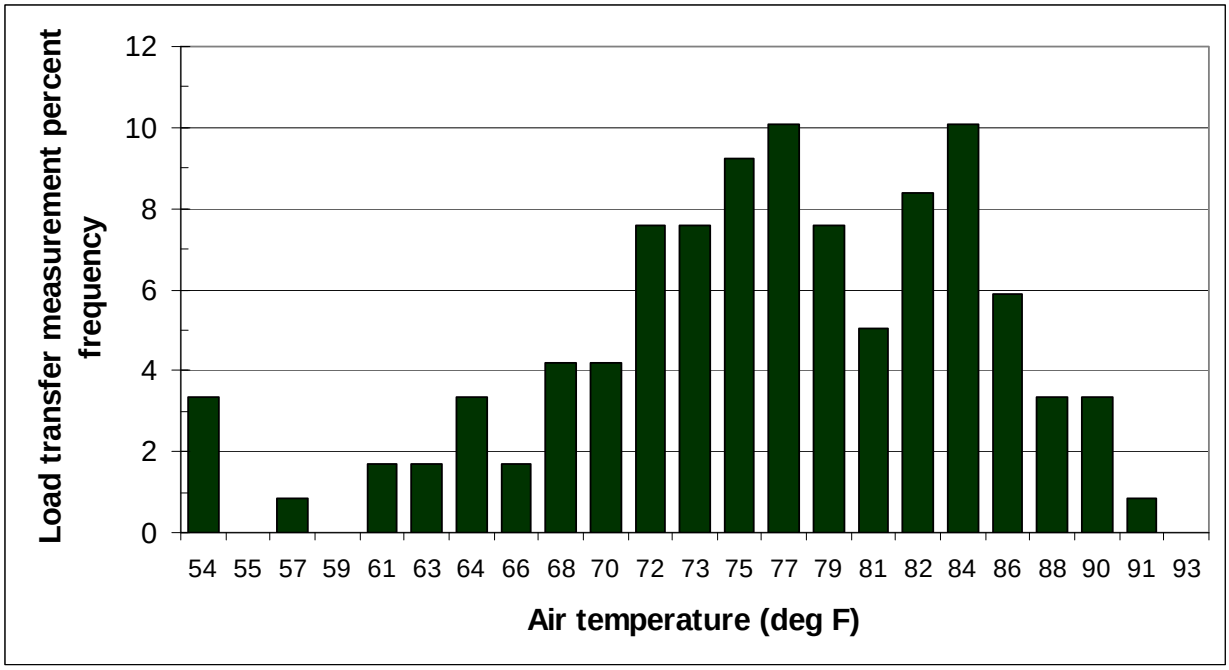

Figure 10. Frequency Distribution of Load Transfer Measurements with Respect to Temperature, June 1990.

Given the approximate nature of the FWD's air and surface temperature measurements, the large percentage of load transfer measurements that were obtained at high temperatures, and the likely contribution of numerous working midslab cracks to variation in joint opening as a function of temperature, it is not surprising that the measured approach and leave joint load transfers show considerable variability as a function of temperature. The graph in Figure 11, which illustrates this variability, suggests three groups of data points:

- Points that follow an upward trend from about 20 percent load transfer at surface temperatures of 70 °F and below, up to load transfers in excess of 80 percent at surface temperatures above about 95 °F.
- A cluster of points with load transfer above 80 percent at surface temperatures in the range of 65 °F to 75 °F.
- A cluster of points with load transfer of about 40 percent to 70 percent at surface temperatures in the range of 45 °F to 60 °F.

Most of the data points in the first group probably represent working joints. The data points in the second group (and perhaps some in the first group as well) represent joints that are not working much at all, perhaps because of the proximity of midslab cracks. The data points in the third group probably represent joints that are working to some degree, but are not opening and closing in response to temperature changes as much as the joints in the first group.

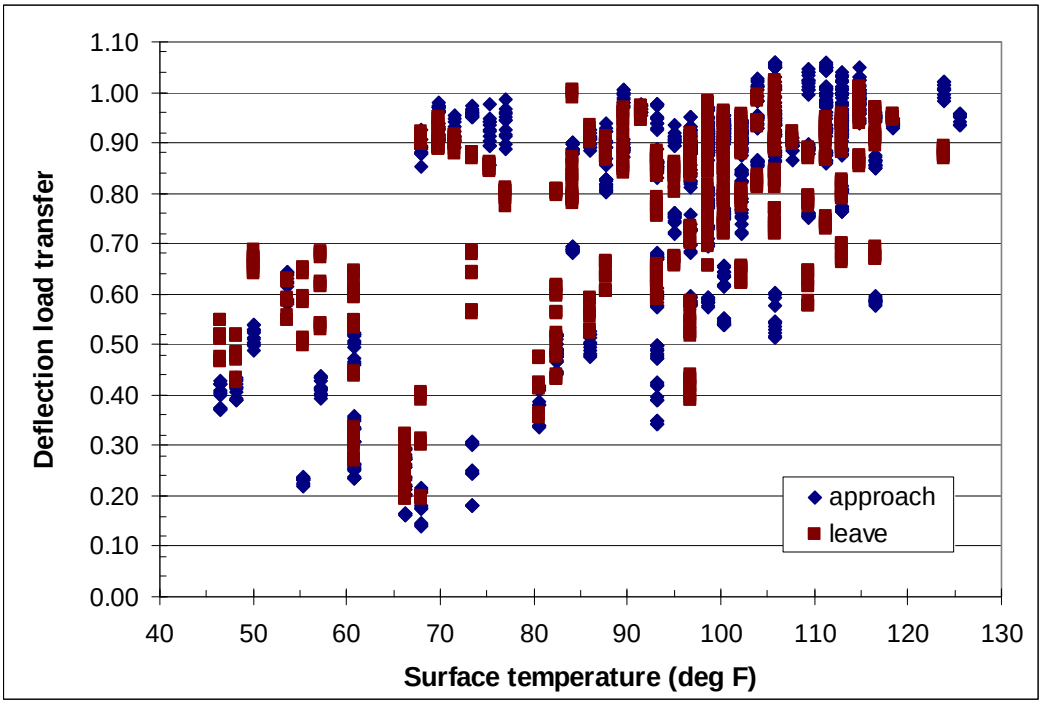

Figure 11. Joint Deflection Load Transfer as a Function of Pavement Surface Temperature, June 1990.

The load transfer at working midslab cracks (at any given pavement surface temperature) may have been equal to or less than the load transfer at working joints at the same temperature. For this analysis, researchers assumed that the variation of load transfer in all working and nonworking joints and cracks combined, with respect to surface temperature, could be represented approximately by the following step function:

- 30 percent load transfer for surface temperatures below 75 °F.
- 50 percent load transfer for surface temperatures between 75 °F and 90 °F.
- 80 percent load transfer for surface temperatures above 90 °F.

It is necessary to make adjustments for load transfer variation as a function of temperature because the slabs are not infinite in size. In fact, given the degree of midslab cracking observed in 1990, clearly many of the slabs were fairly small in size. Not making some reasonable attempt to account for this would result in underestimation of the foundation k value and overestimation of the concrete modulus.

Another aspect of load transfer to consider is how approach side and leave side load transfers compare, joint by joint, at this site. As illustrated in Figure 12:

- At high load transfer levels (for example, at higher temperatures), approach and leave load transfers are comparable.
- At lower load transfer levels (for example, at lower temperatures), load transfer was usually higher on the leave side than on the approach side.

The substantial difference between approach and leave load transfer at many of the same joints is another reason to consider the step function presented earlier sufficiently precise for this analysis.

Maximum Deflection

Maximum deflection refers to the deflection measured at the center of the deflectometer load plate, in the middle of the traffic lane, away from joints and cracks. The magnitude of the maximum deflection and its variability over the length of the project are indications of the magnitude and variability of the stiffness of the pavement structure and foundation combined. When the surface layer of a pavement structure is AC, the maximum deflections need to be normalized with respect to some reference temperature to screen out the effect that changes in AC mix temperature during the day's testing would have on the apparent variability of the maximum deflection over the project length. This is not a concern with the June 1990 data, since all of the sections were bare concrete at that time.

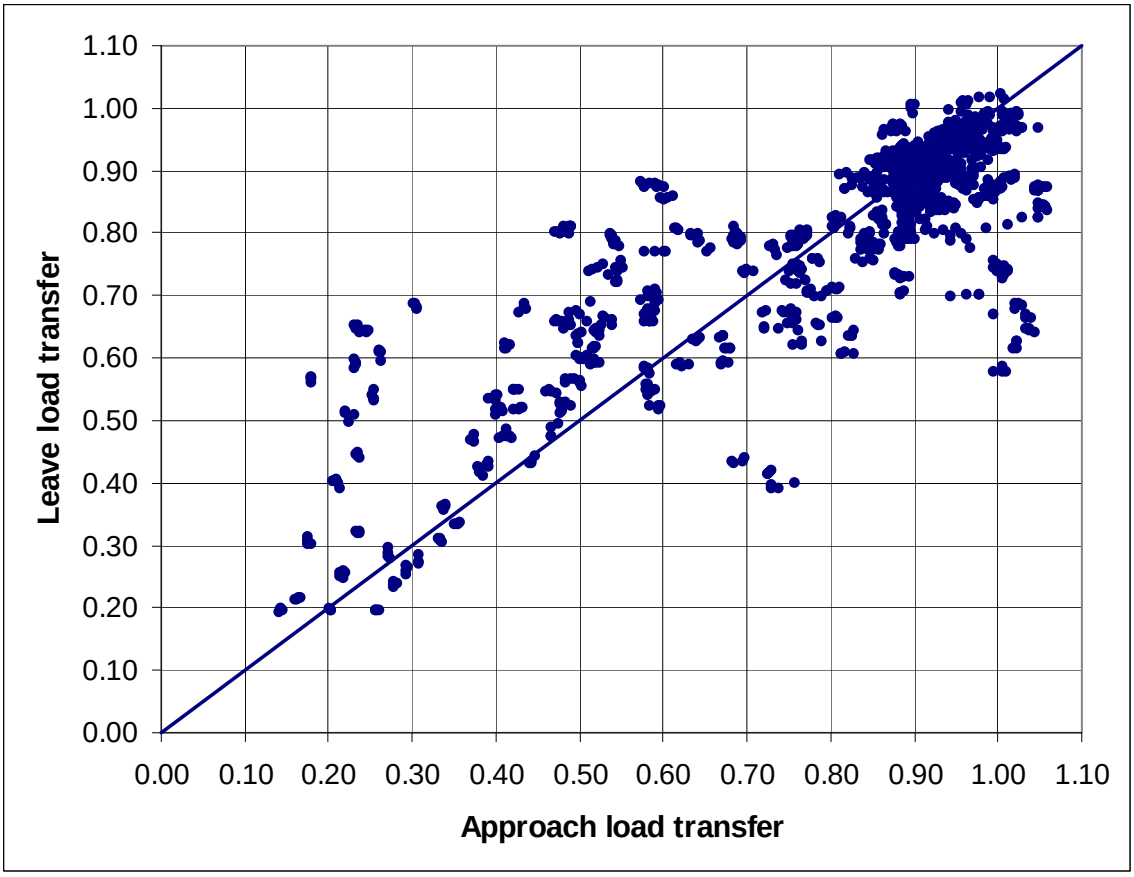

Figure 12. Approach Versus Leave Joint Load Transfer, June 1990.

The maximum deflection measured on a bare concrete slab can be increased—suggesting that the combined stiffness of the pavement and foundation is lower than it really is—if the slab interior is curled up and out of contact with the underlying base as a result of a daytime temperature gradient in the slab. This cannot be checked directly for the June 1990 deflection data because the LTPP database doesn't contain in-pavement temperature measurements from the test sections during the June 1990 round of testing. However, the presence of a temperature gradient substantial enough to lift the slab interior off of the base can be checked by comparing the deflections measured at different load levels. If a curling-induced void is present beneath the slab interior, the slope of the load-deflection line will be greater at lower load levels than at higher load levels (presuming that at higher load levels, the slab is brought into contact with the base). This was observed in only a small percentage of the June 1990 midlane deflection basins, which suggested these deflections were not affected by slab curling.

Figure 13 shows the midslab D0 deflections along the length of the project. Each point represents the average D0 from four load drops at the 9000 pound target load level, where each of the four individual D0 measurements have been normalized to 9000 pounds. The horizontal bars in Figure 13 represent the average D0 for each test section.

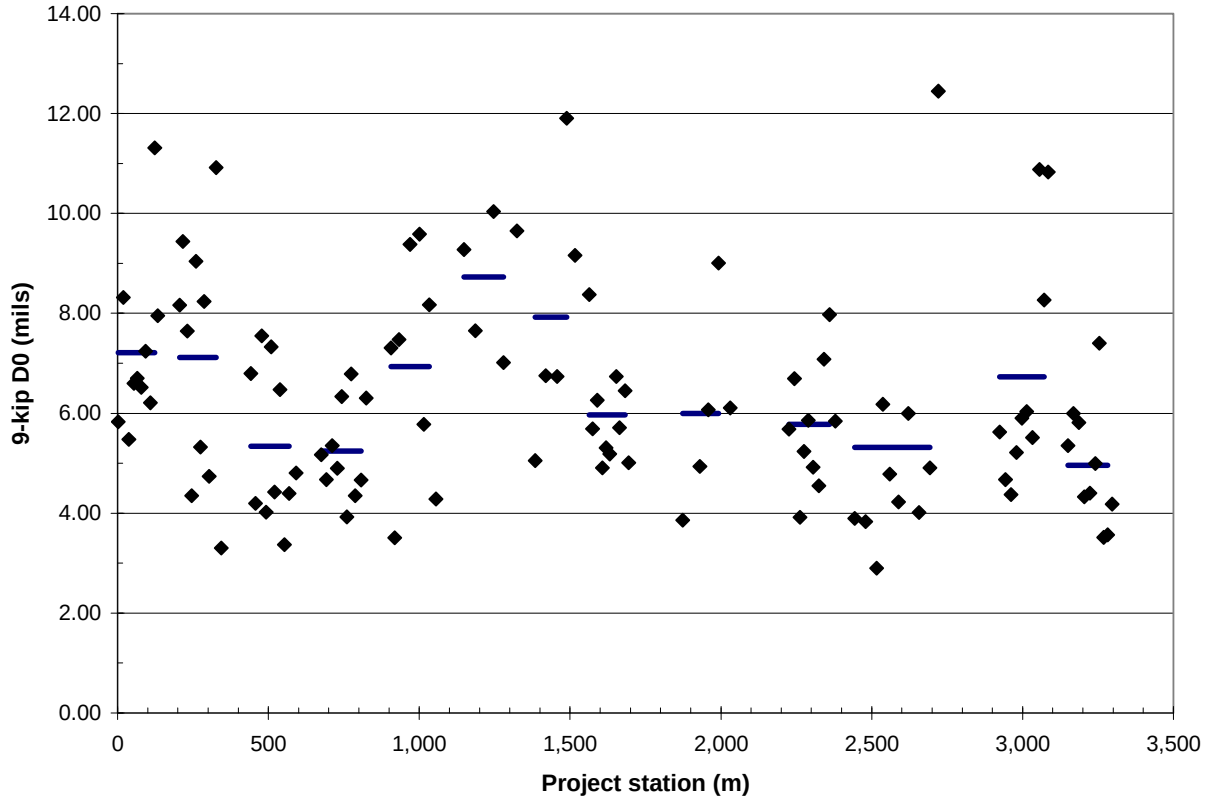

Figure 13. Maximum Deflection at 9000 Pounds along the Project Length, June 1990.

The upward and downward shifts in the test section average D0 deflections are expected, since the first test sections on the west end of the project are in fill, followed by a slight cut, followed by a large fill, followed by an increasingly deep cut. The variation in foundation stiffness due to differences between cut and fill appear to play a large role in the variation in maximum deflection from one test section to the next. The average for the second-to-last test section (040602) deviates from the trend of decreasing average maximum deflection with increasing depth of cut near the east end of the site.

Unusually high deflections at specific points may be the result of a weak foundation or a particularly deteriorated and weak pavement structure at those points.

Static k Value

The static k value of the foundation (granular subbase, fill material, natural subgrade soil, and underlying rock) is calculated from the deflection basin measurements and adjusted for finite slab size and load transfer using closed-form equations derived from the theory of the behavior of plates on dense liquids. Typically for bare concrete pavements, k is backcalculated using the maximum deflection D0 and a deflection basin AREA parameter calculated using two or more deflections away from the load plate, normalized with respect to D0 (to remove the effect of load magnitude).

For asphalt-overlaid concrete pavements, k should be backcalculated using deflections measured away from the load plate, to remove the effect of compression in the AC layer, between the load plate and the concrete slab. For example, k can be backcalculated using D12, the deflection measured 12 inches away from the center of the load plate, and a deflection basin AREA parameter calculated using two or more deflections farther away, normalized with respect to D12 (again, to remove the effect of load magnitude). This “outer AREA” backcalculation approach is advisable when:

- A PCC pavement has an AC surface layer.
- A bare PCC pavement exhibits significant compression (because of exceptional slab thickness such as an airport pavement, exceptional slab weakness such as severe D cracking, an exceptionally stiff foundation such as shallow bedrock, or a combination of these).
- When backcalculation results from deflections measured on bare concrete pavement are to be compared with backcalculation results from deflections measured in later years on that same pavement after an asphalt overlay has been placed.

The estimated static k values along the length of the project are shown in Figure 14. Each point represents the average k value from four load drops at the 9000 pound target load level. The horizontal bars represent the average estimated static k value for each test section. These k values are referred to here as estimated static k values because the backcalculated (dynamic) k value at each point was divided by two to obtain an estimate of the static k value.

Where the average D0 shifts up or down from one test section to the next, the average k value shifts in the opposite direction, as expected. In general (except for the second-to-last section in cut), the test sections with higher k values are those in cut, and the test sections with lower k values are those in fill.

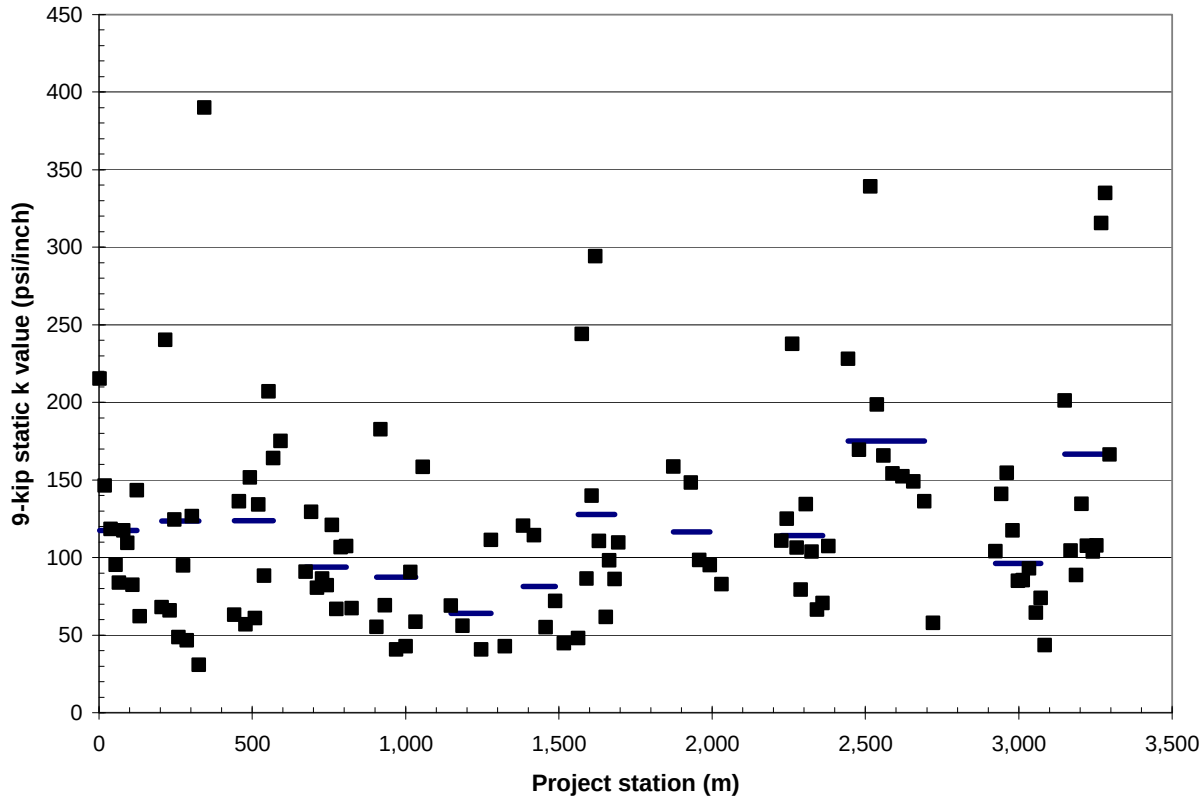

Figure 14. Estimated Static k Value at 9000 Pounds along Project Length, June 1990.

The k value results in Figure 14 show the prevalence of very low estimated static k values. Forty-seven percent of the values are less than 100 psi/inch. Over the length of the project, the average estimated static k value is 119 psi/inch and the median is 106 psi/inch. Even in the cut sections, no test section has a mean estimated static k value greater than 175 psi/inch. These k values are not typical of subgrade soils reported to be silty sand with gravel, clayey sand with gravel, or clayey gravel with sand, much less sandstone bedrock. According to the American Association of State Highway and Transportation Officials (AASHTO) Soil Classification System, the first three are descriptors of A-2 soils—soils that include various granular materials and typically have California Bearing Ratio (CBR) values between 10 percent and 80 percent, and static k values between 150 and 500 psi/inch. However, most of the static k values estimated from the backcalculation results would be typical of fine-grained soils with CBR values of less than 10 percent.

Also, the k value results in Figure 14 indicate the lack of uniformity of foundation stiffness along the length of the project. A foundation that could be considered fairly consistent over the length of a project would have a coefficient of variation (standard deviation as a percentage of the mean) of no more than 20 percent. The coefficient of variation of the Arizona SPS-6 site k values (at least, for the 13 sections deflection tested in June 1990) is 57 percent. Even within the individual test sections (that is, discounting the influence of changes between cut and fill), the coefficients of variation of the estimated static k values range from 23 percent to 90 percent.

Table 7 lists the mean static k value for each test section. The lower average k values are a particular concern for those test sections where the concrete slab was cracked and seated.

Table 7. Arizona SPS-6 Test Section Treatments and Estimated Static k Values.

Test Section	Main Treatments	Mean Static k Value (psi/inch)
040660	Rubblizing and AC overlay	117
040663	Unbonded PCC overlay	123
040608	Crack/seat and AC overlay	123
040607	Crack/seat and AC overlay	93
040606	Lane replacement and AC overlay	87
040659	Crack/seat and AC overlay	64
040661	Crack/seat and AC overlay	81
040604	AC overlay with saw/seal	127
040662	Crack/seat and AC overlay	116
040603	AC overlay	114
040605	Nonoverlay restoration	175
040602	Nonoverlay restoration	96
040601	None	166
040664	AC overlay	*Not tested in June 1990*
040665	Crack/seat and AC overlay	*Not tested in June 1990*
040666	Rubblizing and AC overlay	*Not tested in June 1990*
040667	Crack/seat and AC overlay	*Not tested in June 1990*
040668	AC overlay	*Not tested in June 1990*
040669	Rubblizing and AC overlay	*Not tested in June 1990*

The notable variability of the foundation stiffness along the project length and the large proportion of the project length where the foundation is very weak together call into question whether, in hindsight, this was an appropriate site for a rehabilitation experiment in which the concrete slabs in many of the test sections would be cracked and seated prior to overlay. The findings point to the importance of considering not only treatment type but also differences in foundation stiffness when assessing the relative performance of different test sections at this or any SPS-6 site. They also indicate the value of conducting deflection testing and analysis when selecting sites for rehabilitation treatments such as rubblizing or cracking and seating.

Effective Pavement Modulus

The stiffness of the pavement structure above the subgrade is expressed by the effective pavement modulus (E_{eff}). This parameter reflects the combined contributions of the concrete slab and base layers. It may be calculated using the slab thickness only or using the slab and base thickness together; it does not matter which approach is used so long as the same approach is retained in subsequent calculations to distinguish between the slab modulus and base modulus. For this analysis, effective pavement

modulus values were calculated using LTPP's best estimates of the as-constructed thicknesses of the concrete slabs (Table 1): 7.9 inches for Section 040601, 8.0 inches for Section 040602, 8.3 inches for Section 040603, etc.

Figure 15 shows the effective pavement modulus values along the length of the project. Each point represents the average effective pavement modulus from four load drops at the 9000 pound target load level. The horizontal bars represent the average effective pavement modulus for each test section.

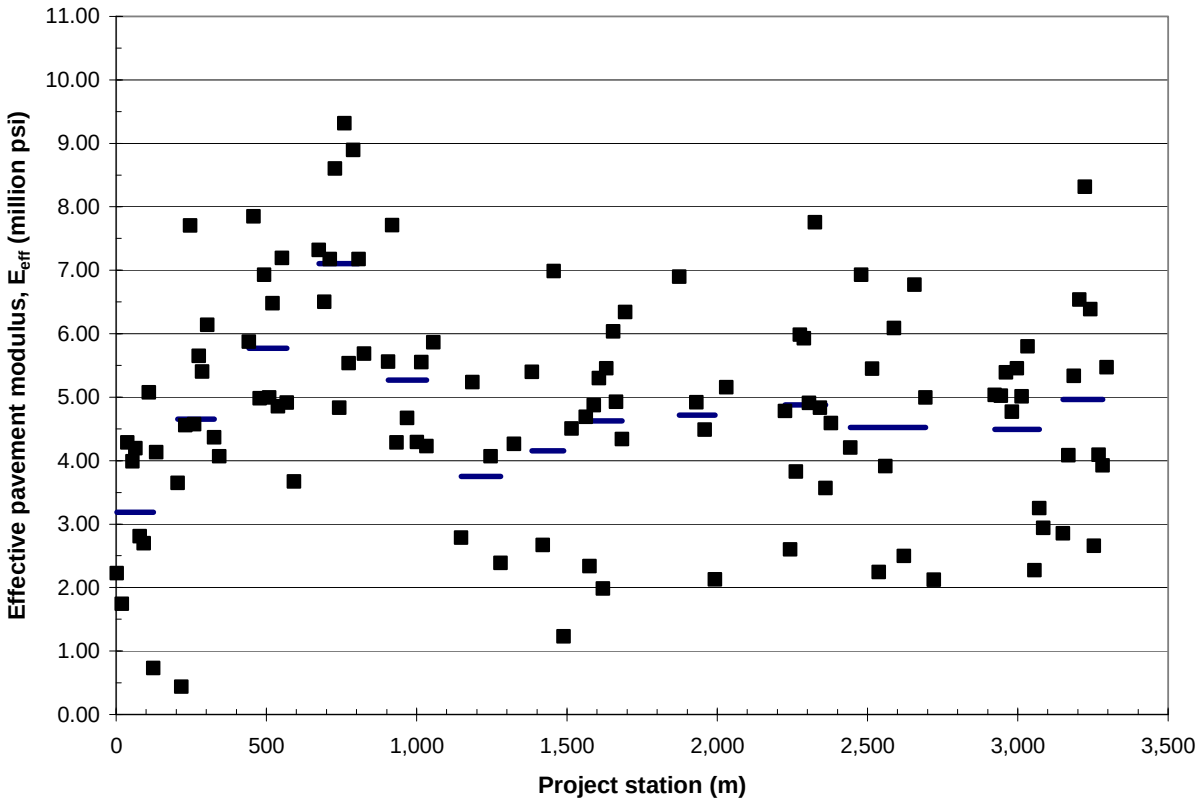

Figure 15. Effective Pavement Modulus at 9000 Pounds along Project Length for Test Sections' Average As-Built Thicknesses.

The overall average effective pavement modulus over the length of the project was 4.84 million psi. The average in Section 040660, the first test section, was 3.18 million psi—considerably lower than the overall project average. The effective pavement modulus values increase in the next three test sections, to an average high of 7.10 million psi in Section 040607, then drop again, and in the last seven of the 13 sections tested in June 1990, level off between 4 million and 5 million psi.

Investigators checked the effective pavement modulus values obtained to ensure they were not biased by either the estimated static k values obtained at the same points or the as-constructed pavement thicknesses used in the calculations. The relationship of effective pavement modulus to each of these

two other parameters has an R^2 of less than 3 percent. Thus, investigators were fairly confident that the variations seen in the effective pavement modulus were due to variations in the thickness of the concrete slab and/or base, and/or variation in the structural integrity of the slab and/or base. If the design slab thickness (8.0 inches) had been used in the effective pavement modulus calculation rather than the as-constructed test section average thicknesses, the effective pavement modulus values would display even greater variability.

The overall average effective pavement modulus, 4.84 million psi; the prevalence of individual effective pavement modulus values less than 5 million psi; and the construction report's comments on the extent of slab cracking all reinforce the finding that the slab had little, if any, remaining structural life in 1990. However, the portion of the project near Sections 040608, 040607, and 040606 appears to be an exception: Many of the effective pavement modulus values obtained for points tested in this region exceeded 6 million psi.

Effective Thickness of Pavement Structure

Another way to look at the overall stiffness of the pavement structure above the subgrade is to turn the effective pavement modulus calculation around: Instead of calculating an elastic modulus as a function of a known slab thickness, the thickness is calculated as a function of an assumed elastic modulus. This yields an indicator of the relative strength of the pavement structure that is easier to visualize than is an elastic modulus.

In this analysis, the effective thickness of the pavement structure at each deflection testing point was calculated assuming a concrete slab elastic modulus of 4.2 million psi. This modulus value was chosen because ADOT's past experience suggests that 28-day compressive strengths of about 5000 to 6000 psi are typical, which correspond to elastic modulus values in the range of about 4.0 million to 4.4 million psi. The effective thickness results are shown in Figure 16.

The effective thicknesses ranged from 3.91 to 11.55 inches, with most values in the range of 7 to 10 inches, and the overall project average was 8.5 inches. This means that the existing pavement had the same average bending stiffness as an 8.5 inch pavement with a concrete modulus of 4.2 million psi; it doesn't mean that the existing pavement had the same remaining structural life as an 8.5 inch pavement with a concrete modulus of 4.2 million psi.

Given that the overall average as-constructed thickness of the concrete was 8.25 inches, the calculated overall average effective thickness of 8.5 inches for the concrete and underlying stabilized and unstabilized base layers together suggests that the base layers contribute only about a quarter of an inch to the bending stiffness of the pavement structure.

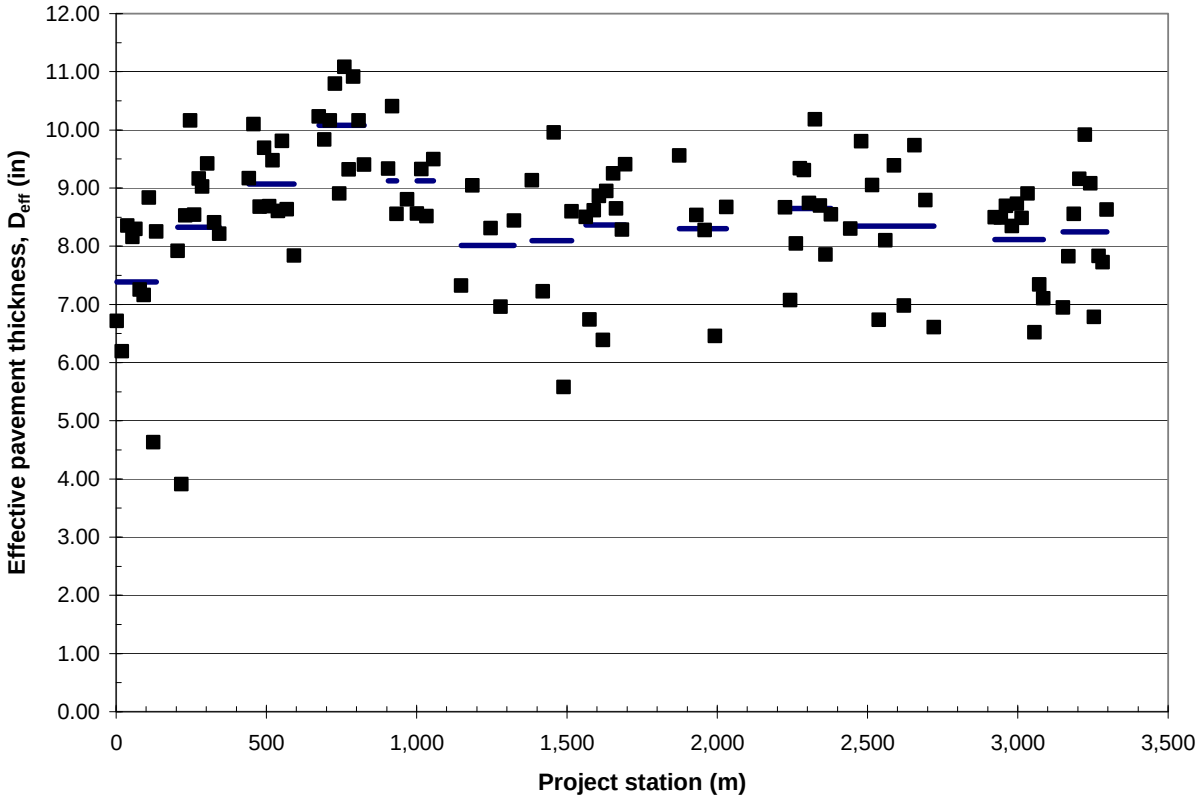

Figure 16. Effective Thickness along Project Length (Assuming 4.2 Million psi Modulus).

Estimation of Concrete Modulus and Base Modulus

The effective pavement modulus can be expressed as separate estimates of the elastic modulus from the concrete slab and from the base. Unfortunately, the state of the art of concrete pavement backcalculation does not provide a closed-form solution for these two pavement layer moduli as a function of the real degree of friction between the two. To solve this problem requires assuming that the slab/base interface is either fully bonded or fully frictionless, and assuming a ratio of the concrete modulus to the base modulus. Whatever results are obtained are thus dependent on the interface condition assumed and the modular ratio assumed.

Investigators obtained a range of solutions for this analysis to assess which were most realistic. Figure 17 shows the overall average concrete elastic modulus, calculated for both the unbonded and bonded interface cases, and as a function of assumed values of the ratio of base modulus to slab modulus. The corresponding base elastic modulus results are shown in Figure 18.

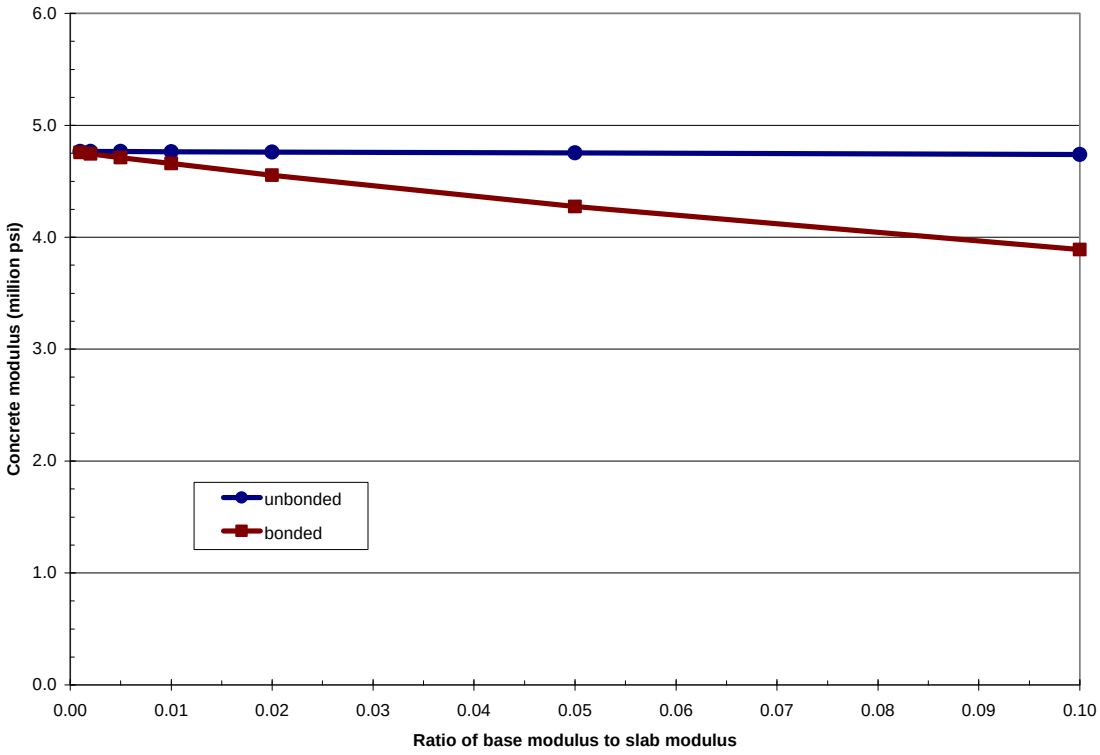

Figure 17. Concrete Elastic Modulus as a Function of Interface Condition and Modular Ratio.

The concrete elastic modulus results show relatively little sensitivity to either the interface condition or the modular ratio. The results suggest that the true overall average concrete elastic modulus is somewhere between about 4.25 and 4.75 million psi. The base elastic modulus results appear to show greater sensitivity, however Figures 17 and 18 have different vertical scales: psi in millions and thousands, respectively. There appears to be almost no difference between the unbonded and bonded solutions for base modulus values up to 225,000 psi, but the true base modulus could be as low as about 25,000 psi or as high as about 250,000 psi. It is difficult to know any more about the stiffness of the base from the deflection results alone. Additional information about the strength or stiffness of the base obtained from laboratory testing or even visual examination in the field would make it easier to determine the elastic modulus of the base and, as a consequence, of the concrete, although as Figures 17 and 18 show, the degree of friction between the slab and the base probably does not matter much.

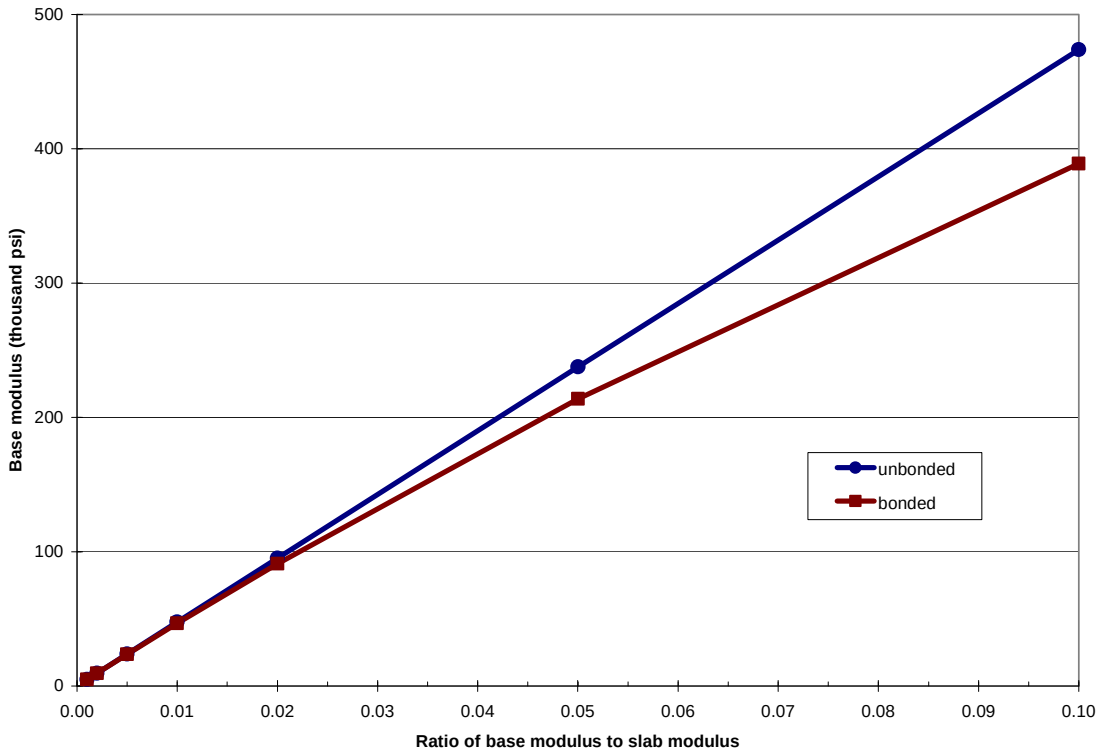

Figure 18. Base Elastic Modulus as a Function of Interface Condition and Modular Ratio.

The remainder of this chapter shows how the deflection response of the Arizona SPS-6 test sections was changed by the rehabilitation treatments applied and how the deflection response subsequently changed over time. For this purpose, it isn't particularly important to know the concrete slab modulus and the base modulus separately. Those results are given here using the June 1990 deflection data to show that the overall stiffness of a multilayer pavement structure can always be decomposed into the stiffness of the individual layers, and to show the relative sensitivity of this decomposition to some of the unknown factors involved. However, the more interesting subject, for the purpose of comparing the performance of the different rehabilitation treatments applied, is the effect of the different rehabilitation treatments on the maximum deflection, and the effective stiffness and effective thickness of the pavement structure as a whole.

ANALYSIS OF DEFLECTIONS MEASURED AFTER REHABILITATION

After rehabilitation, the first 13 sections (ADOT ID numbers 1 through 13) were deflection tested between April 8–12, 1991. The remaining six sections at the site (supplemental sections 040664 through 040669, ADOT ID numbers 14 through 19) were not. The test sections can be placed into the following categories according to the pavement type produced as a result of the rehabilitation work:

- Bare concrete pavement: Section 040601 (the control), Section 040602 (minimum restoration), and Section 040605 (maximum restoration) represent this category. The outer traffic lane was replaced through the full length of Section 040605.
- Asphalt overlay of intact concrete pavement: Sections 040603 and 040606 received asphalt overlays after minimum and maximum repair, respectively. Maximum repair for Section 040606 included, among other things, replacement of the outer traffic lane through the full length of the test section. Section 040604 also received a 4 inch asphalt overlay after minimal repair, but differed from Section 040603 in that in Section 040604, transverse joints were sawed and sealed in the overlay at locations matching the joints in the underlying concrete pavement. Sections 040664 and 040668 also received an asphalt overlay without fracturing of the existing pavement, but were not deflection tested in April 1991.
- Asphalt overlay of cracked and seated concrete pavement: Sections 040607, 040608, 040659, 040661, and 040662 were overlaid after cracking and seating of the existing pavement. Among these, only in Section 040659 was a fabric placed on the cracked and seated concrete prior to placing the asphalt overlay. Sections 040665 and 040667 also received an asphalt overlay after cracking and seating of the existing pavement, but were not deflection tested in April 1991.
- Asphalt overlay of rubblized concrete pavement: Section 040660 and 040666 was overlaid after the existing concrete pavement was rubblized. Section 040669 was also rubblized prior to overlay, but was not deflection tested in April 1991.
- Unbonded concrete overlay of cracked and seated concrete pavement: In Section 040663, the existing concrete pavement was cracked and seated, and covered with a 2 inch AC interlayer and a 10 inch PCC overlay.

Maximum Deflection

The April 1991 midslab D0 deflections along the length of the project are shown in Figure 19. Each point represents the average D0 from four load drops at the 9000 pound target load level, where each of the four individual D0 measurements have been normalized to 9000 pounds. In addition, D0 deflections measured on asphalt-surfaced test sections were normalized to 68 °F using a regression equation based on the 1993 AASHTO Guide's temperature adjustment factor for asphalt surfaces on cement- or pozzolan-treated bases. The horizontal bars in Figure 19 represent the average D0 for each test section. With the exception of the control section (040601, the last section plotted), the first set of post-rehabilitation maximum deflections are lower, more consistent within test sections, and more

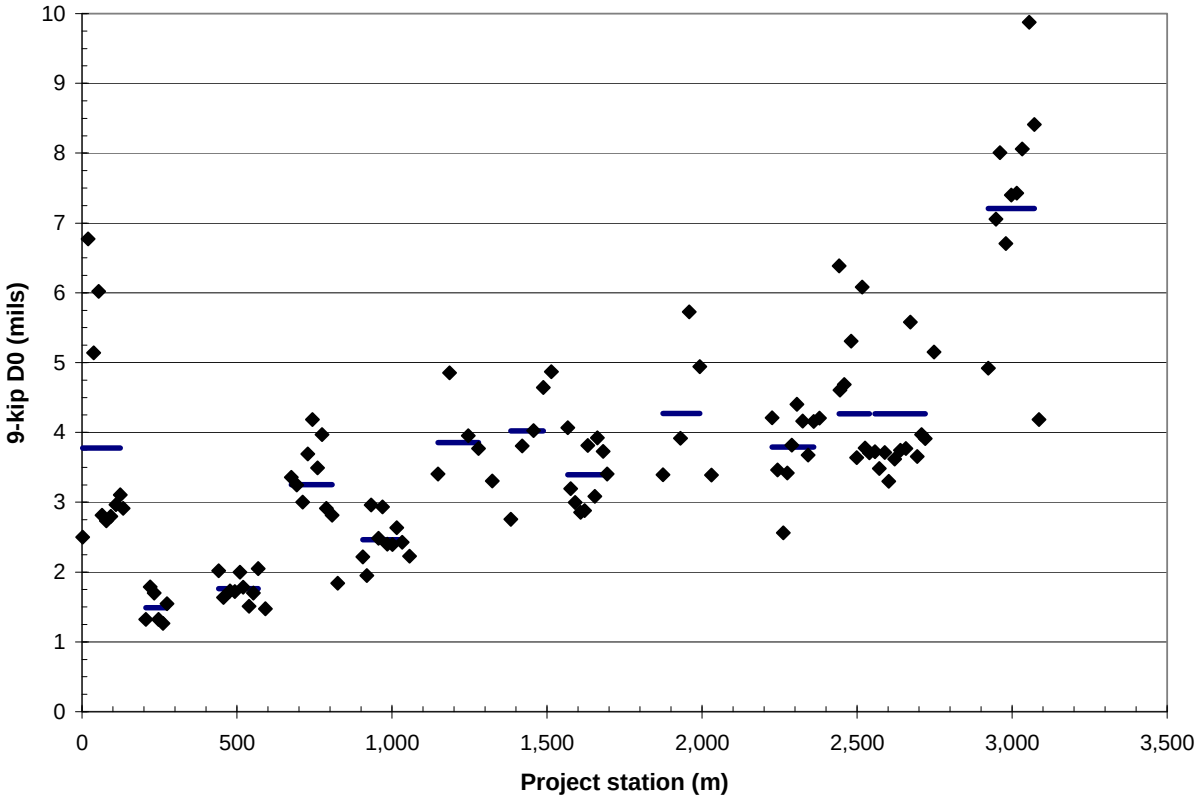

Figure 19. Maximum Deflections along Project Length, April 1991.

consistent from test section to test section than the prerehabilitation maximum deflections shown in Figure 13.

The effect of rehabilitation on the mean maximum deflection in each test section is illustrated in Figure 20. The changes in mean maximum deflection, as a percentage of the prerehabilitation mean, can be examined by rehabilitation treatment group:

- Bare concrete pavement: Mean maximum deflection increased 40 percent in Section 040601, the untreated control; increased 7 percent in Section 040602, which received minimal repair; and decreased 20 percent in Section 040605, in which the entire outer lane was replaced.
- Asphalt overlay of intact concrete pavement: Mean maximum deflection decreased 34 percent in Section 040603 and 43 percent in Section 040604. Both sections received minimal repair; Section 040603 received a 3.4 inch overlay, and Section 040604 received a 3.6 inch overlay along with sawing and sealing of transverse joints. Mean maximum deflection decreased more dramatically (64 percent) in Section 040606, which received a 4.3 inch overlay after complete replacement of the outer lane.

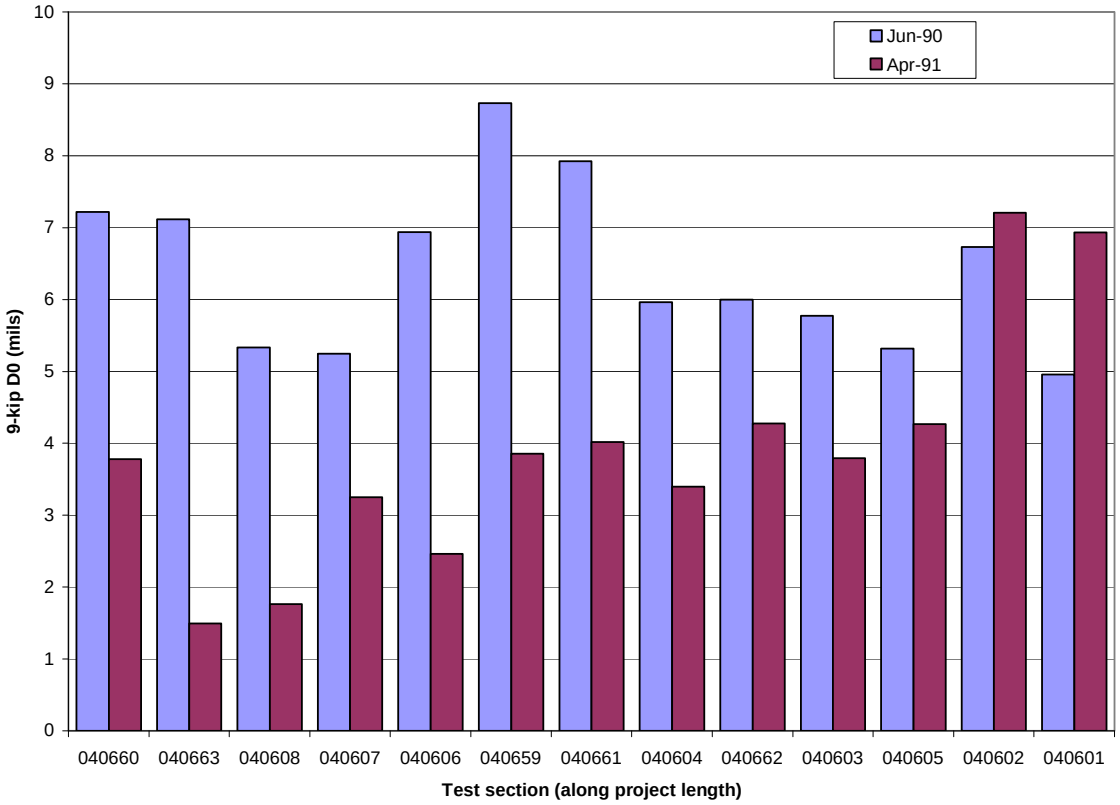

Figure 20. Mean Maximum Deflection Before and After Rehabilitation, April 1991.

- Asphalt overlay of cracked and seated concrete pavement: In Section 040607, which received a 4.3 inch overlay after cracking and seating of the concrete pavement, the decrease in mean maximum deflection (34 percent) was comparable to that of the sections that received an asphalt overlay of comparable thickness without slab fracturing (Sections 040603 and 040604). Mean maximum deflection was more dramatically reduced (67 percent) in the section that received an 8.4 inch overlay after cracking and seating. In Section 040659, in which a fabric was placed on the cracked and seated concrete prior to the overlay, mean maximum deflection was reduced by 56 percent. In Sections 040661 and 040662, the two other cracked and seated sections tested in April 1991, dissimilar reductions in mean maximum deflection were achieved (49 percent versus 29 percent). Both received a 4 inch overlay and no apparent difference in treatment other than that Section 040662 also had subdrains retrofitted.

- Asphalt overlay of rubblized concrete pavement: In Section 040660, which received an 8 inch overlay after rubblizing the existing concrete slab, the mean maximum deflection was reduced 49 percent.
- Unbonded concrete overlay of cracked and seated concrete pavement: The initial result of cracking and seating, a 2 inch asphalt separation layer, and a 10 inch concrete overlay was a 79 percent reduction in mean maximum deflection.

However, rehabilitation treatment is not the only factor that may have contributed to changes in mean maximum deflection between June 1990 and April 1991. The Arizona SPS-6 site is in a mountainous region, probably subject to substantial frost penetration, and it would not be surprising if in April of any year the foundation were stiffer than it would be in June. Were the depth to bedrock fairly uniform along the length of the project, any changes in foundation stiffness due to freezing or thawing would be expected to be fairly uniform in magnitude. However, since the depth of cut or fill varies among the Arizona SPS-6 test sections, the effect of seasonal variation in foundation stiffness will likely vary as well.

Effective Pavement Modulus

Figure 21 shows effective pavement modulus values along the length of the project after rehabilitation. Each point represents the average effective pavement modulus from four load drops at the 9000 pound target load level. The horizontal bars in Figure 21 represent the average effective pavement modulus for each test section. These values were calculated as a function of the thickness of the original concrete slab, as was done with the prerehabilitation deflections, to illustrate the relative effects of different rehabilitation treatments. For example, if an 8 inch concrete slab with a 4 inch asphalt overlay has an effective pavement modulus of 7 million psi, that does not mean that either the concrete or the asphalt has a modulus of 7 million psi, but rather that the asphalt-overlaid concrete structure has the same bending stiffness as an 8 inch slab of 7 million psi concrete.

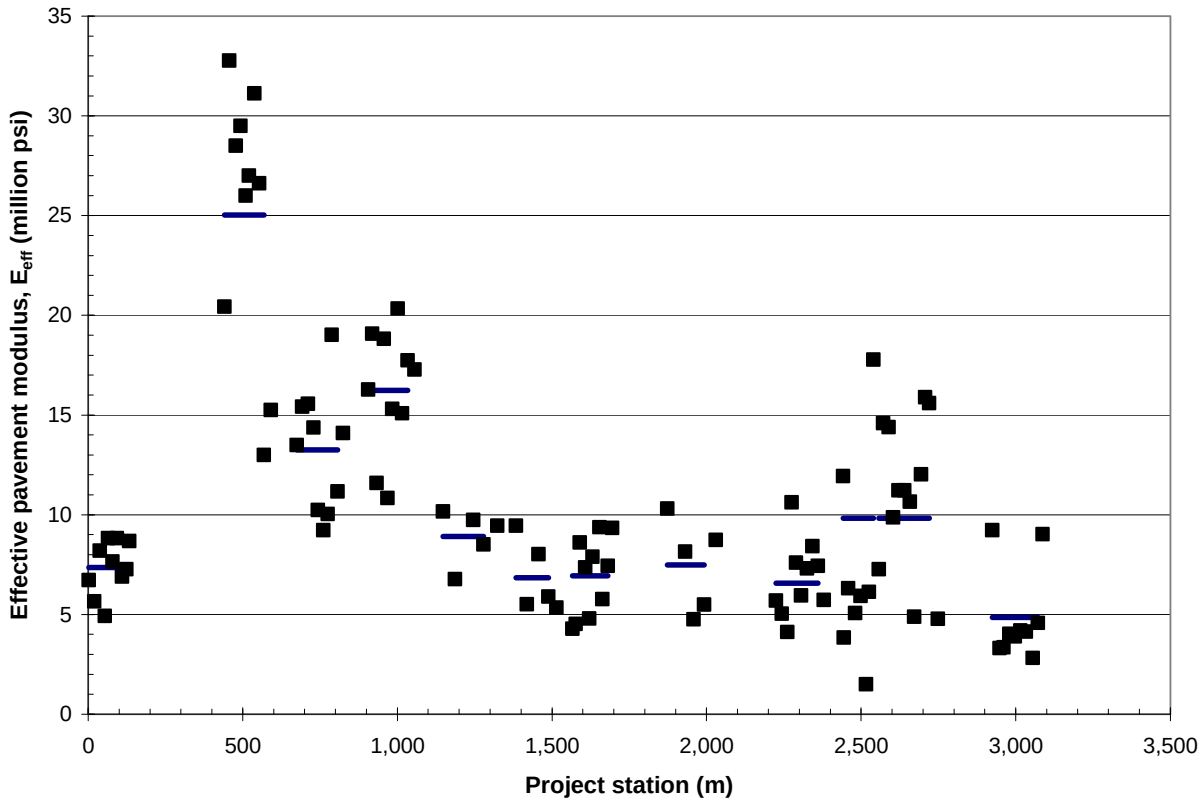

Figure 21. Effective Pavement Modulus along Project Length After Rehabilitation as a Function of Prerehabilitation As-Built Concrete Slab Thicknesses.

The effect of rehabilitation on effective pavement modulus is illustrated in Figure 22. The changes in mean effective pavement modulus, as a percentage of the prerehabilitation mean, can be examined by rehabilitation treatment group:

- Bare concrete pavement: The mean effective pavement modulus decreased by 25 percent in Section 040601, the untreated control section; increased 8 percent in Section 040602, which received minimal repair; and increased 118 percent in Section 040605, in which the entire outer lane was replaced.
- Asphalt overlay of intact concrete pavement: The mean effective pavement modulus increased 35 percent in Section 040603 and 50 percent in Section 040604. Both sections received minimal repair; Section 040603 received a 3.4 inch overlay, and Section 040604 received a 3.6 inch overlayer along with sawing and sealing of transverse joints. Mean effective pavement modulus increased more dramatically (208 percent) in Section 040606, which received a 4.3 inch overlay after complete replacement of the outer lane.

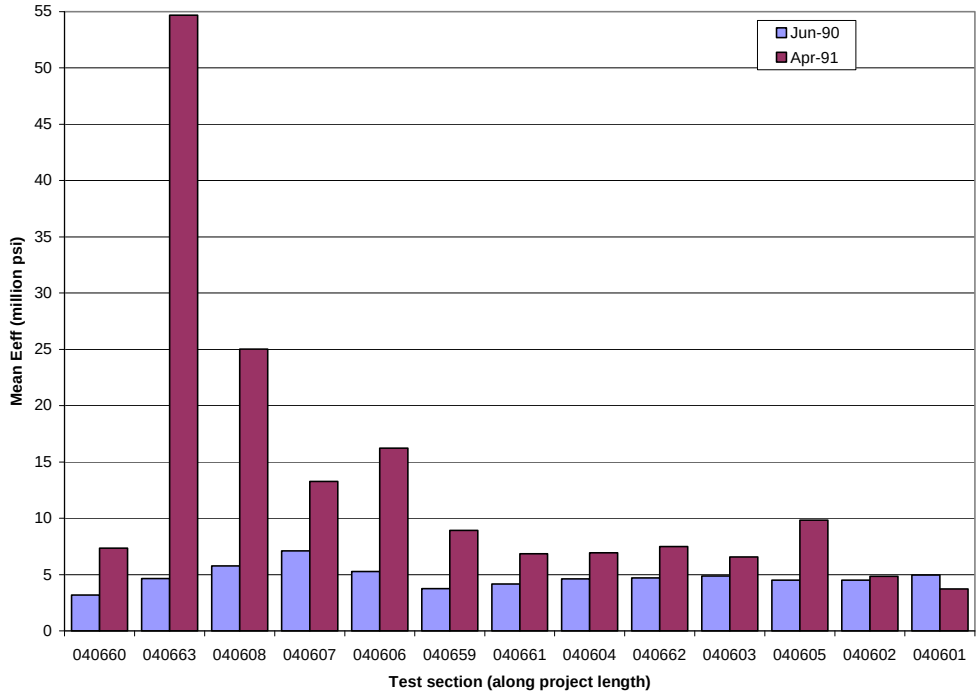

Figure 22. Effective Pavement Modulus Before and After Rehabilitation as a Function of Prerehabilitation As-Built Concrete Slab Thicknesses.

- Asphalt overlay of cracked and seated concrete pavement: The mean effective pavement modulus increased by 87 percent and 333 percent in Sections 040607 and 040608, respectively. Section 040607 received a 4.3 inch overlay, and Section 040608 received an 8.4 inch overlay after cracking and seating of the concrete pavement. In Section 040659, in which a fabric was placed on the cracked and seated concrete prior to the overlay, mean effective pavement modulus increased 138 percent. In Sections 040661 and 040662, the two other cracked and seated supplemental sections tested in April 1991, similar increases in mean effective pavement modulus were 65 percent and 59 percent, respectively. Both sections received a 4 inch overlay.
- Asphalt overlay of rubblized concrete pavement: In Section 040660, which received an 8 inch overlay after rubblizing of the existing concrete slab, the mean effective pavement modulus increased 131 percent.
- Unbonded concrete overlay of cracked and seated concrete pavement: In Section 040663, the initial result of cracking and seating, a 2 inch asphalt separation layer, and a 10 inch concrete overlay was a greater than tenfold (1075 percent) increase in effective pavement modulus.

Effective Thickness of Pavement Structure

The post-rehabilitation effective thickness values along the length of the project are shown in Figure 23. These values were calculated assuming a concrete slab elastic modulus of 4.2 million psi. The pre- and post-rehabilitation mean effective thickness values are compared in Figure 24.

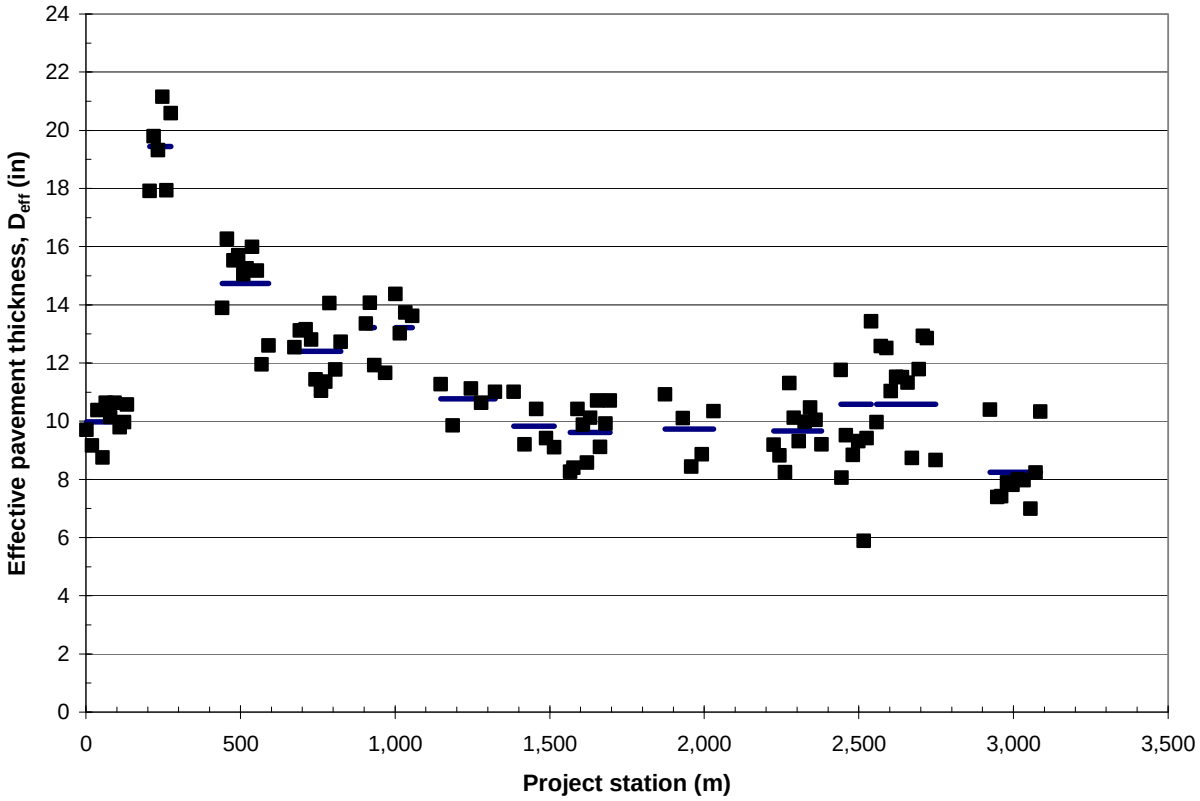

Figure 23. Post-Rehabilitation Effective Pavement Thickness along Project Length (Assuming 4.2 Million psi Modulus).

- Bare concrete pavement: The mean effective pavement thickness decreased 8 percent in Section 040601, the untreated control; increased 2 percent in Section 040602, which received minimal repair; and increased 27 percent in Section 040605, in which the entire outer lane was replaced.
- Asphalt overlay of intact concrete pavement: The mean effective pavement thickness increased 12 percent in Section 040603 and 15 percent in Section 040604. Both sections received minimal repair; Section 040603 received a 3.4 inch overlay and Section 040604 received a 3.6 inch overlay along with sawing and sealing of transverse joints. Mean effective pavement thickness increased more dramatically (45 percent) in Section 040606, which received a 4.3 inch overlay after complete replacement of the outer lane.

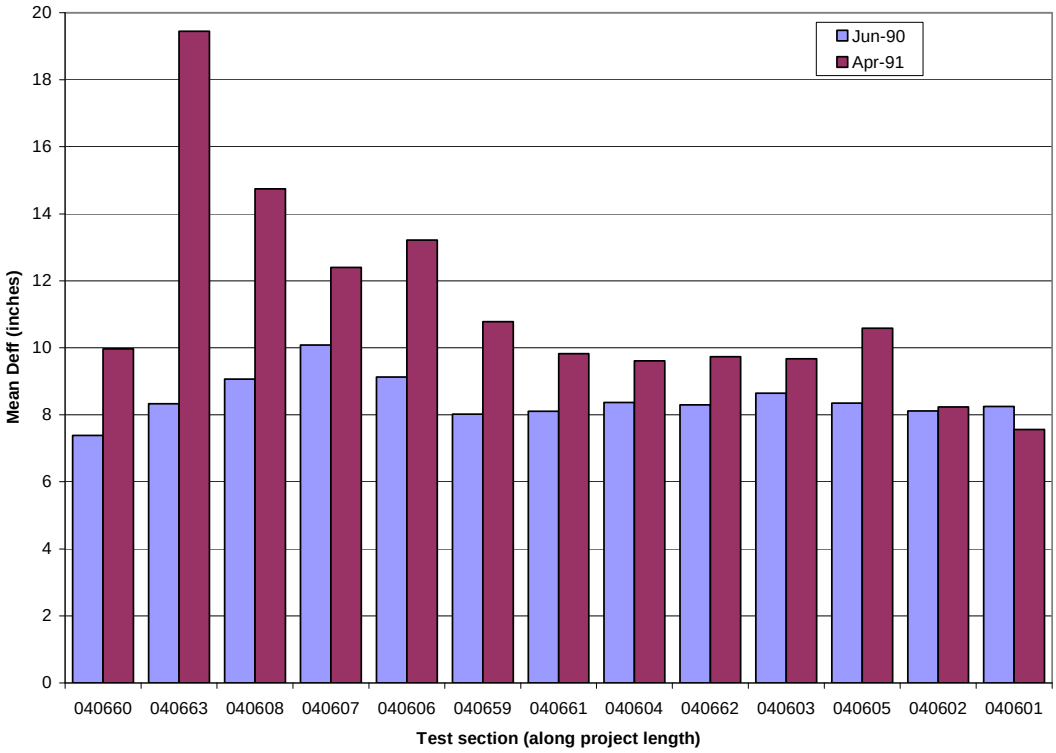

Figure 24. Effective Pavement Thickness Before and After Rehabilitation (Assuming 4.2 Million psi Modulus).

- Asphalt overlay of cracked and seated concrete pavement: The mean effective pavement thickness increased by 23 percent and 63 percent in Sections 040607 and 040608, respectively. Section 040607 received a 4.3 inch overlay and Section 040608 received an 8.4 inch overlay after cracking and seating of the concrete pavement. In Section 040659, in which a fabric was placed on the cracked and seated concrete prior to the overlay, mean effective pavement thickness increased 34 percent. In Sections 040661 and 040662, the two other cracked and seated sections tested in April 1991, both of which received a 4 inch overlay, similar increases in mean effective pavement thickness were observed (21 percent and 17 percent, respectively).
- Asphalt overlay of rubblized concrete pavement: In Section 040660, which received an 8 inch overlay after rubblizing of the existing concrete slab, the mean effective pavement thickness increased 35 percent.
- Unbonded concrete overlay of cracked and seated concrete pavement: In Section 040663, the initial result of cracking and seating, a 2 inch asphalt separation layer, and a 10 inch concrete overlay was a 133 percent increase in effective pavement thickness.

Table 8 lists the test sections in descending order of initial effect of rehabilitation treatment on effective pavement thickness. Not surprisingly, the two greatest increases were achieved by the two thickest overlays: the 10 inch concrete overlay over a 2 inch asphalt separator layer, and the 8 inch asphalt overlay after cracking and seating. Among the several test sections with asphalt overlays nominally 4 inches thick, the next greatest increase was achieved in section 040606 where the old concrete in the outer lane was completely removed and replaced prior to overlay. A 27 percent increase was achieved in Section 040605 simply by replacing the outer lane, with no overlay. This suggests that the additional effect of placing a nominal 4 inch overlay has an effective pavement thickness increase of about 18 percent. This is fairly consistent with the finding that in the two sections where a nominal 4 inch overlay was placed on the old concrete (040604 and 040603), the effective pavement thickness increases were 15 percent and 12 percent, respectively. Overlay thicknesses being roughly equal, crack and seat with fabric and rubblizing achieved greater increases than outer lane slab replacement, while crack and seat without fabric achieved lesser increases. Indeed, the effective pavement thickness increases achieved by cracking and seating and overlaying without fabric were only slightly better than those achieved by overlaying without either cracking and seating or even doing much repair.

Table 8. Initial Effects of Rehabilitation Treatment on Effective Pavement Thickness (Assuming 4.2 Million psi Modulus).

Treatment	Test Section ID	Increase in Effective Pavement Thickness (%)
10 inch unbonded concrete overlay	040663	133
8.4 inch asphalt over crack and seat	040608	63
4.3 inch asphalt over replaced outer lane	040606	45
8 inch asphalt over rubblized concrete	040660	35
4 inch asphalt and fabric over crack and seat	040659	34
No overlay; outer lane replaced	040605	27
4.3 inch asphalt over crack and seat	040607	23
4 inch asphalt over crack and seat	040661	21
4 inch asphalt over crack and seat	040662	17
4 inch asphalt with saw and seal	040604	15
4.5 inch asphalt with minimal repair	040603	12
No overlay; minimal repair	040602	2
Control section: no overlay; no repair	040601	-8

It is important to note that these results reflect only the initial effects of the rehabilitation treatments on effective thickness. These results are potentially interesting in comparison to the different initial construction costs of the different treatments. What is more interesting, however, in comparison to the life-cycle costs of the different treatments is the long-term ranking of the treatments' effects on deflection responses, which are examined in the next section of this report.

EFFECT OF REHABILITATION ON DEFLECTION RESPONSE OVER TIME

This section of the analysis examines the long-term effects of rehabilitation on the deflection response of the Arizona SPS-6 test sections. The deflection data sets in this analysis are all those contained in the LTPP database through October 2002. The occasions on which deflection testing was conducted are shown by test section in Table 9.

Table 9. Arizona SPS-6 Deflection Testing Dates.

	Deflection Testing Dates						
Test Section ID	June 1990	April 1991	Sept 1991	Sept 1994	Oct 1997	Oct 2000	Oct 2002
040601	≅	≅	≅				
040602	≅	≅	≅				
040603	≅	≅	≅	≅	≅	≅	≅
040604	≅	≅	≅	≅	≅	≅	≅
040605	≅	≅	≅				
040606	≅	≅	≅	≅	≅	≅	≅
040607	≅	≅	≅	≅	≅	≅	≅
040608	≅	≅	≅	≅	≅	≅	≅
040659	≅	≅	≅	≅	≅	≅	≅
040660	≅	≅	≅	≅	≅	≅	≅
040661	≅	≅	≅	≅	≅	≅	≅
040662	≅	≅	≅	≅	≅	≅	≅
040663	≅	≅	≅	≅	≅	≅	≅
040664			≅	≅	≅	≅	≅
040665			≅	≅	≅	≅	≅
040666			≅	≅	≅	≅	≅
040667			≅	≅		≅	≅
040668			≅	≅	≅	≅	≅
040669			≅	≅	≅	≅	≅

The long-term trends in deflection response are summarized for bare concrete pavement, asphalt overlay of intact concrete pavement, asphalt overlay of cracked and seated concrete pavement, asphalt overlay of rubblized concrete pavement, and unbonded concrete overlay of cracked and seated concrete pavement.

Bare Concrete Pavement

The test sections in this category are the control Section 040601 and the minimal and intensive restoration Sections 040602 and 040605, respectively. The outer traffic lane was replaced through the full length of Section 040605. Sections 040601 and 040602 were taken out-of-study in April 1992; Section 040605 was taken out-of-study in August 1993. It is not possible to say much about the long-

term deflection response trends of these sections since researchers obtained the last set of deflection measurements for these sections in September 1991.

Maximum Deflection

Figure 25 show the mean maximum deflections at the 9 kip loading level for the three bare concrete test sections. In September 1991 the deflections in Sections 040601 and 040602 were at nearly the same levels as in June 1990. In Section 040605, on the other hand, the mean maximum deflections in September 1991 were slightly higher than in April 1991, which may be due to seasonal variation in the foundation stiffness or simply a slight random variation.

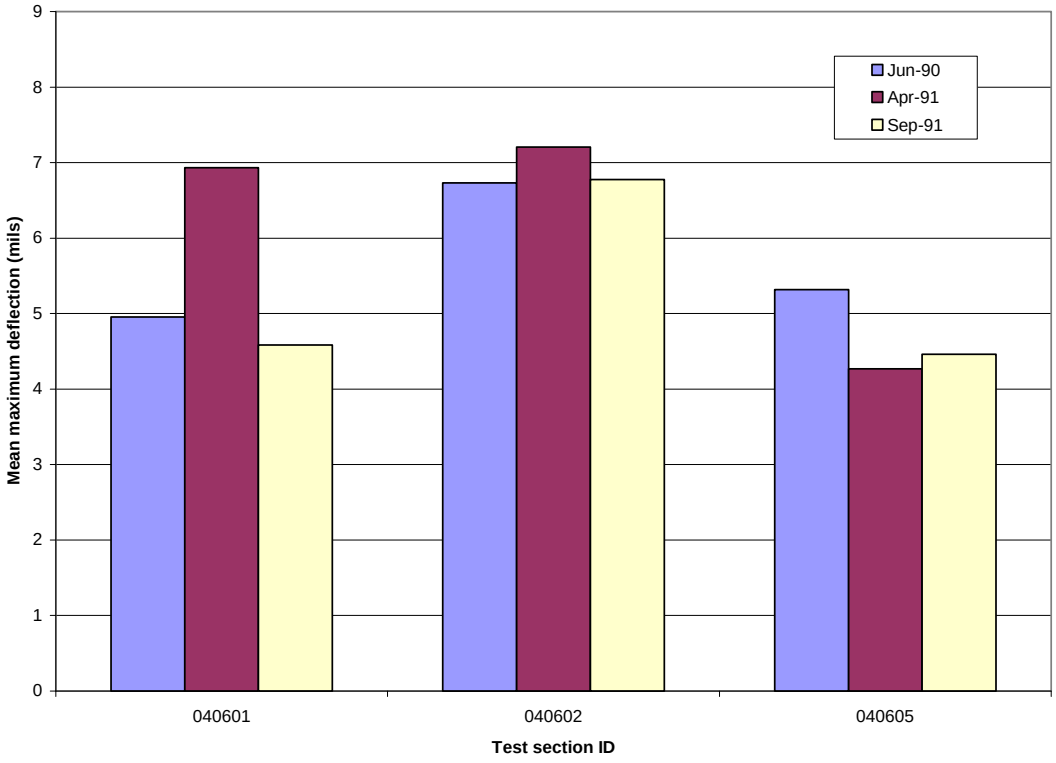

Figure 25. Mean Maximum Deflection Over Time in Bare Concrete Pavement Sections.

Effective Pavement Modulus

Figure 26 shows effective pavement modulus over time for three bare concrete test sections. As noted earlier, the effective pavement modulus decreased by 25 percent between June 1990 and April 1991 in Section 040601; increased by 8 percent in Section 040602, which received minimal repair; and increased by 118 percent in Section 040605, where the entire outer lane was replaced. Five months later, in September 1991, the effective pavement modulus was 20 percent higher than the April 1991 level in the Section 040601, 12 percent higher in Section 040602, and 79 percent higher in Section 040605.

Since there is no ready physical explanation for fluctuations of ±25 percent in the effective pavement modulus over a five-month period, variations of this magnitude from year to year are probably nothing more than random variation. In that context, the relative increases in effective pavement modulus seen in Section 040605 might not be statistically significant. Nonetheless, both the April 1991 and September 1991 results indicate an effective pavement modulus for the new concrete in Section 040605 (9.84 million psi and 8.10 million psi, respectively) that is considerably higher than would be expected in such young concrete. These results suggest that the concrete thickness in the replaced outer lane is greater than the as-constructed thickness (8.3 inches) of the old concrete that was replaced.

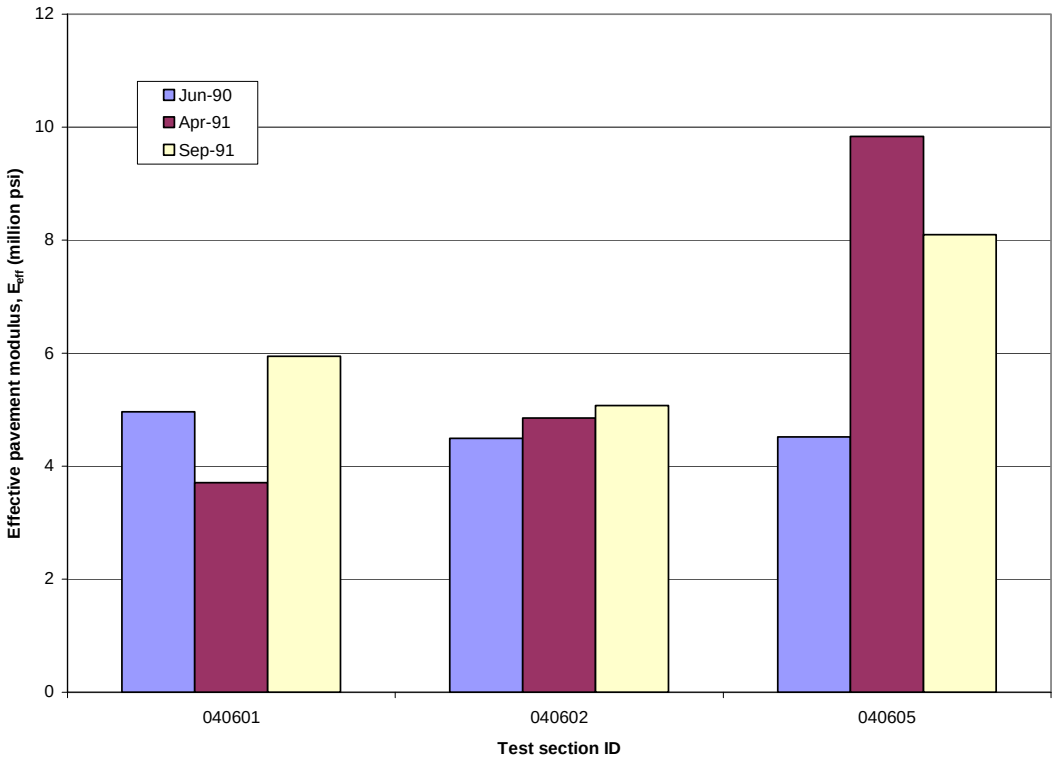

Figure 26. Effective Pavement Modulus Over Time in Bare Concrete Pavement Sections as a Function of Prerehabilitation As-Built Concrete Slab Thickness.

Effective Thickness of Pavement Structure

The mean effective thicknesses of the three bare concrete pavement sections, from the three sets of deflection data available, assuming a concrete modulus of 4.2 million psi, are shown in Figure 27. This comparison reinforces the notion that the pavement structures in Sections 040601 and 040602 were essentially unchanged, while the replacement of the outer lane in Section 040605 produced a notable improvement in the structure. The April 1991 data suggest a 27 percent increase in the effective thickness as a result of the outer lane replacement, and the data from five months later suggest that the effective thickness was 21 percent higher than before the replacement. The difference between the April and September 1991 results is probably not significant. Both results, however, reinforce the impression that the new concrete placed in the outer lane was significantly greater than 8.3 inches thick and/or had an elastic modulus significantly greater than 4.2 million psi within a year after placement.

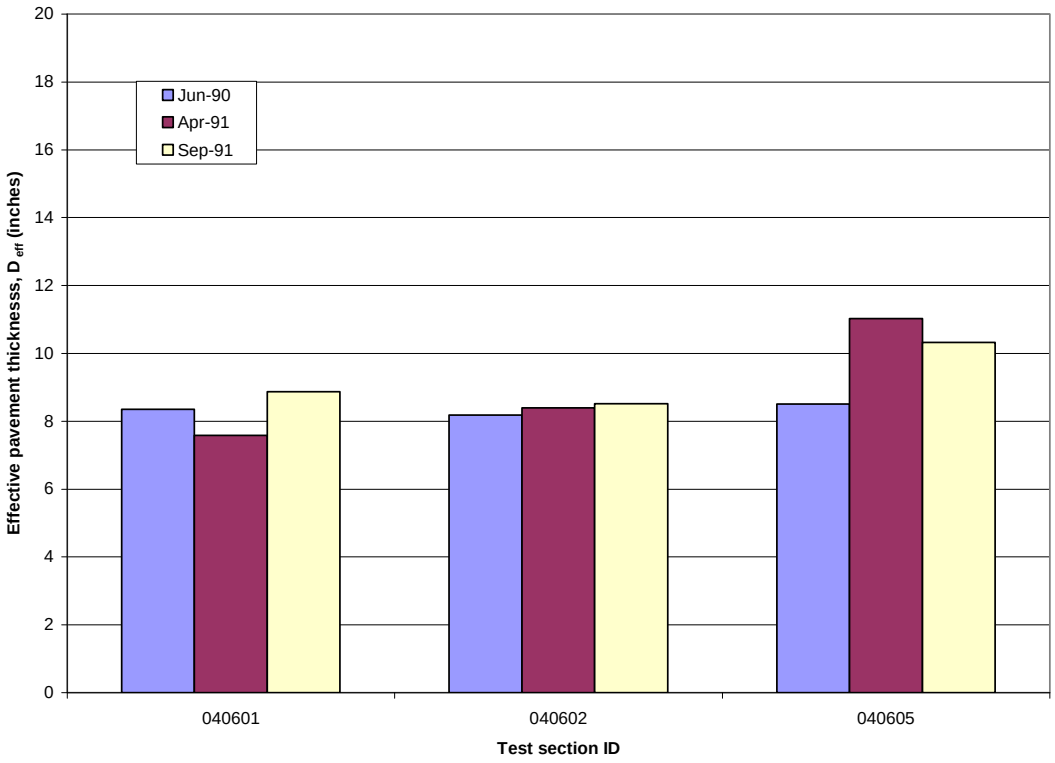

Figure 27. Effective Thickness Over Time in Bare Concrete Pavement Sections (Assuming 4.2 Million psi Modulus).

Given the poor condition of the original pavement, it is not too surprising that Sections 040601 and 040602 were taken out of service so soon after the start of the experiment. The outer lane of Section 040605, on the other hand, appears to have had its structural capacity substantially increased by the lane replacement.

Asphalt Overlay of Intact Concrete Pavement

The test sections in this category are Sections 040603 (4.5 inch asphalt overlay with minimal repair), 040604 (4 inch asphalt overlay with saw and seal), 040606 (4.3 inch asphalt overlay over replaced outer lane), 040664 (6 inch asphalt overlay), and 040668 (6 inch asphalt overlay).

Maximum Deflection

Figure 28 shows the mean maximum deflections at the 9 kip loading level for the asphalt-overlaid concrete sections. No deflections were measured in Sections 040664 or 040668 before September 1991, so pretreatment versus long-term deflection comparisons are not possible for these sections.

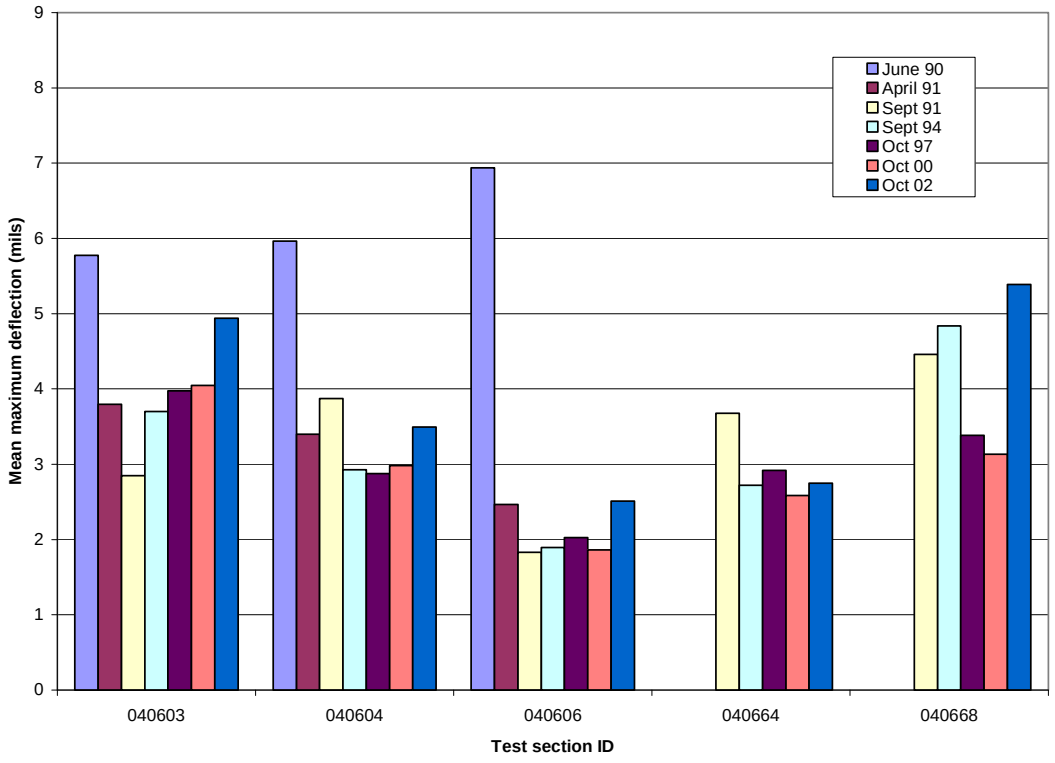

Figure 28. Mean Maximum Deflection Over Time in Asphalt-Overlaid Concrete Sections.

For the three asphalt-overlaid concrete sections for which pretreatment deflections are available, the mean maximum deflection plot illustrates that the deflection reductions were achieved by the overlay treatments. Among the three sections, the most dramatic deflection reductions occurred in Section 040606, where the concrete in the outer traffic lane was replaced before the asphalt overlay was placed. Deflections in all three sections have remained fairly consistent in the 12 years since.

Although deflection reduction due to overlay can't be assessed in Sections 040664 and 040668 (both 6 inch overlays of the existing concrete), post-overlay deflections are at levels comparable to the other

three sections. In Section 040664, the deflections have remained fairly consistent, while in Section 040668, the deflections have been more variable. In both cases, the deflection magnitudes are comparable to those in Sections 040603 and 040604 (4.5 inch and 4 inch overlays of the existing concrete, respectively), and higher than those in Section 040606 (4.3 inch overlay of replaced concrete). It is rather surprising that maximum deflections are no lower in the sections with 6 inch overlays (040664 and 040668) than in the sections with 4 inch and 4.5 inch overlays (040603 and 040604, respectively).

Effective Pavement Modulus

Figure 29 shows the effective pavement modulus over time for the three asphalt-overlaid concrete test sections. This plot illustrates, more clearly than the maximum deflection plot, the relative structural capacity improvements achieved by these different overlay treatments.

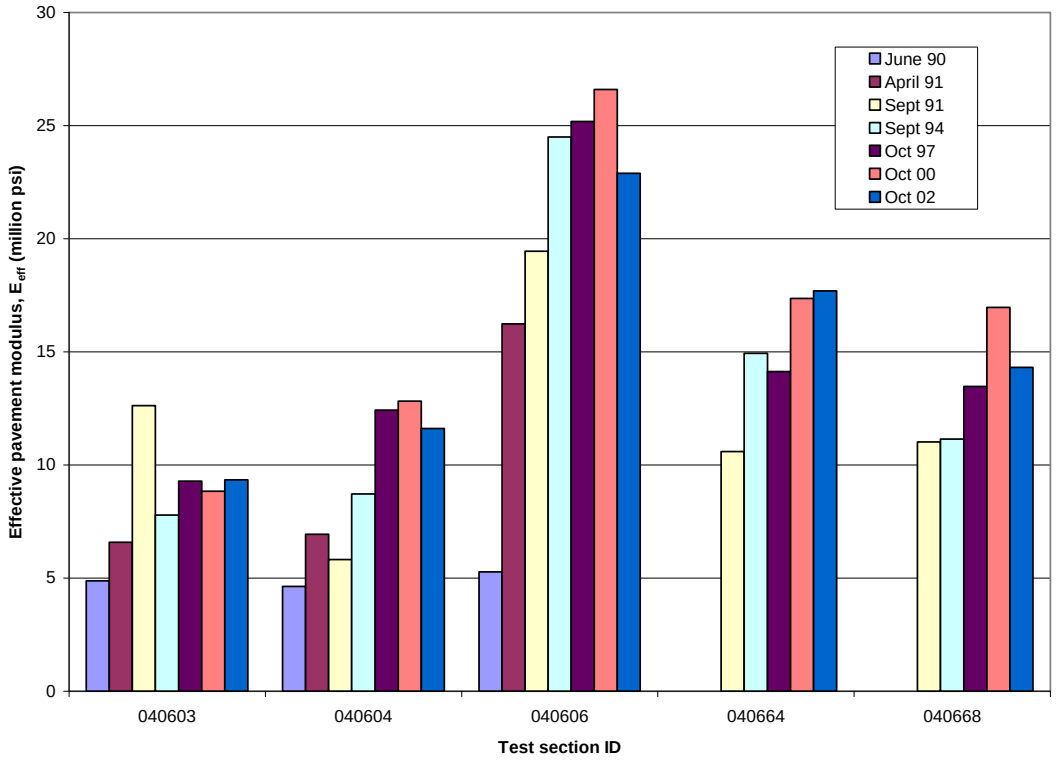

Figure 29. Effective Pavement Modulus Over Time in Asphalt-Overlaid Concrete Pavement Sections as a Function of Prerehabilitation As-Built Concrete Slab Thickness.

Twelve years after the rehabilitation, Section 040606 (4.3 inch overlay of the replaced concrete) remains the section with the highest effective pavement modulus, followed by Sections 040664 and 040668 (6 inch asphalt overlays of the original concrete), which are then followed by Section 040603 (4.5 inch overlay of the original concrete) and Section 040604 (4 inch overlay of the original concrete).

Effective Thickness of Pavement Structure

The effective pavement thickness over time is shown for the three asphalt-overlaid concrete test sections in Figure 30. This plot also illustrates the relative structural capacity improvements achieved by these different overlay treatments. The greatest effective thickness corresponds to Section 040606 (4.5 inch overlay over replaced concrete). Sections 040664 and 040668 (6 inch asphalt overlay) have the next largest effective thicknesses, and Sections 040603 and 040604 (4.5 inch and 4 inch overlays, respectively) have lesser effective thicknesses. In each case, the effective thicknesses have remained fairly consistent between the years 1994 and 2002.

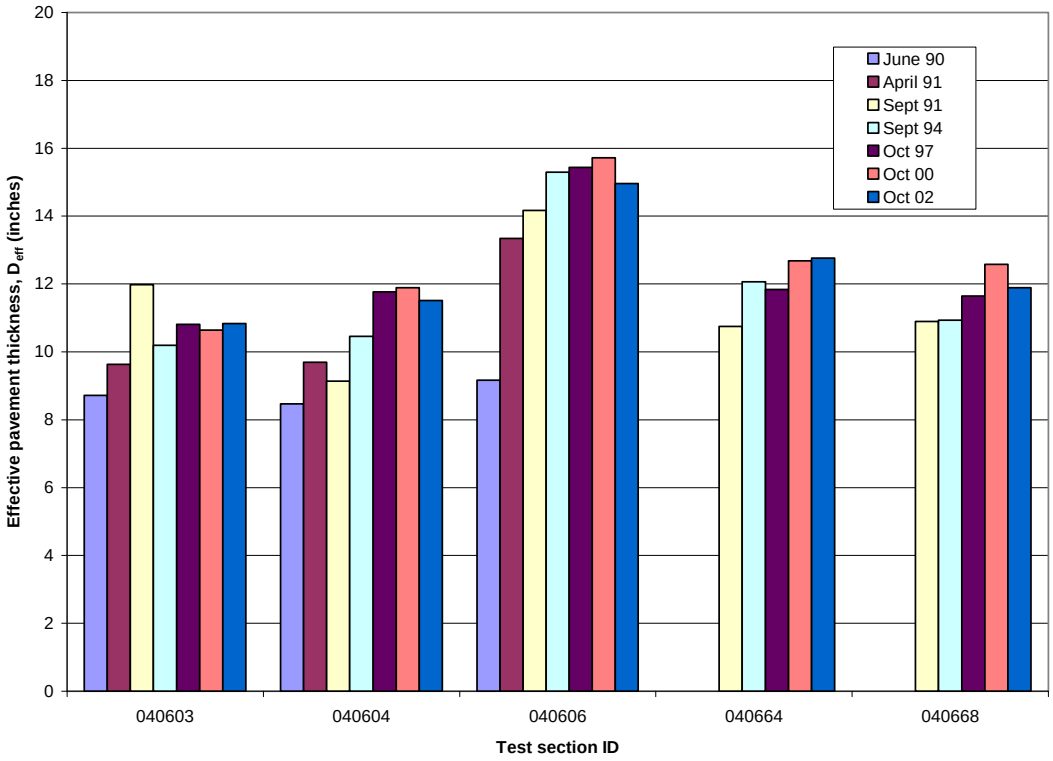

Figure 30. Effective Thickness Over Time in Bare Concrete Pavement Sections (Assuming 4.2 Million psi Modulus).

Asphalt Overlay of Cracked and Seated Concrete Pavement

The following test sections were overlaid with asphalt after cracking and seating of the original concrete pavement: 040607 (4.3 inch overlay), 040608 (8.4 inch overlay), 040659 (fabric and 4 inch overlay), 040661 (4 inch overlay), 040662 (4 inch overlay and subdrains), 040665 (5.5 inch overlay and subdrains), 040666 (5.5 inch overlay and subdrains), and 040667 (5.5 inch overlay and subdrains). Friction courses are not included in the overlay thicknesses listed here, and the sections with 5.5 inch overlays presumably differ in the cracking pattern employed.

Maximum Deflection

Figure 31 shows the mean maximum deflections at the 9 kip loading level for the sections with asphalt overlays of cracked and seated concrete. No deflections were measured in Sections 040665, 040666, or 040667 before September 1991, so pretreatment versus long-term deflection comparisons are not possible for these sections.

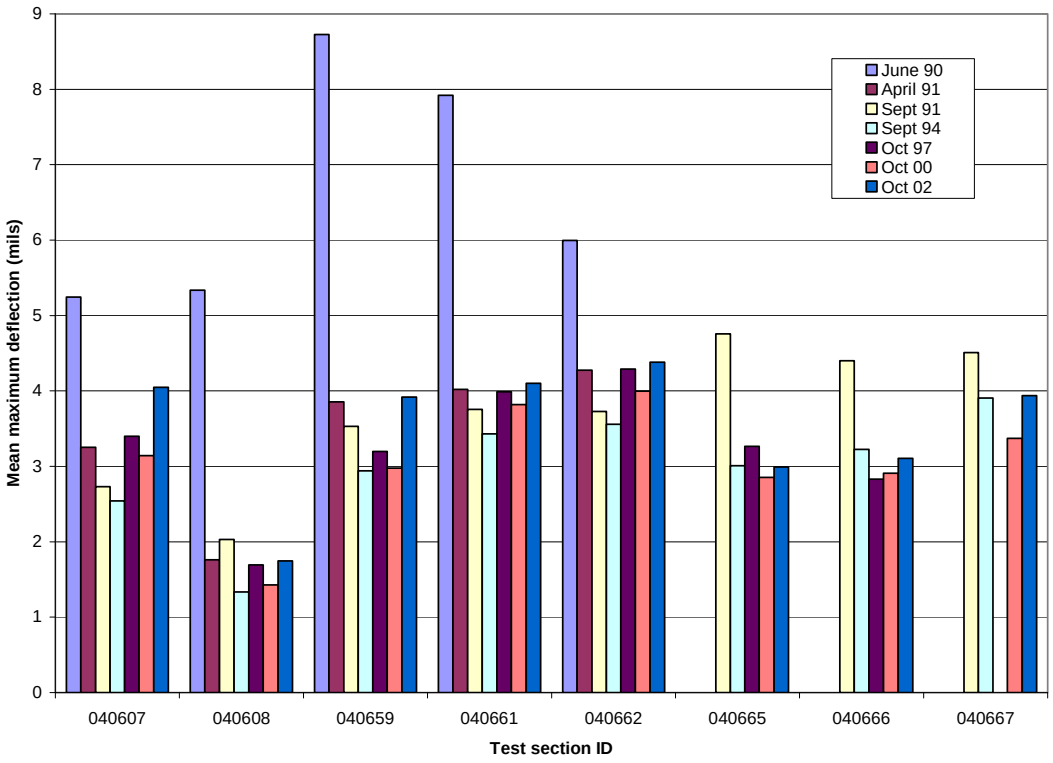

Figure 31. Mean Maximum Deflection Over Time in Crack and Seat Sections.

The 4.3 inch overlay in Section 040607 reduced deflections by about 40 percent, although in the last five years of monitoring, the deflections appear to have been increasing again. The 8.4 inch overlay in Section 040608 reduced deflections by about 66 percent, and the deflections in subsequent years have so far remained steadier.

Section 040659, where a fabric was placed on the cracked and seated concrete before placing the 4 inch overlay, had the highest mean maximum deflection among the sections with pretreatment data available, but the rehabilitation brought deflections down about 50 percent, to about the same level as in Section 040607. The post-overlay deflections in Sections 040661 and 040662 are similar, which suggests that for these sections, the magnitude of deflections after overlay depended more on the thickness of the overlay than on the magnitude of deflections before the overlay.

The plot in Figure 31 shows that in Sections 040665 and 040666, the mean maximum deflections were considerably higher in September 1991 than in subsequent years (during which deflections have remained fairly steady). In Section 040667, the September 1991 deflections were also somewhat higher than the 1994 deflections, but not to the degree seen in Sections 040665 and 040666. This decline in deflections soon after placement of an asphalt overlay, when traffic is still compacting the mix and volatile compounds are still evaporating, is not that uncommon, and is in fact a reason not to read too much into deflections measured soon after asphalt overlay placement. However, if this is the reason that the September 1991 deflections are higher than later deflections in these three sections, it would suggest something different about the AC mix in these sections than in the other sections in this group.

Figure 31 also shows that since 1994, mean maximum deflections have been lower in Sections 040665 and 040666 than in 040667. Given that all three sections had retrofit subdrains and the same overlay thickness, the difference may be due either to differences in foundation stiffness or differences in slab stiffness as a result of different cracking patterns.

Effective Pavement Modulus

Figure 32 shows the effective pavement modulus over time for the crack and seat sections. This plot shows the dramatic difference in structural improvement achieved by Section 040608 (the 8.4 inch overlay) versus the 4 inch and even the 5.5 inch overlays in the other test sections. The effective modulus has since declined somewhat in this section, but even 12 years after the rehabilitation, is still considerably greater than in the other crack and seat sections. The next highest effective pavement modulus levels over time have been in Section 040607 (the 4.3 inch overlay) and 040665 (one of the 6 inch overlays). The remaining 4- and 5.5 inch overlay sections have exhibited similar effective pavement modulus levels. However, the effective pavement modulus levels in the 5.5 inch overlay sections do seem to have increased during the time period monitored.

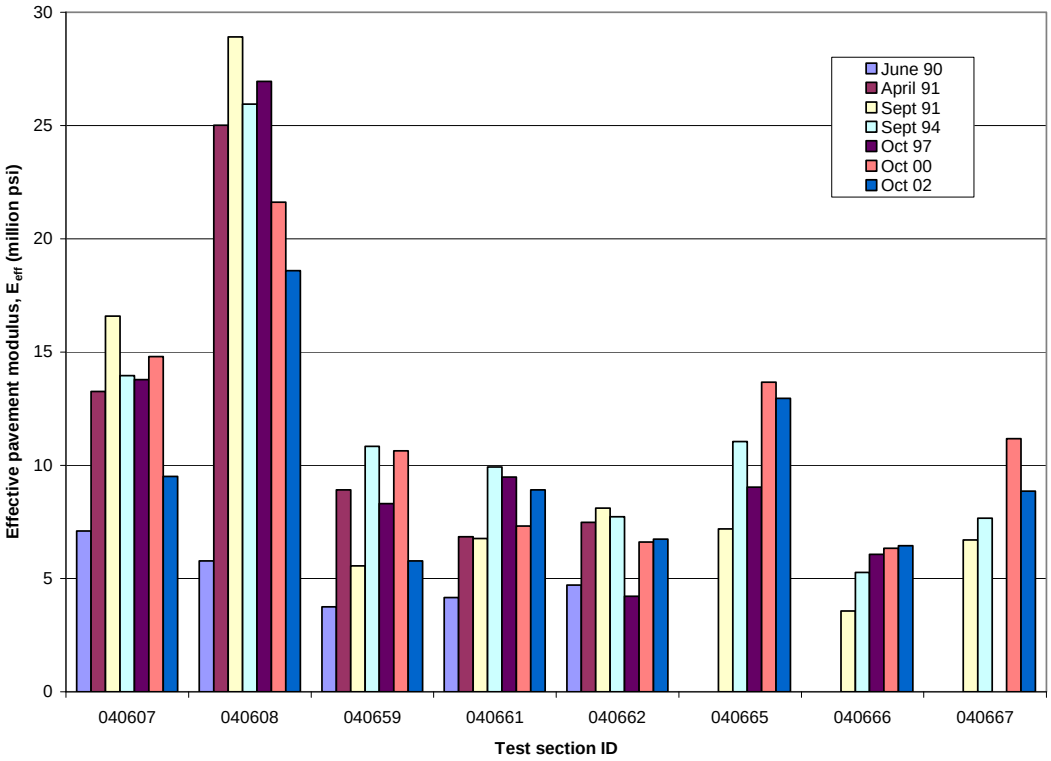

Figure 32. Effective Pavement Modulus Over Time for Crack and Seat Sections as a Function of Prerehabilitation As-Built Concrete Slab Thickness.

Effective Thickness of Pavement Structure

Figure 33 shows the effective thickness over time for the crack and seat sections. This plot illustrates, like the effective modulus plot, the greater structural improvement achieved by the 8.4 inch overlay compared to the overlays in the other test sections. Surprisingly, the effective pavement thicknesses are not, in general, higher in the 5.5 inch overlay sections than in the 4 inch overlay sections. They do, however, seem to be increasing over time in these sections.

Asphalt Overlay of Rubblized Concrete Pavement

This category has two sections: Section 040660 received an 8 inch asphalt overlay and Section 040669 received a 5 inch asphalt overlay after the original concrete was rubblized in each section.

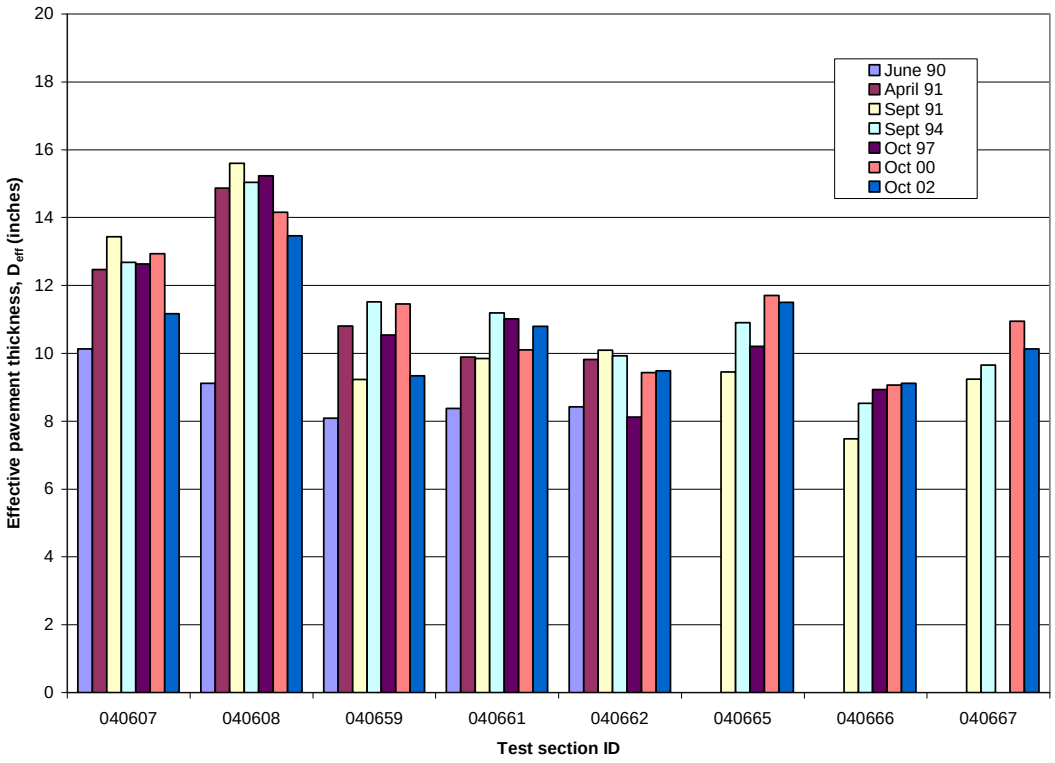

Figure 33. Effective Thickness Over Time for Crack and Seat Sections (Assuming 4.2 Million psi Modulus).

Maximum Deflection

Figure 34 shows the mean maximum deflections over time in the two rubblized sections. Pretreatment deflection measurements are only available for Section 040660. The plot illustrates the substantial reduction in mean maximum deflection—about 50 percent—achieved by the 8 inch overlay, even after rubblizing of the original concrete.

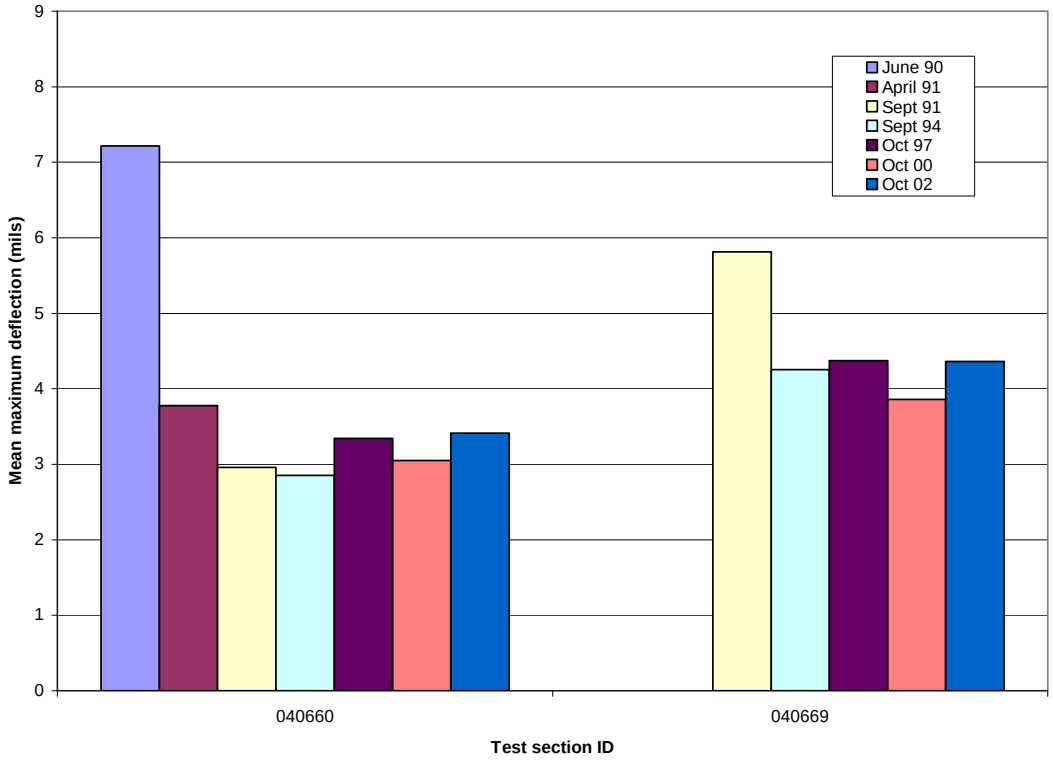

Figure 34. Mean Maximum Deflection Over Time in Rubblized Sections.

In Section 040669, like the nearby crack and seat sections, the September 1991 deflections were higher than in subsequent years. In both of the rubblized test sections, the mean maximum deflections have held fairly steady since 1994. The effect of the thicker overlay in Section 040660 is illustrated by its lower mean maximum deflection levels.

Effective Pavement Modulus

Figure 35 shows the effective pavement modulus values over time for the two rubblized sections. This chart is plotted with the same vertical scale as in Figure 32 to illustrate the lower levels of effective modulus obtained for the rubblized sections compared to the crack and seat sections. However, the effective pavement moduli in both rubblized test sections do appear to have increased over time.

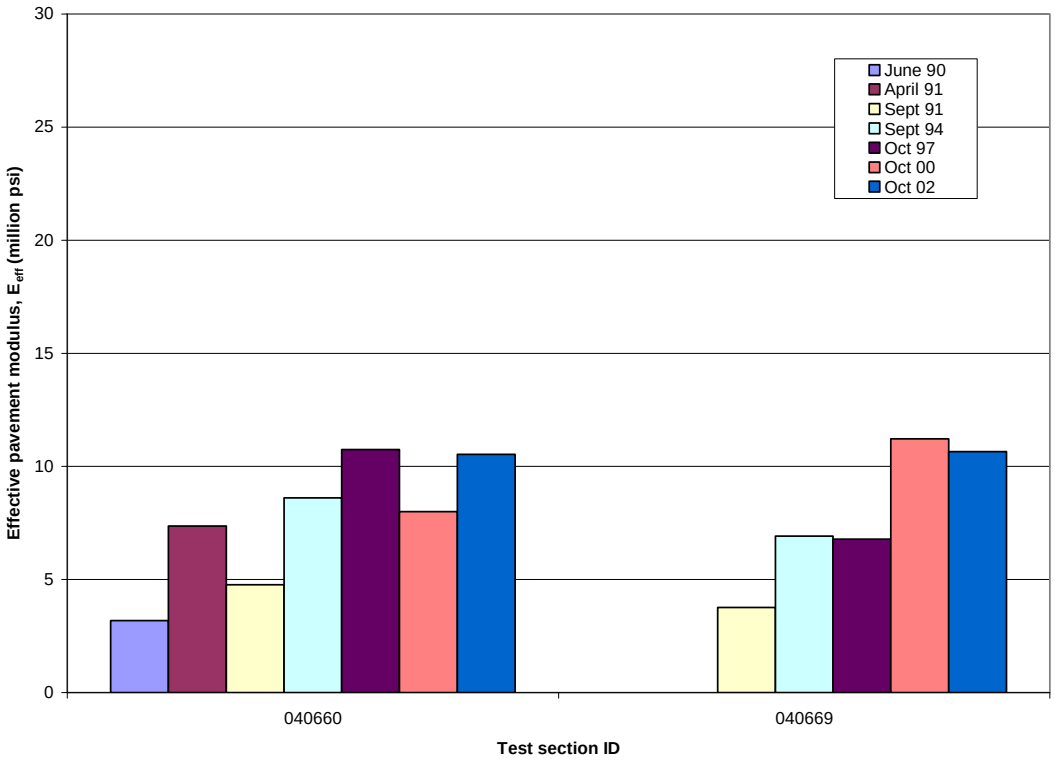

Figure 35. Effective Pavement Modulus Over Time in Rubblized Sections as a Function of Prerehabilitation As-Built Concrete Slab Thickness.

Effective Thickness of Pavement Structure

Figure 36 shows the effective thickness values over time for the two rubblized sections. These are plotted with the same vertical scale as in Figure 33 to illustrate the smaller increases in effective thickness achieved by rubblizing plus overlay compared to crack and seat plus overlay. However, the effective thicknesses do appear to have increased over time.

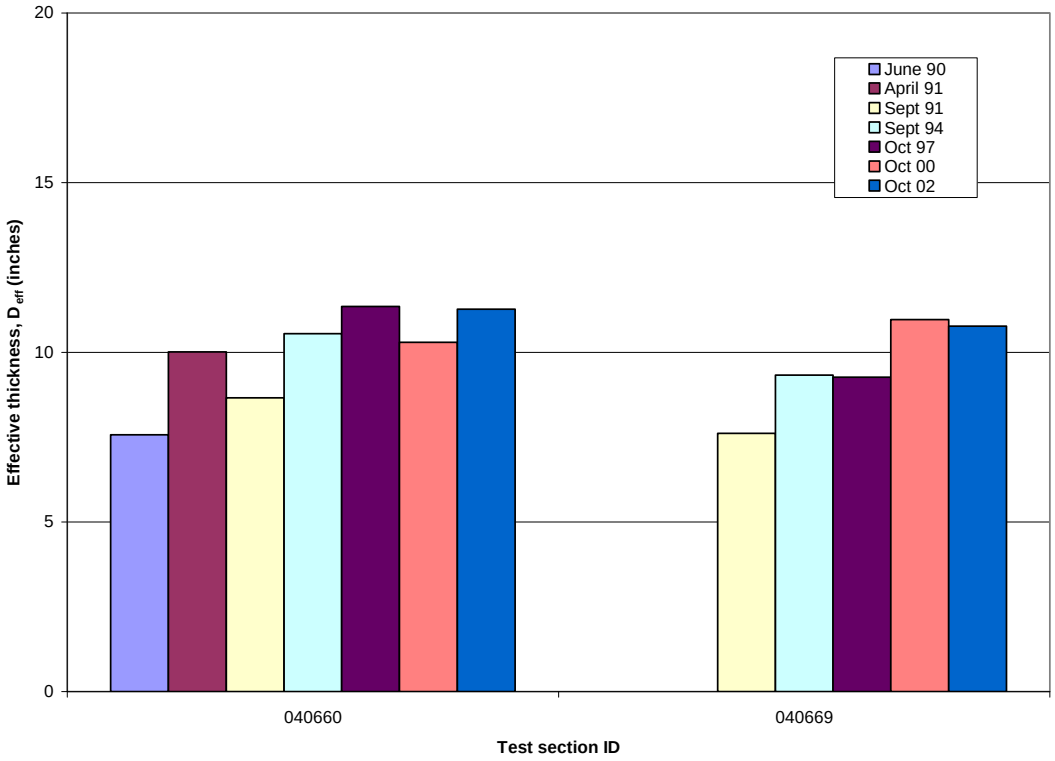

Figure 36. Effective Thickness of Rubblized Sections (Assuming 4.2 Million psi Modulus).

Unbonded Concrete Overlay of Cracked and Seated Concrete Pavement

This category has one section: 040663. Its structure consists of a 10 inch unbonded concrete overlay and 2 inch AC interlayer over the cracked and seated original concrete.

Maximum Deflection

The mean maximum deflections over time in the unbonded overlay section are plotted in Figure 37. The deflections were dramatically reduced by the rehabilitation, although mean maximum deflection appears to have increased slightly in recent years.

Effective Pavement Modulus

Figure 38 shows the section's effective pavement modulus over time. This plot illustrates the dramatic structural improvement achieved by the rehabilitation, although there has been some decrease in the effective pavement modulus in recent years.

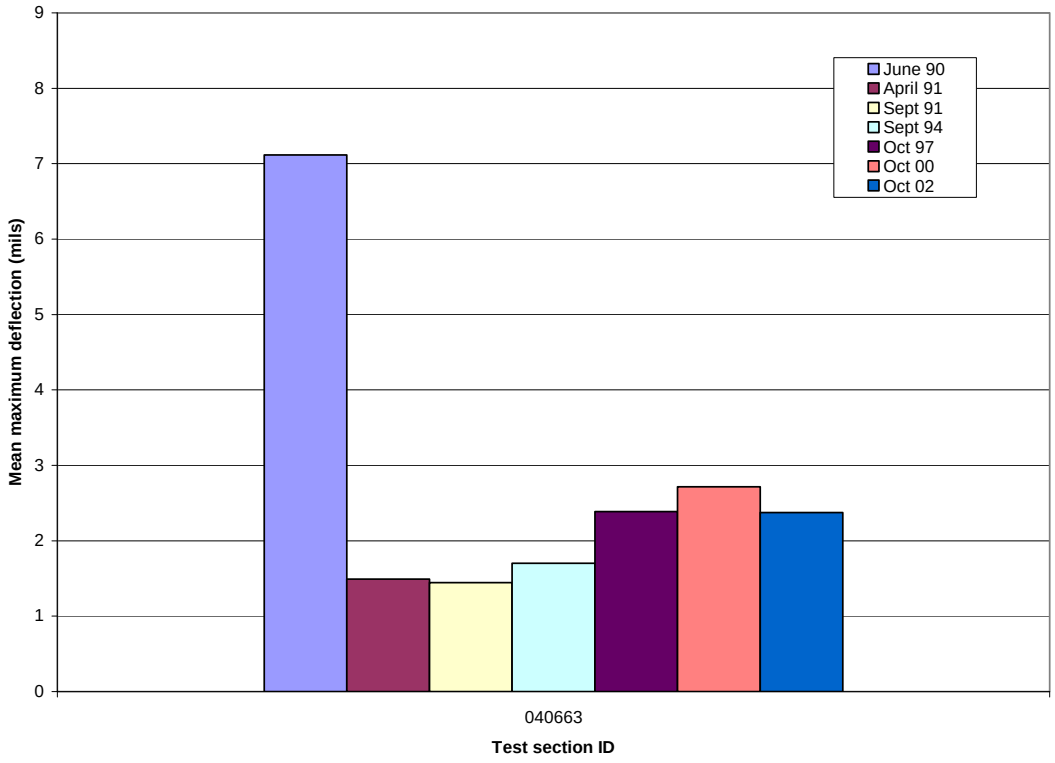

Figure 37. Mean Maximum Deflection Over Time in Unbonded Overlay Section.

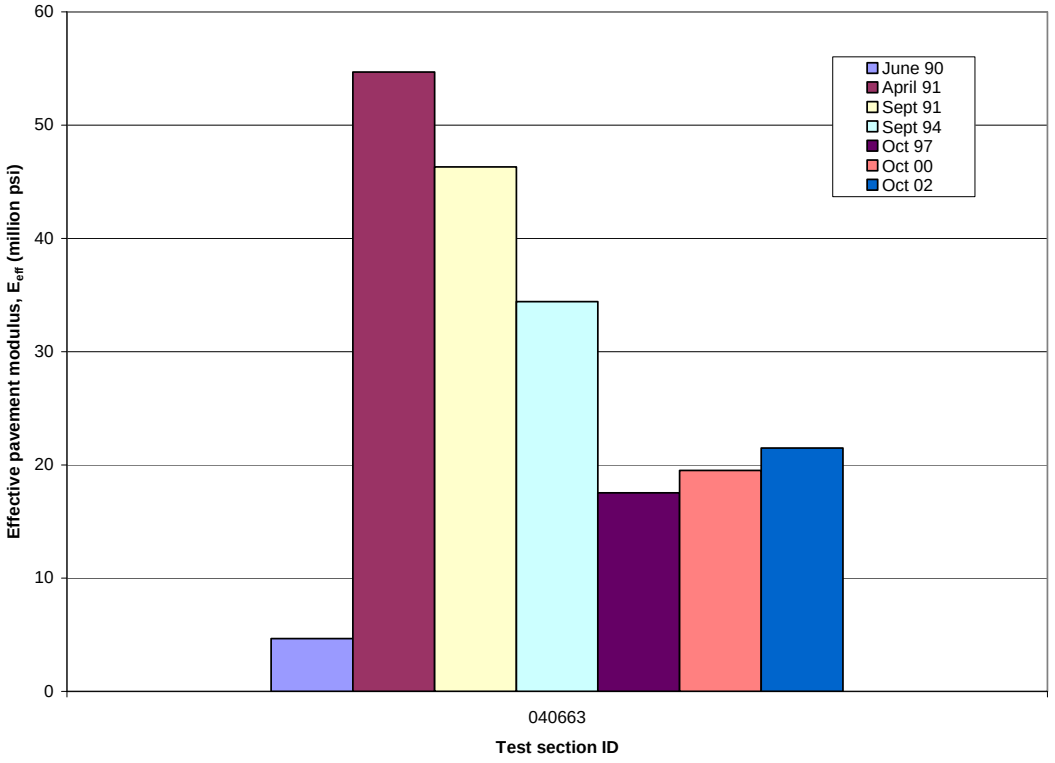

Figure 38. Effective Pavement Modulus Over Time in Unbonded Overlay Section as a Function of Prerehabilitation As-Built Concrete Slab Thickness.

Effective Thickness of Pavement Structure

Figure 39 shows the effective pavement thickness over time for the unbonded overlay section. The rehabilitation more than doubled the effective thickness of the pavement structure, and while there has been some decrease in the effective pavement thickness in recent years, after 12 years it is still almost twice the effective thickness of the pavement prior to rehabilitation.

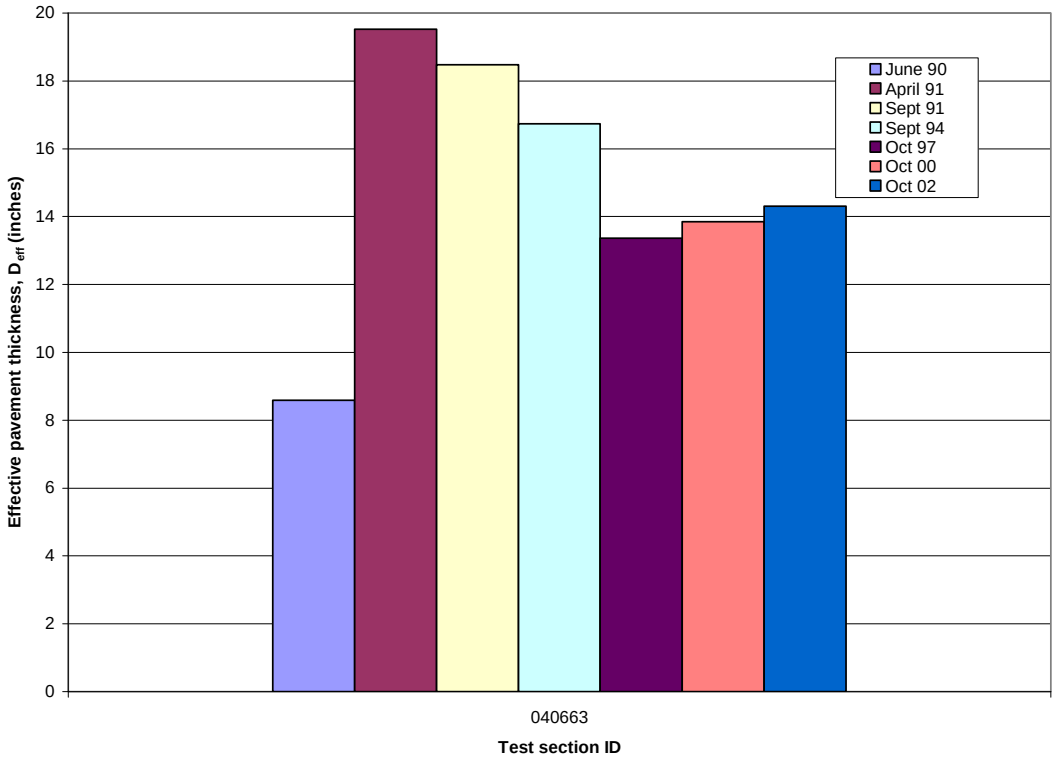

Figure 39. Effective Pavement Thickness Over Time in Unbonded Overlay Section (Assuming 4.2 Million psi Modulus).

SUMMARY OF ANALYSIS OF LONG-TERM DEFLECTION RESPONSE TRENDS

The initial effects of the rehabilitation treatments, in terms of percentage increase in the effective pavement thickness, were summarized in Table 8. This assessment was only possible for sections with pretreatment deflection data. For 10 of these 13 sections, the long-term percent increase in effective pavement thickness can be quantified by directly comparing the pretreatment data to the latest available values (October 2002). Table 10 lists the percent change in effective pavement thickness in decreasing order. Sections 040601, 040602, and 040605 are listed in Table 8 but not in Table 10 because all were removed from the experiment only a few years after it began. For the six sections without pretreatment deflection data available, an indirect comparison was made using the pretreatment (June 1990) average effective thickness of the other 13 sections (8.59 inches).

Another way to compare the long-term deflection response of the sections is in terms of the absolute value of the October 2002 effective pavement thickness. This comparison is possible for all but the three bare concrete sections that were removed from the study long before October 2002. Comparing the sections with respect to absolute values of effective pavement thickness could be construed as not entirely fair since, as has already been shown, the sections weren't all of equal effective thickness before the experiment began. Nonetheless, such a comparison does indicate the relative structural capacities of the pavement sections at the end of the experiment, although the differences among those structural capacities are not necessarily due to the different rehabilitation treatments applied. Table 11 lists the 16 sections in order of decreasing effective pavement thickness in October 2002.

The rehabilitation treatments in Tables 10 and 11 are color-coded for ease of comparison. The two treatments that were clearly most successful in increasing the effective pavement thickness over the long term were the 10 inch unbonded concrete overlay (Section 040663) and the 4.3 inch asphalt overlay of the replaced concrete in the outer traffic lane (Section 040606). The next most effective treatment was the 8.4-inch asphalt overlay of the cracked and seated slab (Section 040608). The 8-inch asphalt overlay of rubblized concrete (Section 040660) actually achieved a slightly greater percent increase in effective pavement thickness than the 8.4 inch asphalt over crack and seat, but its effectiveness in terms of the absolute value of pavement thickness in 2002 was considerably lower. The 5.5 inch asphalt overlay of rubblized concrete (Section 040669) ranked lower than its 8 inch counterpart (Section 040660) both in percent increase and in absolute value of effective pavement thickness. However, the 5.5 inch overlay of rubblized concrete ranked lower than the sections with 5.5-inch overlays of intact concrete, but higher than some of the sections with 5.5-inch overlays of cracked and seated concrete.

The asphalt overlays of intact concrete, color-coded in orange, occupy much of the middle of the ranking in both tables. These overlays ranged from 4 to 5.5 inches thick, and one section (040604) included sawing and sealing of transverse joints. Among these four sections, the 4.5 inch overlay with minimal repair (Section 040603) was less effective in improving pavement thickness than were the two 5.5 inch overlays (Sections 040664 and 040668) and the 4-inch overlay with saw and seal (Section 040604). This latter difference may have less to do with the sawing and sealing of joints in the overlay than with the quantities of unrepaired distress in the different sections prior to overlay.

Table 10. Long-Term Effect of Rehabilitation Treatment in Terms of Percent Increase in Effective Pavement Thickness (D_{eff}) (Assuming 4.2 Million psi Modulus).

Treatment	Test Section ID	Percent Increase in D_{eff} (%)
10 inch unbonded concrete overlay	040663	66
4.3 inch asphalt over replaced outer lane	040606	63
8 inch asphalt over rubblized concrete	040660	49
8.4 inch asphalt over crack and seat	040608	48
5.5 inch asphalt overlay	040664[1]	48
5.5 inch asphalt overlay	040668[1]	38
4 inch asphalt with saw and seal	040604	36
5.5 inch asphalt over crack and seat	040665[1]	34
4 inch asphalt over crack and seat	040661	29
5.5 inch asphalt over rubblized concrete	040669[1]	25
4.5 inch asphalt with minimal repair	040603	24
5.5 inch asphalt over crack and seat	040667[1]	18
4 inch asphalt, fabric over crack and seat	040659	15
4 inch asphalt over crack and seat	040662	12
4.3 inch asphalt over crack and seat	040607	10
5.5 inch asphalt over rubblized concrete	040666[1]	6

[1]No pretreatment deflection data available. Comparisons for these sections were made using the average pretreatment effective thickness of the other 13 sections.

Table 11. Long-Term Effect of Rehabilitation Treatment on Absolute Value of Effective Pavement Thickness (D_{eff}) (Assuming 4.2 Million psi Modulus).

Treatment	Test Section ID	October 2002 D_{eff} (inches)
4.3 inch asphalt over replaced outer lane	040606	14.96
10 inch unbonded concrete overlay	040663	14.30
8.4 inch asphalt over crack and seat	040608	13.47
5.5 inch asphalt overlay	040664	12.76
5.5 inch asphalt overlay	040668	11.89
4 inch asphalt with saw and seal	040604	11.51
5.5 inch asphalt over crack and seat	040665	11.50
8 inch asphalt over rubblized concrete	040660	11.27
4.3 inch asphalt over crack and seat	040607	11.16
4.5 inch asphalt with minimal repair	040603	10.84
4 inch asphalt over crack and seat	040661	10.79
5.5 inch asphalt over rubblized concrete	040669	10.78
5.5 inch asphalt over crack and seat	040667	10.13
4 inch asphalt over crack and seat	040662	9.48
4 inch asphalt, fabric over crack and seat	040659	9.34
5.5 inch asphalt over rubblized concrete	040666	9.11

Occupying much of the lower tier in both rankings are the overlays, ranging in thickness from 4 to 5.5 inches, of cracked and seated slabs. Among these, however, there are some notable differences. For example, Sections 040665, 040667, and 040666 all received 5.5 inch overlays, but the long-term percent increase in effective pavement thickness was 34 percent in 040665, 18 percent in 040667, and only 6 percent in 040666. The three sections are ranked in the same order, and in roughly the same positions in the overall rankings, in terms of the absolute value of effective pavement thickness in October 2002. All other things presumably being equal, these differences are probably due to differences in the slab cracking patterns used.

In summary, the most effective rehabilitation treatments, in terms of long-term increase in effective pavement thickness, were the 4.3 inch asphalt overlay of the replaced outer lane concrete, the 10 inch unbonded concrete overlay of the cracked and seated concrete, and the 8.4 inch asphalt overlay of the cracked and seated concrete. After these three, the most effective treatments, in terms of long-term increase in effective pavement thickness, were the 4 to 5.5 inch asphalt overlays of intact concrete slabs. The 4 to 5.5 inch overlays of cracked and seated or rubblized slabs were less effective. Differences in slab cracking patterns may be responsible for some of the variances in effectiveness among the crack and seat sections of comparable overlay thickness.

CHAPTER 3. SPS-6 DISTRESS ANALYSIS

This chapter describes analyses and results from evaluating distress data collected on the Arizona SPS-6 project using LTPP manual survey techniques. Surface distress provides powerful information regarding the nature and extent of pavement deterioration, which can be used to quantify performance trends as well as to investigate the contribution of design features on service life.

All 19 of the SPS-6 test sections were constructed consecutively and exposed to the same traffic loading, climate, and subgrade conditions, allowing for direct comparisons between layer configurations and design features without confounding effects introduced by different in situ conditions.

Of 19 test sections, 15 received AC overlays, three received no overlay and remained with the existing PCC surface, and one unique case consisted of a 10 inch unbonded concrete overlay (with a 2 inch AC bond breaker). Because distress types vary between the AC and PCC sections, researchers performed distress analyses and made comparisons within each surface type.

AC DISTRESS TYPES

The following distress types lead to deterioration in asphalt surfaces (Huang 1993):

- Fatigue cracking: A series of interconnecting cracks caused by repeated traffic loading. Cracking initiates at the bottom of the asphalt layer where tensile stress is the highest under the wheel load. With repeated loading, the cracks propagate to the surface.
- Longitudinal wheelpath cracking: Cracking parallel to the centerline occurring in the wheelpath. This cracking can be the early stages of fatigue cracking or can initiate from construction-related issues such as paving seams and segregation of the mix during paving. In the latter case, cracking is typically very straight (no meandering).
- Longitudinal non-wheelpath cracking: Cracking parallel to the centerline occurring outside the wheelpath. This cracking is not load-related and can initiate from paving seams or where segregation issues occurred during paving. Cracking can also be caused by tensile forces experienced during temperature changes. Pavements with oxidized or hardened asphalt are more prone to this type of cracking.
- Transverse cracking: Cracking that is predominantly perpendicular to the pavement centerline. Cracking starts from tensile forces experienced during temperature changes. Pavements with oxidized or hardened asphalt are more prone to this type of cracking.
- Block cracking: Cracking that forms a block pattern and divides the surface into approximately rectangular pieces. Cracking initiates from tensile forces experienced during temperature changes. This distress type indicates that the AC has significantly oxidized or hardened.

- Raveling: Wearing away of the surface caused by dislodging of aggregate particles and loss of asphalt binder. Raveling is caused by moisture stripping and asphalt hardening.
- Bleeding: Excessive bituminous binder on the surface that can lead to loss of surface texture or a shiny, glass-like, reflective surface. Bleeding is a result of high asphalt content or low air void content in the mix.
- Rutting: A surface depression in the wheelpaths. Rutting can result from consolidation or lateral movement of material due to traffic loads. It can also signify plastic movement of the asphalt mix because of inadequate compaction, excessive asphalt, or a binder that is too soft given the climatic conditions.

Table 12 provides a summary of flexible pavement distress types and their associated failure mechanisms.

Table 12. Flexible Pavement Distress Types and Failure Mechanisms.

Distress Type	Failure Mechanism	
	Traffic/Load Related	Climate/Materials Related
Fatigue cracking	X	
Longitudinal wheelpath cracking	X	
Longitudinal non-wheelpath cracking		X
Transverse cracking		X
Block cracking		X
Raveling		X
Bleeding		X
Rutting	X	X

PCC DISTRESS TYPES

The following distress types lead to deterioration in concrete surfaces:

- Corner break: A crack that intersects the joint at a distance less than 6 ft (1.8 m) on either side measured from the corner of the slab. Load repetitions combined with the loss of support, poor load transfer across the joint, and thermal curling and moisture warping stresses usually cause corner breaks.
- Durability or “D” cracking: A series of closely spaced, crescent-shaped hairline cracks that appear at the concrete surface adjacent to and roughly parallel to joints, cracks, and slab edges. D cracking is caused by freeze-thaw expansive pressures of certain types of coarse aggregates. The fine surface cracks contain calcium hydroxide residue, which causes a dark coloring of the crack in the immediate surrounding area.
- Faulting of transverse joints and cracks: A difference of elevation across a joint or crack. Faulting is caused in part by a buildup of loose materials under the trailing slab near the joint or crack, or by a depression of the leading slab. The buildup of eroded or infiltrated materials is caused by pumping due to heavy loadings. The upward warp and curl of the

slab near the joint or crack due to moisture and temperature gradients contribute to the pumping condition. Lack of load transfer contributes greatly to faulting.

- Joint seal damage: An accumulation of rocks, soil, or water in a joint. Typical evidence of joint seal damage includes stripping and extrusion of joint sealant, weed growth, hardening of the filler, loss of bond to the slab edge, and lack or absence of sealant in the joint.
- Longitudinal cracks: Cracks that occur parallel to the centerline of the pavement. Longitudinal cracks are often caused by a combination of heavy load repetition, loss of foundation support, curling and warping stress, and improper construction.
- Lane-to-shoulder dropoff: A difference in elevation at the longitudinal joint between pavement edges of the traffic lane and the shoulder. Where the longitudinal joint has faulted, the length of the affected area and the maximum joint faulting should be recorded.
- Map cracking: A network of shallow, fine, or hairline cracks that extend only through the upper surface of the concrete. Map cracking is usually caused by overfinishing of the concrete and can lead to surface scaling, which is the breakdown of the slab surface to a depth of approximately 0.25 to 0.5 inch.
- Patch deterioration: Removing a portion of the original concrete slab and replacing it with concrete or other epoxy materials. Poor construction of the patch, loss of support, heavy load repetitions, lack of load transfer devices, improper or absent joints, and moisture or thermal gradients can all cause this distress.
- Pumping and water bleeding: Material ejected by water through joints or cracks, caused by the deflection of the slab under moving loads. As the water is ejected, it carries particles of gravel, sand, clay, or silt, resulting in a progressive loss of pavement support. Surface staining or accumulation of base or subgrade material on the pavement surface close to joints and cracks is evidence of pumping. Pumping can occur without such evidence, particularly when stabilized bases are used. Water being ejected by heavy traffic loads after a rainstorm can also indicate pumping. Water bleeding occurs when water seeps out of joints or cracks.
- Transverse cracks: Cracking that is predominantly perpendicular to the pavement centerline. These cracks are usually caused by a combination of heavy load repetitions and stresses due to temperature gradient, moisture gradient, and drying shrinkage.
- Spalling (transverse and longitudinal joint or crack): Cracking, breaking, or chipping of the slab edges within 1 ft of the joint or crack. A joint spall usually does not extend vertically through the whole slab thickness, but instead extends to intersect the joint at an angle. Spalling usually results from excessive stresses at the joint or crack, caused by the infiltration of incompressible materials and by subsequent expansion or traffic loading. It can also be caused by the disintegration of concrete, by weak concrete at the joint caused by overworking, or by poorly designed or constructed load transfer devices.

Table 13 summarizes concrete distress types and their associated failure mechanisms.

Table 13. Concrete Distress Types and Failure Mechanisms.

Distress Type	Failure Mechanism	
	Traffic/Load Related	Climate/Materials Related
Corner break	X	
"D" cracking		X
Faulting of transverse joints and cracks	X	
Joint seal damage		X
Longitudinal cracks	X	X
Lane-to-shoulder dropoff	X	
Map cracking		X
Patch deterioration	X	X
Pumping and water bleeding	X	X
Transverse cracks	X	X
Spalling (joints and cracks)		X
Spalling (corner)		X

RESEARCH APPROACH

The analysis began with a review of all distress data collected at each test section to identify suspect or inconsistent information. Researchers used photos and distress maps to verify quantities reported in the database. Because of the subjective nature of the data collection technique (raters had to select distress type and severity based on a set of rules), variation is expected in distress data. The SPS-6 data set was well within the acceptable range of variability.

Along with structural and environmental distress factors, the analyses also incorporated rutting, patching, and other surface defects such as potholes, bleeding, and raveling. Rutting data reported in this study was generated using a 6 ft straightedge reference (Simpson 2001).

The experimental design of the SPS-6 project allowed for replicate data collection for the test sections using asphalt rubber asphalt concrete (ARAC): Sections 040664 and 040668, 040665 and 040667, and 040666 and 040669). This was useful in validating their performance and comparing them with the other rehabilitation methods.

OVERALL PERFORMANCE TREND OBSERVATIONS

While gathering pavement distress data, investigators became aware of a few significant trends affecting the overall pavement performance of the project. These observations were clearly driving issues for this project and were intrinsically important pieces of the distress performance.

All JPCP test sections that did not receive an overlay (040601, 040602, and 040605) had the worst performance of all sections in the SPS-6 experiment. Within only two or three years, these sections had deteriorated to a level that required reconstruction and, therefore, were taken out of the experiment.

The unbonded PCC overlay test section (040663) exhibited excellent performance and had very little distress cracking at the end of the monitoring period. Details about the performance of this section will be discussed further in the PCC performance comparisons section in the report.

In general, the ARAC sections that received an AR-ACFC performed much better than the other AC test sections. Of the sections that received an AC overlay, nearly half received patching during the project. None of the test sections experienced raveling or shoving, and only one section (040603) experienced bleeding.

The overall longitudinal cracking trends are plotted in Figure 40 (crack and seat test sections) and Figure 41 (no preparation, minimum/maximum restoration, and rubblized test sections). The performance trends are relatively consistent and within the expected range of variation. Drops in the longitudinal distress graph are indicative of the maintenance that was performed on the test sections, which masked the distress. A full list of the work history of each site is given in Appendix B.

The overall transverse cracking trends are plotted in Figure 42 (crack and seat test sections) and Figure 43 (no preparation, minimum/maximum restoration, and rubblized test sections). The performance trends are relatively consistent and within the expected range of variation. The drop of longitudinal distress for Sections 040603 and 040662 are indicative of large areas of skin patching, which masked the distress.

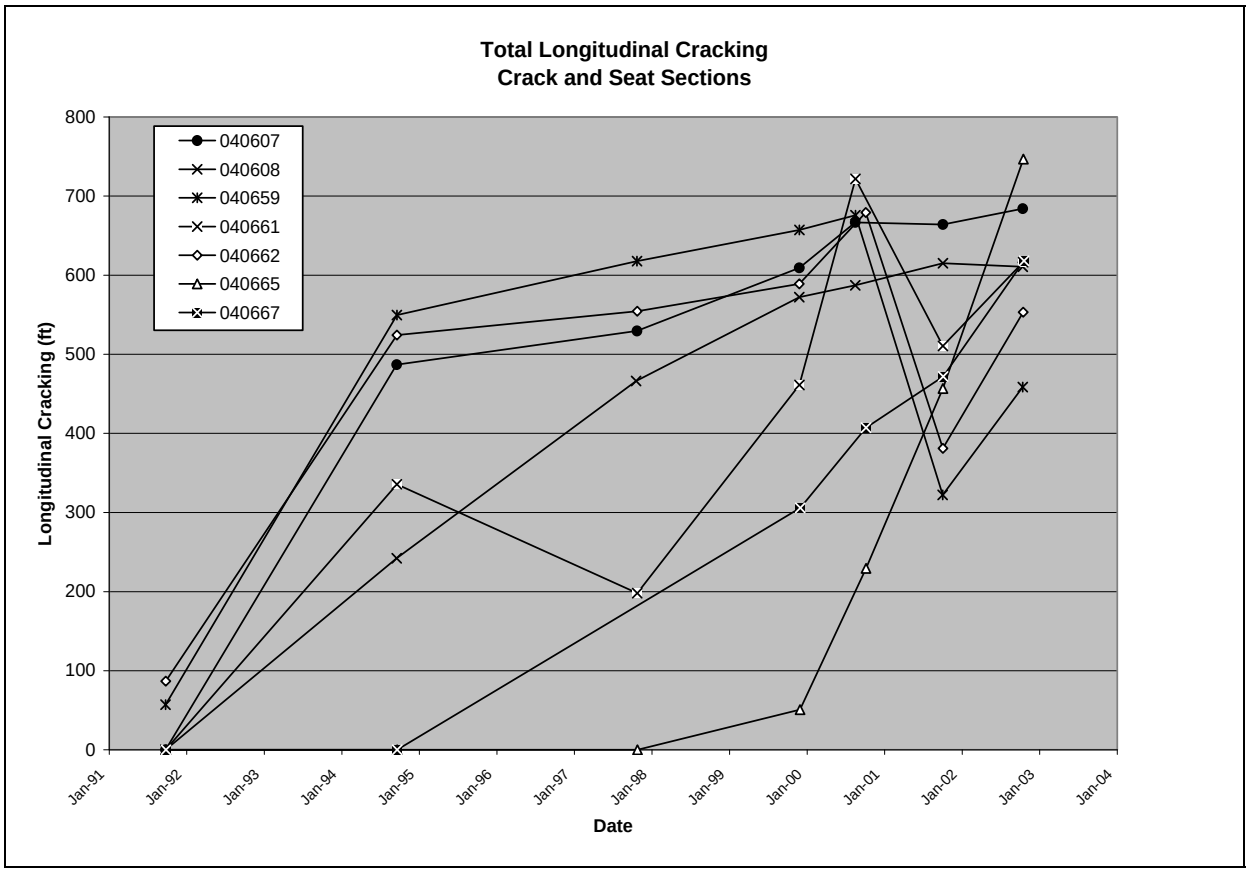

Figure 40. Longitudinal Cracking Trends of the Crack and Seat Test Sections.

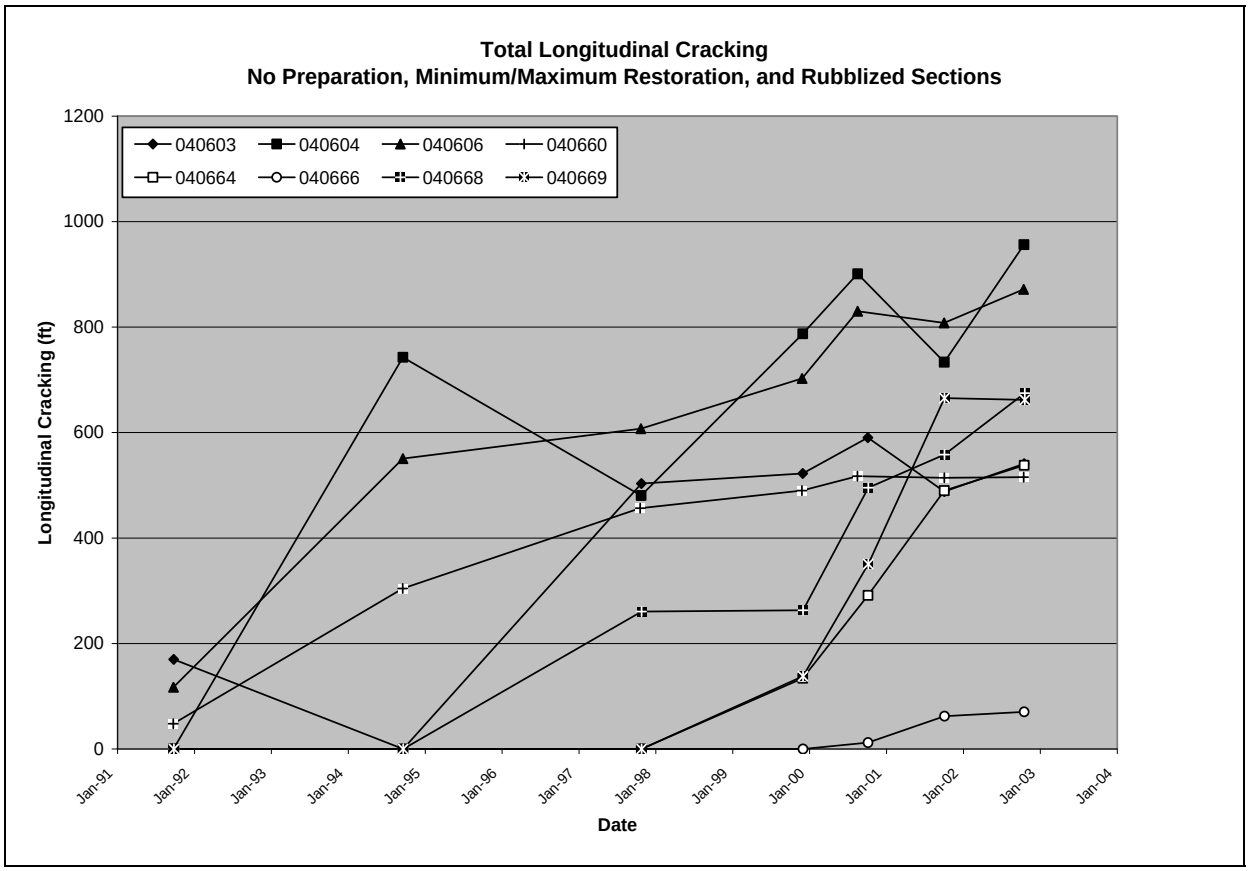

Figure 41. Longitudinal Cracking Trends of the No Preparation, Minimum/Maximum Restoration, and Rubblized Test Sections.

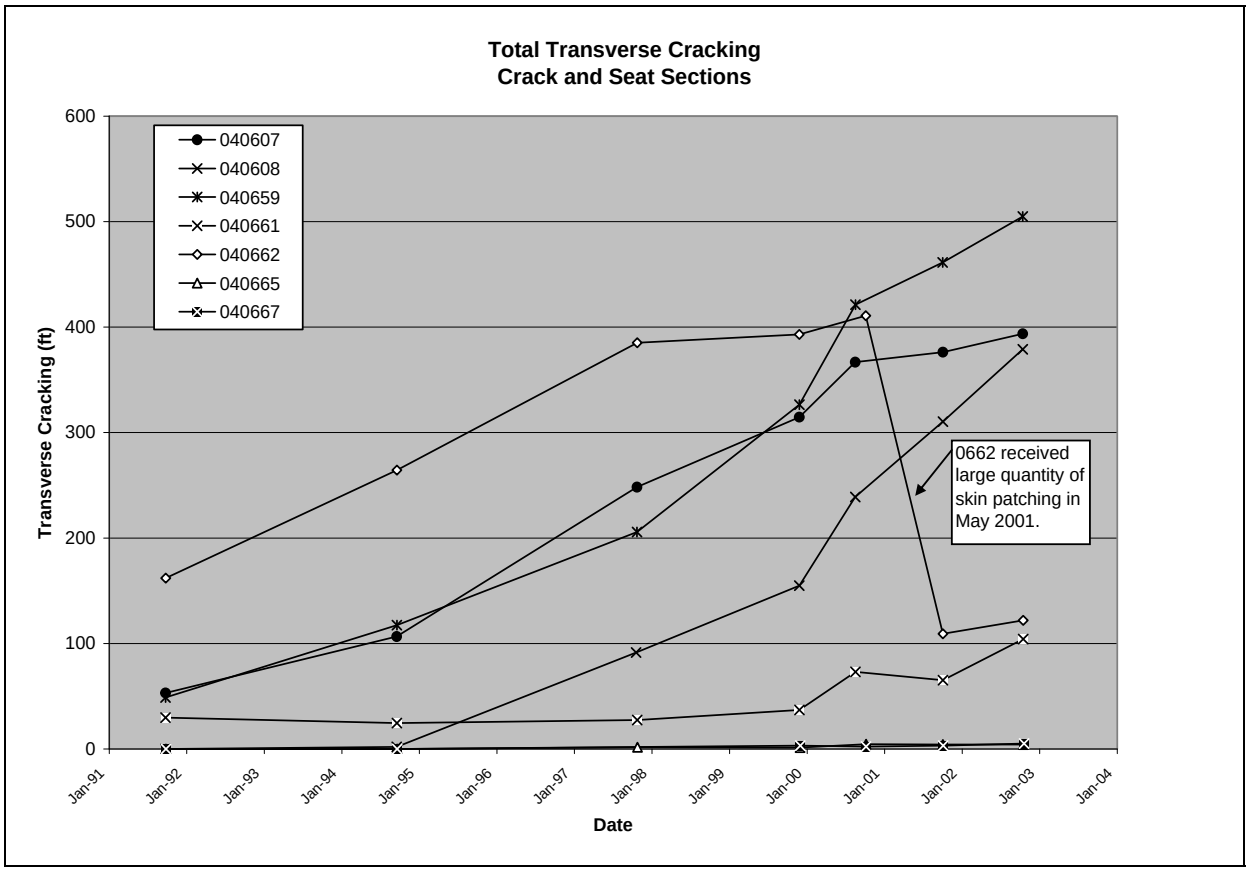

Figure 42. Transverse Cracking Trends of the Crack and Seat Test Sections.

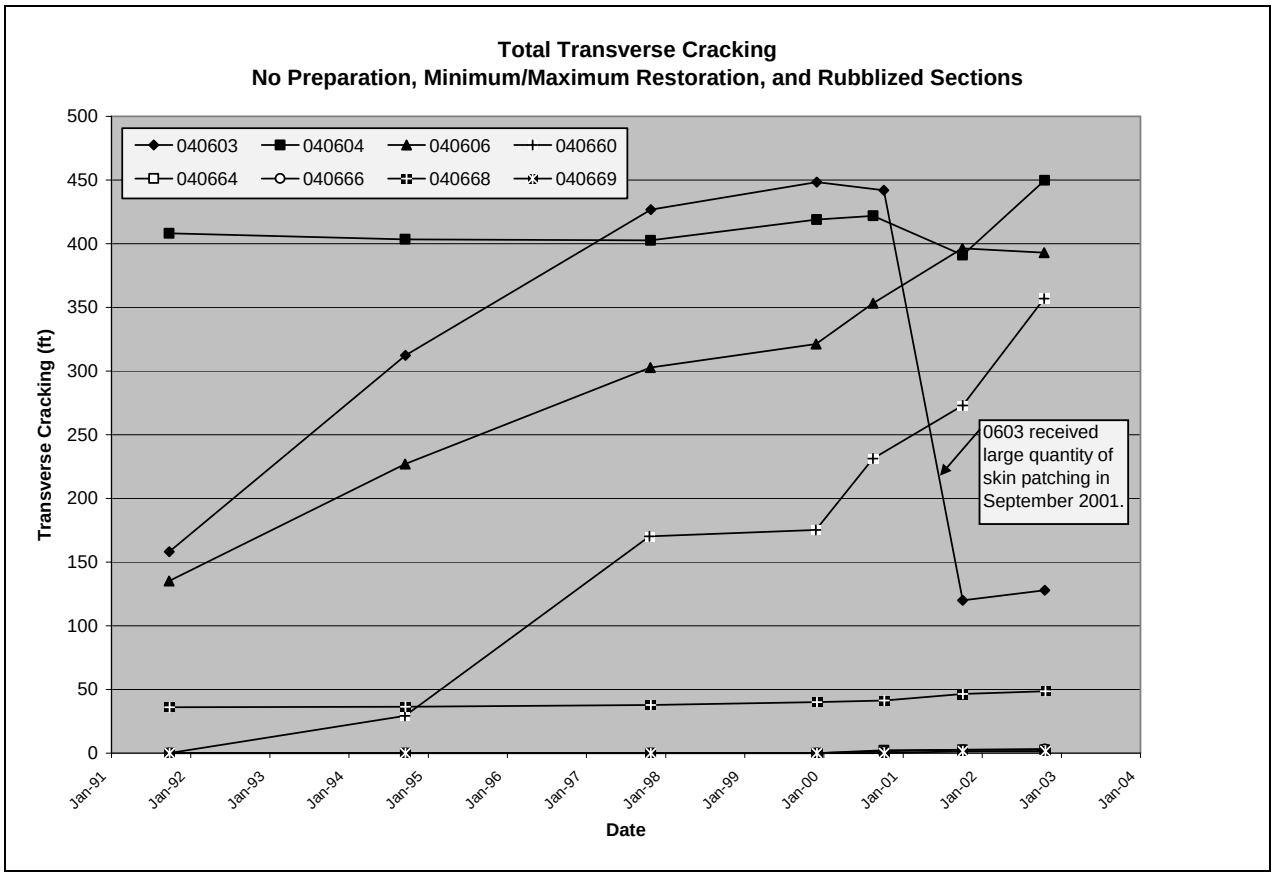

Figure 43. Transverse Cracking Trends of the No Preparation, Minimum/Maximum Restoration, and Rubblized Test Sections.

PERFORMANCE COMPARISONS

As previously mentioned, the SPS-6 test sections were analyzed based on surface type: AC and PCC. Because the distress types vary between the AC and PCC sections, researchers performed distress analyses and made comparisons within each surface type.

AC Performance Comparisons

In-depth analyses and comparisons were conducted for all of the SPS-6 test sections that were rehabilitated with AC overlays. Figure 44 provides a summary of the longitudinal cracking for each section; Figure 45 provides a summary of transverse cracking. Data for both distress charts were collected in October 2000 to avoid confounding the data with large skin patching that was performed on Sections 040603 and 040662 in 2001.

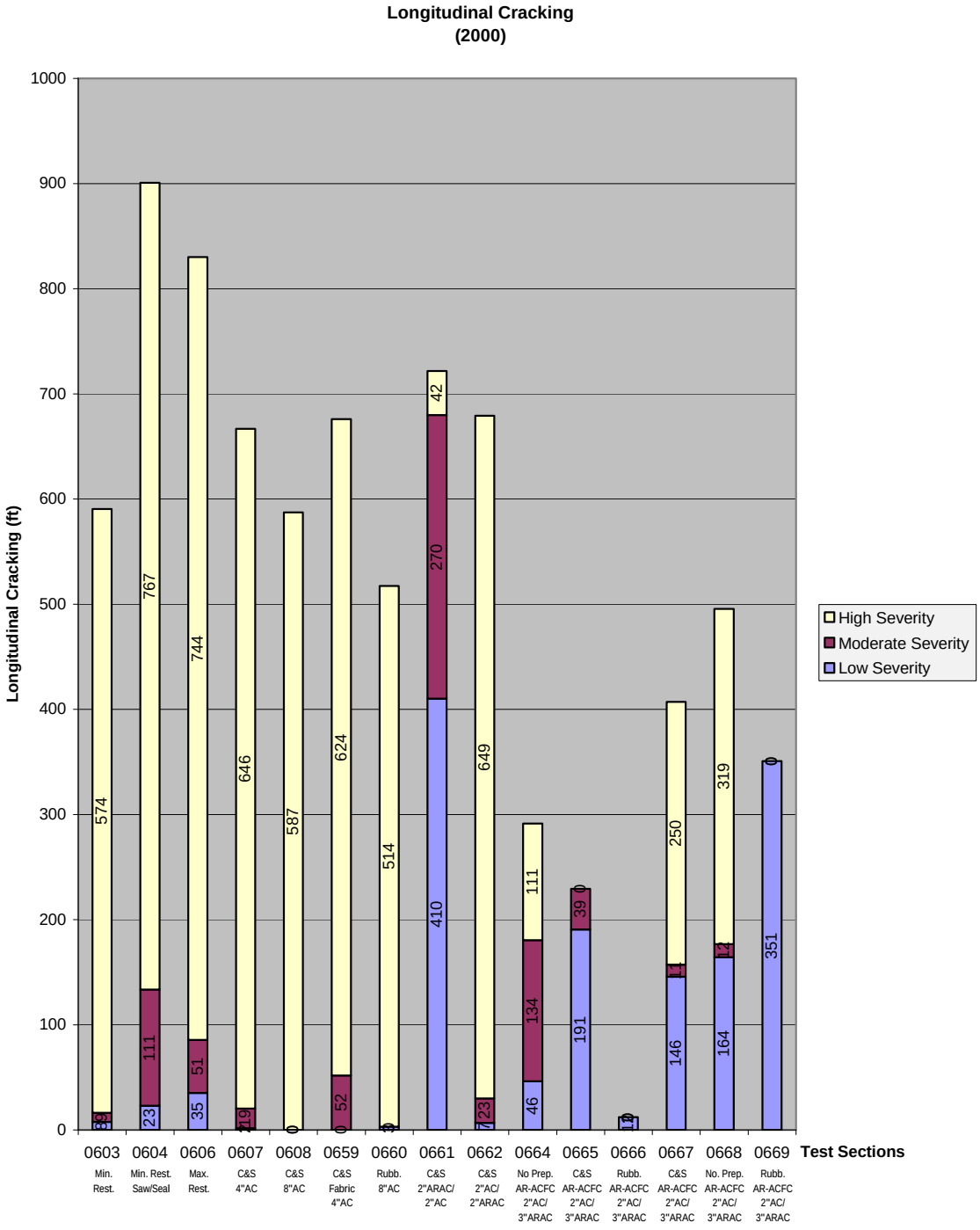

Figure 44. Longitudinal Cracking Summary.

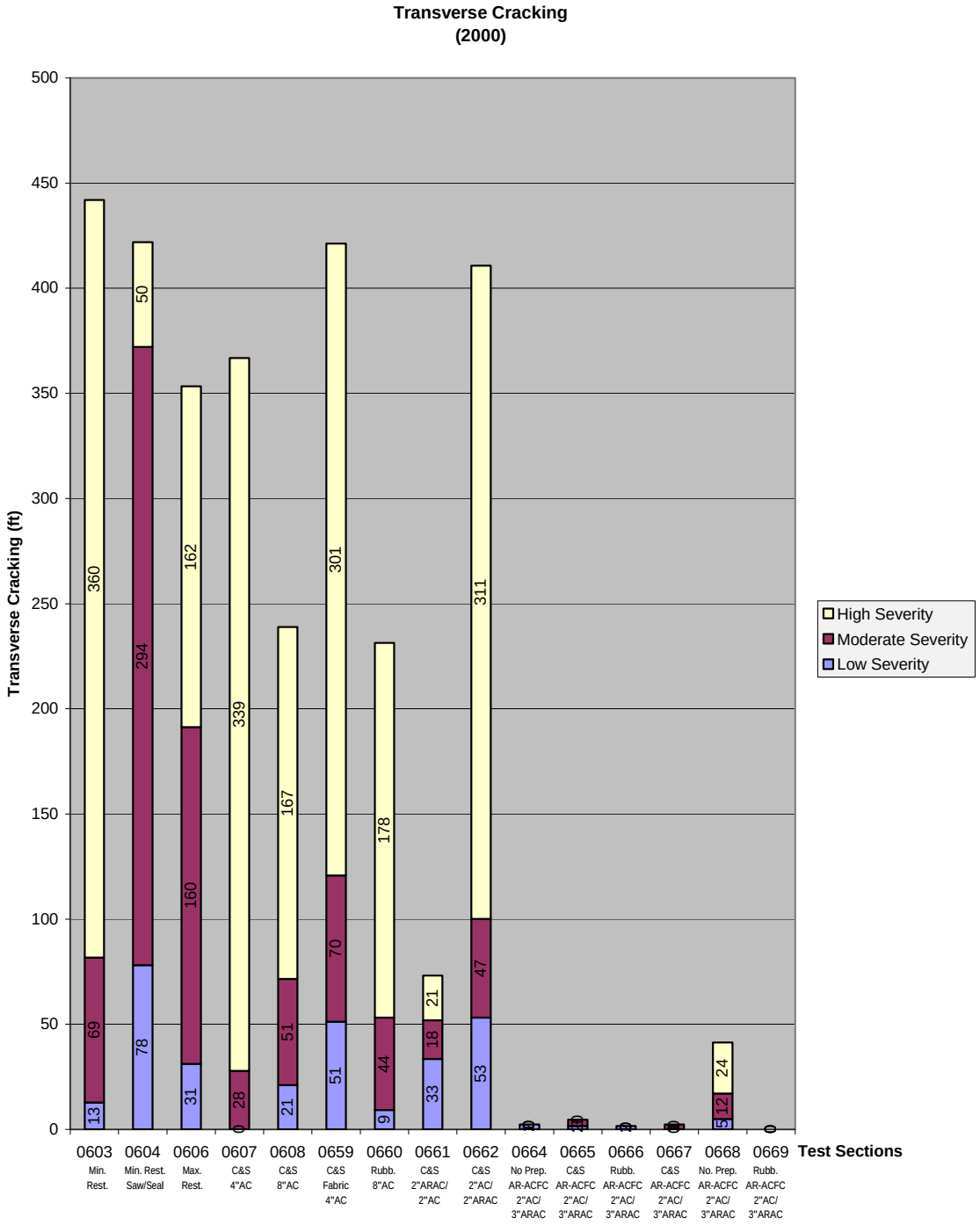

Figure 45. Transverse Cracking Summary.

Figure 46 provides a summary of rutting for each section. Section 040608, which received a crack and seat treatment with an 8 inch overlay, experienced the least amount of rutting among all the test sections. However, all sections exhibited less than 9 mm of rutting after more than seven years in service, which is well below the level required to trigger improvements in most pavement management systems. Therefore, rutting was not the driving factor in the overall condition of the pavement.

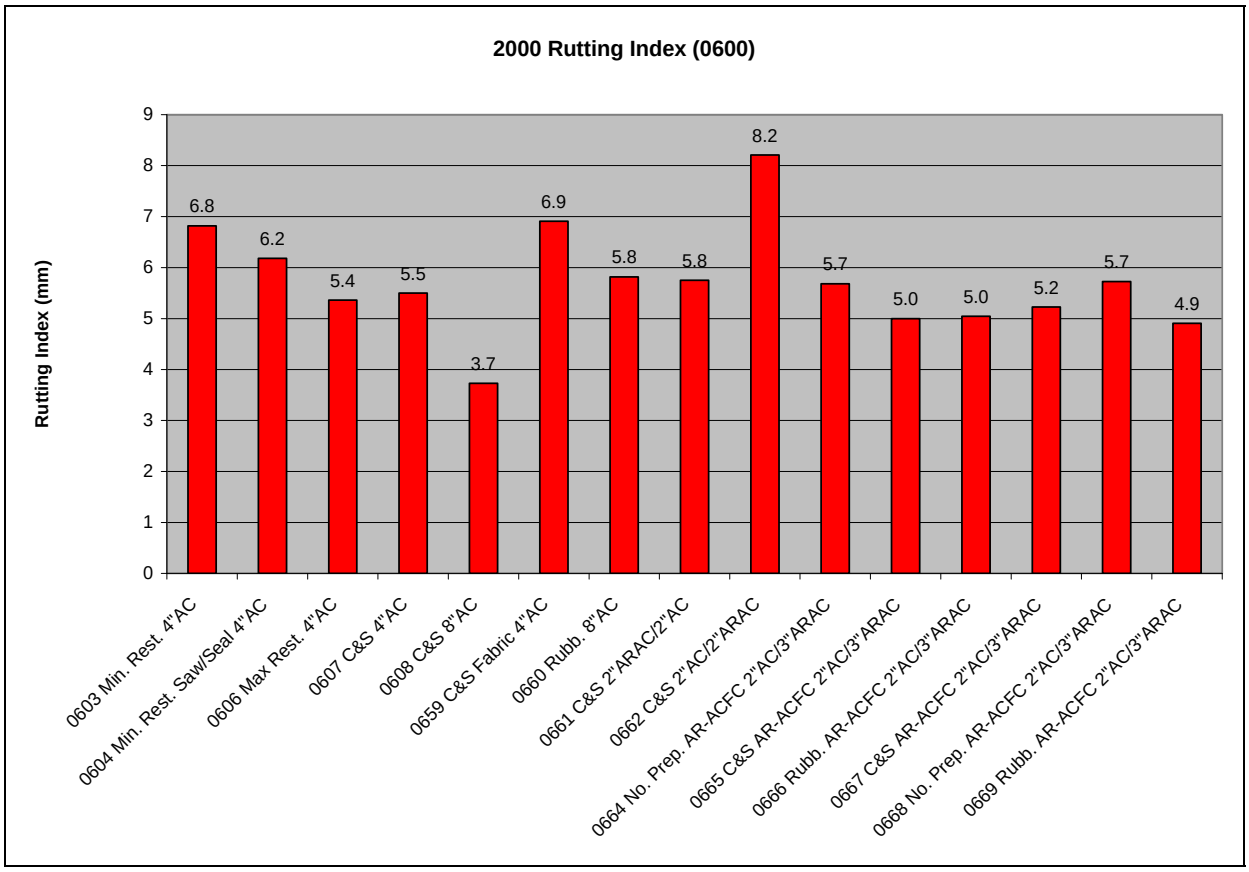

Figure 46. Rutting Index Summary.

Following is a synopsis of the findings and performance from each section, including longitudinal cracking, transverse cracking, rutting, and other circumstances. All overlay thicknesses are reported as nominal. A detailed list of exact thicknesses is available in Table 2.

Minimum/Maximum Restoration Sections

040603 Minimum Restoration (4 inch AC Overlay). Section 040603 exhibited an average performance against longitudinal cracking. Sections 040604 and 040606 experienced similar levels of longitudinal cracking (quantity and severity). Section 040603 also showed both the largest amount and highest severity of transverse cracking among all the sections. However, Sections 040659 and 040662 experienced similar levels of transverse cracking (quantity and distress). Section 040603 performed better against longitudinal cracking than all crack and seat sections with 4 inch AC overlays, the maximum restoration section with a 4 inch AC overlay, and the minimum restoration with a 4 inch saw and seal AC overlay.

040604 Minimum Restoration (4 inch AC Overlay with Saw and Seal). Section 040604 experienced both the largest quantity and highest severity of longitudinal cracking among all the test sections. Only Section 040606 experienced similar quantities and severity levels. This section exhibited large quantities of transverse cracking similar to Sections 040603, 040659, and 040662; however, most of the distress was moderate severity, whereas the other sections were dominantly high severity cracking. With the exception of Section 040661, this section exhibited slightly better transverse cracking resistance than all the crack and seat sections that received a 4 inch AC overlay.

040606 Maximum Restoration (4 inch AC Overlay). This section had very poor performance against longitudinal cracking. Only Section 040604 experienced similar quantities and severity levels of longitudinal cracking. This section exhibited fair to moderate resistance to transverse cracking. Only Section 040607 experienced similar quantities of transverse cracking; however nearly half of the distress was moderate severity, whereas Section 040607 was dominantly high severity cracking. As expected, this section performed slightly better against transverse cracking than the minimum restoration sections; however, with respect to transverse cracking, it also performed better than half of the crack and seat sections with 4 inch overlays.

Crack and Seat Sections

The crack and seat procedure for most of the SPS-6 test sections was intended to produce a nominal crack spacing of 3 × 3 ft. The pavement was then rolled until the broken pieces were seated. However, in two of the ADOT supplemental sections (040665 and 040667), this procedure was intended to produce a 4 × 6 ft cracking pattern. A tack coat was placed prior to overlay.

040607 Crack and Seat (4 inch AC Overlay with 3 × 3 ft Nominal Crack Spacing). This section had fair to moderate performance against longitudinal and transverse cracking. It had similar quantities of longitudinal distress as Sections 040659, 040661, and 040662, and two of those three sections (040659 and 040662) displayed similar levels of cracking severity. Section 040607 exhibited slightly smaller quantities of transverse cracking than Sections 040659 and 040662,

however, it also had slightly larger amounts of high-severity transverse cracking. This section did not outperform Section 040603, which received the minimum restoration with a 4 inch AC overlay.

040659 Crack and Seat (4 inch AC Overlay with Fabric and 3 × 3 ft Nominal Crack Spacing). This section had fair to moderate longitudinal cracking performance, but performed poorly in terms of transverse cracking. It had similar quantities of longitudinal distress as Sections 040607, 040661, and 040662, and two of those three sections (040607 and 040662) displayed similar levels of cracking severity. With respect to longitudinal and transverse cracking, this section performed similarly to Section 040662, which was a crack and seat section with 2 inch AC on top of 2 inch ARAC. However, Section 040659 performed worse than Section 040603 (the minimum restoration section with a 4 inch AC overlay), so no advantage was gained by adding the geotextile fabric.

040661 Crack and Seat (4 inch AC Overlay with 2 inch ARAC on 2 inch AC and 3 × 3 ft Nominal Crack Spacing). Section 040661 had the best performance among all the crack and seat sections with a 4 inch AC overlay. It had moderate longitudinal cracking performance, but exhibited very well against transverse cracking resistance. Though this section had larger quantities of longitudinal cracking than the majority of the test sections, most of the cracks were low and moderate in severity, with very little high severity cracking. With the exception of the six sections (040664 through 040669) that received an AR-ACFC, this section performed better against transverse and longitudinal cracking than all other test sections, including the rubblized and crack and seat sections with 8 inch overlays. Interestingly this section performed significantly better than Section 040662, which had the same layers and layer thicknesses, but the layer orientation was reversed (2 inch AC and 2 inch ARAC). This may suggest that the reflection cracking was top-down.

040662 Crack and Seat (4 inch AC Overlay with 2 inch AC on 2 inch ARAC and 3 × 3 ft Nominal Crack Spacing).
This section had fair to moderate longitudinal cracking performance, but exhibited poor transverse cracking performance. It had similar quantities of longitudinal distress as Sections 040607, 040659, and 040661, and two of those three sections (040607 and 040659) displayed similar levels of cracking severity. Section 040662 performed similarly with respect to longitudinal and transverse cracking as Section 040659, which had a 4 inch overlay and an underlying geotextile fabric layer. This section performed worse than Section 040603, the minimum restoration section with a 4inch AC overlay.

040608 Crack and Seat (8 inch AC Overlay with 3 × 3 ft Nominal Crack Spacing). Section 040608 exhibited an average longitudinal cracking performance and exhibited moderate transverse cracking performance. This section was comparable in its longitudinal and transverse cracking performance to Section 040660, the rubblized section with an 8 inch overlay. Three other sections—040603, 040660, and 040668—had similar quantities of longitudinal cracking, and two

of the three (040603 and 040660) had similar levels of cracking severity. It is surprising that the quantity and severity of longitudinal cracking was similar to Section 040603, which received the minimum restoration and only a 4 inch overlay.

040665 Crack and Seat (AR-ACFC with 2 inch AC on 3 inch ARAC and 4 × 6 ft Nominal Crack Spacing).
Section 040665 performed very well against longitudinal cracking and demonstrated excellent performance against transverse cracking. This section performed slightly better than its replicate, Section 040667. Two other sections (040664 and 040669) showed similar quantities of longitudinal distress; however, the majority of the cracking was low severity, whereas Section 040664 was split between moderate and high severity, and Section 040669 was dominantly high severity cracking. Sections with an ARAC-FC layer and a 3 inch ARAC bottom layer performed better than all other test sections in the project.

040667 Crack and Seat (AR-ACFC with 2 inch AC on 3 inch ARAC and 4 × 6 ft Nominal Crack Spacing). Section 040667 performed well against longitudinal cracking, and demonstrated excellent performance against transverse cracking. This section performed slightly worse than its replicate, Section 040665. Section 040668, which consisted of the same layer types and thicknesses but received no pre-overlay surface preparation, showed similar quantities and severity levels of longitudinal distress. Sections with an ARAC-FC layer and a 3 inch ARAC bottom layer performed better than all other test sections in the project.

Rubblized Sections

040660 Rubblized Section (8 inch AC Overlay). Section 040660 exhibited an average performance against longitudinal cracking and performed moderately well against transverse cracking. This section was comparable in its performance against longitudinal and transverse cracking to Section 040608, the crack and seat section that received an 8 inch overlay. Three other sections—040603, 040608, and 040668—had similar quantities of longitudinal cracking, and two of the three (040603 and 040608) had similar levels of cracking severity. It is surprising that the quantity and severity of longitudinal cracking was similar to Section 040603, which received the minimum restoration and only a 4 inch overlay. It should be noted that a 150 ft segment located 49 ft from the beginning of this section received a 4 to 7 ft over-excavation due to a liquefaction problem during the rubblization process. Subgrade material was replaced with better structural material, and this may have influenced the section's performance.

040666 Rubblized Section (AR-ACFC with 2 inch AC on 3 inch ARAC). Section 0666 performed significantly better than all other sections, including its replicate, Section 040669. After nine years of service and no maintenance, this section showed virtually no longitudinal or transverse cracking. Sections with an ARAC-FC layer and a 3 inch ARAC bottom layer performed better than all other test sections in the project.

040669 Rubblized Section (AR-ACFC with 2 inch AC on 3 inch ARAC). Section 040669 performed well against longitudinal cracking and exhibited excellent performance against transverse cracking. This section performed worse against longitudinal cracking than its replicate, Section 0666. Two other sections—040664 and 040665—showed similar quantities of longitudinal distress; however, the majority of the cracking was high severity, whereas Section 040664 was split between moderate and high severity and Section 040665 was dominantly low cracking. Sections with an ARAC-FC layer and a 3 inch ARAC bottom layer performed better than all other test sections in the project.

No Surface Preparation

040664 No Surface Preparation (AR-ACFC with 2 inch AC on 3 inch ARAC). Section 040664 performed well against longitudinal cracking and exhibited excellent performance against transverse cracking. This section performed better against longitudinal cracking than its replicate, Section 040668. Two other sections—040665 and 040669—showed similar quantities of longitudinal distress, however, the majority of the cracking was moderate to high severity. Section 040665 was dominantly low severity and Section 040669 was dominantly high severity cracking. Sections with an ARAC-FC layer and a 3 inch ARAC bottom layer performed better than all other test sections in the project.

040668 No Surface Preparation (AR-ACFC with 2 inch AC on 3 inch ARAC). Section 040668 performed moderately well against longitudinal cracking and performed very well against transverse cracking. This section performed worse against longitudinal and transverse cracking than its counterpart, Section 040664. Section 040667, a crack and seat section with the same layer types and thicknesses, showed similar quantities and severity levels of longitudinal distress. Section 040661, a crack and seat section with 2 inch ARAC on top of 2 inch AC, showed similar quantities and severity levels of transverse distress. Sections with an ARAC-FC layer and a 3 inch ARAC bottom layer performed better than all other test sections in the project.

PCC Performance Comparisons

Researchers also conducted in-depth analyses and comparisons of the SPS-6 test sections with PCC surfaces. Due to early structural failure of Sections 040601, 040602, and 040605, longitudinal and transverse cracking charts were only generated for Section 040663 (Figure 47).

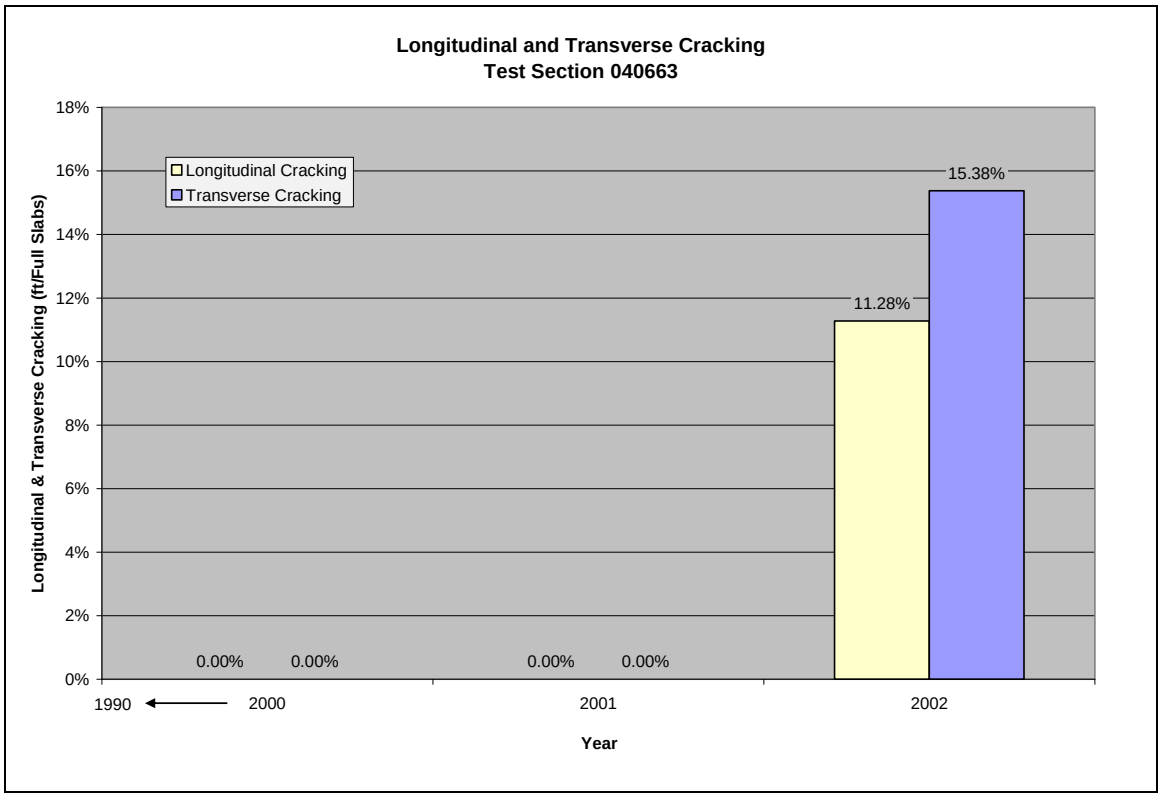

Figure 47. Summary of Longitudinal and Transverse Cracking in Section 040663.

040601 Control Section. Section 040601, the control section, only received the required routine maintenance needed to keep the section safe and functional. This section was placed out of study in late April 1992 due to significant deterioration. At the time it was taken out of study, the majority of the slabs were cracked, and approximately 31 percent of the cracks in the section were high severity.

040602 Minimum Restoration (No Surface Preparation). Section 040602 received minimum restoration, but was placed out of study in late April 1992 due to significant deterioration. At the time it was taken out of study, the majority of the slabs were cracked, and approximately 42 percent of the cracks in the section were high severity.

040605 Maximum Restoration (No Surface Preparation). Section 040605 received maximum restoration, but was placed out of study in early August 1993 due to significant deterioration. At the time it was taken out of study, much of the section consisted of large areas of patching and cracked slabs.

040663 Crack and Seat (10 inch PCC on 2 inch AC). Section 040663 performed very well and was the only PCC that lasted to the end of the monitoring period. In fact, when it was taken out of study in November 2002, it had very little cracking.

DISTRESS KEY FINDINGS

The distress data captured at the project site gave valuable insight into pavement performance, design, management, and construction. Highlights from the SPS-6 distress analysis follow:

- All sections with an ARAC-FC layer and a 3 inch ARAC bottom layer of experienced a significantly higher resistance to longitudinal and transverse reflective cracking.
- The higher performance of the ARAC-FC sections (040664 through 040669) could be partially attributed to the viscosity of the AR, which is more than 10 times that of AC-20 (PG-64-16) at hot-mixing temperatures and, therefore, can be applied to an open-graded friction course (OGFC) at a rate of 9 percent to 10 percent by weight of the mix. This extra coating thickness is believed to increase durability, slow aging, and help retard reflective cracking.
- When overlay thickness increased to 8 inches, rubblized sections and crack and seat sections yielded approximately the same performance.
- Reflection cracking is believed to originate from the bottom of the layers. However, while the findings from this study don't definitively show top-down cracking, the test section performances may point to it.
- In this study, both minimum and maximum restorations of PCC slabs were not long-term improvement solutions.
- Section 040663, the 10 inch unbonded PCC overlay (with a 2 inch AC bond breaker), had the highest performance among all of the test sections in the SPS-6 experiment.
- The rubblized section (040666) with AR-ACFC and 2 inch AC on 3 inch ARAC had the highest performance among all sections that received AC overlays in the SPS-6 experiment.
- All sections performed well with regard to rut resistance. Rutting would not have triggered a rehabilitation event for any of the test sections.
    - Section 040661 (2 inch ARAC on 2 inch AC) performed much better than Section 040662 (2 inch AC on 2 inch ARAC). This is interesting as the ARAC layer is believed to retard reflection cracking.
    - The thin layer of ARAC-FC may have contributed to the higher performance of Sections 040664 through 040669.
    - Geotextile fabric, which is also believed to help prevent reflection cracking, did not seem to improve the performance of Section 040659.

CHAPTER 4. SPS-6 ROUGHNESS ANALYSIS

This chapter characterizes the surface roughness of the test sections throughout their service life and links the observations to records of pavement distress and its development. Road profile measurements were collected on this site about once per year starting with the winter after it was opened to traffic. This study analyzed the profiles in detail by calculating their roughness values, examining the spatial distribution of roughness within them, viewing them with post-processing filters, and examining their spectral properties. These analyses provided details about the roughness characteristics of the road and also provided a basis for quantifying and explaining the changes in roughness with time.

PROFILE DATA SYNCHRONIZATION

Profile data were collected at the Arizona SPS-6 site on 15 dates from April 9, 1990 through October 28, 2002 (Table 14). Raw profile data were available for all visits. Each visit produced a minimum of six repeat profile measurements. Visit 00 took place before the original rehabilitation and only included Sections 040601 through 040663. Visit 01 took place soon after the original rehabilitation and excluded Sections 040660, 040663, 040608, and 040607 because data collection was triggered in an incorrect location. Sections 040601, 040602, and 040605 were removed from the study after visit 04. In visits 02 through 08, the raw measurements covered the entire site in one long profile. In visits 09 through 13, the raw measurements covered "leading" Sections 040603 through 040663 in one profile and "trailing" Sections 040664 through 040669 in another.

Table 14. Profile Measurement Visits of the SPS-6 Site.

Visit	Date	Time	Repeats	Sections Missing
00	April 9, 1990	19:14	7	040664-040669
01	Sept. 27, 1990		7	040607, 040608, 040660, 040663
02	Sept. 16, 1991	12:32-14:15	6-7	—
03	Feb. 27, 1992	00:56	6	—
04	Feb. 12, 1993	14:29-17:13	9	—
05	Jan. 21, 1994	06:24-08:33	9	—
06	May 2, 1995	14:04-16:57	9	—
07	Feb. 19, 1997	11:06-13:11	9	—
08	April 17, 1998	10:16-11:33	7	—
09	March 2, 1999	10:36-12:28	7	—
10	March 14, 2000	10:43-12:17	7	—
11	Aug. 17, 2000	10:40-12:39	8-9	—
12	Feb. 7, 2001	10:50-12:46	9	—
13	Feb. 15, 2002	10:24-12:21	9	—
14	Oct. 28, 2002	17:52-19:54	9	—

DATA EXTRACTION

Profiles of individual test sections were extracted directly from the raw measurements. Raw profiles provided data recorded at a short interval of 0.98 inch for visits 07 through 13 and 0.77 inch for visit 14. The raw profiles included multiple (if not all) test sections within each pass. As such, they provided the opportunity to refine the consistency of section boundaries over time.

Three indicators helped extract the correct profile segments from the long raw measurements: the design layout, event markers in the raw profiles showing the start and end of each section, and automated searching for the longitudinal offset between repeat measurements.

CROSS CORRELATION

Searching for the longitudinal offset between repeat profile measurements that provides the best agreement between them is a helpful way to refine their synchronization. This can be done by inspecting filtered profile plots, but it is very time-consuming. Visual assessment is also somewhat subjective when two profiles do not agree well, which is often the case when measurements are made a year or more apart. In this study, investigators used an automated procedure rather than visual inspection to find the longitudinal offset between measurements.

The procedure is based on a customized version of cross correlation (Karamihas 2004). In this procedure, a basis measurement is designated that is considered to have the correct longitudinal positioning. A candidate profile is then searched for the longitudinal offset that provides the highest cross correlation to the basis measurement. A high level of cross correlation requires a good match of profile shape, the location of isolated rough spots, and overall roughness level. Therefore, the correlation level is often only high when the two measurements are synchronized. When the optimal offset is found, a profile is extracted from the candidate measurement with the proper overall length and endpoint positions. For the remainder of this discussion, this procedure will be referred to as automated synchronization.

For this application, cross correlation was performed after the International Roughness Index (IRI) filter was applied to the profiles rather than using the unfiltered profiles. This helped assign the proper weighting to relevant profile features. In particular, it increased the weighting of short-wavelength roughness that may be linked to pavement distress. This enhanced the effectiveness of the automated synchronization procedure. The long-wavelength content within the IRI output helped ensure that the longitudinal positioning was nearly correct, and the short-wavelength content was able to leverage profile features at isolated rough spots to fine-tune the positioning.

VISITS 01 THROUGH 14

For visits 01 through 14, profiles of individual test sections were extracted from the raw measurements using the following steps:

1. Establish a basis measurement for each section from visit 02. This was done using the event markers from a raw measurement. The first repeat measurement was used for this. Event markers appeared at the start and end of every section. The locations of the event markers were compared to the layout provided in the construction report (Austin Research Engineers 1992). Unlike the event markers for the later visits, the events markers from repeat 1 of visit 02 exhibited a linear relationship with the section starting locations listed in the construction report. In particular, the event markers for Section 040663 were not consistent with the construction report in later visits.
2. Automatically synchronize the other eight repeats from visit 02 to the basis set.
3. Automatically synchronize measurements from the next visit to the current basis set.
4. Replace the basis set with a new set of synchronized measurements from the first repeat of the current visit.
5. Repeat steps 3 and 4 until visit 14 is complete.

A basis set for visit 01 was extracted from repeat 1 using automated synchronization to the basis set from visit 02. Then remaining repeat measurements were synchronized to the new basis set.

VISIT 00

Visit 00 was difficult to synchronize to later visits because it took place before major rehabilitation of the test sections. A basis set of measurements from visit 01 only produced a significant match for Sections 040601 and 040602 because all the other test sections received extensive surface preparation, and most of them received a subsequent overlay. To further complicate matters, the profiles from visit 00 included several spurious event markers.

For visit 00, profiles of individual test sections were extracted from the raw measurements using the following steps:

1. Extract basis measurements of Sections 040601 and 040602 from repeat 1 of visit 00 using automated synchronization to visit 02 profiles.
   Repeat 2 from visit 02 was selected for this purpose since it was more consistent to the longitudinal distance measurement in visit 00 than the other repeats.
2. Extrapolate the expected boundaries of the remaining test sections and extract a basis set from repeat 1 of visit 00. Assume a linear relationship between the design layout and the distribution of sections within the profile, given the distance between Sections 040601 and 040602 found using automated synchronization.
3. Automatically synchronize the other repeat measurements to the new basis set from visit 00.

SPECIAL OBSERVATIONS

Section 040668: The construction report listed Section 040668 as 400 ft long. However, the event markers in the raw profile for the start and end of the section appeared 500 ft apart in all visits. Investigators assumed that the section was 500 ft long. Note that this affects the profiles for Section 040669, which start at the end of Section 040668.

Sections 040601, 040602, and 040605: The data extraction and synchronization procedures described above produced profile boundaries that were quite consistent with LTPP database profiles for Sections 040603, 040604, and 040606 through 040608. In most cases, the synchronized data overlapped profiles from the LTPP database by more than 99 percent. This was not the case for Sections 040601, 040602, and 040605. LTPP database profiles of Section 040601 led the actual section start by more than 50 ft in visit 00 and lagged the actual section start by nearly 200 ft in visit 03. LTPP database profiles of Section 040602 from visit 00 led the actual section start by about 40 ft in visit 00 and lagged the section start by at least 175 ft in visits 02 through 04. For Section 040605, LTPP database profiles from visit 00, 02, and 04 led the actual section start by about 10 to 30 ft.

LONGITUDINAL DISTANCE MEASUREMENT

The basis measurements for visit 02, established in step 1 above, were set using the event markers in one raw profile measurement (the first repeat). The locations of these markers agreed very well, but not perfectly, with the layout provided in the construction report. For example, a least-squares linear fit was drawn between the layout of the event markers and the starting locations listed in the construction report. For the leading group of sections (from the start of the site to the end of Section 040603), the slope of the fit was 0.9932. This implies that the longitudinal distance measurement made by the profiler was consistent with the construction report to within 0.68 percent, and that the profiler measured distances slightly longer than expected. No individual section boundary deviated from the best fit line by more than 1 ft.

The other eight repeats from visit 02 were automatically synchronized to the basis set. When the layout of section starting locations for the leading group of sections was compared to the locations listed in the construction report for each of these repeats, the slope of the linear fit ranged from 0.9971 to 1.0023. Thus, the longitudinal distance measurement for the nine profile measurements of visit 02 was consistent within 0.52 percent.

Figure 48 shows the disagreement in longitudinal distance measurement for each visit of the leading group of sections, using the event markers from repeat 1 of visit 02 as a reference. The leading group terminates at the end of Section 040601 for visits 00 through 04, and at the end of Section 040603 for the other visits. In the figure, a range of disagreement for each visit exists because up to nine repeat profile measurements were made. The variation between repeat

measurements from the same visit appears as the width of each bar in the figure. Since the longitudinal distance measurement was based on the rotation of a drive wheel, the variations were most likely caused by variations in speed, lateral wander, and tire inflation pressure (Karamihas et al. 1999). If tire inflation pressure were the dominant cause, the disagreement would grow more negative (or less positive) with each successive repeat measurement as the tire heated up because the tire rolling radius would increase; the profiler would register less wheel rotation for the same travel distance. This appeared to be the case for visits 08 through 13. However, the effect was weak, which indicates that the tires were warmed up to some extent before the measurements began. Only visit 02 exhibited a level of disagreement between repeat measurements that may interfere with the analyses described in this report.

The variation between visits in Figure 48 is caused by differences in distance measurement instrument calibration. The longitudinal distance measured by a profiler is not true horizontal distance. It always includes some additional component because the profiler must travel up and down the undulations in the road. This component can be minimized by calibrating the profiler to true horizontal distance. However, if a profiler operates on a road with grade changes and

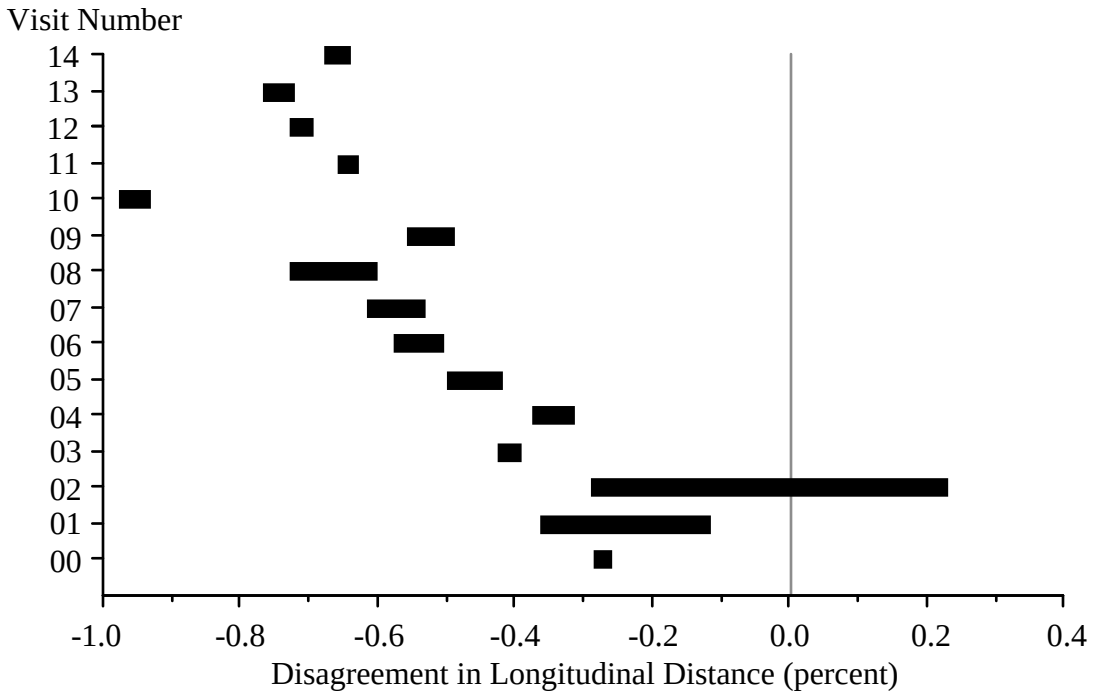

Figure 48. Consistency in Longitudinal Distance in the Leading Sections.

roughness that are not similar to the site used for longitudinal distance measurement calibration, some error will exist. Tire inflation pressure must also be close to the level that existed during calibration for consistent results.

Modest inconsistency in longitudinal distance measurement between visits is not critical as long as the profiles of individual sections are extracted using event markers or automated synchronization rather than longitudinal distance from the start of each raw profile measurement. A high level of inconsistency, however, could interfere with comparisons between profile features and distress surveys. Errors in profile index values, such as the IRI, are also roughly of the same order as errors in longitudinal distance measurement (Karamihas et al. 1999). With the exception of visit 02, longitudinal distance was measured with enough consistency to avoid bias in the IRI values above 1 percent.

Figure 49 shows the disagreement in longitudinal distance measurement for the trailing group of sections (040664 through 040669). Overall, the disagreement is similar to that observed for the leading group with the exception that earlier visits were less repeatable.

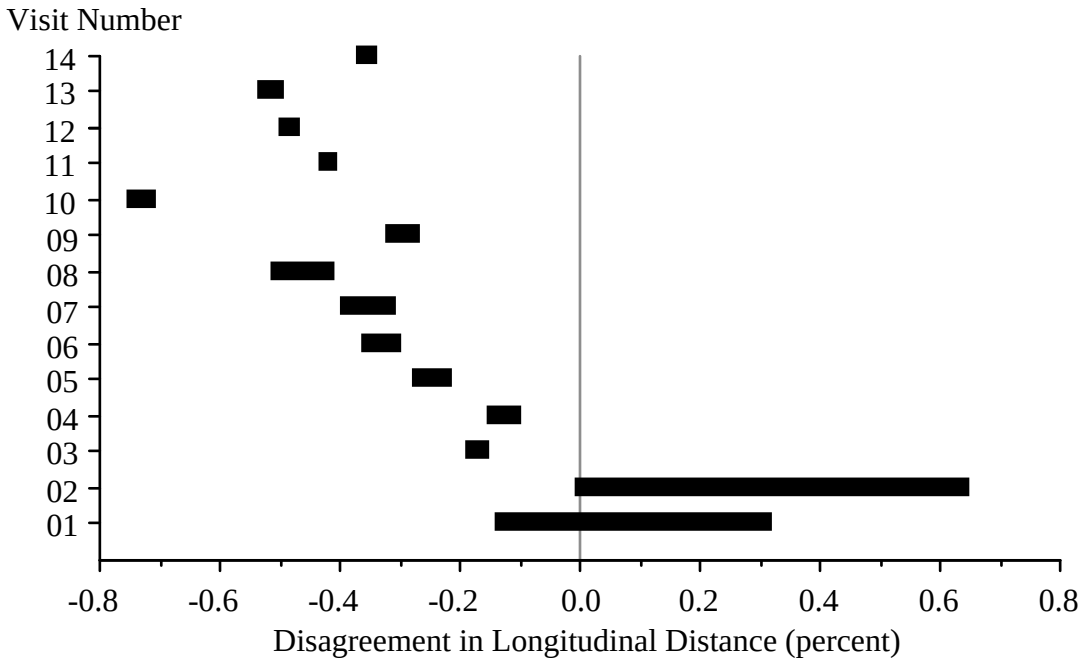

Figure 49. Consistency in Longitudinal Distance in the Trailing Sections.

DATA QUALITY SCREENING

Investigators performed data quality screening to select repeat profile measurements from each visit of each section. Among the group of available runs, investigators selected the five measurements that exhibited the best agreement with each other. In this case, agreement between any two profile measurements was judged by cross-correlating them after applying the IRI filter and then comparing the output signals rather than the overall index (Karamihas 2004). High correlation by this method requires that the overall roughness as well as the details of the profile shape that affect the IRI agree.

The IRI filter was applied before correlation in this case for several reasons:

- Direct correlation of unfiltered profiles places a premium on very long wavelength content, but ignores much of the contribution of short wavelength content.
- Correlation of IRI filter output emphasizes profile features in (approximate) proportion to their effect on the overall roughness.
- Correlation of IRI filter output provides a good trade-off between emphasizing localized rough features at distressed areas in the pavement and placing too much weight on the very short-duration, narrow features (spikes) that are not likely to agree between measurements because the IRI filter amplifies short wavelength content, but attenuates macrotexture, megatexture, and spikes.
- A relationship has been demonstrated between the cross-correlation level of IRI filter output and the expected agreement in overall IRI (Karamihas 2004).

Note: This method was performed with a special provision for correcting modest longitudinal distance measurement errors.

Each comparison between profiles produced a single value that summarized their level of agreement. When nine repeat profile measurements were available, they produced a total of 36 correlation values. Any subgroup of five measurements could be summarized by averaging the relevant 10 correlation values. The subgroup that produced the highest average was selected, and the other repeats were excluded from most of the analyses discussed in the rest of this report. Since the number of available profiles ranged from six to nine, the number of measurements that were excluded ranged from one to four. Tables 15 through 33 list the selected repeats for each visit of each section, and the composite correlation level that they produced.

The process for selecting five repeat measurements from a larger group is similar to the practice within LTPP except that it is based on composite agreement in profile rather than the overall index value. The correlation levels listed in Tables 15 through 33 provide an appraisal of the agreement between profile measurements for each visit of each section. When two profiles produce a correlation level above 0.82, their IRI values are expected to agree within 10 percent most (95 percent) of the time. Above this threshold, the agreement between profiles is usually acceptable for studying the influence of distresses on profile. When two profiles produce a correlation level above 0.92, they are expected to agree within 5 percent most of the time. Above this threshold, the agreement between profiles is good. Correlation above 0.92 often depends on consistent lateral tracking of the profiler, and may be very difficult to achieve on highly distressed surfaces. The IRI values provided in this report will be the average of five observations, which will tighten the tolerance even further.

Table 15. Selected Repeats of Section 040601.

Visit	Repeat Numbers					Composite Correlation
00	5	6	7	8	9	0.949
01	3	4	6	7	8	0.814
02	1	2	3	4	5	0.835
03	1	3	5	6	7	0.870
04	1	2	5	6	9	0.703

Table 16. Selected Repeats of Section 040602.

Visit	Repeat Numbers					Composite Correlation
00	2	4	6	7	8	0.978
01	5	6	7	8	9	0.952
02	1	4	5	6	7	0.959
03	1	3	5	6	7	0.952
04	1	2	3	4	6	0.956

Table 17. Selected Repeats of Section 040603.

Visit	Repeat Numbers					Composite Correlation
00	1	2	5	6	8	0.923
01	4	5	6	8	9	0.900
02	1	2	3	5	6	0.835
03	1	4	5	6	7	0.814
04	3	4	5	8	9	0.846
05	1	2	3	4	5	0.866
06	2	3	5	6	7	0.884
07	1	2	6	7	9	0.927
08	1	3	5	6	7	0.972
09	1	3	4	5	7	0.955
10	1	2	3	4	7	0.985
11	1	2	3	8	9	0.972
12	1	2	3	5	6	0.973
13	1	2	7	8	9	0.959
14	1	3	4	7	9	0.919

Table 18. Selected Repeats of Section 040604.

Visit	Repeat Numbers					Composite Correlation
00	2	6	7	8	9	0.958
01	4	5	6	7	8	0.932
02	2	3	4	5	6	0.892
03	1	4	5	6	7	0.863
04	3	4	7	8	9	0.870
05	1	2	3	7	9	0.843
06	4	6	7	8	9	0.883
07	3	4	6	7	8	0.926
08	2	3	5	6	7	0.883
09	2	3	4	6	7	0.915
10	1	2	3	5	6	0.956
11	4	5	6	8	9	0.974
12	1	2	3	5	6	0.956
13	1	2	3	6	7	0.964
14	1	3	4	5	9	0.925

Table 19. Selected Repeats of Section 040605.

Visit	Repeat Numbers					Composite Correlation
00	4	5	6	8	9	0.958
01	3	4	5	6	8	0.906
02	1	2	3	5	7	0.914
03	1	3	4	5	6	0.943
04	3	5	6	7	8	0.944

Table 20. Selected Repeats of Section 040606.

Visit	Repeat Numbers					Composite Correlation
00	1	2	7	8	9	0.934
01	4	5	7	8	9	0.929
02	1	2	5	6	7	0.850
03	1	3	4	6	7	0.864
04	1	4	5	8	9	0.854
05	2	5	6	7	9	0.903
06	2	3	5	6	8	0.892
07	3	4	6	7	9	0.904
08	2	3	4	5	7	0.917
09	2	4	5	6	7	0.950
10	1	3	5	6	7	0.927
11	1	2	6	8	9	0.963
12	1	3	5	7	9	0.967
13	1	3	6	8	9	0.976
14	1	2	5	6	8	0.947

Table 21. Selected Repeats of Section 040607.

Visit	Repeat Numbers					Composite Correlation
00	2	5	6	8	9	0.890
02	1	3	5	6	7	0.821
03	1	3	4	5	6	0.864
04	1	4	6	7	9	0.839
05	2	5	6	8	9	0.891
06	3	5	6	7	8	0.854
07	2	3	6	7	8	0.933
08	2	3	4	5	6	0.922
09	2	4	5	6	7	0.969
10	1	2	4	6	7	0.960
11	2	3	5	7	8	0.956
12	2	3	4	7	9	0.966
13	2	3	5	6	8	0.965
14	1	2	4	5	6	0.880

Table 22. Selected Repeats of Section 040608.

Visit	Repeat Numbers					Composite Correlation
00	1	4	6	7	8	0.963
02	1	2	5	6	7	0.868
03	1	3	4	5	7	0.834
04	1	2	6	8	9	0.863
05	4	5	6	7	9	0.905
06	2	3	6	8	9	0.805
07	2	4	5	6	9	0.883
08	2	3	4	5	7	0.784
09	1	2	3	4	6	0.906
10	1	3	4	5	6	0.899
11	3	4	5	6	8	0.919
12	1	2	3	4	8	0.910
13	1	2	5	7	9	0.898
14	3	4	5	7	8	0.852

Table 23. Selected Repeats of Section 040659.

Visit	Repeat Numbers					Composite Correlation
00	2	3	4	5	6	0.949
01	3	5	6	7	8	0.943
02	2	3	5	6	7	0.911
03	1	3	5	6	7	0.824
04	1	3	5	6	8	0.878
05	1	2	3	4	9	0.915
06	1	2	3	5	6	0.827
07	3	4	5	8	9	0.923
08	2	4	5	6	7	0.949
09	1	2	3	4	7	0.902
10	2	4	5	6	7	0.912
11	2	3	5	6	9	0.953
12	1	2	3	4	6	0.970
13	2	3	5	8	9	0.963
14	3	4	5	7	8	0.940

Table 24. Selected Repeats of Section 040660.

Visit	Repeat Numbers					Composite Correlation
00	2	4	6	8	9	0.959
02	1	3	4	5	7	0.941
03	3	4	5	6	7	0.913
04	1	2	4	5	6	0.913
05	2	5	6	7	9	0.957
06	3	4	6	7	9	0.949
07	4	5	6	8	9	0.971
08	1	3	4	6	7	0.958
09	1	2	3	4	7	0.979
10	1	2	3	4	5	0.973
11	1	2	3	6	9	0.980
12	2	3	7	8	9	0.980
13	1	4	6	7	9	0.977
14	1	3	5	6	9	0.865

Table 25. Selected Repeats of Section 040661.

Visit	Repeat Numbers					Composite Correlation
00	3	5	6	7	9	0.986
01	1	3	5	6	7	0.937
02	1	4	5	6	7	0.886
03	1	3	5	6	7	0.837
04	3	5	6	8	9	0.790
05	2	3	5	7	8	0.871
06	1	5	6	7	9	0.853
07	1	2	3	4	5	0.907
08	2	3	4	5	6	0.879
09	1	2	3	5	6	0.831
10	1	2	4	6	7	0.934
11	1	3	4	7	8	0.964
12	1	2	5	6	7	0.959
13	2	3	4	6	7	0.962
14	1	4	5	6	8	0.894

Table 26. Selected Repeats of Section 040662.

Visit	Repeat Numbers					Composite Correlation
00	1	2	4	6	7	0.963
01	1	2	5	6	8	0.910
02	1	3	4	5	7	0.900
03	3	4	5	6	7	0.906
04	1	2	3	4	7	0.857
05	2	4	5	6	8	0.925
06	2	3	4	7	9	0.842
07	2	3	4	6	9	0.948
08	1	2	3	4	7	0.958
09	1	2	4	5	6	0.941
10	1	2	4	5	7	0.970
11	1	4	6	8	9	0.972
12	2	3	5	6	8	0.947
13	1	3	4	5	7	0.961
14	1	2	5	8	9	0.904

Table 27. Selected Repeats of Section 040663.

Visit	Repeat Numbers					Composite Correlation
00	1	5	6	8	9	0.981
02	1	3	4	5	7	0.920
03	3	4	5	6	7	0.926
04	1	4	5	6	8	0.911
05	1	3	4	5	8	0.934
06	1	3	6	8	9	0.909
07	3	5	6	8	9	0.949
08	1	2	4	5	7	0.901
09	2	3	5	6	7	0.947
10	2	3	4	5	7	0.944
11	1	3	5	6	9	0.931
12	1	3	5	6	7	0.954
13	1	4	6	8	9	0.955
14	1	6	7	8	9	0.909

Table 28. Selected Repeats of Section 040664.

Visit	Repeat Numbers					Composite Correlation
01	2	4	5	7	8	0.856
02	2	3	4	5	6	0.907
03	1	3	5	6	7	0.912
04	5	6	7	8	9	0.861
05	4	6	7	8	9	0.868
06	4	5	7	8	9	0.891
07	1	2	3	6	9	0.926
08	1	3	4	5	7	0.898
09	1	2	3	5	7	0.920
10	1	2	3	4	6	0.934
11	1	3	4	5	7	0.936
12	1	4	5	7	9	0.943
13	1	2	3	4	7	0.952
14	3	4	6	7	9	0.853

Table 29. Selected Repeats of Section 040665.

Visit	Repeat Numbers					Composite Correlation
01	5	6	7	8	9	0.841
02	1	3	4	5	6	0.907
03	1	3	5	6	7	0.940
04	1	3	5	7	9	0.902
05	1	3	4	6	9	0.919
06	2	4	5	8	9	0.905
07	2	3	5	6	9	0.940
08	2	3	4	6	7	0.902
09	1	2	3	4	7	0.908
10	1	2	4	5	6	0.932
11	1	3	4	6	7	0.942
12	1	3	4	7	8	0.950
13	2	3	6	8	9	0.948
14	2	3	6	7	9	0.891

Table 30. Selected Repeats of Section 040666.

Visit	Repeat Numbers					Composite Correlation
01	4	6	7	8	9	0.807
02	1	2	4	5	6	0.895
03	1	3	5	6	7	0.940
04	2	3	4	6	8	0.880
05	2	3	5	7	9	0.889
06	2	4	5	8	9	0.870
07	3	5	6	7	9	0.902
08	1	2	4	6	7	0.908
09	3	4	5	6	7	0.902
10	1	2	4	5	6	0.912
11	3	4	6	7	8	0.914
12	1	3	5	6	8	0.942
13	1	2	3	6	7	0.918
14	1	2	3	7	8	0.882

Table 31. Selected Repeats of Section 040667.

Visit	Repeat Numbers					Composite Correlation
01	2	5	6	7	9	0.914
02	1	2	3	4	6	0.957
03	1	4	5	6	7	0.955
04	1	2	4	5	6	0.949
05	2	3	5	6	9	0.947
06	2	5	6	7	9	0.943
07	1	2	4	6	8	0.965
08	1	3	4	5	6	0.959
09	2	3	4	5	6	0.956
10	1	2	3	4	5	0.964
11	1	2	4	6	7	0.968
12	1	3	4	7	9	0.971
13	2	5	6	7	8	0.972
14	1	2	7	8	9	0.927

Table 32. Selected Repeats of Section 040668.

Visit	Repeat Numbers					Composite Correlation
01	4	6	7	8	9	0.682
02	2	3	4	5	6	0.861
03	1	3	4	6	7	0.890
04	1	2	7	8	9	0.849
05	2	3	6	8	9	0.873
06	1	3	4	6	8	0.864
07	1	2	3	6	7	0.890
08	1	3	4	5	6	0.863
09	2	3	4	5	6	0.873
10	1	2	3	5	6	0.901
11	1	2	3	4	8	0.900
12	1	2	3	5	8	0.915
13	2	5	6	7	9	0.918
14	1	2	7	8	9	0.826

Table 33. Selected Repeats of Section 040669.

Visit	Repeat Numbers					Composite Correlation
01	1	3	4	7	8	0.852
02	2	3	4	5	6	0.932
03	1	3	4	5	7	0.952
04	1	3	5	6	8	0.931
05	1	2	5	6	7	0.924
06	4	5	7	8	9	0.932
07	2	3	7	8	9	0.944
08	2	4	5	6	7	0.918
09	3	4	5	6	7	0.940
10	1	2	3	4	6	0.947
11	2	4	5	6	8	0.955
12	1	2	4	7	9	0.962
13	1	2	3	4	6	0.945
14	1	2	5	6	8	0.878

Overall, most of the groups of measurements listed in Tables 15 through 33 exhibited acceptable correlation, and nearly half of them exhibited good or excellent correlation. Agreement was lowest overall for visits 01 through 04. Agreement improved significantly for the later visits, and was good or excellent on every section in visits 10 through 13.

Any group of repeat measurements that produced a composite correlation level below 0.82 was investigated using filtered plots, and they are discussed here along with other cases of low but acceptable correlation.

In many cases, correlation was diminished because of modest disagreement in the severity of narrow bumps that had reflected upward from the original joints. Diminished correlation was most prevalent in visit 02 of Sections 040603 and 040607; visit 03 of Sections 040603, 040608, and 040661; visit 04 of Sections 040607 and 040661; and visit 06 of Section 040608.

Uncorrelated short wavelength content diminished the correlation in a few cases: visit 01 of Section 040665, visit 04 of Section 040661, visit 08 of Section 040608, and visit 09 of Section 040661. In the latter two cases, the effect of the resulting “chatter” that appeared in the profiles was severe. Visit 01 of Section 040668 also showed diminished correlation because of severe chatter in the right-side profiles.

Other observations are given below:

- Section 040601, visit 01: Inconsistency in the severity of deep narrow dips at distressed joints reduced the correlation level.
- Section 040601, visit 02: Three of the seven profiles (repeats 5–7) did not cover the entire section. Repeat 5 was selected because it was the longest, but the lack of seven viable repeat measurements left no room for exclusion of profiles with other problems.
- Section 040601, visit 04: Repeat numbers 4–8 exhibited artificial roughness caused by lost lock (Evans and Eltahan 2000). This was the least severe in Repeats 5 and 6, but this condition significantly diminished the composite correlation level.
- Section 040608, visit 14: These measurements included several deep spikes on the right side. Repeat measurements did not agree on their severity. The measurements also did not agree on the shape of a very rough section of pavement on the left side from 365 to 390 ft into the section. Evidence of this rough section first appeared in visit 08.
- Section 040659, visits 03 and 06: These visits showed general disagreement in short wavelength content, including some uncorrelated upward spikes.
- Section 040662, visit 06: These measurements did not agree on the shape, severity, or existence of a 6 ft wide bump in the right-side profile about 160 ft from the start of the section.
- Section 040666, visit 01: These profiles showed general disagreement in short wavelength content, primarily on the left side.
- Section 040668, visit 01: This group included poorly correlated short wavelength content in the left-side profiles.
- Section 040668, visit 14: This visit showed general disagreement in short wavelength content on both the left and right side. In particular, repeat 1 agreed with the others to a much lesser extent than they agreed with each other.

SUMMARY ROUGHNESS VALUES

Figures 50 through 68 show the left and right IRI values for each pavement section over its monitoring period. For most of the sections, this includes at least 28 summary IRI values: two per visit over 14 visits (Table 14). The figures show the IRI values versus time in years. In this case, “years” refers to the number of years between the measurement date and the date that the site was opened to traffic after rehabilitation (October 6, 1990). Fractions of a year are estimated to the nearest day.

To supplement the plots, Appendix C lists the IRI, Half-car Roughness Index (HRI), and Ride Number (RN) of each section for each visit. These roughness values are the average of the five repeat measurements selected in the data quality screening. These are not necessarily the same five repeat measurements selected for the LTPP database. Appendix C also provides the standard deviation of IRI over the five repeat measurements. This helps identify erratic roughness values that result from transverse variations in profile caused by surface distresses.

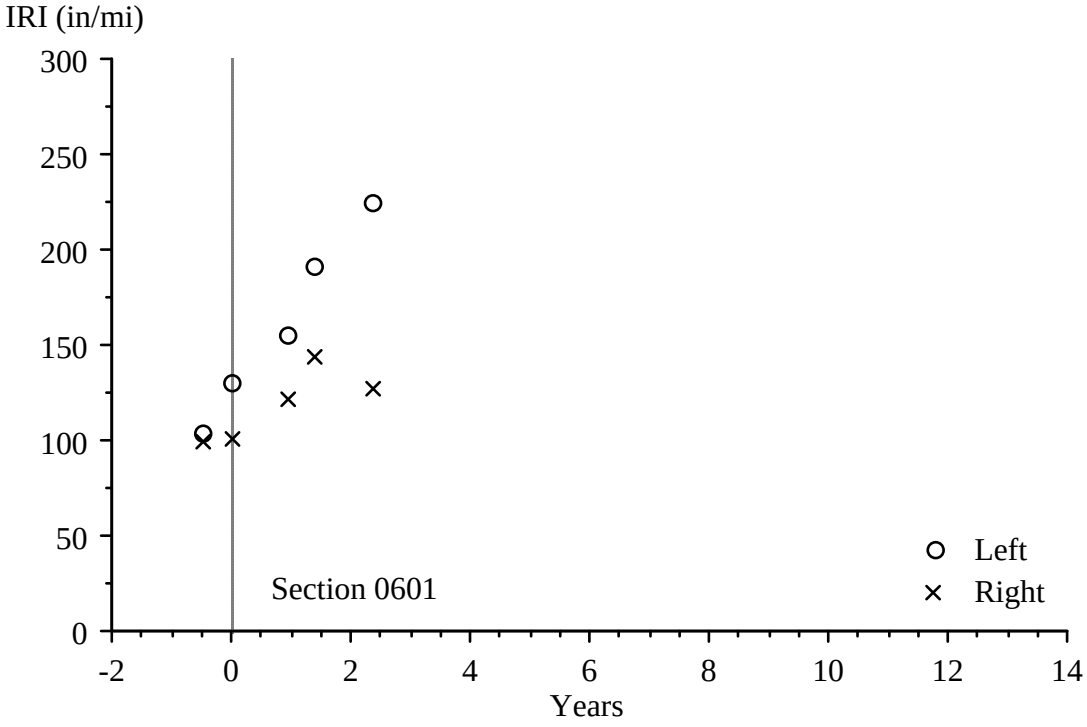

Figure 50. IRI Progression of Section 040601.

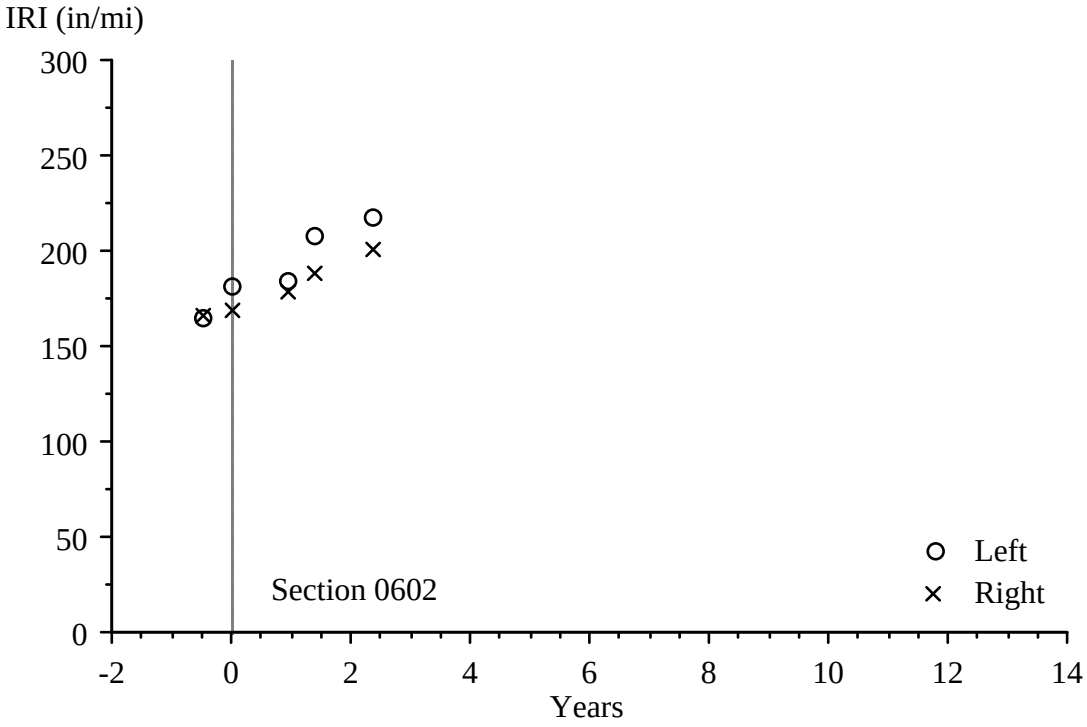

Figure 51. IRI Progression of Section 040602.

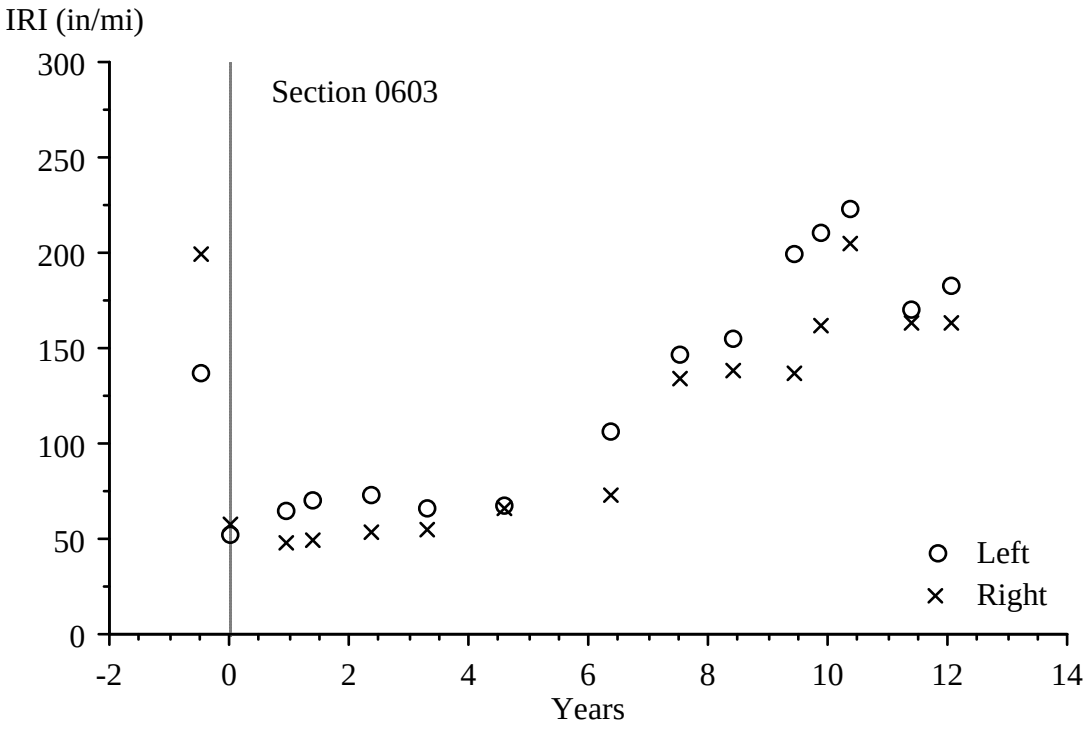

Figure 52. IRI Progression of Section 040603.

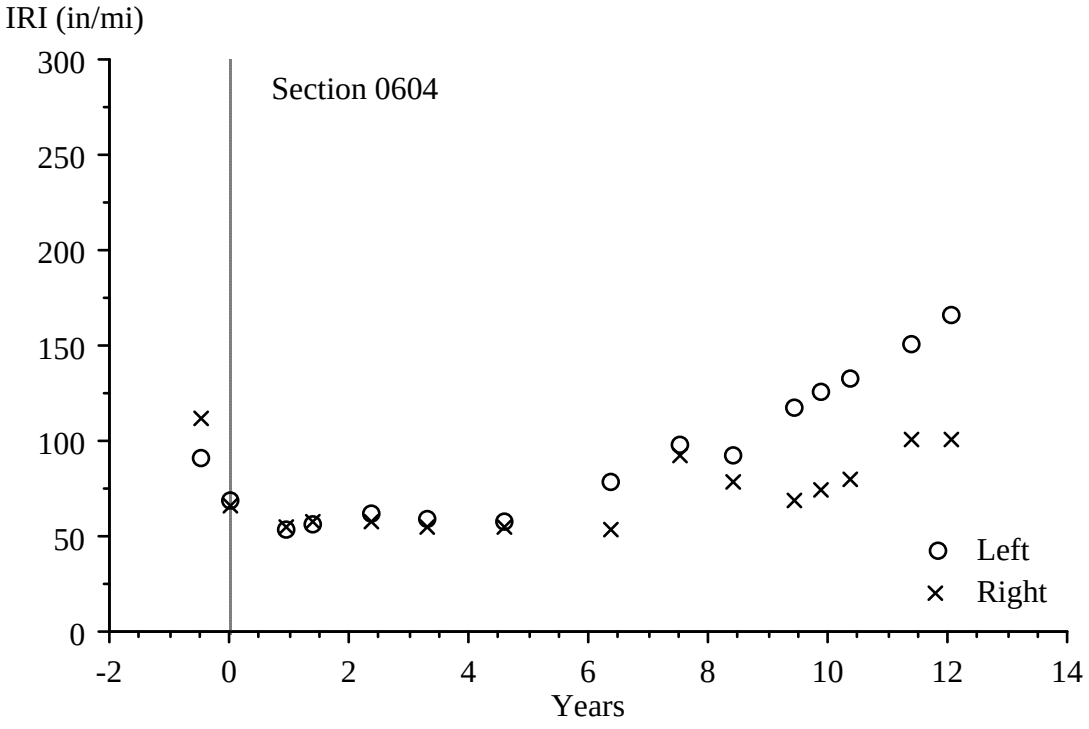

Figure 53. IRI Progression of Section 040604.

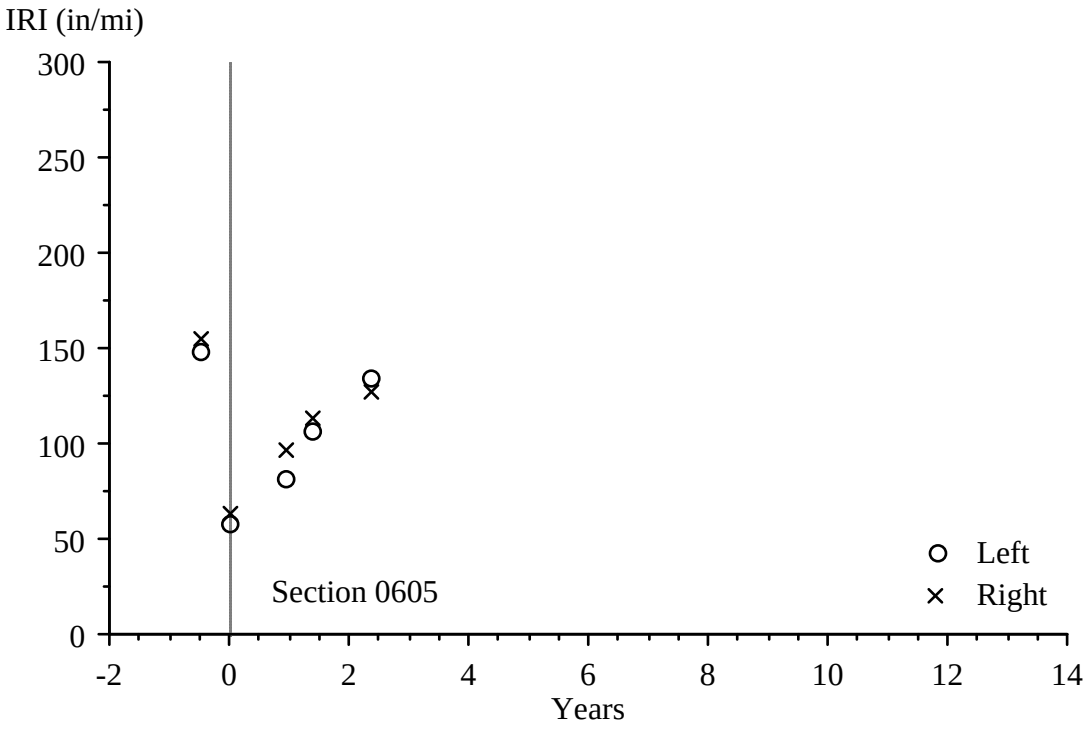

Figure 54. IRI Progression of Section 040605.

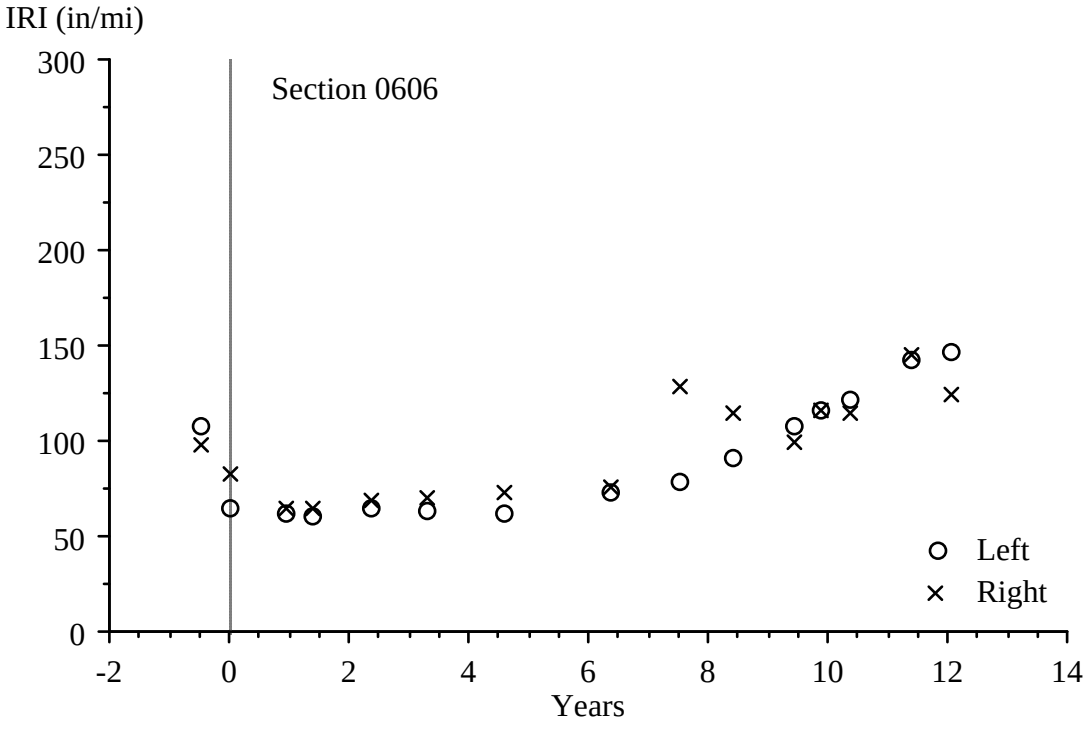

Figure 55. IRI Progression of Section 040606.

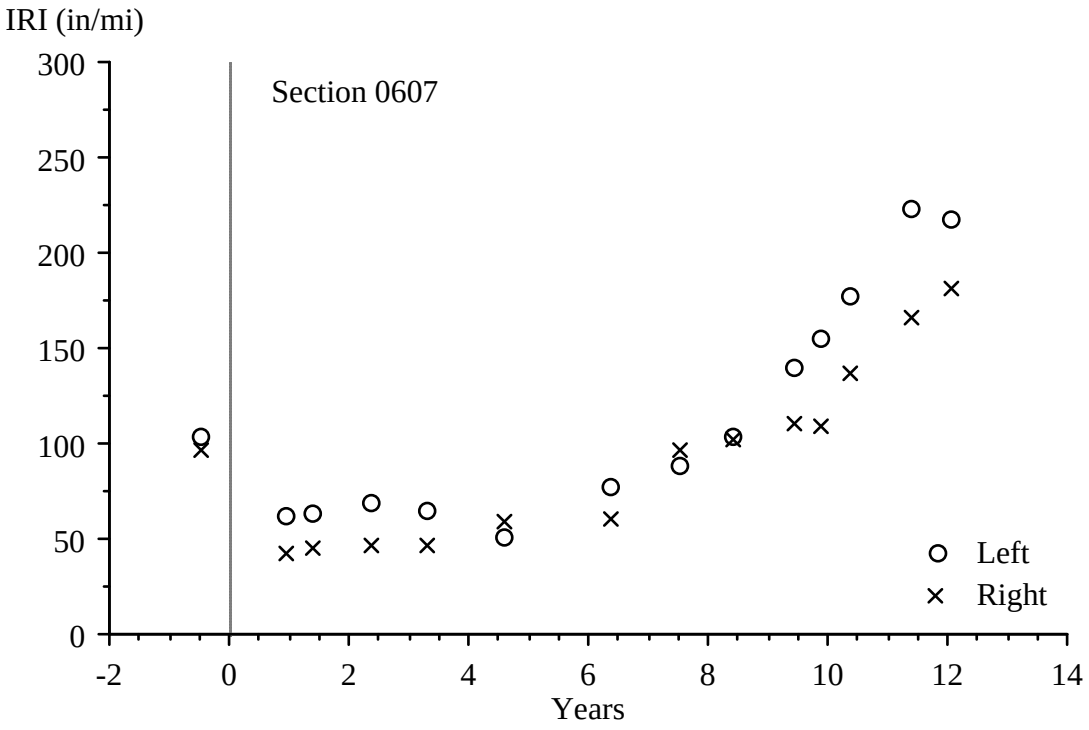

Figure 56. IRI Progression of Section 040607.

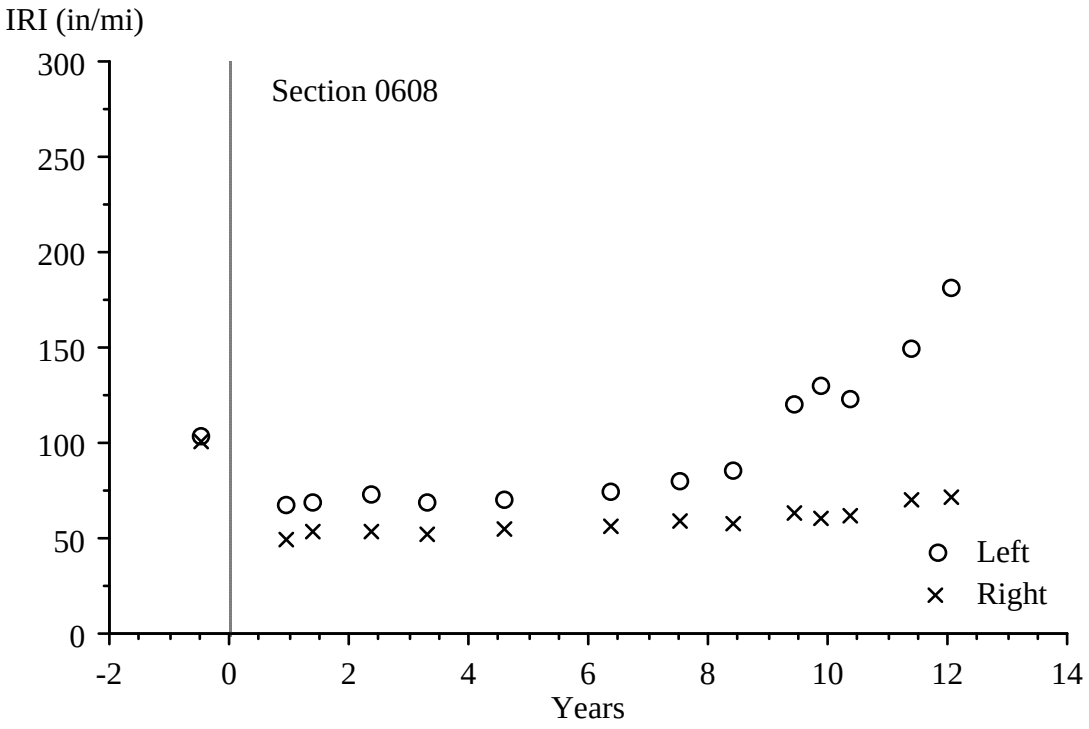

Figure 57. IRI Progression of Section 040608.

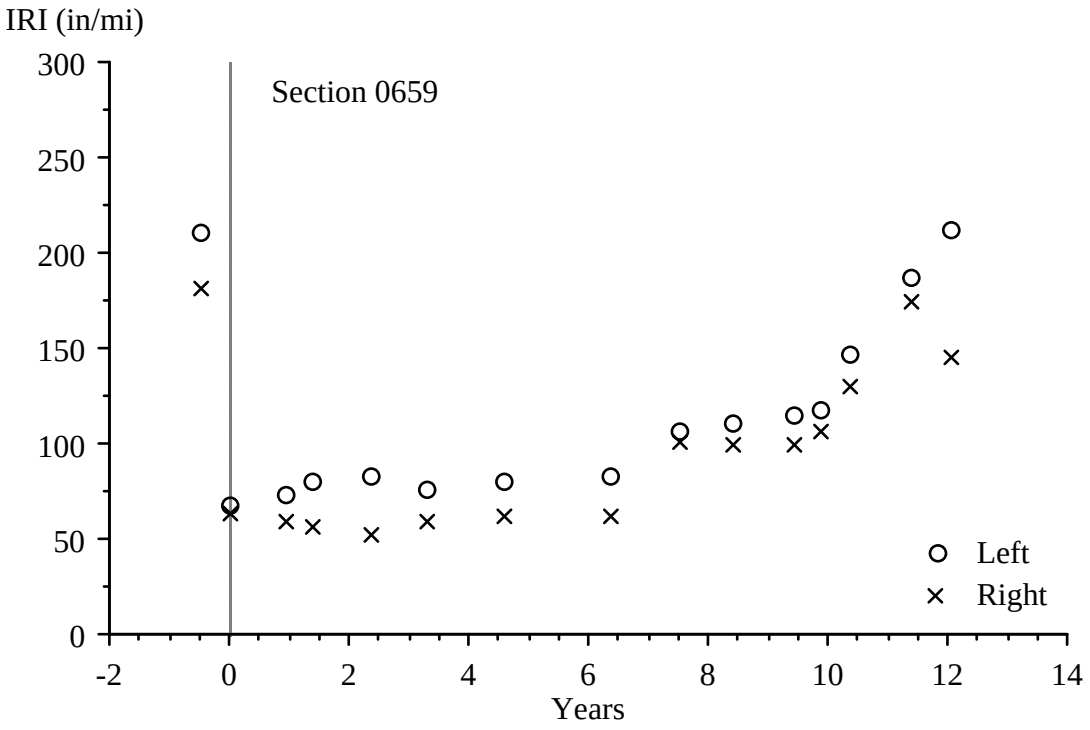

Figure 58. IRI Progression of Section 040659.

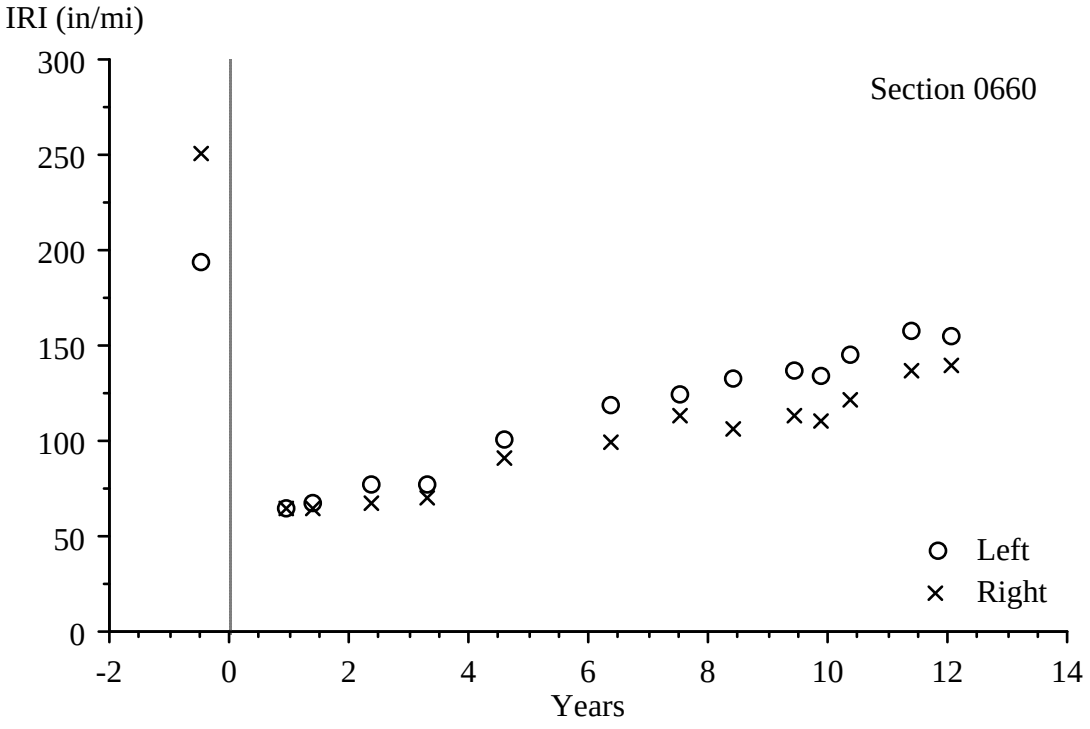

Figure 59. IRI Progression of Section 040660.

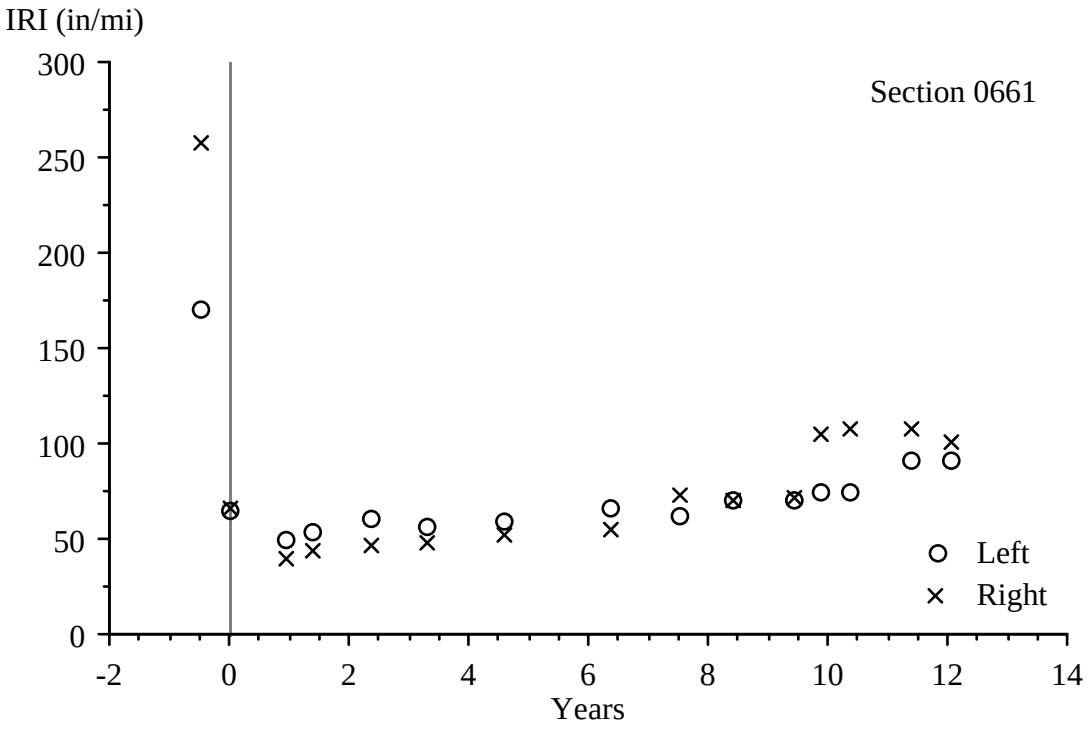

Figure 60. IRI Progression of Section 040661.

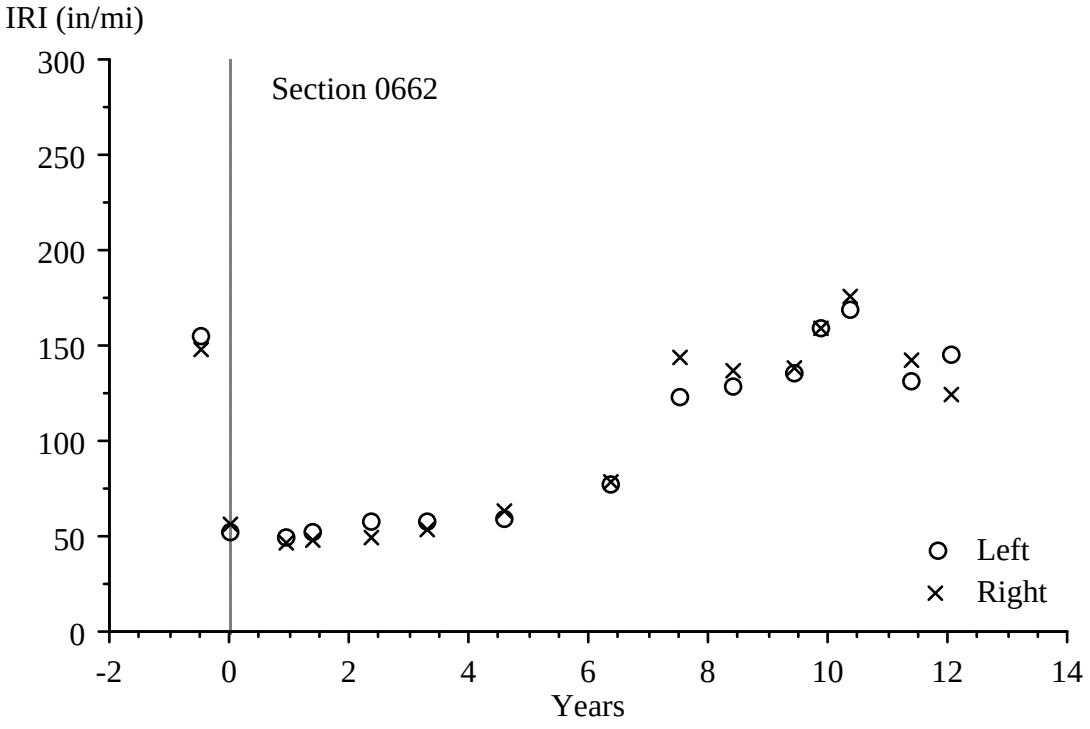

Figure 61. IRI Progression of Section 040662.

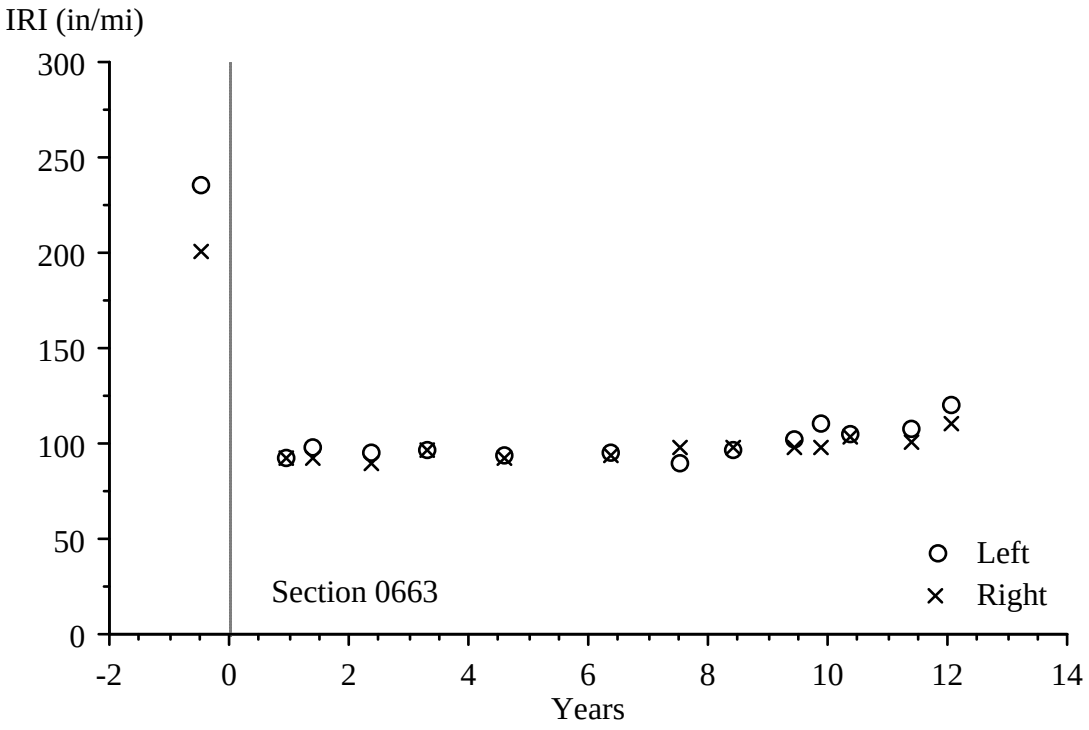

Figure 62. IRI Progression of Section 040663.

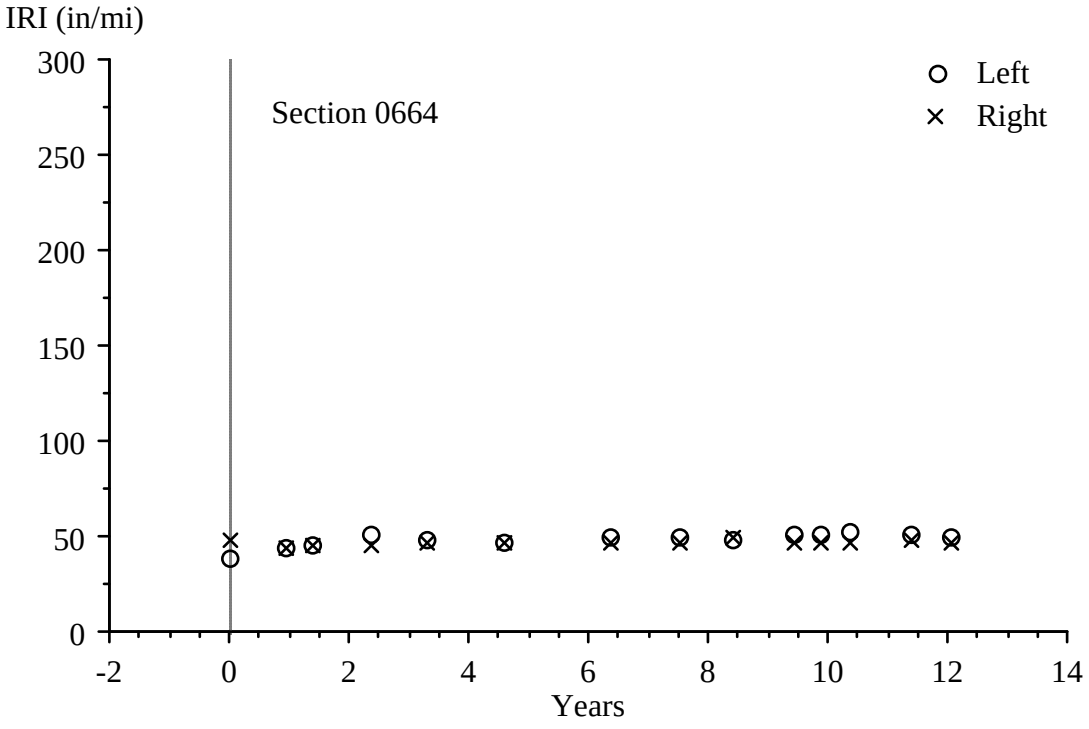

Figure 63. IRI Progression of Section 040664.

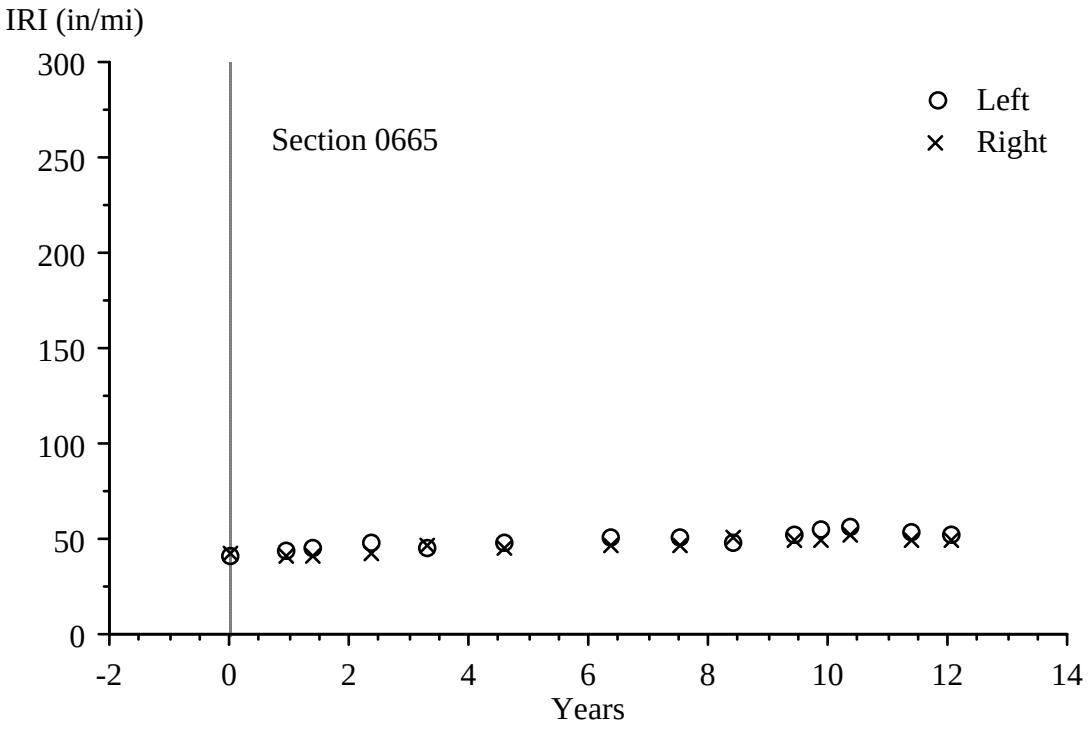

Figure 64. IRI Progression of Section 040665.

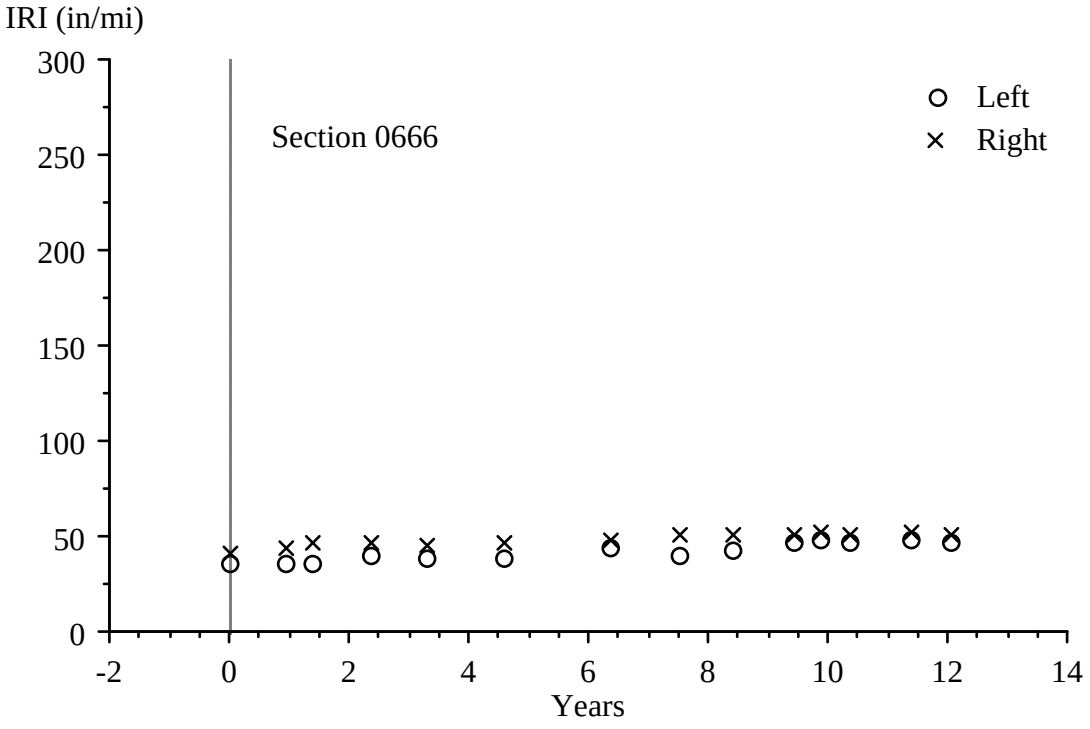

Figure 65. IRI Progression of Section 040666.

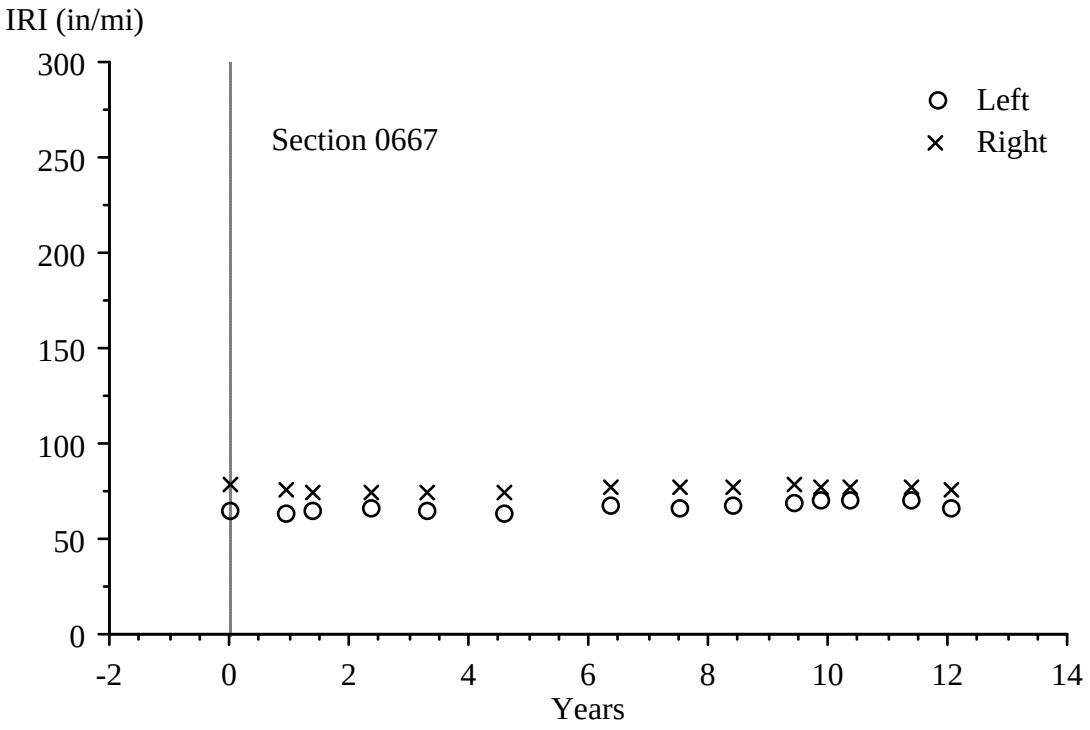

Figure 66. IRI Progression of Section 040667.

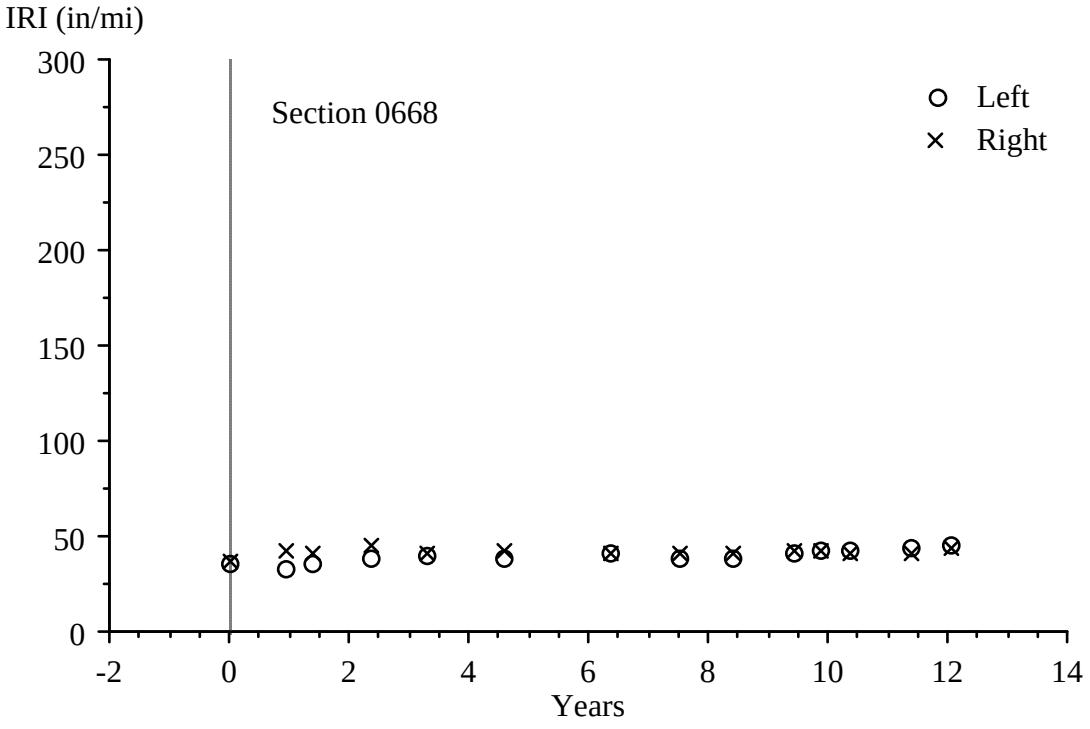

Figure 67. IRI Progression of Section 040668.

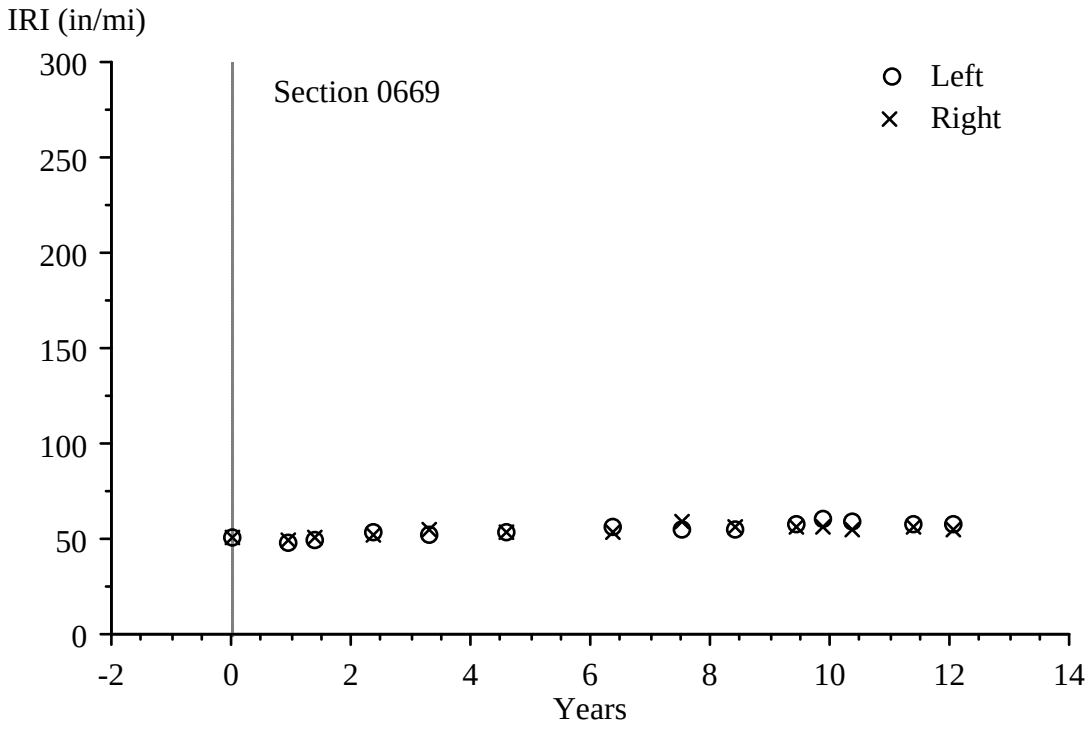

Figure 68. IRI Progression of Section 040669.

Figures 50 through 68 provide a snapshot of the roughness history of each pavement section. The remainder of this report is devoted to characterizing the profile content that made up the roughness and explaining the profile features that contributed to roughness progression.

PROFILE ANALYSIS TOOLS

Investigators used various analytical techniques to study the profile characteristics of each pavement section and their change with time. These tools help study roughness, roughness distribution, and roughness progression of each test section, including concentrated roughness that may be linked to pavement distress. The discussion of each analysis and plotting method is brief; Sayers and Karamihas (1996) provide more details about these methods.

Summary Roughness Values

Left IRI, right IRI, Mean Roughness Index (MRI), HRI, and RN values were calculated. Appendix C provides the average value of each index for each visit of each section. This report's discussion of roughness emphasizes the left and right IRI. Nevertheless, comparing the progression of HRI and RN to the MRI offers additional information about the type of roughness that is changing. For example, a low HRI value relative to MRI indicates roughness that exists on only one side of

the lane. Further, aggressive degradation of RN without a commensurate growth in MRI signifies that the developing roughness is biased toward short wavelength content.

Filtered Profile Plots

A simple way to learn about the type of roughness that exists within a profile is to view the trace. For example, Figure 69 shows the raw profile trace for five visits of Section 040603 throughout its monitoring history. The plot shows that the long wavelength content, or the trend, in each plot is quite consistent with time. Of particular interest is the consistency in long wavelength content between the profile measured in April 1990, which occurred before rehabilitation, and the profile measured in September 1990, which occurred after placement of a 4 inch AC overlay.

Figure 69 illustrates some features of the roughness and its progression on Section 040603. The profile measured before rehabilitation includes multiple disturbances in a saw-tooth shape. The downward steps at the trailing edge of each “tooth” are joint faults, and the saw-tooth shape is present as a result of the associated slab tilt.

Several short-duration disturbances such as bumps and dips appear in the profile measured in May 1995 that do not appear in the September 1990 profile. In the two subsequent visits shown, roughness progresses with time in the form of narrow dips. Transverse cracking and the associated surface deformation at the borders of the cracks caused most of the narrow dips and small bumps.

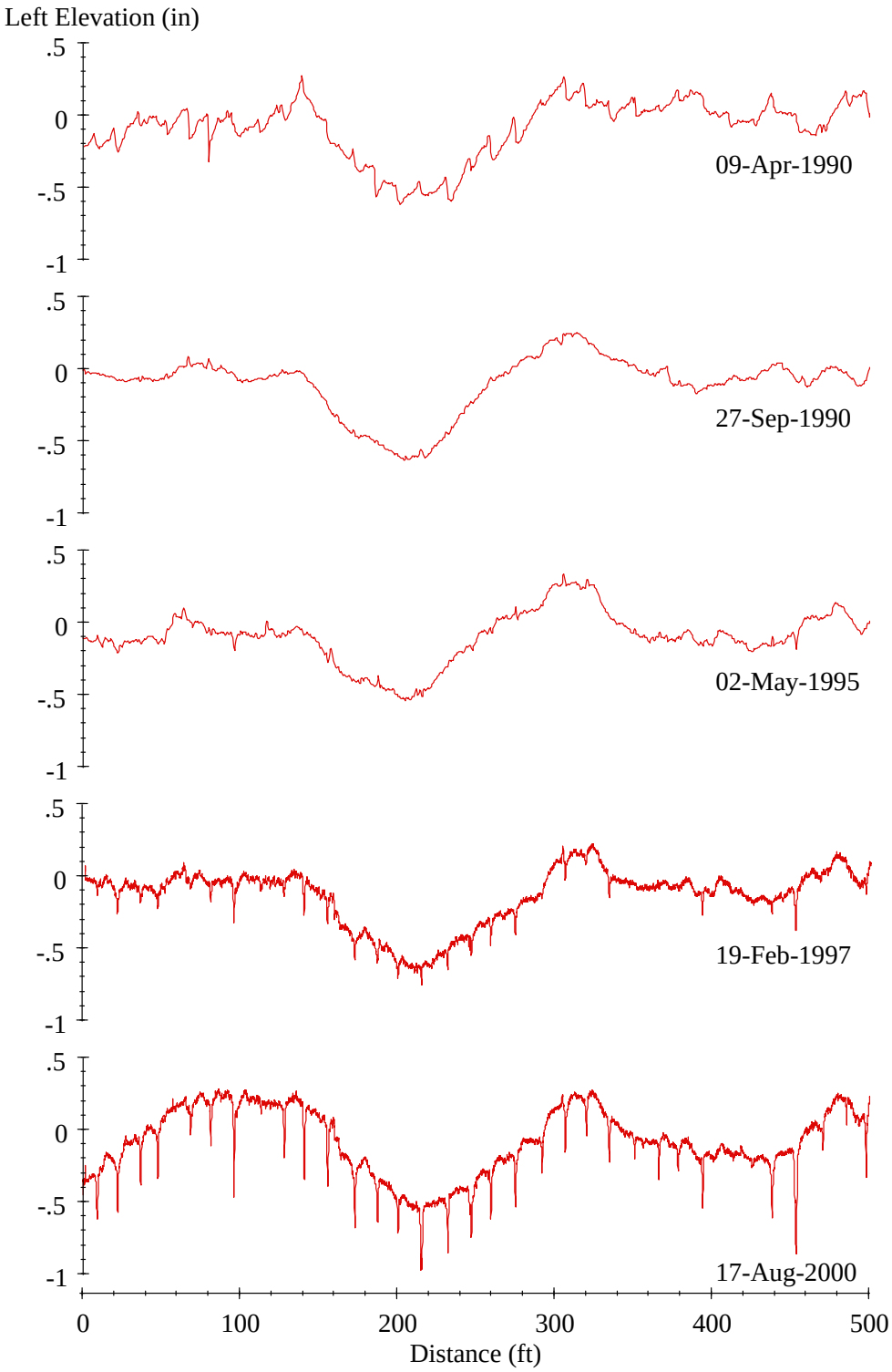

Figure 69. Raw Profiles of Section 040603.

By August 2000 the narrow dips are deep and numerous, standing out in the raw profile plot. However, the raw profile plot is not ideal for recognizing when the dips first appear or

characterizing their shape and width. Figure 70 provides a closer look at one of the dips after a moving average anti-smoothing filter is applied using a base length of 10 ft. This high-pass filter removes much of the roughness in the profile associated with changes in elevation over distances longer than 10 ft (including the long trends visible in Figure 69) and leaves most of the very short duration changes in elevation intact.

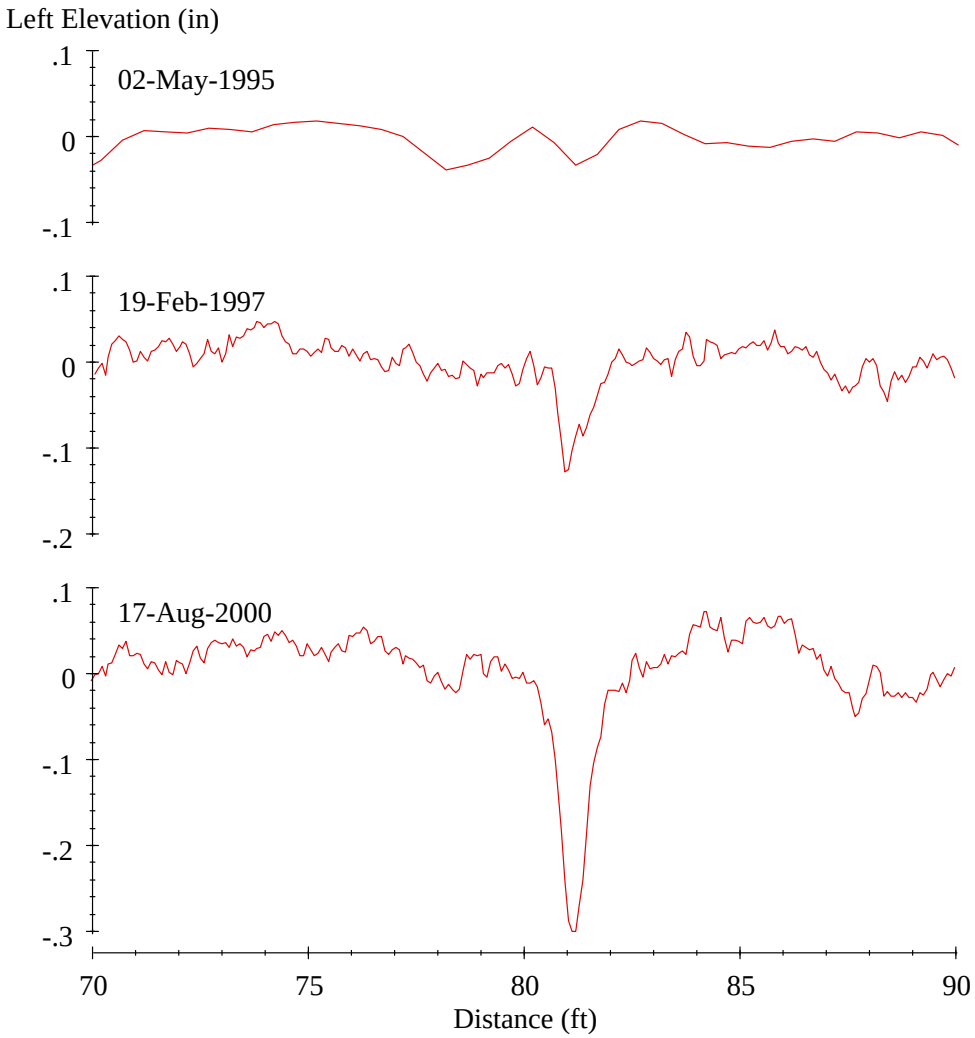

Figure 70. High-Pass Filtered Profiles of Section 040603.

Figure 70 shows a clear progression in the depth of the dip—from a small ripple in May 1995 to a deep, narrow dip in August 2000. An important feature of the dip is its width. The dip is about 1 ft wide, which is much wider than the crack that caused it. This dip is likely to degrade ride quality and penalize the IRI value much more than a narrower dip with the same depth.

Any of the dips that stand out in the February 1997 profile measurements appear as much shallower dips in the same location in May 1995. (This was the case on all of the test sections

with significant transverse cracking.) The change in severity between these two measurement dates has two potential causes. First, the dip itself may have grown more severe. However, the dip was rated as medium severity in distress surveys in August 1994, October 1997, and December 1999. (In October 2000 and later, the crack was rated as high severity.) Second, the profile measurement was made with a K.J. Law T-6600 in 1995 and an International Cybernetics Corporation (ICC) MDR 4086L3 in 1997. This is important because the T-6600 used a height sensor footprint with a transverse dimension of 1.5 inches and a longitudinal dimension of 0.24 inch, whereas the MDR 4086L3 used a point laser with a 0.06 inch diameter (Perera and Kohn 2005). The large footprint of the T-6600 may have blunted the dips.

Profiles of Section 040603 late in the monitoring history (starting in August 2000) included narrow dips throughout the entire section and in the same locations where joint faults appeared in the prerehabilitation profiles. Figure 71 illustrates the close relationship. The figure shows segments from both profiles after application of a moving average anti-smoothing filter with a base length of 10 ft. In the faulted profile of April 1990, the filter distorts the faults, and they appear as abrupt downward changes in elevation that follow each upward spike. However, the filter makes the faults easier to see.

Figure 71 shows that the narrow dips in Section 040603 appear in the same pattern and in the same locations as the faults on the left side of the lane, which occurred in a pattern that approximated the original joint spacing of 15-13-15-17 ft. On the right side (not shown), the same pattern of faults before rehabilitation and narrow dips caused by transverse cracks late in the monitoring history is also present. However, the pattern is shifted about 1 ft downstream because of the skewed saw cuts. The synchronization process itself did not guarantee this alignment. Profiles collected before rehabilitation were only aligned to those afterward using data within Section 040601 and extrapolation over the rest of the site.

Many of the test sections in this SPS-6 project exhibited the same behavior. The profiles included narrow dips at transverse cracks that could be linked to joints through faulting detected in the prerehabilitation profiles.

Two types of filtered plots were inspected for every visit of every test section:

- Raw profiles: A plot of a profile with no filtering except the filters applied before conversion to an ASCII format. In some cases, a moving average anti-smoothing filter was applied with a base length of 100 ft.
- Short wavelength: A plot of a profile anti-smoothed using a moving average with a base length of 10 ft.

These plots were used to screen the profiles for changes with time and other features.

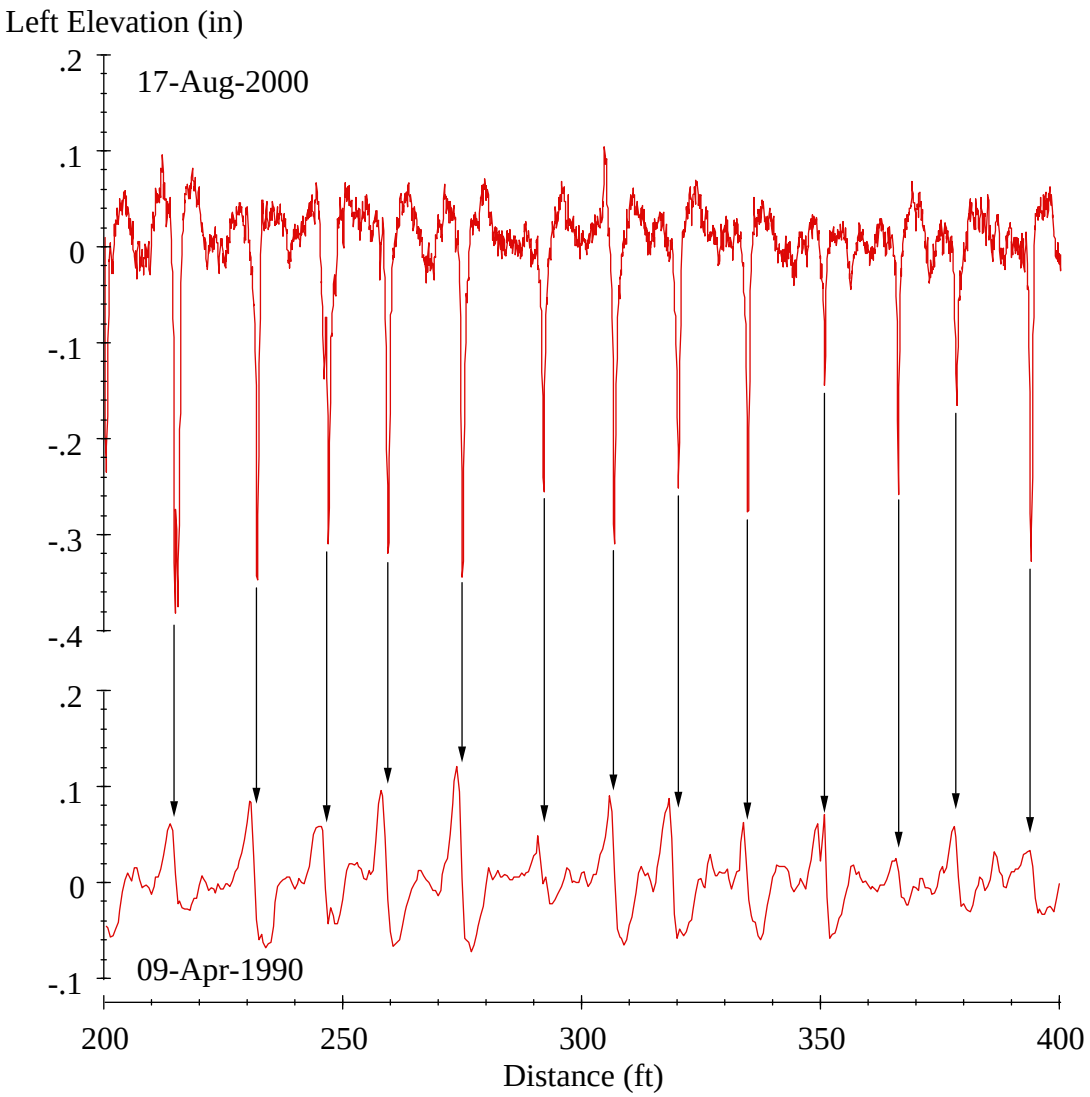

Figure 71. Joint and Crack Locations on Section 040603.

The raw profiles provided a broad view of the surface properties and an opportunity to identify the roughest features within a given test section. The short wavelength elevation plots provided a closer view of key features of interest because short-duration features such as faults and narrow dips stood out more readily. The most common features studied using the short wavelength plots were: (a) joint faulting, (b) narrow dips at saw cuts, (c) narrow dips at transverse cracks, (d) deep dips at potholes, and (e) short wavelength content of high amplitude over areas of high-severity fatigue and rough patching.

Roughness Profile Plots

A roughness profile provides a continuous report of road roughness using a short segment length. Instead of summarizing the roughness by providing the IRI for an entire pavement section, the roughness profile shows the details of how IRI varies with distance along the section. It does this by using a sliding window to display the IRI of every possible segment of given base length along the pavement (Sayers 1990).

A roughness profile displays the spatial distribution of roughness within a profile. As such, it can be used to distinguish road sections with uniform roughness from sections with roughness levels that change over their length. Further, the roughness profile can pinpoint locations with concentrated roughness and provide an estimate of the contribution of a given road disturbance to the overall IRI.

Figure 72 is a roughness profile of Section 040660 measured in September 1991. The roughness profile was generated using a base length of 100 ft, that is, every point in the plot shows the IRI of a 100 ft segment of road, starting 50 ft upstream and ending 50 ft downstream. No data are shown over the 50 ft at each end of the section because the plot was generated using a profile that terminated at the section boundaries. The plot shows that the first 250 ft of the section are more than twice as rough as the last 200 ft.

The profile featured in Figure 72 was measured shortly after rehabilitation, and it represents the status of the section just after rehabilitation. The construction process itself caused the roughness in the first half of the section. Figure 73 is an elevation profile that corresponds to Figure 72 after application of a moving average anti-smoothing filter with a base length of 100 ft. This figure shows that the roughness is caused by some very long duration features. The long dip running 30 to 90 ft from the start of the section deteriorated over time, and eventually became so rough by growing in depth that a skin patch was placed over it.

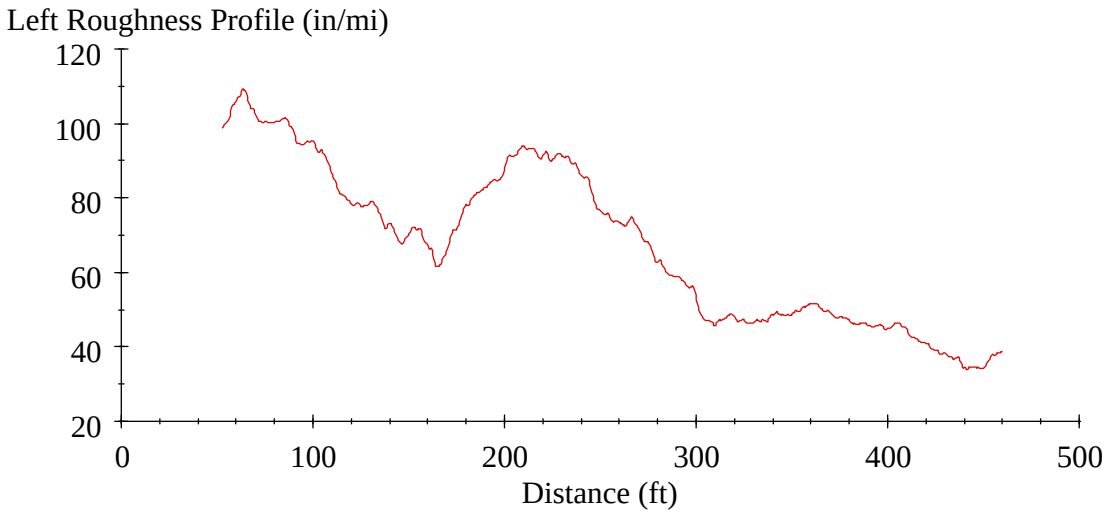

Figure 72. Roughness Profile of Section 040660 (100 ft Base Length, September 1991).

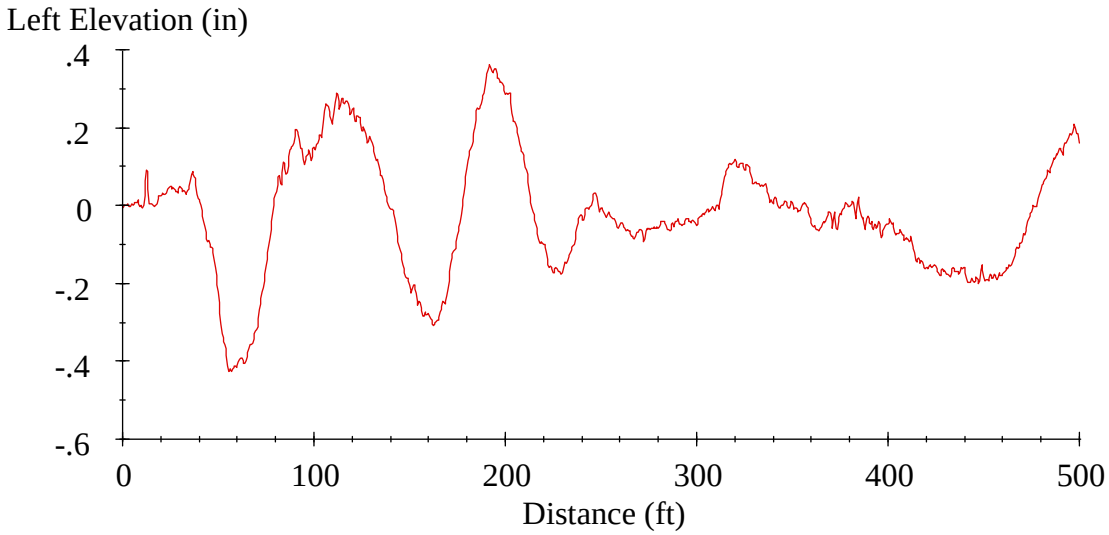

Figure 73. Elevation Profile of Section 040660 (September 1991).

Figure 74 shows how a roughness profile can help find localized roughness and quantify its impact on the overall roughness of a test section. This figure shows the roughness profile of Section 040603 for the three most recent profiles given in Figure 69. The plot was generated using a 5 ft base length, so each point shows the contribution to the IRI that has accumulated over 5 ft. A base length of 25 ft is more standard for the purpose of seeking localized roughness (AASHTO 2008; Swan and Karamihas 2003). But a short base length was required to isolate the closely spaced dips in this section and easily identify roughness. For example, many of the dips highlighted in Figure 71 produced peak values greater than 400 inches/mi in Figure 74. Since

these peaks correspond to roughness over 1 percent of the test section length, they each account for more than 4 inches/mi of the section's overall IRI.

Figure 75 shows how a roughness profile can help find and quantify isolated roughness. The figure shows the right roughness profile of Section 040661 from August 2000 using a 25 ft base length. With this base length, the area of concern about 375 ft from the start of the section is easy to identify. The peak value there is about 678 inches/mi, which is more than 575 inches/mi above the prevailing roughness level surrounding it. This is a difference of 575 inches/mi over 25 ft. Since that value represents the roughness over just 5 percent of the segment, it suggests that a rough feature here increased the overall IRI of the section by nearly 29 inches/mi.

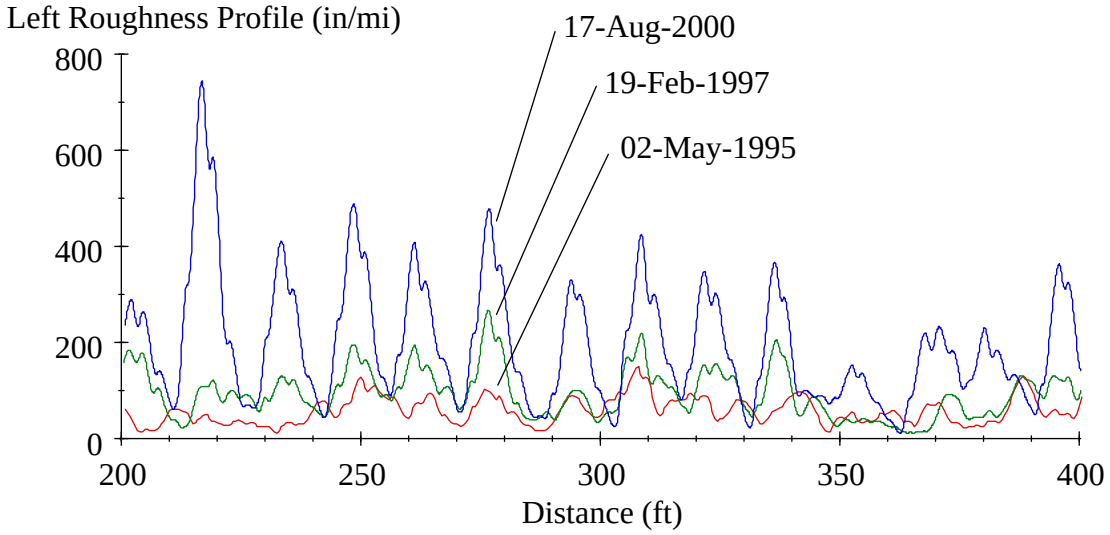

Figure 74. Roughness Profiles of Section 040603 (5 ft Base Length).

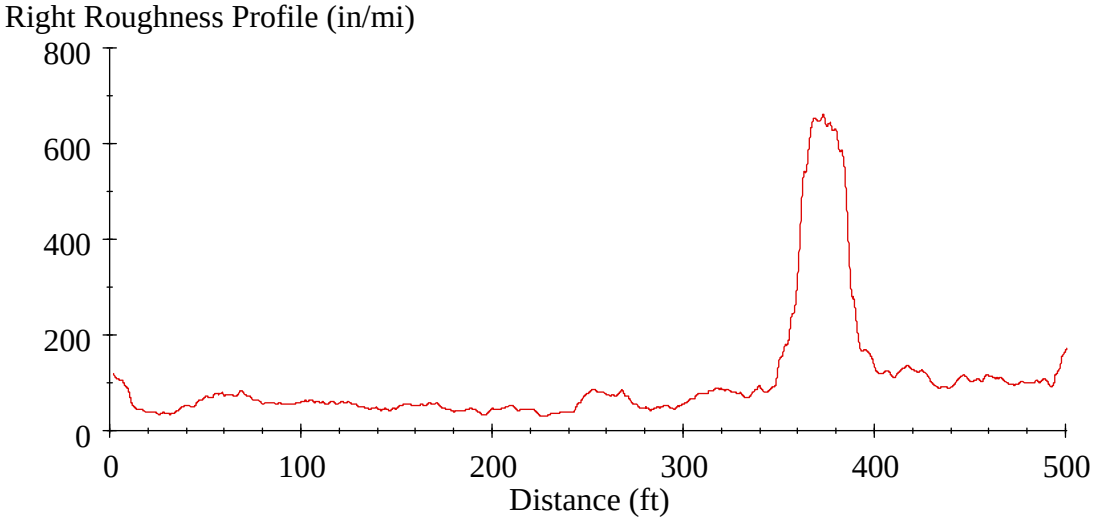

Figure 75. Right Side Roughness Profile of Section 040661 (August 2000).

Figure 76 shows the elevation profile of Section 040661 that produced the roughness profile in Figure 75. The profile includes a significant dip and significant disturbances within the dip. Figure 77 is a photograph of the distress that caused the disturbance. Significant localized fatigue is present between the fog line and about 5 ft into the section from the right side. This fatigue cracking developed in the winter and spring of 1999–2000 and is consistent with a "soft spot" in the pavement structure, possibly caused by excessive water buildup in the unbound layers. Many of the fines have pumped up to the pavement surface and are visible in Figure 77.

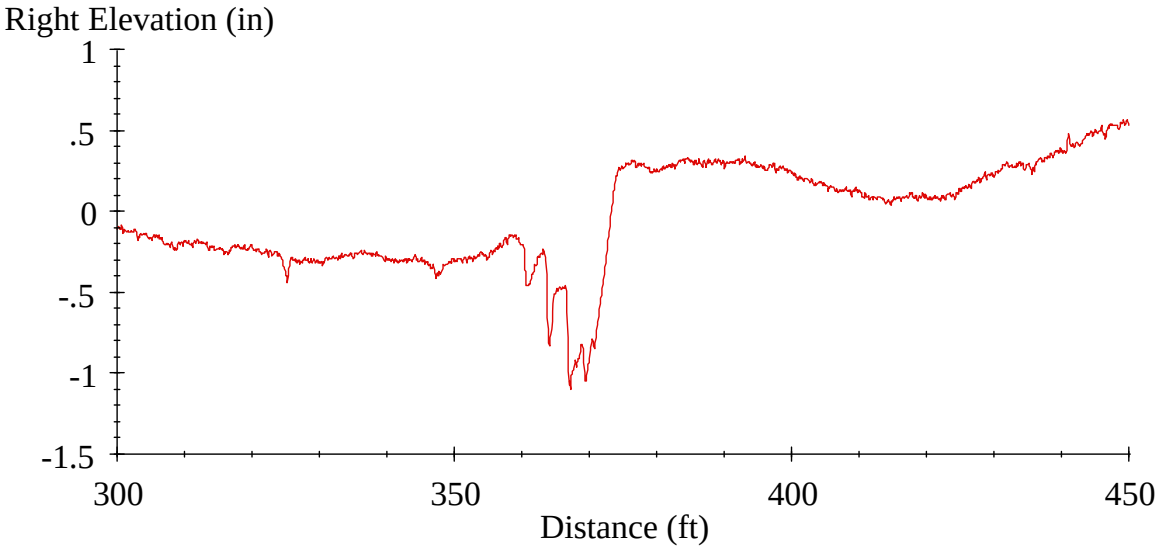

Figure 76. Right Side Elevation Profile of Section 040661 (August 2000).

In this section, the roughness was obvious using all three sources of information: the elevation profile, roughness profile, and distress survey data. But this isn't always the case. The roughness profile provided a systematic method of prioritizing rough features for further analysis. Any area is considered to have localized roughness when the roughness profile (with a base length of 25 ft) reaches a peak value that is greater than 2.5 times the average IRI for the whole section. Of the 1225 profile pairs analyzed in this study, 372 included localized roughness on the left side and 203 included localized roughness on the right side. Detection of localized roughness prompted more careful examination of the filtered elevation profiles, distress surveys and maintenance records.

Figure 77. A Fatigued Area with Pumping on Section 040661 (August 2000).

Power Spectral Density Plots

A power spectral density (PSD) plot of an elevation profile shows the distribution of its content within each waveband. An elevation profile PSD is displayed as mean square elevation versus wave number, which is the inverse of wavelength. A PSD plot is generated by performing a Fourier transform on a profile. The PSD's value in each waveband is derived from the Fourier coefficients and represents the contribution to the overall variance of the profile in that band.

Often, the wavebands used in a PSD plot are given a uniform spacing on a log scale. In this study, PSDs were typically displayed using 12 bands per octave. In other words, the center of each waveband was a factor of $2^{1/12}$ larger than the waveband to its left on the plot and a factor of $2^{1/12}$ smaller than the waveband to its right. This spacing provided enough detail to search for roughness that was isolated at a given wavelength, but enough averaging to eliminate spurious content that is common when PSDs are displayed using a linear wave-number scale. PSD plots were also calculated from the slope profile rather than the elevation profile because the content of a slope PSD typically covers fewer orders of magnitude than an elevation PSD. This aided in interpreting the plots.

PSD plots provided a very useful breakdown of the content within the profiles from this study. In particular, the plots revealed; (a) cases in which significant roughness is concentrated within a given waveband; (b) the type of content that dominates the profile, such as long, medium, or short wavelength; (c) the effectiveness of rehabilitation in eliminating roughness over each waveband; (d) the type of roughness that increases with time; and (e) the type of roughness that is stable with time.

Figure 78 shows the PSD of the left profile for Section 040604 measured in February 1997 and February 2001. This PSD plot includes several noteworthy features:

- The plot shows the PSD of slope rather than elevation; the vertical axis has units of slope^2/(wave number), as opposed to elevation^2/(wave number).
- The plot covers a range of wave numbers from 0.01 to 1 cycle/ft. This includes the range that affects IRI most.
- The spectral content from about 25 to 100 ft (wave numbers between 0.01 to 0.04 cycle/ft) did not change significantly with time.
- The spectral content for wavelengths below 25 ft increased between visits. Roughness in this range progressed in every visit from 1997 through 2001.
- In both profile measurement visits, the trend in the PSD grew in content with decreasing wavelength (increasing wave number) for wavelengths below 10 ft. This should be interpreted cautiously, however, because a single anomalous reading in the elevation profile or a single severe narrow dip would appear on a PSD plot this way. Alternatively, it may indicate uniform growth in short wavelength roughness over the entire length of the profile. In this case, the growth was caused by narrow dips in the profile at saw cuts that were placed over the underlying PCC joints and grew rougher as the sealant deteriorated.

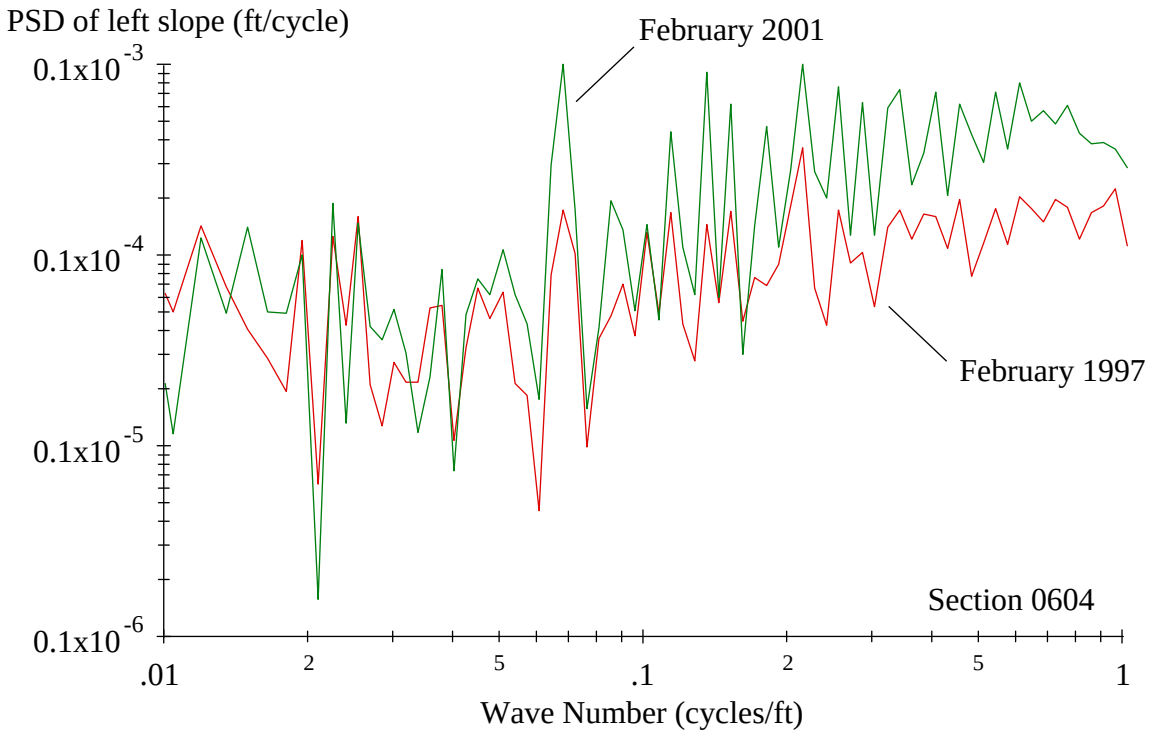

Figure 78. PSD of Section 040604 Profile (Left Side).

- The peak at about 0.067 cycle/ft indicates emerging periodic roughness concentrated at a wavelength of about 15 ft. This is present in the PSD because enough transverse cracks (and associated dips) appeared to form a pattern with a spacing of roughly 15 ft. The narrow dips were present in both visits, but they were much more severe in February 2001.

Each of the final four observations listed above provide important information about the nature of the roughness on Section 040604 and its progression. However, the PSD provides no information about where the roughness exists within the section. Further, if the roughness within a profile is concentrated in a single location, the PSD plot may provide misleading information. The filtered profile plots and the roughness profiles discussed below provide a more complete assessment of the roughness on a given pavement.

The PSD plot provides insight into the filtering practices of the profiler that made the measurements. Figure 79 is the PSD of the left profile of Section 040664 for profiles measured in September 1990, February 1997, and October 2002 over the maximum range allowed by the section length and sample interval. The measurements were made by a K.J. Law DNC 690 (1990 through 1995), a T-6600 (1997 through 2001), and an MDR 4086L3 (2002).

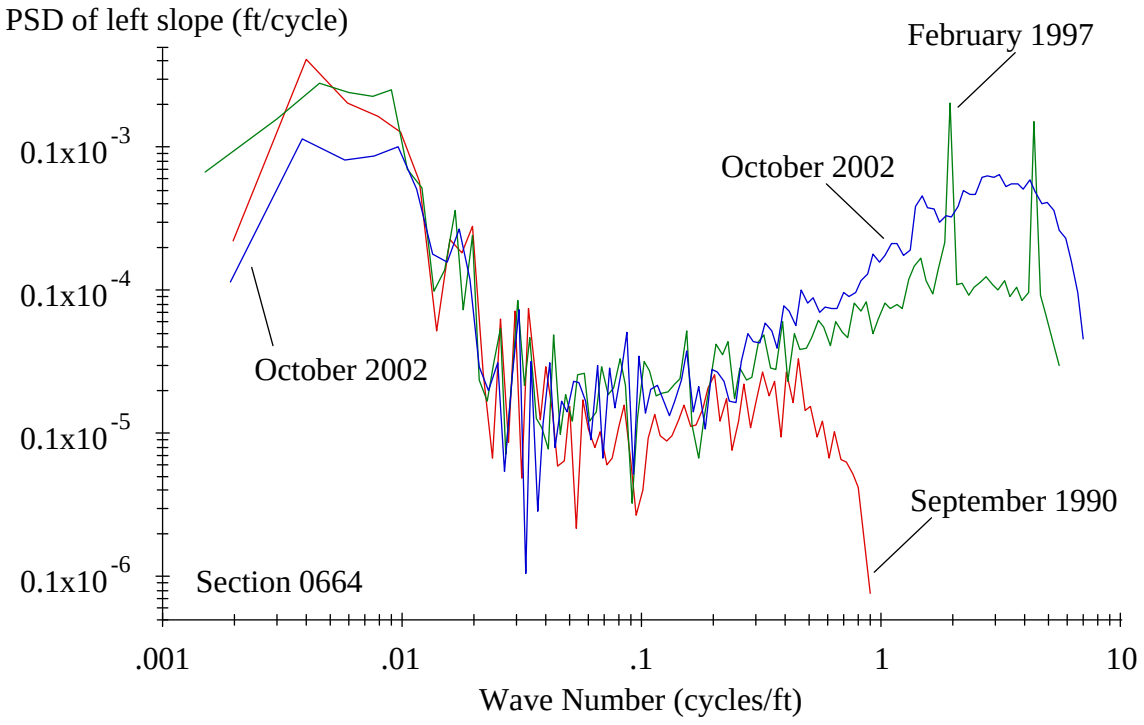

Figure 79. PSD of Section 040664 Profiles (Left Side).

Key observations about this plot include:

- Content at wave numbers below 0.01 cycle/ft (wavelengths above 100 ft) dominates the content in the PSD from September 1990. This is a common trait in the PSD plot for an elevation profile collected just after an overlay is placed since the process of placing an overlay often leaves little short wavelength roughness, but changes the long wavelength trends in the road very little.
- The spectral content for wave numbers between 0.01 and 0.25 cycle/ft (100 and 4 ft) is about the same in all three visits. This range affects IRI the most (Karamihas 2005).
- The spectral content differs for very long wavelengths (low wave numbers). This is not caused by a change in the true profile of the section but is the result of the changes in profiler and an associated change in the high-pass filtering methods (Perera and Kohn 2005). In particular, the content below a wave number of 0.01 cycle/ft is much lower in October 2002 after the transition from K.J. Law profilers to the MDR 4086L3 profiler.
- The spectral content in each trace decreases at short wavelengths (high wave numbers) near the end of the plotted range. This is an artifact of low-pass filtering applied at the time of the measurement, which is a combination of digital filtering and height sensor footprint (Karamihas 2005). Since each profiler stores data at a different interval, each profile applies a low-pass filter with a different cutoff value.
- The PSD plot for February 1997 includes a spike at a wave number of about 1.9 cycles/ft and another at a higher value. This is also an artifact of the measurement process, but the source is unclear. The spikes were present in all of the T-6600 profiler measurements. However, the spikes did not occur at the same wave number in each visit or in each repeat measurement within a given visit. The wave number where the left-most spike occurred ranged from about 1.67 to 3.06 cycles/ft.

The PSD plots provided significant information about the three profilers used to make measurements throughout the life of this SPS-6 project. The plots also helped to study slab-related effects within prerehabilitation profiles and profiles of sections with PCC surfaces. However, most of the insight into the behavior of AC overlays over time came from elevation profile plots and roughness profile plots.

Distress Surveys and Maintenance Records

Once the analysis and plotting was completed, all of the observations were compared to the manual distress survey performed on each section. Manual distress surveys were available for each section starting in 1991 and including up to six other visits throughout the rest of the study. This provided a means of relating profile features to known distresses. For this SPS-6 project, one observation was common: Dips that grew progressively rough with time were often found in the vicinity of transverse cracks or saw cuts, which in turn appeared in the locations where joint faulting was detected before rehabilitation.

Observations of changes in profile properties were also compared to maintenance records. For example, Sections 040603, 040659, 040660, and 040661 received skin patching that affected their roughness late in the project.

DETAILED OBSERVATIONS

This section summarizes observations from the study of roughness index progression, filtered profile plots, roughness profile plots, PSD plots, and distress surveys. In many cases, similar behavior was noted for multiple sections. Appendix D provides much more detailed observations. The test sections are grouped by overlay type:

- Sections 040601, 040602, and 040605 did not receive an overlay.
- Sections 040603, 040604, 040606, 040607, and 040659 each received a 4 inch AC overlay.
- Sections 040661, 040662, and 040664 through 040669 each received an overlay constructed with a combination of ARAC and AC.

Prerehabilitation

Before rehabilitation, all of the test sections included roughness that could be linked to faulting, spalling, corner breaks, shattered slabs, or other slab effects. However, the level of roughness and distress varied significantly along the site. This may have affected the relative performance of each rehabilitation alternative. Often groups of adjacent test sections had similar properties. Table 34 lists the roughness level, number of faulted joints, and an estimate of the faulting magnitude for the test sections in this study.

Table 34. Prerehabilitation Roughness.

Section	MRI (inch/mi)	Portion of Joints with Faulting	Faulting Magnitude (inch)
040660	196	All	0.05–0.40
040663	218	All	0.05–0.30
040608	103	Most	0–0.10
040607	100	None	—
040606	104	Few	0–0.10
040659	223	Most	0.05–0.25
040661	215	All	0.05–0.25
040604	102	Most	0–0.15
040662	152	Most	0–0.15
040603	169	All	0.05–0.30
040605	152	All	0.05–0.25
040602	166	All	0.05–0.30
040601	102	Few	0–0.1

No Overlay

Distress at joints accounted for most of the roughness in all three sections at the end of their service life. Faulting caused much of the roughness on Sections 040602 and 040605 before surface preparation, and faulting caused most of the roughness at the end of their service life. Section 040601 was not faulted before surface preparation; narrow dips at joints, rather than faulting, caused most of the roughness at the end of its service life.

- Section 040601 (routine surface preparation): The MRI of this section increased from 102 to 177 inches/mi in less than three years before it was taken out of the study. Most of the roughness and its increase were caused by narrow dips at spalled joints. Some of the dips grew to as wide as 4 ft and up to 1 inch deep.
- Section 040602 (minimum surface preparation): This section's MRI increased from 166 to 210 inches/mi in less than three years before it was taken out of the study. Faulting at joints and midslab cracks and the associated tilting of the pieces caused most of the roughness and its increase. Localized roughness was observed at a map cracked slab.
- Section 040605 (maximum surface preparation): The MRI of this section decreased from 152 to 61 inches/mi as a result of the surface preparation. It then increased to 131 inches/mi in less than three years before it was taken out of the study. Faulting at joints and midslab cracks and the associated tilting of the pieces caused most of the roughness and its increase over time. The roughness properties (types of features and spectral content, but not spatial distribution) were very similar in the last profiling visit to those of the section before surface preparation.

PCC Overlay

- Section 040663: This section received a 10 inch unbonded overlay over a 2 inch AC course. The MRI of this section decreased from 218 to 93 inches/mi as a result of the rehabilitation. It then increased very little in the next seven years—23 inches/mi over the monitoring history.

  Narrow dips appeared at a regular spacing of 15 ft throughout the section, and the increase in their depth caused most of the increase in roughness over time. No significant distress was observed on this section. Since the dips at the joints were narrow and did not include significant faulting, the increase in MRI did not cause a commensurate reduction in ride quality. The removal and subsequent replacement of weigh-in-motion scales on the test section caused a somewhat erratic change in roughness over the second half of the monitoring history.

AC Overlay: 4 Inch

- Section 040603 (minimum surface preparation): The MRI of this section increased by 12 inches/mi over the first five years after rehabilitation, then increased at a much higher rate to a peak value of 214 inches/mi by the 11th year. Transverse cracking at the locations of the underlying joints caused most of the roughness progression, and a narrow dip appeared over most of the joints by the seventh year after rehabilitation. By the 11th year, most of the dips were 1 to 2 ft wide and at least 0.25 inch deep. Subsequent skin patching over the last 380 ft of the section reduced the MRI by about 40 inches/mi. Narrow dips still appeared at most of the joints, but they were less severe.
- Section 040604 (saw and seal): The MRI of this section decreased from 218 to 93 inches/mi as a result of the rehabilitation. It then increased very little in the next seven years—23 inches/mi over the monitoring history. Narrow dips that appeared at saw cuts as the sealant wore away caused the increase in roughness. By the end of the monitoring history, narrow dips appeared at most of the saw cuts that were 1 to 1.5 ft wide and up to 0.3 inch deep.
- Section 040606 (maximum surface preparation): The MRI of this section increased by 1 inch/mi over the first six years after rehabilitation, then increased at a higher rate to a peak value of 145 inches/mi by the 11th year. Transverse cracking at the locations of the underlying joints caused most of the roughness progression, and a narrow dip appeared within the profiles over most of the joints by the end of the monitoring period. By the final visit, most of the dips were 1 to 2 ft wide and at least 0.2 inch deep. However, a small number of dips at high-severity transverse cracks stood out as more severe than the rest. Nothing was detected in the prerehabilitation profiles that could explain the most severe dips.
- Section 040607 (crack and seat): The MRI of this section increased by 14 inches/mi over the first six years after rehabilitation, then increased at a higher rate to a peak value of 200 inches/mi by the end of the monitoring period. Transverse cracking at the locations of the underlying joints caused the majority of the roughness progression, and a narrow dip appeared within the profiles over most of the joints by the end of the monitoring period. Several dips 1 to 2 ft wide and more than 1 in deep appeared where high severity transverse cracks were recorded. Gouges in the pavement, a longitudinal crack, an area of fatigued pavement, and a patch in poor condition also contributed to roughness of the left side of the lane in the last three years of the experiment.
- Section 040659 (fabric/crack and seat): The MRI of this section increased by 7 inches/mi over the first six years after rehabilitation, then increased at a higher rate to a value of 179 inches/mi by the end of the monitoring period. Transverse cracking at the locations of the underlying joints caused the majority of the roughness progression, and a narrow dip appeared within the profiles over about half of the joints by the end of the monitoring period. Most of the dips were less than 1 ft wide and less than 0.5 inch deep. However, a few dips more than 1 inch deep appeared at cracks with fatigue in the

wheelpath. Localized roughness appeared at potholes, in an area of high severity fatigue with potholes, and at a fatigued area with a patch.

AC Overlay: 8 Inch

- Section 040608 (crack and seat): The MRI of this section increased by 68 inches/mi over the post-rehabilitation monitoring history. This included five times as much growth in the IRI of the left side compared to the right side. A 20 ft long fatigued area on the left side of the lane with rough patches at both ends caused more of the roughness progression than any other feature and accounted for 40 to 60 inches/mi of roughness on the left side in the final profiling visit. Transverse cracking caused the majority of the roughness progression on the right side of the lane and some of the roughness progression on the left side of the lane. A narrow dip appeared within the profiles over most of the locations where transverse cracks were recorded. The cracks may have appeared at the locations of underlying joints, but this could not be confirmed.
- Section 040660 (rubblize): The MRI of this section increased by 83 inches/mi over the post-rehabilitation monitoring history. Three types of distress caused the progression in roughness: (a) narrow dips at transverse cracks, (b) localized roughness at a 20 ft long fatigued area on the right side, and (c) roughness at the leading and trailing edge of a long dip 50 to 90 ft from the start of the section. A skin patch was placed over the long dip, but this did not completely remove the dip and it added roughness at the borders of the patch.

Rubblized AC Overlay

- Section 040661 (crack and seat, ARAC/AC): The MRI of this section increased erratically after rehabilitation from a minimum value of 45 inches/mi to a final value of 97 inches/mi. Three features accounted for the majority of the post-rehabilitation increase in roughness. First, an area about 15 ft long appeared on the right side with pumping and several cracks in 1999 and 2000 and caused severe localized roughness in 2000. Second, the leading edge of a skin patch placed in 2001 (extending from the rough area to the end of the section) caused localized roughness on both sides. Third, the skin patch itself was rougher than the pavement it covered, with the exception of the area where the patch covered cracking and pumping.
- Section 040662 (crack and seat, ARAC/AC): The MRI of this section increased after rehabilitation from a minimum value of 55 to 173 inches/mi in 2001. A skin patch decreased the roughness to 137 inches/mi, although the transition at the start of the patch caused localized roughness. Transverse cracking at the locations of the underlying joints caused most of the roughness progression, and a narrow dip appeared within the profiles over most of the joints by the end of the monitoring period.

- Section 040664 (no surface preparation): This section was very smooth throughout the monitoring history. The initial MRI value was 44 inches/mi, and the MRI only ranged from 48 to 50 inches/mi from February 1993 until October 2002. The roughest portion of the section occurred from 350 to 400 ft from the start because of a very long dip over that range.
- Section 040665 (crack and seat): This section was very smooth throughout the monitoring history. The MRI progressed from an initial value of 43 inches/mi to a final value of 51 inches/mi, but was roughest in February 2001 with an MRI value of 55 inches/mi. In all visits, a rise in elevation of about 0.2 inch appeared about 200 ft from the start of the section, followed by a series of small bumps. These features were harsh enough to qualify as localized roughness in the left side profiles.
- Section 0666 (rubblize): This section was very smooth throughout the monitoring history. The MRI progressed somewhat steadily from an initial value of 39 inches/mi to a value of 49 inches/mi in March 2000, then it held steady for the rest of the monitoring period. No localized roughness appeared on this section. However, the roughest locations within the section were found at two bumps 4 to 6 ft long and about 0.1 inch high. These did not correspond to any observed distress.
- Section 040667 (crack and seat): This section experienced little change in roughness throughout the monitoring history, with a total range in MRI of 70 to 74 inches/mi. Content in the wavelength range from 45 to 60 ft accounted for most of the MRI. Localized roughness (or nearly so) was detected in the profiles because of a long bump near the middle of the section with a sharp crest.
- Section 040668 (no surface preparation): This section was very smooth throughout the monitoring history. The MRI increased from 37 to 45 inches/mi. The profiles included a small amount of roughness isolated at a wavelength of 15 ft, and the right side profiles included some content isolated at a wavelength of 7.5 ft. In the second half of the monitoring history, small dips 0.5 ft long and up to 0.25 inch deep appeared at the only three locations where distress survey recorded slightly skewed transverse cracks that spanned the entire lane. No localized roughness was detected.
- Section 040669 (rubblize): This section remained smooth throughout the monitoring history. The MRI ranged from 49 to 59 inches/mi. Content in the 45 to 60 ft wavelength range accounted for most of the MRI. Localized roughness was detected in the left side profiles because of a sharp slope change at the apex of a very long bump. This was not nearly as severe on the right side.

SUMMARY

This section provided details about the prerehabilitation and post-rehabilitation roughness of the road. It also provided a basis for quantifying and explaining the changes in roughness with time and relating the observations to distress and maintenance.

Table 35 summarizes the observations for the sections that received an overlay. The table includes the roughness progression, the distresses that contributed to the roughness progression, and the prerehabilitation status of each section. The table also lists MRI values immediately after rehabilitation, 6.4 years after, at the end of the project, and the overall post-rehabilitation range.

Prerehabilitation status did not have a clear relationship to post-rehabilitation roughness progression. However, any comparison of performance by surface preparation technique should consider the roughness and faulting levels that were present before rehabilitation. For example, among the test sections that received a 4 inch AC overlay, roughness progressed more slowly on the section with maximum surface preparation (040606) than on the section with minimum surface preparation (040603). On both sections, roughness progressed due to reflective cracking. However, the lower roughness progression on Section 040606 may have been caused by a combination of the additional surface preparation and status of the joints before rehabilitation. The prerehabilitation status of Sections 040664 through 040669 is unknown, but was reported as being similar to that of the other test sections in this project.

Table 35 shows that the most prevalent contributor to roughness in this project was reflective and transverse cracking. Late in the history of the project, transverse and reflective cracking often dominated as a source of roughness in the roughest sections. Table 35 identified the sections with localized roughness. Since an instance of localized roughness required that the severity stand out relative to the rest of the section, the threshold for localized roughness was lower on smooth sections than on rough sections. Localized roughness was often associated with a particular type of distress cited in the distress surveys. In some cases, such as on Sections 040665, 040667, and 040669, localized roughness occurred directly after rehabilitation and was probably built in.

Figure 80 summarizes the roughness progression of all of the sections that received an overlay. The figure shows the entire range of MRI values observed in post-rehabilitation profile measurements with a gray bar. (Appendix C provides values for each visit.) The figure also provides markings at two landmark visits. First, the value 6.4 years after rehabilitation is marked to distinguish sections with high initial MRI or roughness that progressed early from those that may have held their roughness for several years before losing their functional performance. Second, the final value (12 years after rehabilitation) is also marked, and the test sections are sorted using this value in the figure.

At a glance, Figure 80 shows that sections with ARAC/AC overlay progressed in roughness much less than the rest of the sections. While the PCC overlay started out rougher than the rest, it progressed in roughness very little over the 12-year life of the project. Finally, Sections 040603 and 040662 reached peak roughness values much higher than their final roughness because they both received skin patching that reduced their roughness.

A summary of the surface roughness performance of the 19 test sections follows:

- Roughness on the six sections with a rubberized friction course covering 2 inches of ARAC on top of 3 inches of AC (040664 through 040669) progressed very little after rehabilitation.
- The seven supplemental sections constructed with ARAC over AC (040661 and 040664 through 040669) outperformed the other test sections with an asphalt overlay.
- Using 2 inches of ARAC over 2 inches of AC (Section 040661) provided a significant improvement in smoothness compared to using 2 inches of AC over 2 inches of ARAC (Section 040662). Only the latter exhibited significant reflective cracking.
- The unbonded concrete overlay (Section 040663) was the roughest in the first visit after rehabilitation among all of the sections that received an overlay. However, the section increased in roughness very slowly and held its functional performance and structural integrity at the surface throughout the entire monitoring history.
- Roughness on the pavement with a crack and seat and an 8 inch AC overlay (Section 040608) progressed more slowly than its rubblized counterpart (Section 040659) and much more slowly than its counterpart with a 4 inch AC overlay (Section 040607).
- Disturbances at transverse cracks dominated the roughness on of the sections with a 4 inch AC overlay (040603, 040604, 040606, 040607, and 040659) by the end of the experiment. (These were reflective cracks in all of the sections except 040604, where the cracks were sawed and sealed.) However, they did not all perform equally.
    - These sections retained their smoothness quite well for the first six years, at which point roughness began to increase aggressively—particularly for sections receiving minimal restoration.
    - The saw and seal section (040604) and the section with maximum restoration (040606) finished the experiment with the lowest roughness and the least amount of roughness at transverse cracks.
    - Among the sections with minimum restoration (040603 and 040604), the saw and seal section (040604) was affected by roughness at transverse cracks the least, but wearing away of the sealant took its toll by the end of the experiment. In contrast, the section without saw and seal (040603) included rough reflective cracks over each underlying joint.
    - Both sections with crack and seat (040607 and 040659) included roughness caused by other distress in addition to reflective cracks. Roughness progressed less rapidly on the section with geotextile (040659), but neither section outperformed saw and seal (040604) or maximum restoration (040606).

Table 35. Summary of Roughness Behavior.

Section	040603	040607	040659	040606	040604	040660	040608	040663
Overlay material	AC	AC	AC	AC	AC	AC	AC	PCC/AC
Overlay thickness (inches)	4	4	4	4	4	8	8	10/2
Surface preparation	Min.	CS	F/CS	Max.	SS	Rub.	CS	CS
MRI (inch/mi)								
Minimum	55	53	66	64	55	65	59	93
6.4 years after rehabilitation	91	69	73	75	67	110	66	95
Final	173	200	179	137	135	148	127	117
Range	55–214	53–200	66–181	64–145	55–135	65–148	59–127	93–117
Contributors to roughness								
Reflective cracking	?	?	?	?				
Transverse cracking					?	?		
Longitudinal cracking			?					
Fatigue		?	?			?	?	
Potholes			?					
Patches		?	?				?	
Gouges		?						
Transition at skin patch								
Cracks and pumping								
Localized roughness	?	?	?			?	?	
Prerehabilitation								
Roughness (MRI)	M	L	H	L	L	H	L	H
Faulting severity	H	L	H	L	M	H	M	H

Surface preparation: crack and seat (CS), fabric/crack and seat (F/CS), maximum (Max.), minimum (Min.), rubblize (Rub.), saw and seal (SS).
Roughness: high (H) (> 170 inches/mi), medium (M) (120–170 inches/mi), low (L) (< 120 inches/mi).
Faulting severity: high (H), medium (M), low (L).

Table 35. Summary of Roughness Behavior (Continued).

Section	040662	040661	040665	040667	040664	040668	040666	040669
Overlay material	AC	ARAC	ARAC	ARAC	ARAC	ARAC	ARAC	ARAC
Overlay thickness (inches)	2	2	2	2	2	2	2	2
Surface preparation	CS	CS	CS	CS	None	None	Rub.	Rub.
MRI (inch/mi)								
Minimum	49	45	43	70	44	37	39	49
6.4 years after rehabilitation	79	61	49	73	49	42	47	56
Final	136	97	51	73	49	45	49	58
Range	49-173	45-100	43-55	70-74	44-50	37-45	39-50	49-59
Contributors to roughness								
Reflective cracking	?							
Transverse cracking								
Longitudinal cracking								
Fatigue								
Potholes								
Patches								
Gouges								
Transition at skin patch	?	?						
Cracks and pumping		?						
Localized roughness	?	?	?	?				?
Prerehabilitation								
Roughness (MRI)	M	H						
Faulting severity	M	H						

Note: Sections 040664 through 040669 also included a 0.5 inch AR-ACFC layer.
Surface preparation: crack and seat (CS), rubblize (Rub.).
Roughness: high (H) (> 170 inches/mi), medium (M) (120-170 inches/mi).
Faulting severity: high (H), medium (M).

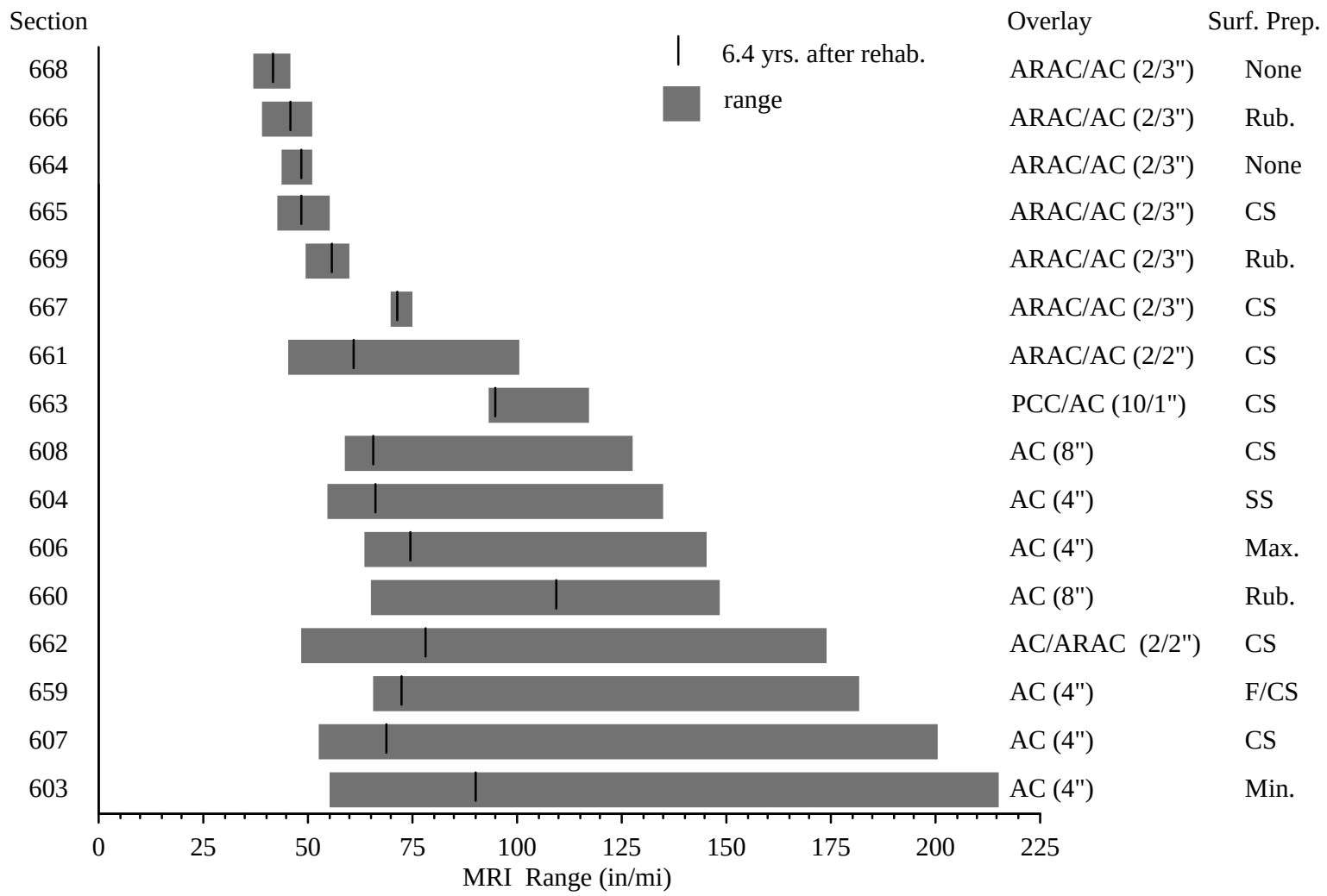

Figure 80. Roughness Summary.

- The three sections not receiving overlays (040601, 040602, and 040605) reached their terminal serviceability within three years. Performing the maximum rehabilitation activities (Section 040605) on the PCC only extended the service life by one year as compared to the routine maintenance and minimum restoration sections, but the section offered better functional performance (that is, less roughness) over the interval between rehabilitation and terminal serviceability.
- In 2000, Sections 040603, 040661, and 040662 received substantial thin overlay patching covering up to 70 percent of the test sections. Sections 040660 and 040659 also received patching to a lesser extent in 1999. Patching did not always decrease roughness, and localized roughness sometimes appeared at the borders of the patches.

CHAPTER 5. CONCLUSIONS AND RECOMMENDATIONS

ADOT initiated this project to study the performances of various rehabilitation techniques and integrated this study into a large JPCP rehabilitation project along I-40. Surface distress, deflection, and profile data were used as the basis for performance evaluation and were each analyzed as part of the study.

The SPS-6 project offers a unique opportunity to directly compare performance of various rehabilitation techniques while reducing the confounding effect of other variables such as traffic loading, climate, and subgrade conditions. However, findings drawn from this evaluation must be considered carefully. The conclusions are based on one set of in situ conditions; observations from other climate or loading scenarios may differ from those noted within this report. Therefore, findings reported may be unique to the conditions and construction of this site.

Despite these issues, the data captured at the project provides valuable insight into pavement performance, design, management, and construction. Following is a summary of lessons learned from the performance data collected at the SPS-6:

- All sections with an AR-ACFC layer and a bottom layer of 3 inches of ARAC experienced a significantly higher resistance to longitudinal and transverse reflective cracking.
- The higher performance of the AR-ACFC sections (040664 through 040669) could be partially attributed to the viscosity of the AR, which is more than 10 times greater than AC-20 (PG-64-16) at hot-mixing temperatures and, therefore, can be applied to an OGFC at a rate of 9 percent to 10 percent by weight of the mix. This extra coating thickness is believed to increase durability, slow down aging, and help retard reflective cracking (Way 1999).
- When overlay thickness increased to 8 inches, rubblized sections as well as crack and seat sections yielded approximately the same performance.
    - Reflection cracking is believed to originate from the bottom of the layers. However, though the findings from this study do not definitively show top-down cracking, the test section performances may point to it.
    - There was much better performance in Section 040661 (2 inches of ARAC on 2 inches of AC) than Section 040662 (2 inches of AC on 2inches of ARAC). This is interesting as the ARAC layer is believed to retard reflection cracking.
    - The thin layer, or AR-ACFC, may have contributed to the higher performance of Sections 040664 through 040669.
    - Geotextile fabric, which is also believed to help prevent reflection cracking, did not seem to improve the performance of Section 040659.

- In this study, minimum restoration and maximum restoration of PCC slabs were not long-term improvement solutions. Maximum restoration only extended the service life by one year as compared to the routine maintenance and minimum restoration.

- The 10 inch unbonded PCC overlay with a 2 inch AC bond breaker (Section 040663) had the highest performance among all of the test sections in the SPS-6 experiment.
- The rubblized section with AR-ACFC and 2 inches of AC on 3 inches of ARAC had the highest performance among all sections that received AC overlays in the SPS-6 experiment.
- The most effective rehabilitation treatments, in terms of long-term increase in effective pavement thickness, were the 4.3 inch asphalt overlay of the replaced outer lane concrete, the 10 inch unbonded concrete overlay of the cracked and seated concrete, and the 8.4 inch asphalt overlay of the cracked and seated concrete. After these three, the most effective treatments, in terms of long-term increase in effective pavement thickness, were the 4 to 5.5 inch asphalt overlays of intact concrete slabs. The 4 to 5.5 inch overlays of cracked and seated or rubblized slabs were less effective. Differences in slab cracking patterns may be responsible for some of the differences in effectiveness among the different crack and seat sections of comparable overlay thickness.
- All sections performed well with regard to rut resistance. Rutting would not have triggered a rehabilitation event for any of the test sections.
- The test sections experienced very few structurally related distresses and, therefore, the PCC preparations appeared to provide a solid foundation for reasonable pavement life.
- The test sections did not equally share the same structural capacity prior to rehabilitation; therefore, the post-rehabilitation differences in structural capacity cannot solely be attributed to the rehabilitation treatments.

In this study, the data did not explicitly show that reflective cracking originated from the top-down; however, the data suggested that this could be a possibility. Further studies should be performed to verify top-down or bottom-up reflective cracking so that rehabilitation strategies can better mitigate it in future projects.

REFERENCES

American Association of State Highway and Transportation Officials. 2008. *Standard Specification for Pavement Ride Quality When Measured Using Inertial Profiling Systems*. Publication AASHTO MP 17-08. Washington, D.C.: American Association of State Highway and Transportation Officials.

Austin Research Engineers, Inc. 1992. *SPS-6: Rehabilitation of Jointed Portland Cement Concrete Pavements: Construction Report*. Publication FHWA-AZ92-379-II. Washington, D.C.: Federal Highway Administration.

Evans, L. D., and A. Eltahan. 2000. *LTPP Profile Variability*. Publication FHWA-RD-00-113. McLean, Virginia: Federal Highway Administration.

Hall, K. T., M. I. Darter, and C-M Kuo. 1995. "Improved Methods for Selection of K Value for Concrete Pavement Design." *Transportation Research Record: Journal of the Transportation Research Board* 1505: 128-136.

Huang, Y. H. 1993. *Pavement Analysis and Design*. Englewood Cliffs, New Jersey: Prentice-Hall.

Karamihas, S. M. 2004. "Development of Cross Correlation for Objective Comparison of Profiles." *International Journal of Vehicle Design* 36(2/3): 173-193.

Karamihas, S. M. 2005. *Critical Profiler Accuracy Requirements*. Report UMTRI-2005-24. Ann Arbor, Michigan: University of Michigan Transportation Research Institute.

Karamihas, S. M., T. D. Gillespie, R. W. Perera, and S. D. Kohn. 1999. *Guidelines for Longitudinal Pavement Profile Measurement*. NCHRP Report No. 434. Washington, D.C.: National Cooperative Highway Research Program.

Miller, J., and W. Bellinger. 2003. *Distress Identification Manual for the Long-Term Pavement Performance Program*. Publication FHWA-RD-03-031. McLean, Virginia: Federal Highway Administration.

Perera, R. W., and S. D. Kohn. 2005. *Quantification of Smoothness Index Differences Related to Long-Term Pavement Performance Equipment Type*. Publication FHWA-HRT-05-054. McLean, Virginia: Federal Highway Administration.

Sayers, M. W. 1990. "Profiles of Roughness." *Transportation Research Record: Journal of the Transportation Research Board* 1260: 106-111.

Sayers, M. W., and S. M. Karamihas. 1996. *Interpretation of Road Roughness Profile Data*. Publication FHWA-RD-96/101. McLean, Virginia: Federal Highway Administration.

Simpson, A. L. 2001. *Characterization of Transverse Profiles*. Publication FHWA-RD-01-024. McLean, Virginia: Federal Highway Administration.

Swan, M., and S. M. Karamihas. 2003. "Use of a Ride Quality Index for Construction Quality Control and Acceptance Specifications." *Transportation Research Record: Journal of the Transportation Research Board* 1861: 10-16.

Way, G. 1999. "Flagstaff I-40 Asphalt Rubber Overlay Project: Nine Years of Success." *Proceedings of the Transportation Research Board 78th Annual Meeting*.

APPENDIX A: CONSTRUCTION DEVIATIONS

040601 (Control Section):

- The only work done in this section was to replace the asphalt shoulders after milling them.

040602 (Minimum Restoration):

- 22.5 ft slabs replaced at beginning of section. Should be OK since it was 571ft long; should still have at least 500ft of length.
- Fine aggregate mixture design for patch material value is large. Units were not good. One bag mix = 0.58 lf. Typically mixed was 4-bag quantities approx 2.3 cf or less than 0.01 cubic yard (27cf).

040603 (Minimum Restoration):

- Spall repair operations on July 6, 1990, failed to clean some joints.
- Poor workmanship on spall repair June 28, 1990. Sloppy cuts, mix too wet, cold and floating joints. Unapproved aggregate. Used on last two joints (repair).
- Contractor repair poor workmanship (item above) on July 16, 1990, poured set-45 July 16, 1990. Total replaced = 23.35sf. Added some 13.5sf also. One of these joints repaired was poured complete, that is, no bond breaker used for transverse joint. Sawed later. Spall was too deep for good bond breaker.
- When done with pour July 12, 1990, drove loader over last joint repair. Needs to be replaced by contractor -4.7sf.
- Fine aggregate mix design for patch material value large because units were not good.
- During construction, multiple lifts were placed on different dates for the same layer.

040604 (Saw and Seal, Minimum Restoration):

- Fine aggregate mixture design for patch material value is large. Units were not good. One bag mix =0.58 lf. Typically mixed was 4-bag quantities approx 2.3 cf or less than 0.1 cubic yard (27cf).
- During construction, multiple lifts were placed on different dates for the same layer.

040605 (Maximum Restoration):

- No contractor quality control on site July 17, 1990.
- Trencher made a spall in new PCC July 25, 1990 (Scofield).
- Fine aggregate mixture design for patch material value is large. Units were not good. One bag mix = 0.58 lf. Typically mixed was 4-bag quantities approx 2.3 cf or less than 0.1 cubic yard (27cf).

040606 (Maximum Restoration):

- Although not in plans, longitudinal tie bars were added to the design. However, a test cut into the adjacent lane PCC showed the concrete to be in too poor

condition for placement of tie bars. Also, no tie bars were placed in any of this test section. There was some confusion over the mix design grading. They used #57. doweled required 57 undoweled 467. It seems they used the right one (Scofield diary, Donman conversation, June 20, 1990).

- Fine aggregate mixture design for patch material value is large. Units were not good. One bag mix = 0.58 lf. Typically mixed was 4-bag quantities approx 2.3 cf or less than 0.1 cubic yard (27cf).
- During construction, multiple lifts were placed on different dates for the same layer.

040607 (Crack and Seat):

- During construction, multiple lifts were placed on different dates for the same layer.

040608 (Crack and Seat):

- During construction, multiple lifts were placed on different dates for the same layer.

040659 (Fabric/Crack and Seat):

- Non-standard section contains binder and fabric. Binder. AC-20 placed at 0.18 gallons/sq. yard. Fabric: amoco 4597 paving fabric, 3500 sq. yard.
- Contractor didn't tack the overlap on transverse joints. He had some difficulty making 12 inch transverse laps.
- Outside (distress lane) shoulder also has binder and fabric.
- During construction, multiple lifts were placed on different dates for the same layer.

040660 (Rubblize):

- This section was a rubblization section. Subsequent overlay began to deflect considerably. A skin patch 3 inches thick was placed; the cracks re-appeared after rolling. (Only a pneumatic roller was used to avoid exacerbating the situation with a vibratory roller.) It was decided to excavate the failure region in lieu of bridging it with more AC. The failure area was 49 ft into the section and 150 ft long. The trench dug was 12 ft wide, 7 ft deep for the first 25 ft. After that, it was 4 ft deep for remainder of 150 ft. the rest of the details can be seen on constr. data forms 3. Work occurred on Monday, Aug. 6, 1990. Section was rubblized using custom war watong with water tanks having 7 to 12 inch wide steel shoe, 2000 lbf, 44 times per second. During construction, multiple lifts placed on different dates for the same layer.

040661 (Crack and Seat):

- Used an older blaw-knox paver with an extended screen when layer 7-ARAC rubber placed on Aug. 9, 1990.
- During construction multiple lifts were placed on different dates.

040662 (Crack and Seat):

- Rubberized asphalt placed Aug. 9, 1990 at 7:10 p.m. and was rolled till 8:15 p.m. It started raining at 7:45 p.m.

- During crack and seat height of drop 43 to 44 inches, spacing from 32 to 40 inches; typically spacing 34 to 36 inches. Roller used for seating only two-thirds full of water (near tank) and front tank was empty. They filled, don't know how much done with empty and part-empty tanks.

040663 (Crack and Seat):

- No notes available.

040664 (No Surface Preparation):

- During construction, multiple lifts were placed on different dates.

040665 (Crack and Seat):

- No notes available.

040666 (Rubblize):

- Section was rubblized using custom war wagon with water tanks having 7 to 12 inch wide steel shoe, 2000 lbf, 44 times per second.
- Nov. 1, 2002: Taken out of study.

040667 (Crack and Seat):

- No notes available.

040668 (No Surface Preparation):

- No notes available.

040669 (Rubblize):

- Section was rubblized using custom war wagon with water tanks having 7 to 12 inch wide steel shoe, 2000 lbf, 44 times per second.

APPENDIX B: SITE WORK HISTORY

After original construction in June through October 1990, the following maintenance activities were performed:

040601 (Control Section):

- 11/15/91: Partial depth patching of PCC pavements at joints (sq. yards).
- 04/30/92: Taken out of study.

040602 (Minimum Restoration):

- 06/11/90: Partial depth patching of PCC pavement other than at joint (sq. yards).
- 06/11/90: Crack sealing (linear ft).
- 06/11/90: Transverse joint sealing (linear ft).
- 06/11/90: Lane-shoulder longitudinal joint sealing (linear ft).
- 06/11/90: AC shoulder replacement (sq. yards).
- 04/30/92: Taken out of study.

040603 (Minimum Restoration):

- 06/11/90: Partial depth patching of PCC pavement other than at joint (sq. yards).
- 06/11/90: Asphalt concrete overlay (sq. yards).
- 03/08/95: Crack sealing (linear ft).
- 10/01/99: Patch pot holes—hand spread, compacted with truck (no. of holes).
- 09/11/01: Skin patching (hand tools/hot pot to apply liquid asphalt and aggregate) (sq. Yards).
- 11/01/02: Taken out of study.

040604 (Saw and Seal, Minimum Restoration):

- 06/11/90: Transverse joint sealing (linear ft).
- 06/11/90: Partial depth patching of PCC pavement other than at joint (sq. yards).
- 06/11/90: Asphalt concrete overlay (sq. yards).
- 06/11/90: Grooving surface (sq. yards).
- 06/11/90: Saw and seal.
- 03/08/95: Crack sealing (linear ft).
- 11/01/02: Taken out of study.

040605 (Maximum Restoration):

- 06/11/90: Crack sealing (linear ft).
- 06/11/90: Transverse joint sealing (linear ft).
- 06/11/90: Lane-shoulder longitudinal joint sealing (linear ft).
- 06/11/90: Full depth transverse joint repair patch (sq. yards).
- 06/11/90: Partial depth patching of PCC pavement other than at joint (sq. yards).

- 06/11/90: PCC slab replacement (sq. yards).
- 06/11/90: Grinding surface (sq. yards).
- 06/11/90: Longitudinal subdrains (linear ft).
- 06/11/90: Joint load transfer restoration in PCC pavements (linear ft).
- 07/01/91: Partial depth patching of PCC pavements at joints (sq. yards).
- 08/01/93: Taken out of study.

040606 (Maximum Restoration):

- 06/11/90: Full depth transverse joint repair patch (sq. yards).
- 06/11/90: Partial depth patching of PCC pavement other than at joint (sq. yards).
- 06/11/90: PCC slab replacement (sq. yards).
- 06/11/90: AC shoulder replacement (sq. yards).
- 06/11/90: Asphalt concrete overlay (sq. yards).
- 06/11/90: Longitudinal subdrains (linear ft).
- 03/07/95: Crack sealing (linear ft).
- 11/01/02: Taken out of study.

040607 (Crack and Seat):

- 06/11/90: Fracture treatment of PCC pavement as base for new AC surface (sq. yards).
- 06/11/90: Asphalt concrete overlay (sq. yards).
- 06/11/90: Longitudinal subdrains (linear ft).
- 03/07/95: Crack sealing (linear ft).
- 05/01/00: Patch pot holes—hand spread, compacted with truck (no. of holes).
- 11/01/02: Taken out of study.

040608 (Crack and Seat):

- 06/11/90: Fracture treatment of PCC pavement as base for new AC surface (sq. yards).
- 06/11/90: Asphalt concrete overlay (sq. yards).
- 06/11/90: Longitudinal subdrains (linear ft).
- 03/07/95: Crack sealing (linear ft).
- 05/01/00: Patch pot holes—hand spread, compacted with truck (no. of holes).
- 11/01/02: Taken out of study.

040659 (Fabric/Crack and Seat):

- 06/11/90: Fracture treatment of PCC pavement as base for new ac surface (sq. yards).
- 06/11/90: Asphalt concrete overlay (sq. yards).
- 06/11/90: Longitudinal subdrains (linear ft).
- 03/07/95: Crack sealing (linear ft).
- 08/29/97: Patch pot holes—hand spread, compacted with truck (no. of holes).
- 09/28/99: Patch pot holes—hand spread, compacted with truck (no. of holes).
- 05/01/00: Patch pot holes—hand spread, compacted with truck (no. of holes).

- 11/01/02: Taken out of study.

040660 (Rubblize):

- 06/11/90: Fracture treatment of PCC pavement as base for new AC surface (sq. yards).
- 06/11/90: Asphalt concrete overlay (sq. yards).
- 06/11/90: Longitudinal subdrains (linear ft).
- 06/11/90: Asphalt concrete overlay (sq. yards).
- 03/07/95: Crack sealing (linear ft).
- 09/28/99: Skin patching (hand tools/hot pot to apply liquid asphalt and aggregate) (sq. yards).
- 06/01/00: Patch pot holes—hand spread, compacted with truck (no. of holes).
- 11/01/02: Taken out of study.

040661 (Crack and Seat):

- 06/11/90: Fracture treatment of PCC pavement as base for new AC Surface (sq. yards).
- 06/11/90: Asphalt concrete overlay (sq. yards).
- 06/11/90: Longitudinal subdrains (linear ft).
- 06/11/90: Asphalt concrete overlay (sq. yards).
- 03/08/95: Crack sealing (linear ft).
- 09/11/01: Skin patching (hand tools/hot pot to apply liquid asphalt and aggregate) (sq. yards).
- 11/01/02: Taken out of study.

040662 (Crack and Seat):

- 06/11/90: Fracture treatment of PCC pavement as base for new AC surface (sq. yards).
- 06/11/90: Asphalt concrete overlay (sq. yards).
- 06/11/90: Longitudinal subdrains (linear ft).
- 06/11/90: Asphalt concrete overlay (sq. yards).
- 03/08/95: Crack sealing (linear ft).
- 06/01/00: Manual premix spot patch (hand spreading and compacting with roller) (sq. yards).
- 06/01/00: Patch pot holes—hand spread, compacted with truck (no. of holes).
- 05/01/01: Skin patching (hand tools/hot pot to apply liquid asphalt and aggregate) (sq. yards).
- 11/01/02: Taken out of study.

040663 (Crack and Seat):

- 06/11/90: Fracture treatment of PCC pavement as base for new AC surface (sq. yards).
- 06/11/90: Asphalt concrete overlay (sq. yards).
- 06/11/90: Portland cement concrete overlay (sq. yards).
- 06/11/90: Longitudinal subdrains (linear ft).

- 09/28/99: Partial depth patching of PCC pavements at joints (sq. yards).
- 11/01/02: Taken out of study.

040664 (No Surface Preparation):

- 06/11/90: Asphalt concrete overlay (sq. yards).
- 06/11/90: Longitudinal subdrains (linear ft).
- 06/11/90: Asphalt concrete overlay (sq. yards).
- 11/01/02: Taken out of study.

040665 (Crack and Seat):

- 06/11/90: Fracture treatment of PCC pavement as base for new AC surface.
- 06/11/90: Asphalt concrete overlay (sq. yards).
- 06/11/90: Longitudinal subdrains (linear ft).
- 06/11/90: Asphalt concrete overlay (sq. yards).
- 11/01/02: Taken out of study.

040666 (Rubblize):

- 06/11/90: Fracture treatment of PCC pavement as base for new AC surface.
- 06/11/90: Asphalt concrete overlay (sq. yards).
- 06/11/90: Longitudinal subdrains (linear ft).
- 06/11/90: Asphalt concrete overlay (sq. yards).
- 11/01/02: Taken out of study.

040667 (Crack and Seat):

- 06/11/90: Fracture treatment of PCC pavement as base for new AC surface.
- 06/11/90: Asphalt concrete overlay (sq. yards).
- 06/11/90: Longitudinal subdrains (linear ft).
- 06/11/90: Asphalt concrete overlay (sq. yards).
- 11/01/02: Taken out of study.

040668 (No Surface Preparation):

- 06/11/90: Asphalt concrete overlay (sq. yards).
- 06/11/90: Longitudinal subdrains (linear ft).
- 06/11/90: Asphalt concrete overlay (sq. yards).
- 11/01/02: Taken out of study.

040669 (Rubblize):

- 06/11/90: Fracture treatment of PCC pavement as base for new AC surface.
- 06/11/90: Asphalt concrete overlay (sq. yards).
- 06/11/90: Longitudinal subdrains (linear ft).
- 06/11/90: Asphalt concrete overlay (sq. yards).
- 11/01/02: Taken out of study.

APPENDIX C: ROUGHNESS VALUES

This appendix lists the left International Roughness Index (IRI), right IRI, mean roughness index (MRI), Half-car Roughness Index (HRI), and Ride Number (RN) values for each visit of each section. The roughness values are the average for five repeat runs. The five runs were selected from a group of as many as nine by automated comparison of profiles, as described in the report. Values of standard deviation are also provided for left and right IRI to reveal cases of high variability among the five measurements. However, the screening procedure used to select five repeats usually helped reduce the level of scatter.

The discussion of roughness in the report emphasizes the left and right IRI. Nevertheless, the other indexes do provide useful additional information. MRI is simply the average of the left and right IRI value. HRI is calculated by converting the IRI filter into a half-car model (Sayers 1989). This is done by collapsing the left and right profile into a single profile in which each point is the average of the corresponding left and right elevation. The IRI filter is then applied to the resulting signal. The HRI is very similar to the IRI, except that side-to-side deviations in profile are eliminated. The result is that the HRI value for a pair of profiles will always be lower than the corresponding MRI value. Comparing the HRI and MRI value provides a crude indication of the significance of roll (i.e., side-by-side variation in profile) to the overall roughness. When HRI is low compared to MRI, roll is significant. This is common among asphalt pavements (Karamihas et al. 1995). Certain types of pavement distress, such as longitudinal cracking, may also cause significant differences between HRI and MRI.

Figure 81 compares the HRI to MRI for all of the profile measurements that are covered in this appendix. This includes 1225 pairs of roughness values. The figure shows a best fit line and a line of equality. The slope of the line is 0.865. This is close to values observed for asphalt pavement.

RN has shown a closer relationship to road user opinion than the other indexes (Sayers and Karamihas 1996). As such, it may help distinguish the segments from each other by ride quality. Further, the effect on RN may help quantify the impact of that distress on ride when the roughness of a section is dominated by a particular type of distress. In particular, a very low RN value coupled with moderate IRI values indicates a high level of short wavelength roughness, and potential sensitivity to narrow dips and measurement errors caused by coarse surface texture.

Table 36 provides the roughness values. The tables also list the date of each measurement and the time in years since the site was opened to traffic. Negative values indicate measurements that were made before rehabilitation.

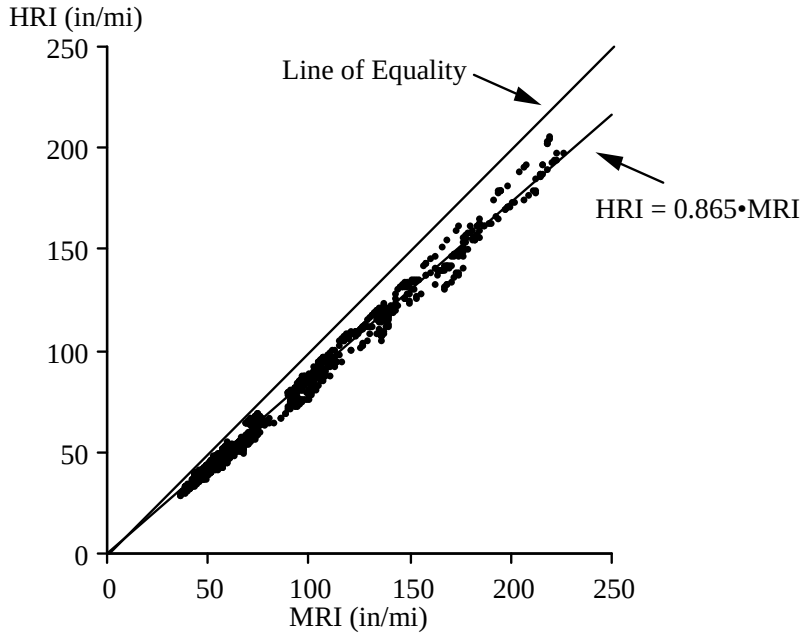

Figure 81. Comparison of HRI to MRI.

Table 36. Roughness Values.

Section	Date	Years	Left IRI (in/mi)		Right IRI (in/mi)		MRI	HRI	RN
			Ave	St Dev	Ave	St Dev	(in/mi)	(in/mi)	
0601	09-Apr-90	-0.49	104	0.7	102	1.7	103	83	2.84
0601	27-Sep-90	-0.02	131	6.3	102	1.3	116	97	2.19
0601	16-Sep-91	0.94	156	5.1	122	1.1	139	118	1.95
0601	27-Feb-92	1.39	191	12.6	145	5.8	168	144	1.77
0601	12-Feb-93	2.35	225	13.3	128	6.6	177	155	1.87
0602	09-Apr-90	-0.49	166	2.1	167	0.8	166	140	2.65
0602	27-Sep-90	-0.02	182	2.3	170	1.4	176	149	2.58
0602	16-Sep-91	0.94	185	2.1	179	1.6	182	156	2.50
0602	27-Feb-92	1.39	208	6.0	188	2.9	198	171	2.35
0602	12-Feb-93	2.35	218	2.7	202	4.3	210	178	2.20
0603	09-Apr-90	-0.49	138	7.4	200	2.6	169	155	2.43
0603	27-Sep-90	-0.02	52	0.9	58	1.9	55	44	4.12
0603	16-Sep-91	0.94	66	2.5	49	1.2	57	48	3.83
0603	27-Feb-92	1.39	71	2.0	50	1.5	61	50	3.81
0603	12-Feb-93	2.35	73	3.0	55	1.1	64	52	3.66
0603	21-Jan-94	3.29	66	0.5	56	2.3	61	49	3.68
0603	02-May-95	4.57	68	1.0	67	1.6	67	54	3.56
0603	19-Feb-97	6.37	107	2.8	74	2.9	91	73	3.05
0603	17-Apr-98	7.53	148	1.7	134	1.8	141	121	1.98
0603	02-Mar-99	8.40	155	1.4	140	3.3	147	127	2.03
0603	14-Mar-00	9.44	200	0.9	138	1.3	169	142	1.90
0603	17-Aug-00	9.86	211	2.0	163	4.8	187	162	1.70
0603	07-Feb-01	10.34	224	1.7	205	3.7	214	187	1.45

Table 36. Roughness Values (Continued).

Section	Date	Years	Left IRI (in/mi)		Right IRI (in/mi)		MRI (in/mi)	HRI (in/mi)	RN
			Ave	St Dev	Ave	St Dev			
0603	15-Feb-02	11.36	171	2.4	164	2.7	168	133	2.06
0603	28-Oct-02	12.06	183	2.0	164	3.4	173	139	1.96
0604	09-Apr-90	-0.49	91	1.5	113	1.4	102	87	3.06
0604	27-Sep-90	-0.02	69	1.0	67	0.7	68	55	3.91
0604	16-Sep-91	0.94	55	0.7	55	1.2	55	44	3.83
0604	27-Feb-92	1.39	57	1.6	58	2.1	58	46	3.71
0604	12-Feb-93	2.35	62	1.8	58	2.2	60	48	3.66
0604	21-Jan-94	3.29	59	0.8	55	3.4	57	45	3.71
0604	02-May-95	4.57	58	1.0	55	0.3	57	44	3.82
0604	19-Feb-97	6.37	79	1.5	55	0.8	67	52	3.56
0604	17-Apr-98	7.53	99	3.4	93	6.8	96	77	2.64
0604	02-Mar-99	8.40	93	3.5	79	2.7	86	68	3.00
0604	14-Mar-00	9.44	119	1.7	70	1.0	94	74	2.98
0604	17-Aug-00	9.86	126	0.5	75	0.6	101	83	2.91
0604	07-Feb-01	10.34	134	1.3	81	2.3	107	87	2.78
0604	15-Feb-02	11.36	152	1.9	101	1.6	127	104	2.54
0604	28-Oct-02	12.06	167	6.3	102	4.0	135	112	2.41
0605	09-Apr-90	-0.49	149	2.6	155	1.5	152	133	2.88
0605	27-Sep-90	-0.02	58	0.6	64	0.9	61	54	3.99
0605	16-Sep-91	0.94	82	0.4	97	1.0	89	80	3.33
0605	27-Feb-92	1.39	107	2.3	114	2.2	111	100	2.94
0605	12-Feb-93	2.35	135	2.0	127	3.2	131	119	2.88
0606	09-Apr-90	-0.49	109	2.6	99	1.4	104	88	3.04
0606	27-Sep-90	-0.02	66	1.4	83	3.4	74	63	3.94
0606	16-Sep-91	0.94	62	1.4	65	1.4	64	54	3.89
0606	27-Feb-92	1.39	61	1.7	66	2.1	64	54	3.83
0606	12-Feb-93	2.35	65	1.0	69	2.4	67	57	3.72
0606	21-Jan-94	3.29	64	1.9	70	0.9	67	58	3.73
0606	02-May-95	4.57	62	1.3	74	0.9	68	58	3.81
0606	19-Feb-97	6.37	74	2.0	76	1.8	75	66	3.42
0606	17-Apr-98	7.53	79	4.0	129	1.9	104	92	2.66
0606	02-Mar-99	8.40	91	1.8	115	2.4	103	91	2.70
0606	14-Mar-00	9.44	108	1.1	100	4.6	104	93	2.64
0606	17-Aug-00	9.86	117	1.1	116	1.8	116	106	2.49
0606	07-Feb-01	10.34	122	1.3	115	3.2	118	107	2.32
0606	15-Feb-02	11.36	144	1.0	146	1.9	145	132	1.90
0606	28-Oct-02	12.06	148	2.5	125	4.0	137	124	1.98
0607	09-Apr-90	-0.49	104	1.1	97	2.2	100	85	2.29
0607	16-Sep-91	0.94	62	1.9	43	2.0	53	43	3.88
0607	27-Feb-92	1.39	64	0.9	46	0.6	55	45	3.80
0607	12-Feb-93	2.35	69	2.6	47	1.5	58	47	3.73
0607	21-Jan-94	3.29	65	1.6	48	0.6	56	47	3.80
0607	02-May-95	4.57	51	2.1	60	1.0	55	45	3.78

Table 36. Roughness Values (Continued).

Section	Date	Years	Left IRI (in/mi)		Right IRI (in/mi)		MRI (in/mi)	HRI (in/mi)	RN
			Ave	St Dev	Ave	St Dev			
0607	19-Feb-97	6.37	78	1.1	61	1.2	69	58	3.55
0607	17-Apr-98	7.53	88	4.5	97	1.6	93	82	2.63
0607	02-Mar-99	8.40	104	1.2	103	1.0	103	91	2.49
0607	14-Mar-00	9.44	141	3.1	111	1.9	126	112	2.21
0607	17-Aug-00	9.86	156	2.4	110	2.5	133	120	2.11
0607	07-Feb-01	10.34	177	3.8	138	1.6	158	144	1.75
0607	15-Feb-02	11.36	223	2.2	167	1.4	195	180	1.40
0607	28-Oct-02	12.06	218	13.3	182	2.7	200	185	1.08
0608	09-Apr-90	-0.49	105	0.6	102	1.3	103	91	3.16
0608	16-Sep-91	0.94	68	1.8	50	1.8	59	48	3.83
0608	27-Feb-92	1.39	69	2.3	54	0.7	61	50	3.79
0608	12-Feb-93	2.35	74	2.0	54	0.8	64	52	3.69
0608	21-Jan-94	3.29	70	0.9	52	0.7	61	49	3.77
0608	02-May-95	4.57	71	3.6	56	1.0	64	51	3.66
0608	19-Feb-97	6.37	74	1.2	57	0.9	66	52	3.63
0608	17-Apr-98	7.53	80	5.2	60	1.2	70	56	3.32
0608	02-Mar-99	8.40	87	3.1	58	0.7	72	57	3.21
0608	14-Mar-00	9.44	121	3.6	64	0.8	93	76	2.74
0608	17-Aug-00	9.86	131	1.3	61	1.3	96	81	2.54
0608	07-Feb-01	10.34	123	4.8	62	1.1	93	79	2.52
0608	15-Feb-02	11.36	150	2.2	71	2.5	111	94	2.07
0608	28-Oct-02	12.06	182	7.3	72	1.8	127	112	1.67
0659	09-Apr-90	-0.49	211	6.8	181	2.0	196	170	2.17
0659	27-Sep-90	-0.02	68	1.4	64	1.1	66	56	4.11
0659	16-Sep-91	0.94	74	1.6	60	1.1	67	56	3.99
0659	27-Feb-92	1.39	80	3.4	57	3.1	69	58	3.91
0659	12-Feb-93	2.35	84	2.2	52	1.2	68	57	3.90
0659	21-Jan-94	3.29	76	0.9	60	1.0	68	57	3.94
0659	02-May-95	4.57	80	3.5	63	0.9	71	59	3.82
0659	19-Feb-97	6.37	83	0.6	62	1.0	73	61	3.62
0659	17-Apr-98	7.53	107	2.2	102	1.6	104	90	2.64
0659	02-Mar-99	8.40	112	4.5	100	1.8	106	89	2.70
0659	14-Mar-00	9.44	115	0.3	100	5.3	107	91	2.79
0659	17-Aug-00	9.86	118	2.3	107	2.5	113	98	2.61
0659	07-Feb-01	10.34	148	2.2	131	2.1	139	121	1.98
0659	15-Feb-02	11.36	187	4.0	175	2.2	181	160	1.36
0659	28-Oct-02	12.06	213	7.1	146	4.4	179	159	1.54
0660	09-Apr-90	-0.49	194	1.0	251	3.1	223	197	1.81
0660	16-Sep-91	0.94	65	0.8	65	0.3	65	55	4.07
0660	27-Feb-92	1.39	68	1.2	66	0.8	67	57	4.02
0660	12-Feb-93	2.35	77	1.1	68	0.5	73	62	3.89
0660	21-Jan-94	3.29	77	0.3	71	0.8	74	65	3.97
0660	02-May-95	4.57	102	0.9	92	1.4	97	87	3.58

Table 36. Roughness Values (Continued).

Section	Date	Years	Left IRI (in/mi)		Right IRI (in/mi)		MRI (in/mi)	HRI (in/mi)	RN
			Ave	St Dev	Ave	St Dev			
0660	19-Feb-97	6.37	119	0.8	101	2.2	110	96	3.26
0660	17-Apr-98	7.53	125	2.2	114	1.2	119	108	2.87
0660	02-Mar-99	8.40	133	0.9	107	1.1	120	109	2.94
0660	14-Mar-00	9.44	138	0.5	114	1.1	126	112	2.80
0660	17-Aug-00	9.86	135	0.6	111	0.7	123	110	2.83
0660	07-Feb-01	10.34	146	0.8	122	1.6	134	119	2.58
0660	15-Feb-02	11.36	158	0.8	138	1.1	148	133	2.23
0660	28-Oct-02	12.06	156	2.5	140	8.4	148	133	1.93
0661	09-Apr-90	-0.49	171	1.9	259	0.9	215	189	2.25
0661	27-Sep-90	-0.02	66	1.5	67	1.1	66	50	4.08
0661	16-Sep-91	0.94	50	0.3	41	0.9	45	37	4.22
0661	27-Feb-92	1.39	55	1.4	44	1.2	50	41	4.18
0661	12-Feb-93	2.35	61	2.0	47	1.1	54	44	4.08
0661	21-Jan-94	3.29	57	1.2	49	1.0	53	43	4.11
0661	02-May-95	4.57	60	1.2	53	1.6	56	45	4.01
0661	19-Feb-97	6.37	66	1.5	56	1.1	61	49	3.81
0661	17-Apr-98	7.53	63	1.7	74	1.3	68	55	3.46
0661	02-Mar-99	8.40	71	3.2	71	4.5	71	56	3.62
0661	14-Mar-00	9.44	71	1.0	72	0.8	72	58	3.54
0661	17-Aug-00	9.86	75	0.5	106	0.7	90	75	2.96
0661	07-Feb-01	10.34	75	0.7	108	1.3	92	75	3.04
0661	15-Feb-02	11.36	92	1.5	109	1.7	100	80	3.20
0661	28-Oct-02	12.06	92	3.1	102	2.7	97	76	3.16
0662	09-Apr-90	-0.49	156	3.3	148	2.0	152	126	2.73
0662	27-Sep-90	-0.02	52	1.1	57	0.5	55	43	4.26
0662	16-Sep-91	0.94	50	0.9	47	0.8	49	41	4.19
0662	27-Feb-92	1.39	53	1.6	48	0.7	51	43	4.16
0662	12-Feb-93	2.35	58	2.8	50	0.7	54	45	4.07
0662	21-Jan-94	3.29	58	1.2	54	1.2	56	46	4.07
0662	02-May-95	4.57	60	0.8	63	1.6	62	51	3.85
0662	19-Feb-97	6.37	78	1.2	80	0.9	79	65	3.30
0662	17-Apr-98	7.53	124	1.8	145	1.9	134	116	2.12
0662	02-Mar-99	8.40	129	6.0	138	0.6	133	115	2.13
0662	14-Mar-00	9.44	136	0.9	139	1.2	138	117	2.10
0662	17-Aug-00	9.86	160	2.3	160	2.8	160	139	1.90
0662	07-Feb-01	10.34	170	5.3	177	2.3	173	149	1.68
0662	15-Feb-02	11.36	132	1.0	143	2.3	137	112	2.32
0662	28-Oct-02	12.06	146	1.3	125	1.6	136	108	2.16
0663	09-Apr-90	-0.49	235	2.2	201	1.2	218	204	2.16
0663	16-Sep-91	0.94	94	1.2	93	1.6	93	81	3.47
0663	27-Feb-92	1.39	98	1.9	93	1.5	96	85	3.40
0663	12-Feb-93	2.35	97	1.3	90	1.9	93	83	3.38
0663	21-Jan-94	3.29	97	1.7	97	2.3	97	87	3.42
0663	02-May-95	4.57	95	1.6	93	1.9	94	84	3.39

Table 36. Roughness Values (Continued).

Section	Date	Years	Left IRI (in/mi)		Right IRI (in/mi)		MRI (in/mi)	HRI (in/mi)	RN
			Ave	St Dev	Ave	St Dev			
0663	19-Feb-97	6.37	96	1.4	95	0.9	95	85	3.26
0663	17-Apr-98	7.53	91	2.7	98	2.6	94	83	3.07
0663	02-Mar-99	8.40	97	2.8	99	1.6	98	84	3.02
0663	14-Mar-00	9.44	103	1.3	98	2.0	101	89	2.94
0663	17-Aug-00	9.86	111	2.0	99	1.6	105	95	2.88
0663	07-Feb-01	10.34	106	0.9	104	1.2	105	95	2.79
0663	15-Feb-02	11.36	108	1.9	102	1.5	105	96	2.93
0663	28-Oct-02	12.06	121	1.8	112	1.1	117	107	2.16
0664	27-Sep-90	-0.02	40	1.8	48	1.3	44	38	4.23
0664	16-Sep-91	0.94	44	1.0	44	1.7	44	38	4.34
0664	27-Feb-92	1.39	46	0.3	45	1.7	46	40	4.29
0664	12-Feb-93	2.35	52	0.9	46	0.8	49	42	4.17
0664	21-Jan-94	3.29	49	2.1	47	1.6	48	41	4.18
0664	02-May-95	4.57	47	1.6	48	1.5	48	40	4.15
0664	19-Feb-97	6.37	51	0.7	47	0.7	49	41	4.12
0664	17-Apr-98	7.53	50	1.3	47	1.1	49	41	3.92
0664	02-Mar-99	8.40	48	0.9	50	0.9	49	40	4.01
0664	14-Mar-00	9.44	51	0.8	48	0.6	50	41	4.05
0664	17-Aug-00	9.86	52	0.8	47	0.3	49	40	4.08
0664	07-Feb-01	10.34	53	1.1	47	0.3	50	42	4.09
0664	15-Feb-02	11.36	52	0.9	49	0.3	50	41	4.06
0664	28-Oct-02	12.06	50	0.8	47	1.1	49	41	3.96
0665	27-Sep-90	-0.02	42	1.2	43	0.8	43	38	4.30
0665	16-Sep-91	0.94	44	1.5	42	0.8	43	40	4.42
0665	27-Feb-92	1.39	46	0.5	41	0.2	44	40	4.39
0665	12-Feb-93	2.35	49	1.0	43	0.6	46	41	4.32
0665	21-Jan-94	3.29	46	0.7	47	0.7	46	42	4.29
0665	02-May-95	4.57	48	0.5	46	0.7	47	42	4.29
0665	19-Feb-97	6.37	51	1.0	47	0.3	49	43	4.17
0665	17-Apr-98	7.53	51	0.4	48	0.6	50	43	3.94
0665	02-Mar-99	8.40	49	0.3	51	0.7	50	44	4.03
0665	14-Mar-00	9.44	53	0.8	50	0.6	52	44	4.11
0665	17-Aug-00	9.86	55	0.9	50	0.1	52	45	4.09
0665	07-Feb-01	10.34	57	0.7	52	0.3	55	47	4.11
0665	15-Feb-02	11.36	54	0.9	50	0.7	52	44	4.10
0665	28-Oct-02	12.06	53	1.6	50	0.8	51	44	4.02
0666	27-Sep-90	-0.02	37	1.7	42	1.8	39	33	4.21
0666	16-Sep-91	0.94	36	0.7	45	0.9	40	34	4.37
0666	27-Feb-92	1.39	36	0.1	47	1.1	42	35	4.34
0666	12-Feb-93	2.35	40	1.4	47	0.7	44	36	4.17
0666	21-Jan-94	3.29	38	0.6	46	0.7	42	34	4.20
0666	02-May-95	4.57	39	1.1	48	1.0	44	35	4.19
0666	19-Feb-97	6.37	45	0.9	49	1.5	47	37	4.11

Table 36. Roughness Values (Continued).

Section	Date	Years	Left IRI (in/mi)		Right IRI (in/mi)		MRI	HRI	RN
			Ave	St Dev	Ave	St Dev	(in/mi)	(in/mi)	
0666	17-Apr-98	7.53	41	0.8	51	1.3	46	37	3.88
0666	02-Mar-99	8.40	43	0.6	51	1.1	47	37	4.03
0666	14-Mar-00	9.44	47	0.7	51	1.2	49	41	4.05
0666	17-Aug-00	9.86	49	0.7	52	0.8	50	41	4.01
0666	07-Feb-01	10.34	47	1.1	52	0.5	49	40	4.05
0666	15-Feb-02	11.36	48	1.1	52	1.1	50	41	4.03
0666	28-Oct-02	12.06	47	0.6	52	1.5	49	40	4.00
0667	27-Sep-90	-0.02	66	1.5	79	0.9	72	67	4.08
0667	16-Sep-91	0.94	63	1.1	76	1.3	70	66	4.26
0667	27-Feb-92	1.39	65	1.2	74	0.8	70	65	4.25
0667	12-Feb-93	2.35	66	0.7	75	0.9	71	66	4.13
0667	21-Jan-94	3.29	66	0.4	75	0.8	70	66	4.15
0667	02-May-95	4.57	64	0.2	75	1.3	70	65	4.14
0667	19-Feb-97	6.37	68	0.9	77	0.3	73	67	4.06
0667	17-Apr-98	7.53	67	0.3	78	0.7	73	67	3.86
0667	02-Mar-99	8.40	68	0.6	78	0.9	73	67	3.97
0667	14-Mar-00	9.44	69	1.0	79	0.7	74	68	4.01
0667	17-Aug-00	9.86	72	0.6	77	0.6	74	69	4.00
0667	07-Feb-01	10.34	71	0.9	77	0.5	74	68	4.02
0667	15-Feb-02	11.36	70	0.7	78	0.4	74	68	4.00
0667	28-Oct-02	12.06	67	1.6	76	1.4	72	65	3.89
0668	27-Sep-90	-0.02	36	1.6	38	1.0	37	30	4.22
0668	16-Sep-91	0.94	34	1.2	43	1.9	38	33	4.38
0668	27-Feb-92	1.39	37	1.9	42	0.6	39	34	4.35
0668	12-Feb-93	2.35	40	1.3	47	1.4	43	38	4.21
0668	21-Jan-94	3.29	40	1.9	41	1.2	41	35	4.24
0668	02-May-95	4.57	39	0.8	43	1.6	41	35	4.21
0668	19-Feb-97	6.37	42	1.4	42	0.9	42	34	4.15
0668	17-Apr-98	7.53	39	1.2	42	1.7	40	33	3.93
0668	02-Mar-99	8.40	38	0.5	42	1.4	40	33	4.07
0668	14-Mar-00	9.44	41	0.3	43	1.6	42	35	4.05
0668	17-Aug-00	9.86	42	0.8	43	1.1	43	35	4.07
0668	07-Feb-01	10.34	43	1.1	41	1.0	42	35	4.08
0668	15-Feb-02	11.36	44	0.6	42	0.7	43	36	4.06
0668	28-Oct-02	12.06	45	1.4	45	1.3	45	37	3.90
0669	27-Sep-90	-0.02	51	1.5	52	1.0	52	47	4.17
0669	16-Sep-91	0.94	48	0.6	51	1.6	49	45	4.46
0669	27-Feb-92	1.39	50	1.0	52	0.5	51	46	4.40
0669	12-Feb-93	2.35	54	0.5	53	1.0	54	48	4.29
0669	21-Jan-94	3.29	53	1.4	55	0.6	54	48	4.27
0669	02-May-95	4.57	54	0.5	54	0.5	54	49	4.23
0669	19-Feb-97	6.37	57	0.9	55	0.5	56	50	4.13
0669	17-Apr-98	7.53	55	0.9	59	1.7	57	52	3.88

Table 36. Roughness Values (Continued).

Section	Date	Years	Left IRI (in/mi)		Right IRI (in/mi)		MRI	HRI	RN
			Ave	St Dev	Ave	St Dev	(in/mi)	(in/mi)	
0669	02-Mar-99	8.40	56	0.6	57	1.0	56	51	4.04
0669	14-Mar-00	9.44	58	0.6	57	0.4	57	52	4.10
0669	17-Aug-00	9.86	61	0.7	57	0.7	59	54	4.09
0669	07-Feb-01	10.34	59	0.3	56	0.4	58	53	4.13
0669	15-Feb-02	11.36	59	1.1	57	0.8	58	52	4.10
0669	28-Oct-02	12.06	59	0.9	55	1.5	57	50	3.98

References

Karamihas, S. M., T.D. Gillespie, and S. M. Riley. 1995. "Axle Tramp Contribution to the Dynamic Wheel Loads of a Heavy Truck." *Proceedings of the 4th International Symposium on Heavy Vehicle Weights and Dimensions*, Ann Arbor, Michigan. Ed. C. B. Winkler.

Sayers, M. W. 1989. "Two Quarter-Car Models for Defining Road Roughness: IRI and HRI." *Transportation Research Record* 1215: 165-172.

Sayers, M. W. and S. M. Karamihas. 1996. "Estimation of Rideability by Analyzing Road Profile." *Transportation Research Record* 1536: 110-116.

APPENDIX D: DETAILED OBSERVATIONS

This appendix provides detailed observations from the roughness trends, profiles, and distress surveys of each section within the Arizona Specific Pavement Studies 6 project. Observations regarding profile features are made using power spectral density (PSD) plots, filtered elevation profile plots, and roughness profiles.

Typically, roughness profiles provided the most information about the location of features that affected the International Roughness Index (IRI) most, including areas of localized roughness. In this appendix, roughness profiles were made using a base length of 25 ft unless otherwise specified. An area is considered to have localized roughness when the roughness profile (with a base length of 25 ft) reaches a peak value that is greater than 2.5 times the average IRI for the whole section. Detection of localized roughness usually prompted more careful examination of the filtered elevation profiles.

SECTION 040601

Roughness: The IRI of the left side increased from 104 to 225 inches/mi in less than three years. The IRI values vary significantly within the last two visits before this section was taken out of the study. The IRI of the right side increased from 102 inches/mi in visit 00 to 122 inches/mi in visit 04, but reached a peak value of 145 inches/mi in visit 03. The Half-car Roughness Index (HRI) was about 20 inches/mi below the Mean Roughness Index (MRI) throughout the monitoring history.

Elevation profile plots: The elevation profiles were fairly consistent throughout the monitoring period in the medium wavelength range, and very consistent in the long wavelength range, but not very consistent in the short wavelength range.

In visit 00 a disturbance appeared at the majority of the joints. This included some shallow bumps, some narrow dips, and some faults up to 0.1 inch deep. Narrow dips appeared in the left side profiles 3 ft, 17 ft, 62 ft, 122 ft, 257 ft, 273 ft, 289 ft, 302 ft, and 498 ft from the start of the section. The dips were usually less that 2 ft wide and were up to 0.3 in deep. In the range from 257 to 302 ft from the start of the section, the dips were wider along the trailing edge. From visit 00 through visit 03, the dips grew in number and severity until many of them were more than 0.3 inch deep. In visit 03 narrow dips appeared throughout the section with a spacing that roughly followed a 15-13-15-17 ft pattern. The pattern was not as obvious in visit 04. However, some of the dips were still more severe. For example, a narrow dip up to 1 inch deep appeared about 360 ft from the start of the section, and a dip 6 ft wide and about 0.6 inch deep appeared about 257 ft from the start of the section.

Narrow dips also appeared in the right-side profiles, but there were fewer of them and they were less severe in most cases. The most noteworthy dip in the right side profiles appeared about 411 ft from the start of the section. It was about 0.2 inch deep in visit 01, but more than 4

ft wide. By visit 03, its depth had grown beyond 0.5 inch. In visit 04, another dip that was about 0.5 inch deep and more than 2 ft wide appeared 34 ft from the start of the section.

Roughness profile plots: Many of the narrow dips within the profiles contributed significantly to roughness, and the instances of significant roughness at narrow dips increased with each visit.

By visit 03, the left side profiles included increased roughness at all of the narrow dips in a regular pattern. Localized roughness appeared in the left side profiles 360 ft from the start of the section in visit 04. The roughness at the deep dip there contributed more than 20 inches/mi to the roughness of the entire section.

The dip in the right side profile 411 ft from the start of the section consistently contributed significant roughness to the section. In visit 03, localized roughness appeared 156 ft and 411 ft from the start of the section. In visit 04, the dip 34 ft from the start of the section also caused localized roughness.

PSD plots: PSD plots for the left side profiles included a spike at 15 ft and elevated content at some upper harmonics (7.5 ft, 5 ft) in every visit. In some cases, PSD plots from the right side profiles also showed some roughness that stood out at a wavelength of 25.5 ft. The spectral content was high in the short wavelength range because of spikes that appeared in the profile at joints. The short wavelength content grew significantly with time.

Distress surveys: Distress data were only available for September 26, 1991. The survey confirmed that the spikes within the profile appeared at the joints. Significant distress was recorded at many of the joints, although the joints where the roughness was worst did not always correspond to those with the most distress.

Maintenance history: Partial depth patching (47 sq. ft) was performed on this section in November 1991.

SECTION 040602

Roughness: The IRI increased steadily on the left side from 166 to 218 inches/mi and on the right side from 167 to 202 inches/mi in less than three years. The HRI was 14 percent to 16 percent below the MRI.

Elevation profile plots: Before rehabilitation the entire section was faulted. Faults appeared with a pattern that closely approximated the saw cut spacing 15-13-15-17 ft. (The actual pattern was closer to 14.8-12.9-15.1-16.9 ft.) Each fault on the right side appeared about 1 ft downstream of a fault on the left side from the same joint. Faults 0.05 to 0.3 inch deep appeared in the left side and faults 0.05 to 0.15 inch deep appeared on the right side.

The profiles from both sides include abrupt downward steps of up to 0.2 inch throughout the entire section followed by a fairly steep upward slope. The downward steps are typically 7 to 15 ft apart. A very large downward step appeared about 561 ft from the start of the section. In many of the profile measurements, the step was 0.7 inch downward on the left side and 0.5 inch downward on the right side.

Roughness profile plots: Many of the downward steps within the profiles contributed significant roughness to the section, and the roughness at these locations grew steadily with time. The severity of roughness caused by the downward steps was uniform along the section, with the exception of a moderate increase in roughness on the left side in the last 100 ft of the section. Localized roughness appeared 561 ft from the start of the section.

PSD plots: Much of the roughness in the left side profiles was concentrated at a wavelength of 14.8 ft as well as 11.9, 8.4, 7.5, and 6.6 ft. On the right side, roughness was concentrated at 14.8 ft, 8.6 ft, and 7.5 ft.

Distress surveys: Distress data were only available for September 26, 1991. Although faulting measurements were not reviewed for this study, the downward steps followed by an upward slope provide clear profiles of faulted slabs and half slabs that are often tilted over the first several feet after the faults. The localized roughness about 561 ft from the section start appears in a location where map cracking that was recorded in the September 26, 1991 distress survey.

SECTION 040603

Roughness: Rehabilitation decreased the IRI from 138 to 52 inches/mi on the left side and from 200 to 58 inches/mi on the right side. After rehabilitation, the MRI held somewhat steady in visits 01 through 06, then increased more rapidly throughout the rest of the monitoring history. The HRI was 8 percent below the MRI before rehabilitation and 13 percent to 21 percent below MRI after rehabilitation.

Elevation profile plots: Before rehabilitation the entire section was faulted. Faults appeared with a pattern that crudely approximated the saw cut spacing 15-13-15-17 ft. (The actual pattern was closer to 15.1-12.7-15.4-16.8 ft.) Each fault on the right side appeared about 1 ft downstream of a fault on the left side from the same joint. Faults 0.05 to 0.2 inch deep appeared in the left side and faults 0.05 to 0.3 inch deep appeared on the right side.

The profiles did not change much in visits 01 through 06. In visit 07, narrow dips appeared in a regular pattern that resembled the underlying joint spacing over much of the section on the left side and in several locations on the right side. The dips were up to 2 ft wide. The dips grew to up to 0.4 inch deep (with a few exceptions) by visit 12, but were less severe in visits 13 and 14. On the right side some dips also appeared at center slab locations near the middle of the section.

The section included a few dips that stood out as more severe than the others: (a) 453 ft from the start of the section on the left side that began growing in starting with visit 04, (b) 438 ft from the start of the section on the left side that stood out in visit 10 and later, (c) 141 ft from the start of the section that stood out on the left side starting in visit 08 and was more than 2 ft wide and 1 inch deep by visit 14; (d) 96 ft from the start of the section that first stood out on the left side in visit 05 and first stood out in visit 09 on the right side; and (e) 201 ft from the start of the section on the right side that first stood out in visit 09.

The dips in visits 13 and 14 were less severe than the dips in visit 12. Profiles from visit 13 and 14 included a sharp rise of 0.2 inch on the left and 0.35 inch on the right about 120 ft from the start of the section. At visit 13, the long wavelength content had changed downstream of the rise, but not upstream.

Roughness profile plots: The left side profiles did not include localized roughness, although the dip 438 ft from the start of the section caused a very high value in the short base length roughness profile. The dip 97 ft from the start of the section caused localized roughness on the right side in visits 13 and 14.

PSD plots: Before rehabilitation the PSD plots included content concentrated around a wavelength of 15 ft, 7.5 ft, 5 ft, etc. The content below a wavelength of 20 ft, and especially below 5 ft, increased over visits 01 through 12. Content at wavelengths between 1 and 20 ft decreased significantly between visits 12 and 13.

Distress surveys: Distress surveys included transverse cracks throughout the monitoring history. Transverse cracks were noted at some locations in September 1991 including the 97 ft, 141 ft, 201 ft, and 458 ft from the start of the section, where the deepest narrow dips eventually appeared in the profiles. The dip 438 ft from the start of the section was first noted as a transverse crack in September 1994. By December 1999, transverse cracks that covered the entire width of the lane appeared in a regular pattern that matched the joint spacing of the underlying pavement. Per the LTPP Distress Identification Manual, transverse cracks were not recorded on the skin patch in visits 13 and 14. Narrow dips in the profile at the same pattern found in earlier visits confirm the presence of the cracks.

Maintenance history: Crack sealing (700 ft) was performed on this section in March 1995. The section received skin patching over 4400 sq. ft in September 2001.

SECTION 040604

Roughness: Rehabilitation decreased the IRI from 91 to 69 inches/mi on the left side and from 113 to 67 inches/mi on the right side. After rehabilitation, the MRI did not increase significantly in visits 01 through 07 and increased more rapidly throughout the rest of the monitoring history. The HRI was 14 percent below the MRI before rehabilitation and 17 percent to 23 percent below MRI after rehabilitation.

Elevation profile plots: Before rehabilitation the majority of joints in this section were faulted. Faults up to 0.15 inch deep (with the exception of one 0.4 inch deep fault) appeared with a pattern that crudely approximated the saw cut spacing 15-13-15-17 ft, with some gaps at joints without faulting. When faults appeared on both sides at the same joint, the fault on the right side appeared about 1 ft downstream of the fault on the left. In many cases, a smaller fault appeared between the larger faults (at a center slab position).

The profiles before rehabilitation also included a dip 158 ft from the start of the section on the left side 0.2 inch deep. Dips up to 0.2 inch deep also appeared in the right side 280 ft, 401 ft, and 429 ft from the start of the section.

Post-rehabilitation profiles inherited much of the long wavelength content that was present before rehabilitation.

Visit 01 profiles included more short wavelength content over the first 220 ft than the rest of the section on the left side. Visit 01 left side profiles also included a dip 5 ft wide and 0.15 ft deep about 163 ft from the start of the section and a sharp upward step of 0.15 inch over 2 ft near 227 ft from the start of the section. Visit 01 agreed with the later visits in long wavelength content, but agreed only somewhat in the medium wavelength range and not at all in the short wavelength range.

Profile features were consistent in visits 02 through 06 on the right side and in visits 02 through 07 on the right side. Afterward, the narrow dip began to appear in the profiles throughout much of the section, starting with dips 1 ft wide and up to 0.1 inch deep of the left side in visit 07. By visit 14, the dips appeared on both sides in a regular pattern over the last 440 ft of the section. The dips were up to 0.3 inch deep on the left side and up to 0.2 inch deep in the right side. These dips appeared in the same locations where faults were detected in visit 00 profiles. Two of the repeat measurements in visit 14 included a dip 0.7 inch deep 213 ft from the start of the section.

On the left side, a bump 5 ft long and 0.15 inch deep appeared 380 ft from the start of the section in visits 02 through 14. Short wavelength content in the left side profiles was higher over the first half section in visits 07 through 14.

Roughness profile plots: The narrow dips at the joints caused most of the roughness and its progression over visits 07 through 14. No localized roughness was detected on this section.

PSD plots: Before rehabilitation the PSD plots included elevated content in the range of wavelengths from 15 to 16 ft. The PSD plots were fairly consistent over visits 02 through 07. Spectral content increased in the wavelength range shorter than 5 ft over the rest of the

monitoring history. Content isolated at 15 ft and upper harmonics (7.5 ft, 5 ft, etc.) also increased throughout visits 07 through 14.

Distress surveys: Distress surveys show slightly skewed, sealed saw cuts throughout the entire section after rehabilitation. In October 1997 the seals were intact across the lane at the majority of the saw cuts, but not intact at any of the saw cuts by December 1999.

Maintenance history: Crack sealing (450 ft) was performed on this section in March 1995.

SECTION 040605

Roughness: Rehabilitation decreased the IRI from 149 to 58 inches/mi on the left side and from 155 to 64 inches/mi on the right side. Over less than three years after rehabilitation, the IRI increased to 135 inches/mi on the left and 127 inches/mi on the right. The HRI was 10 percent to 12 percent below the MRI.

Elevation profile plots: Before rehabilitation the entire section was faulted. Faults 0.05 to 0.25 inch deep appeared with a pattern that crudely approximated the saw cut spacing 15-13-15-17 ft. (The actual pattern was closer to 15.1-13.0-14.8-16.7 ft.) Each fault on the right side appeared about 1 ft downstream of a fault on the left side from the same joint. The left side profiles included a dip 0.4 inch deep and 1.5 ft wide that was 897 ft from the start of the section.

The visit 01 profiles (after rehabilitation) do not include the faults. Many areas of visit 01 profiles include 12 to 18 ft intervals in a “bowl” shape, in which the ends of the area are up to 0.1 inch higher than the center.

By visit 03, faulting appears throughout the profiles that are 6 to 15 ft apart. On the left side, a steep upward slope typically follows the faults. Many of these are simply narrow downward spikes with an aggressive leading edge. The faults and spikes grow in severity by visit 04. On the right side, a constant upward slope typically follows the faults to the next fault.

The right side profiles in visits 02 through 04 included a dip about 2 ft wide and up to 1 inch deep that appeared about 5 ft from the start of the section.

Roughness profile plots: The majority of the roughness within this section occurred at the joints, both before and after rehabilitation. Many of the faults within the profiles contributed significant roughness to the section, and the roughness at these locations grew steadily with time after visit 01. The severity of roughness caused by the faults was fairly uniform along the section. An exception was severe localized roughness in the right side profile in the first 10 ft of the section. By visit 04, this was severe enough to add 12 inches/mi to the roughness of the entire section. Localized roughness also appears on the left side about 897 ft from the start of the section in visits 00 and 04.

PSD plots: Some of the roughness in the profiles was concentrated at a wavelength of 15 ft and 7.5 ft. PSD plots from the left side also included spikes at about 8.5 ft and 12 ft. The spectral content decreased significantly in the wavelength range below 20 ft between visit 00 and 01, but hardly at all for wavelengths above 20 ft. After visit 01, the content for wavelengths below 20 ft steadily grew with time until the visit 04 PSD plots were very similar to those from visit 00. (The spatial distribution of roughness was not the same, only the distribution of roughness within each wavelength range.)

Distress surveys: Distress data were only available for April 12, 1991 and September 26, 1991. Although faulting measurements were not reviewed for this study, the downward steps followed by an upward slope provide clear profiles of faulted slabs and half slabs that are often tilted over the first several feet after the faults. The localized roughness at the narrow dip found on the right side at the start of the section corresponds to a distressed joint. Rough narrow dips also appeared at other joints where distress was noted, but many distressed joints were noted without corresponding localized roughness.

SECTION 040606

Roughness: Rehabilitation decreased the IRI from 109 to 66 inches/mi on the left side and from 99 to 83 inches/mi on the right side. After rehabilitation the IRI of the left side progressed at an increasing rate to 148 inches/mi over the monitoring history. The IRI of the right side progressed at an increasing rate to a final value of 125 inches/mi, but some erratic values appeared in visits 08, 09, and 14. The HRI was 15 percent below the MRI before rehabilitation and 9 percent to 16 percent below MRI after rehabilitation with values that decreased with time.

Elevation profile plots: Before rehabilitation the section exhibited early signs of faulting both at joints and at midslab positions, but faults greater than 0.1 inch were rare. Many of the faults seemed to appear as upward step changes in elevation. The left side profiles included several narrow dips: 37 ft from the start of the section 0.4 inch deep and 2 ft wide, 66 ft from the start of the section 0.2 inch deep and 1.5 ft wide, 186 ft from the start of the section 0.15 inch deep and 1.5 ft wide, and 461 ft from the start of the section 0.25 inch deep and 1.5 ft wide. The left side profiles also included two more severe dips that were about 5 ft wide: 173 to 178 ft from the start of the section about 0.1 inch deep with a round shape and 413 to 418 ft from the start of the section about 0.25 ft deep with a rectangular shape.

By visit 05, three small bumps appeared along the section. The bumps were 2 to 3 ft wide and up to 0.1 inch high, and remained throughout the rest of the monitoring history. Narrow dips about 1 ft wide and up to 0.1 inch deep appeared along the section in visit 07 with an irregular spacing. By visit 10, more than 20 narrow dips appeared that were up to 0.3 inch deep. (Once exception was a dip 0.7 inch deep and 370 ft from the section start on the right side.) By visit 13 narrow dips appeared with a pattern that approximated the underlying joint pattern, with dips missing at four joint locations.

The most severe dips on the left side were: (a) 0.7 inch deep, 85 ft from the start of the section, (b) 0.7 inch deep (in two of five repeat measurements), 205 ft from the start of the section, (c) 1 inch deep, 221 ft from the start of the section, (d) 0.6 inch deep, 266 ft from the start of the section, (e) 0.4 to 0.8 inch deep, 369 ft from the start of the section; and, (f) 0.5 to 1 inch deep (depending on which repeat measurement is plotted), 445 ft from the start of the section.

The most severe dips on the right side were: (a) 0.6 inch deep, 86 ft from the start of the section, (b) 0.3 to 0.5 inch deep (depending on which repeat measurement is plotted), 207 ft from the start of the section, (c) 0.5 inch deep, 267 ft from the start of the section; and (d) 0.4 to 0.6 inch deep (depending on which repeat measurement is plotted), 370 ft from the start of the section.

The dips were less severe on the right side in visit 14 than in visit 13 in some locations.

Roughness profile plots: Before rehabilitation, the deep dip on the left side 413 to 418 ft from the start of the section was severe enough to qualify as localized roughness.

The profiles did not include any localized roughness after rehabilitation. However, more roughness was detected in the presence of the deepest dips (such as those listed above) than in other locations. Further, very short interval roughness profiles confirm that the narrow dips account for most of the roughness on this section.

PSD plots: Before rehabilitation the PSD plots included elevated content at wavelengths of 15 ft, 7.5 ft, etc. From visit 07 through 14, the roughness grew in two wavelength ranges: (a) at about 15 ft, and (b) in the range below 10 ft. The exception was visit 13 on the right side, which included higher content than visits 12 and 14 in both ranges.

Distress surveys: The prerehabilitation distress survey shows a corner break on the left side where localized roughness was detected, and the profile shows localized settlement within the corner break.

By August 2000 transverse cracks appeared with a pattern that approximated the underlying joint spacing with a few gaps. This pattern of transverse cracks developed gradually over the previous four distress surveys starting in September 1991.

The locations and first appearance of narrow dips in the profiles corresponds closely with the locations and first appearance of transverse cracks in the distress surveys. Further, the absence of a transverse crack at the location of an underlying joint is usually accompanied by the lack of a narrow dip in the profile.

Maintenance history: Crack sealing (640 ft) was performed on this section in March 1995.

SECTION 040607

Roughness: Rehabilitation decreased the IRI from 104 to 62 inches/mi on the left side and from 97 to 43 inches/mi on the right side. After rehabilitation, the MRI held somewhat steady in visits 01 through 06, then increased more rapidly throughout the rest of the monitoring history with a final value of 200 inches/mi. The HRI was 15 percent below the MRI before rehabilitation and 7 percent to 18 percent below MRI after rehabilitation with values that decreased with time.

Elevation profile plots: Before rehabilitation the profiles over the first half of the section included narrow dips up to 0.15 inch deep on both sides in a pattern that crudely approximated the joint spacing of 15-13-15-17 ft. The second half of the section included a few narrow bumps at joints. Four deep narrow dips about 2 ft wide appeared in the profiles: 289 ft from the start of the section 0.9 inch deep on the right side, 21 ft from the start of the section 0.3 inch deep on the left side, 201 ft from the start of the section 0.65 inch deep on the left side, and 261 ft from the start of the section 0.3 inch deep on the left side.

Visit 02 profiles included seven small bumps along the section. The bumps were 2 to 4 ft wide and up to 0.15 inch high. The highest bump appeared 369 ft from the start of the section. Some of the bumps, including the one 369 ft from the start of the section, remained throughout the monitoring history.

Visit 07 profiles included a bump 0.2 inch high and about 3 ft wide that was 235 ft from the start of the section.

Narrow dips (1 to 3 ft wide and up to 0.2 inch deep) appeared in visit 07 profiles at five locations on both sides of the lane. The dips increased in number and severity throughout the rest of the monitoring period. By visit 14 narrow dips appeared with a pattern that approximated the underlying joint pattern, with dips missing at five joint locations on the left side and six joint locations on the right side.

Short wavelength profile plots revealed some locations with roughness that stood out visually compared to the rest of the section. On the left side:

A narrow dip appeared 132 ft from the start of the section. In visit 09, it was 0.5 ft wide and 0.5 inch deep. By visit 13, the dip had grown to over 1 ft wide and 0.9 inch deep.

Narrow dips about 1 ft wide appeared 148 ft, 172 ft, 189 ft, 219 ft, and 249 ft from the start of the section. These dips appeared in visits 07 and 08, and increased in severity to 0.8 to1 inch deep by visit 14.

In visit 10, a rough area appeared 277 to 289 ft from the start of the section. This included a narrow dip at the start and chatter (rapid changed in elevation within a 0.1 inch band) over the

rest of the area. By visit 14, the area was quite rough, starting with a dip 1 ft wide and over 1.2 inches deep.

In visit 11, a rough area appeared 397 to 411 ft from the start of the section. This included chatter (rapid changed in elevation within a 0.1 inch band) over entire area followed by a narrow dip at the end. By visit 13, the area was quite rough. In visit 14, the chatter was no longer present, but a narrow dip appeared at both ends.

In visit 09, a dip 1 ft wide and 0.6 inch deep appeared 445 ft from the start of the section just downstream of a shallow bump.

On the right side:

- Narrow dips grew to more than 1 inch deep 39 ft, 173 ft, 190 ft, 219 ft, 353 ft, and 411 ft from the start of the section by visit 14.

Roughness profile plots: Before rehabilitation, the deep dips on the left side 201 ft from the start of the section and on the right side 289 ft from the start of the section were severe enough to qualify as localized roughness.

Throughout the post-rehabilitation monitoring history, the bumps and narrow dips discussed above caused areas of much greater roughness than the surrounding pavement. However, two features were so rough that they qualified as localized roughness when compared to the overall section average: (a) the narrow bump 445 ft from the start of the section on the left side in visit 09, and (b) the narrow bump 277 ft from the start of the section on the left side preceding the rough area in visit 12. This dip alone contributed over 20 inches/mi to the overall roughness of the section.

PSD plots: Before rehabilitation the PSD plots included elevated content on the right side at wavelengths of 15 ft, 12.5 ft, and 7 ft and on the left side at wavelengths of 25 ft, 15 ft, 12.5 ft, and 7.5 ft.

After rehabilitation, much more growth in spectral content occurred after visit 08 than before. On the left side, the content grew in the wavelength range under 10 ft up to visit 09, then grew in the wavelength range below 50 ft through the rest of the monitoring history. On the right side, the largest growth was found in the wavelength range below 10 ft between visits 08 and 09.

Distress surveys: Distress surveys show transverse cracking throughout the monitoring history. Four transverse cracks that covered the width of the lane were recorded in 1991. The number of transverse cracks grew steadily with time. By October 2002, 30 transverse cracks appeared with a pattern that approximated the underlying joint spacing, with a few gaps.

The pattern and first appearance of narrow dips in the profiles correspond with the locations and first appearance of transverse cracks in the distress surveys. Further, the absence of a transverse crack at the location of an underlying joint is usually accompanied by the lack of a narrow dip in the profile. Often, the deepest dips were found in the profile in the same locations where the distress survey cited high severity cracks, and the shallowest dips were found in the profile where the distress survey recorded medium and low severity cracks.

Distress surveys show a longitudinal crack from 395 to 413 ft from the start of the section on the left side of the lane starting in August 2000. This explains the narrow dip and chatter found in the profile starting in visit 11.

Distress surveys show an area of fatigued pavement from 276 to 287 ft from the start of the section on the left side starting in December 1999. This area became a stretch of moderately fatigued pavement deteriorating into a small area of highly fatigued pavement by August 2000. Starting in August 2000, a 1 sq. ft patch in very poor condition appeared at the lead end of this area. These features explain the localized roughness found in the profile starting 277 ft from the start of the section.

Distress surveys include a high severity transverse crack about 445 ft from the start of the section starting in December 1999. In December 1999 the survey indicated the presence of a "splattered fox carcus" (sic) on the left side of the lane just downstream of the crack. In August 2000 the survey showed gouges over an area on the left side of the lane just downstream of the crack. These odd features correspond to the localized roughness cited above for visit 09. (The area continued to be as rough in later visits, but the roughness level was overcome by the rest of the section after visit 09.)

Maintenance history: Crack sealing (550 ft) was performed on this section in March 1995. In May 2000 potholes were hand-patched and compacted by a truck. No corresponding changes in the profile were detected between visits 10 and 11.

SECTION 040608

Roughness: Rehabilitation decreased the IRI from 105 to 68 inches/mi on the left side and from 102 to 50 inches/mi on the right side. After rehabilitation, the IRI on the left side held somewhat steady in visits 02 through 09, then increased more rapidly throughout the rest of the monitoring history. The IRI on the right side grew at a steady, modest rate to 72 inches/mi over the monitoring history. The HRI was 12 percent to 21 percent below the MRI.

Elevation profile plots

Before rehabilitation: The majority of joints in this section were faulted up to 0.1 inch deep. Faults appeared with a pattern that closely approximated the saw cut spacing 15-13-15-17 ft,

with some gaps at joints without faulting and some joints with narrow dips rather than faults. When faults appeared on both sides at the same joint, the fault on the right side appeared about 1 ft downstream of the fault on the left. In some cases, a smaller fault appeared between the larger faults (at a center slab position). The most severe narrow dips were: a dip 3 ft wide, 0.25 inch deep and 93 ft from the start of the section; and a dip 2 ft wide, 0.25 inch deep and 409 ft from the start if the section.

After rehabilitation, left side: Visits 02 through 14 profiles included bumps 2 to 4 ft wide and up to 0.2 inch high that were 189 ft, 210 ft, and 238 ft from the start of the section. The most severe was 210 ft from the start.

Two narrow dips, 367 ft and 386 ft from the start of the section, appeared in visit 08. They were less than 2 ft wide. The leading dip was 0.1 inch deep and the trailing dip was 0.2 inch deep. The dips bounded an area of high short wavelength roughness (i.e., chatter) in three of the five repeat measurements. This appeared in all five repeats of visits 09 through 14:

- In visit 09 the trailing dip was 0.4 inch deep with very heavy chatter in one repeat.
- In visit 10 the leading dip was 0.4 inch deep, the trailing dip was 0.6 inch deep, and both dips were 2 ft wide. Two other dips emerged within the bounded area.
- In visit 11 the leading dip was 1.6 inch deep and the trailing dip was 0.6 inch deep.
- In visit 12 the leading dip was 0.7 inch deep and the trailing dip was 0.8 inch deep. The chatter in the bounded area was reduced, and the dip that had appeared in visit 10 was not present.
- In visit 13, the dips at the edges had reduced in severity, but the two dips inside the area had reappeared. Of the four dips, the most severe was 1.2 inch deep, and was 372 ft from the start of the section.
- In visit 14, the severity of the dips was not consistent over the five repeat measurements. In the most severe case, some of the dips were 2 inch deep.

After rehabilitation, right side: Visits 02 through 08 included elevated medium wavelength roughness from 175 to 215 ft.

In visit 09 narrow dips up to 0.15 inch deep appeared in four locations. The dips grew in number (to 14) and severity through the rest of the monitoring history. In visit 14, dips under 0.5 ft wide but more than 1.5 inch deep appeared 471 and 490 ft from the start of the section.

Roughness profile plots: In visits 02 through 07, one or more of the bumps 189 ft, 210 ft, and 238 ft from the start of the section on the left side caused localized roughness.

The rough area 367 through 386 ft from the start of the section on the left side caused localized roughness in visits 08 through 14. With the exception of visit 12, the severity of roughness in this area progressed with time. For example, the roughness in this area contributed 35 inches/mi to

the overall roughness of the section in visit 11, and 40 to 60 inches/mi to the overall roughness of the section in visit 14.

Localized roughness was detected about 201 ft from the start of the section in some repeat measurements from 03 through 08. Roughness was elevated in that location throughout the rest of the monitoring history.

PSD plots: Before rehabilitation the PSD plots included a relatively high contribution from longer (30 to 60 ft) wavelength content than most of the other sections.

After rehabilitation, the left side PSD plots showed little change through visit 07. Roughness grew in the range of wavelengths below 10 ft in visits 08 and 09, and in the wavelength range below 100 ft after visit 09.

After rehabilitation, the right side PSD plots showed change through visit 07. Roughness grew erratically in the range of wavelengths below 5 ft in visits 08 through 13, and in the wavelength range below 10 ft in visit 14.

Distress surveys: No transverse cracks or fatigue were recorded in the 1991 and 1994 distress surveys. Distress surveys from 1997 through 2002 included increasingly more transverse cracks, and the October 2002 survey included 13 transverse cracks that covered the width of the lane and several others that did not. The locations of narrow dips found within the profiles correspond to the locations of these cracks.

The October 1997 distress survey included a longitudinal crack along the wheelpath in the left side of the lane 366 through 386 ft from the start of the section. A transverse crack across the entire lane appeared at the trailing end. All of the subsequent distress surveys recorded an area of high severity fatigue where the longitudinal cracks were recorded in 1997. These four surveys also recorded small (1 to 1.5 sq. ft) patches on one or both sides of the fatigued area (366 and 386 ft from the start of the section). Starting in August 2000 the surveys showed a transverse crack across the lane at the start of the fatigued area.

Maintenance history: Crack sealing (240 ft) was performed on this section in March 1995. In May 2000 potholes were hand-patched and compacted by a truck.

SECTION 040659

Roughness: Rehabilitation decreased the IRI from 211 to 68 inches/mi on the left side and from 181 to 64 inches/mi on the right side. After rehabilitation, the IRI on both sides held fairly steady over visits 01 through 07, and then rose at an increasing rate over the rest of the monitoring period. The HRI was 12 percent to 17 percent below the MRI.

Elevation profile plots: Before rehabilitation the entire section was faulted. Faults appeared with a pattern that approximated the saw cut spacing 15-13-15-17 ft. Each fault on the right side appeared about 1 ft downstream of a fault on the left side from the same joint. Over most of the section, the magnitude of faulting ranged from 0.05 to 0.2 inch. However, the area from 390 to 480 ft from the start of the section included faulting as deep as 0.4 inch. A pattern over much of this area indicated that there were a series of shattered slabs, and the slab pieces were tilting.

The profiles before rehabilitation also included a long dip from 265 to 320 ft from the start of the section about 0.7 inch deep.

In visits 02 through 06 the most obvious roughness was at a narrow bump 31 ft from the start of the section and a narrow dip 51 ft from the start of the section on the left side.

Short duration and short wavelength roughness, such as narrow dips and patches of chatter, increased from visits 08 through 14.

Narrow dips up to 1 ft wide and 0.3 inch deep appeared at 11 locations in visit 08. The number and severity of these dips increased through the rest of the monitoring history and increased in severity most in visits 11 through 13. By visit 14, the profiles included narrow dips at 19 locations on the left side and 21 narrow dips on the right side. Most of the dips were 0.2 to 0.5 inch deep, with a few exceptions described below.

Plots of elevation in the short wavelength range revealed a few severe features:

- A dip 115 ft from the start of the section that grew to 2 ft wide and 1 inch deep on the right side by visit 14.
- An area of increased short wavelength roughness, including several dips and short sunken areas (up to 0.6 inch deep), that appeared 266 to 272 ft from the start of the section on the left side in visits 08 and 09. Roughness of this kind was also found in visits 12 through 14, but it was not found in all repeat measurements.
- A dip 290 ft from the start of the section on the left side 0.3 ft wide that grew to more than 1.5 inches deep in visit 14.
- A dip about 0.5 ft wide and 0.3 in deep that appeared 492 ft from the start of the section on the left side in visit 14. In one of the repeat measurements, the dip was nearly 2 in deep.

Roughness profile plots: Before rehabilitation, the severely tilted slab and abrupt upward step caused severe localized roughness on the left side.

By visit 06, the bump and dip 31 ft and 51 ft from the start of the section, respectively, were severe enough to classify as localized roughness.

Severe localized roughness appeared 115 ft from the start of the section on the right side. In visit 13, this area contributed more than 25 inches/mi to the overall IRI of the section. However, the roughness here was about half as severe in visits 12 and 14.

The area of roughness about 265 through 275 ft from the start of the section caused localized roughness in visits 08 and 09, and in two repeat measurements in visit 14. (This area stood out as rougher than the rest of the section in every visit starting with visit 08.)

PSD plots: Before rehabilitation the PSD plots included very slightly elevated content at wavelengths of 15 ft and 7.5 ft. Throughout the rest of the monitoring history, the content in the PSD plots below a wavelength of 20 ft grew over time.

Distress surveys: All of the narrow dips in visits 08 through 14 all appeared in locations where transverse cracks were recorded. Often, the widest and deepest dips appeared at transverse cracks that included small areas of fatigue in the wheelpath. However, not all transverse cracks caused a dip in the profiles.

The 2 ft wide dip 115 ft from the start of the section appeared at a transverse crack with a small area of fatigue. A photo taken in August 2000 shows that this is a fatigued area that had been patched.

An area of fatigue was recorded in the left wheelpath 265 to 275 ft from the start of the section in December 1999. This accounts for the area of localized roughness described above for visits 08 and 09. Subsequent distress surveys show a long area of high severity fatigue here, and a photo from October 2002 shows the narrow area of fatigued pavement with a few narrow potholes.

Maintenance history: Crack sealing (470 ft) was performed on this section in March 1995. In August 1997, September 1999, May 2000, and September 2001, potholes were hand-patched and compacted by a truck.

SECTION 040660

Roughness: Rehabilitation decreased the IRI from 194 to 65 inches/mi on the left side and from 251 to 65 inches/mi on the right side. After rehabilitation, the IRI on both sides rose at a steady rate over the rest of the monitoring period. The HRI was 12 percent below the MRI before rehabilitation and 9 percent to 15 percent below MRI after rehabilitation with values that decreased overall with time.

Elevation profile plots: Before rehabilitation the majority of joints in this section were faulted, including all of the joints in the last 400 ft of the section. Faults 0.05 to 0.25 inch deep appeared with a pattern that closely approximated the saw cut spacing 15-13-15-17 ft. When faults appeared on both sides at the same joint, the fault on the right side appeared about 1 ft

downstream of the fault on the left. In many cases, a smaller fault appeared between the larger faults (at a center slab position).

The profiles before rehabilitation also included three severe dips: a dip 3 ft wide and 1.25 inches deep that appeared 48 ft from the start of the section on the right side, a dip 3 ft wide and 0.5 inch deep that appeared 43 ft from the start of the section on the left side, and a dip 5 ft and 0.5 inch deep that appeared 52 ft from the start of the section on the left side.

After rehabilitation the roughness in the long wavelength range was greater in the first half of the section than in the second half. The profiles did not change significantly in visits 02 through 05. The profiles included a dip from 50 to 90 ft from the start of the section. In visit 06, the dip grew to more than 1 inch deep on the left side and 0.6 inch deep on the right side. On the left side, the dip included rapid changes in elevation at the leading and trailing edges, such that it appears as a sunken area.

The dip grew deeper through visit 09, and its roughest feature was a downward change in elevation at the leading edge of more than 1 inch over a distance of 2.5 ft. The dip was half as severe in visits 10 through 14, and it was preceded by an upward step in elevation of more than 0.3 inch over a few feet starting about 35 ft from the start of the section. The dip was followed by a downward change in elevation of 0.3 inch over 5 ft starting about 95 ft from the start of the section. A narrow dip appears within the larger dip about 52 ft from the start of the section. This is at the start of the low area within the dip.

Starting in visit 07, narrow dips appeared on both sides that grew in severity over time about 112 ft and 149 ft from the start of the section. By visit 14, the dips were about 2 ft wide and 0.3 inch deep. A bump also appeared 202 ft from the start of the section, which grew in severity through visit 14. By visit 14, the bump was 3 ft wide and 0.5 inch high on the left side.

A rough area with much higher short wavelength content than the surrounding profile appeared on the right side from 260 to 280 ft from the start of the section. In later visits the chatter in this area included an overall vertical range of 0.4 inch. This area is followed by a very narrow dip 290 ft from the start of the section that grew in severity through visit 14, when it was about 0.3 ft wide and over 2 inches deep. On the left side, an area with similar properties appeared 290 to 310 ft from the start of the section. In addition, shallow bumps developed 251 and 268 ft from the start of the section.

Roughness profile plots: Before rehabilitation the three dips mentioned above caused extreme localized roughness. For example, the 1.25 inch deep dip on the right side contributes 31 inches/mi to the overall roughness of the section.

After rehabilitation the first half of the section was consistently more than twice as rough as the second half of the section on the left side. The dip from 50 to 90 ft from the start of the section

contributed significantly to the overall roughness. For example, localized roughness appeared at the steep downward slope in the profile at the leading edge of the dip, which contributed more than 30 inches/mi to the overall IRI of the section on the left side in visits 07 through 09 and about 15 inches/mi to the overall IRI on the right side. Localized roughness also appeared at the trailing edge of the dip, and it contributed about 20 inches/mi to the overall roughness on the left side and over 10 inches/mi to the overall roughness in the right side. In visits 10 and later, the leading edge was half as rough.

The bumps, narrow dips, and areas of increased short wavelength content contributed to increased roughness at their locations. The only feature that caused localized roughness was the area of chatter from 260 to 280 ft from the start of the section on the right side.

PSD plots: Before rehabilitation the PSD plots included slightly elevated content at wavelengths of 15 ft and 7.5 ft. Overall, the content was very uniform over the wavelength range that affects the IRI. Throughout the rest of the monitoring history, the content in the PSD plots below a wavelength of 30 ft grew over time.

Distress surveys: The dip at 112 ft, the dip at 149 ft, the bump at 202 ft, and the dip at 290 ft all correspond to high severity transverse cracks recorded in all of the distress surveys beginning in December 1999. The localized roughness found on the right side 260 to 280 ft from the start of the section corresponds to an area of fatigue in the wheelpath. The fatigue in this area was rated as low severity or medium severity in all of the distress surveys beginning in December 1999.

Maintenance history: Crack sealing (80 ft) was performed on this section in March 1995. The section received skin patching over 800 sq. ft in September 1999. The skin patching extended between 33 to 98 ft from the start of the section.

SECTION 040661

Roughness: Rehabilitation decreased the IRI from 171 to 66 inches/mi on the left side and from 259 to 67 inches/mi on the right side. After rehabilitation, the IRI on both sides increased at a somewhat erratic but increasing rate over the rest of the monitoring period. The HRI was 12 percent below the MRI before rehabilitation and 17 percent to 23 percent below the MRI after rehabilitation.

Elevation profile plots: Before rehabilitation the entire section was faulted. Faults appeared with a pattern that approximated the saw cut spacing 15-13-15-17 ft. Each fault on the right side appeared about 1 ft downstream of a fault on the left side from the same joint. The magnitude of faulting ranged from 0.05 to 0.25 inch. The profiles also included a few V-shaped dips that only appeared on one side or the other. These were most likely partial slabs tilted downward followed by partial slabs tilted upward. The most severe cases appeared on the left side 61 to 70 ft from the start of the section (0.7 inch deep), on the left side from 320 to 326 ft from the start

of the section (0.6 inch deep), on the left side 347 to 357 ft from the start of the section (0.5 inch deep), and on the right side 117 to 127 ft from the start of the section (0.9 inch deep). Multiple instances of this feature appeared from 340 to 360 ft from the start of the section on the right side.

Few features stood out in visits 01 through 06. The largest feature in the short wavelength elevation plots was a bump 0.1 inch high and about 2 ft wide that appeared 127 ft from the start of the section on the left side. In the later visits, some shallow (0.1 inch high) bumps appeared on the left side in the area 205 to 225 ft from the start of the section. In visits 08 and 09, and some repeats in visit 10, a dip 0.15 inch deep and 3 ft wide appeared on the right side starting 273 ft from the start of the section.

In visit 10, a rough area appeared 360 to 375 ft from the start of the section on the right side. This area included three consecutive dips, including a dip 0.4 inch deep and 3 ft wide with a sharp trough. In visit 11, the area included three much more severe dips, and some very sharp changes in elevation at the transitions (two 0.5 inch downward steps and a rise in elevation of 1 inch over 4 ft of pavement). By visit 12, the profiles included a rough sunken area about 0.5 inch below the prevailing pavement that extended from 361 ft from the start of the section to 376 ft from the start of the section. The roughness was not present after visit 12.

Profiles from visits 13 and 14 included two steep upward changes in elevation on the left side: (1) a 0.4 inch rise in elevation over 2 ft starting 264 ft from the start of the section, and (2) a 0.2 inch rise in elevation over less than 1 ft starting 286 ft from the start of the section. The second upward step was the leading edge of a 6 ft wide bump. On the right side the profiles rose 0.6 inch over 3 ft starting 265 ft from the start of the section. The right side profiles also included a downward step of about 0.2 inch that appeared 346 ft from the start of the section.

Roughness profile plots: Before rehabilitation, the tilted, fractured slab components mentioned above caused highly elevated roughness in the left side and localized roughness in the right side.

The progression in roughness on the right side in visits 07 through 09 occurred primarily at the disturbances described above 273 ft and 360 to 375 ft from the start of the section. The area 360 to 375 ft from the start of the section on the right side progressed in roughness and caused severe localized roughness in visits 11 and 12. Roughness at this area alone contributed 32 inches/mi to the overall IRI of the section in visit 11 and 27 inches/mi to the overall IRI of the section in visit 12.

In visits 13 and 14, the upward steps about 265 ft from the start of the section on both sides caused localized roughness. On the right side, the roughness was higher downstream of the step.

PSD plots: Before rehabilitation the PSD plots included very slightly elevated content at wavelengths of 15 ft and 7.5 ft. After rehabilitation, roughness progression was not isolated to any particular waveband.

Distress surveys: The distress surveys recorded an area with pumping and a network of cracks on the right side of the lane in August 2000. This area extended from 361 to 374 ft from the start of the section. This was not present in December 1999 or October 2001.

Maintenance history: Crack sealing (25 ft) was performed on this section in March 1995. The section received skin patching over 2100 sq. ft in September 2001. The disturbances discussed above for visits 13 and 14 occurred at the leading edge of the skin patch.

SECTION 040662

Roughness: Rehabilitation decreased the IRI from 156 to 52 inches/mi on the left side and from 148 to 57 inches/mi on the right side. After rehabilitation, the IRI held somewhat steady in visits 01 through 06, increased rapidly over the next two visits, and changed erratically over a wide range of rough values throughout the rest of the monitoring history. The HRI was 13 percent to 22 percent below the MRI.

Elevation profile plots: Before rehabilitation the majority of joints in this section were faulted. Faults 0.05 to 0.15 inch deep appeared with a pattern that approximated the saw cut spacing 15-13-15-17 ft, with some gaps at joints without faulting. When faults appeared on both sides at the same joint, the fault on the right side appeared about 1 ft downstream of the fault on the left. The profiles also included a 2 ft wide dip about 0.3 inch deep on the left side 182 ft from the start of the section and a 2 ft wide dip about 0.35 inch deep on the right side 156 ft from the start of the section.

Before rehabilitation, the area from 380 to 430 ft from the start of the section included several abrupt elevation and slope changes. The profile appeared to indicate the presence of three slabs that had shattered into multiple fragments. The severity was greatest on the right side.

In visits 02 through 05, three features stood out in the short wavelength plots: (a) a bump 0.15 inch high from 34 to 42 ft on the left side, (b) a 2 ft wide bump 0.1 inch high at 101 ft on the left side, (c) a dip 0.15 inch deep from 455 to 460 ft on the left side, and (d) a dip 0.15 inch deep (in visit 05) preceded by a small bump at 378 ft on the right side. Visit 06 also included a bump 0.2 inch high and 4 ft wide at 239 ft on the left side and a few narrow bumps and dips on the right side.

In visit 07, several dips 1 to 4 ft wide appeared in locations with either no dip or a very shallow dip in visit 06. The deepest dips were: (a) 0.15 inch deep, 43 ft from the start of the section on the left side, (b); about 0.2 inch deep, 116 ft from the start of the section on the left side and (c) 117 ft from the start of the section on the right side; (d) 0.3 inch deep, 377 ft from the start of

the section on the left side; (e) 0.2 inch deep, 378 ft from the start of the section on the right side; and(f) 0.2 inch deep, 452 ft from the start of the section on the left side.

Visit 08 profiles included narrow dips in a pattern that approximately matched the spacing of underlying joints on both sides, with a few joint locations omitted in the last third of the section. The dips grew in severity through visit 12, which included dips 0.1 to 0.8 inch deep.

Visit 13 profiles were very similar to those of visit 12 over the first 135 ft of the section. A 0.35 inch upward step appeared 135 ft from the start of the section. The rest of the section included dips in the same locations as in visit 12, but much less severe. Visit 14 profiles were very similar to visit 13 profiles, except that a 1 ft wide dip grew from 0.4 inch deep to 0.8 inch deep. The most severe dip in visits 13 and 14 was 0.5 inch deep and 4 ft wide. It appeared about 421 ft from the start of the section on the right side.

Roughness profile plots: Before rehabilitation, the three fractured slabs mentioned above caused localized roughness in the right side profiles.

The narrow dip 377 ft from the start of the section on the left side caused localized roughness in visit 09, but not in visit 08 or visit 10. On the right side, the dip 421 ft from the start of the section contributed more than 10 inches/mi to the overall IRI of the section starting in visit 11.

In visits 08 and later, most of the roughness of this section was concentrated at narrow dips in a regular pattern.

Roughness profiles show a decrease in roughness after visit 12 for the portion of the section past 150 ft from the start of the section on the left side and past 170 ft from the start of the section on the right side. However, in visit 13 the smoother area was preceded by localized roughness.

PSD plots: Before rehabilitation the PSD plots included elevated content at a wavelength of 15 ft on both sides, but this was overwhelmed by highly elevated content in the right side PSD plot in the wavelength range from 12 to 13.5 ft.

The increase in roughness over time primarily occurred in the wavelength range below 10 ft. In visit 08 and later, weak evidence of content from the underlying slabs appeared.

Distress surveys: The pattern and first appearance of narrow dips in the profiles correspond with the locations and first appearance of transverse cracks in the distress surveys. Further, the absence of a transverse crack at the location of an underlying joint is usually accompanied by the lack of a narrow dip in the profile. Often, the deepest dips were found in the profile in the same locations where the distress survey cited high severity cracks, and the shallowest dips were found in the profile where the distress survey recorded medium and low severity cracks.

Maintenance history: Crack sealing (490 ft) was performed on this section in March 1995. The section received skin patching in May 2001. The skin patching reduced the roughness of the section overall, but the transition caused localized roughness.

SECTION 040663

Roughness: Rehabilitation decreased the IRI from 235 to 94 inches/mi on the left side and from 201 to 93 inches/mi on the right side. After rehabilitation, the IRI held somewhat steady in visits 02 through 09 then increased erratically in visits 10 through 14. By visit 14, the IRI of the left side was 121 inches/mi and the IRI of the right side was 112 inches/mi. The HRI was 6 percent below the MRI before rehabilitation and 8 percent to 14 percent below the MRI after rehabilitation.

Elevation profile plots: Before rehabilitation the entire section was faulted. Faults 0.05 to 0.3 inch deep appeared with a pattern that crudely approximated the saw cut spacing 15-13-15-17 ft. (The actual pattern was closer to 14.7-13.5-14.7-17.3 ft.) Each fault on the right side appeared about 1 ft downstream of a fault on the left side from the same joint. Faults of lesser magnitude also appeared in the center of some slabs.

The elevation profiles were consistent in visits 02 through 06. In visits 07 though 14, narrow dips appeared with a very regular spacing of 15 ft throughout the section. (Evidence of narrow dips that had passed through the low-pass filter native to the profiler was also present in visits 02 through 06.) The narrow dips were roughly 0.2 to 0.3 inch deep in visits 07 through 13, but ranged from 0.3 to 1.0 inch deep in visit 14.

Narrow dips also appeared 409 and 411 ft from the start of the section. In visits 10 through 12 a single dip 0.4 inch deep and about 1.5 ft wide was there instead. These features were not present in visits 13 and 14.

All of the narrow dips appeared at the same location on both sides of the lane. (The profile features indicate that this section was built with a fixed joint spacing of 15 ft and no skew.)

The profiles also include a 0.75 inch rise over the 10 ft leading up to the section on the right side and a ride about half as severe in the left side.

Roughness profile plots: An area of elevated roughness appears about 410 ft from the start of the section on the right side in visits 08, 09, and 12. An area of slightly elevated roughness also appeared 410 ft from the start of the section on the left side in visits 11 through 14. These were not severe enough to classify as localized roughness.

An area of severe localized roughness appears just ahead of the test section and just behind the end of the test section on both sides.

PSD plots: Before rehabilitation the PSD plots included strong content isolated at wavelengths of 15 ft and 7.5 ft.

After rehabilitation the PSD plots included slightly elevated content at a wavelength of 15 ft. The PSD plots for visit 14 included significantly higher content for wavelengths below 2 ft than in the other visits. This was caused by the narrow dips.

Distress surveys: No distress appeared within the wheelpaths of this section over the monitoring period. Photographs and distress survey forms show that the peculiar roughness about 410 ft from the start of the section appeared at the site of some weigh-in-motion scales. A bending plate scale was in that location during visits 08 and 09. An asphalt patch appeared in that location in visits 10 through 12, and a new scale was there during visits 13 and 14.

The photos also show that the severe localized roughness at the section boundaries was caused by transitions from asphalt pavement to concrete and back to asphalt.

Maintenance history: The section received two partial depth patches at joints in September 1999.

SECTIONS 040664 THROUGH 040669

Prerehabilitation information was not collected on sections 040664 through 040669, but it was observed that the pavement condition was similar to those of 040601 through 040663. The observations below pertain to post-rehabilitation data only.

SECTION 040664

Roughness: The IRI of the left side increased erratically from 40 to 50 inches/mi over the monitoring period, with a peak value of 53 inches/mi in visit 12. The IRI of the right side held within a range from 44 to 50 inches/mi over the entire monitoring period, with an initial value of 48 inches/mi and a final value of 47 inches/mi. The HRI was 13 percent to 19 percent below the MRI.

Elevation profile plots: The elevation profiles were fairly consistent throughout the monitoring period in the medium wavelength range, and very consistent in the long wavelength range, but not very consistent in the short wavelength range.

The profiles included a long dip from about 350 to 400 ft from the start of the section. On the right side, a bump about 0.15 inch high appeared from 360 to 370 ft from the start of the section (within the dip). The right side profiles included a bump about 0.15 inch high from 110 to 116 ft from the start of the section.

Roughness profile plots: A rough area appears from 350 to 430 ft from the start of the section on both sides. On the left side, this area has an average roughness of about 90 to 100 inches/mi. On the right side, the overall roughness is lower, but a peak appears about 415 ft from the start of the section with a maximum value over 110 inches/mi in most visits. The right side roughness profiles also included peaks about 116 ft from the start of the section that ranged from 80 to 100 inches/mi.

PSD plots: The spectral content is skewed toward very long wavelength content. On the right side, a minor peak appears in the PSD plots at about 15 ft, but it is not a significant contributor to the roughness.

Distress surveys: No distress appeared within the wheelpaths of this section over the monitoring period. Nothing in the distress surveys explain the two bumps described above.

SECTION 040665

Roughness: The IRI of the left side increased erratically from 42 to 53 inches/mi over the monitoring period, with a peak value of 57 inches/mi in visit 12. The IRI of the right side increased overall from 43 to 50 inches/mi and half of the increase occurred between visits 04 and 05. The HRI was 8 percent to 15 percent below the MRI.

Elevation profile plots: The elevation profiles were fairly consistent throughout the monitoring period in the medium wavelength range and very consistent in the long wavelength range. Both sides of the lane included an increase in elevation of up to 0.2 inch over 5 ft of longitudinal distance ending 200 ft from the start of the section. This was followed by a series of small bumps over the next 20 ft. The bumps and the sudden rise in elevation were more severe on the left side.

Roughness profile plots: The roughness was not evenly distributed throughout the section. In particular, peaks appeared in the roughness profiles about 210 ft from the start of the section. These were caused by the upward change in elevation and the bumps that followed, as described above. The series of bumps on the left side caused an area of localized roughness, with peak values in the roughness profiles above 140 inches/mi in visits 03 through 14 about 212 ft from the start of the section.

The right side roughness profiles from visit 12 include a rough area in the first 50 ft of the section. This is caused by a roughly 20 ft long bump at the very start of the section. This does not appear in the left side profiles or in any other visit.

PSD plots: The spectral content is skewed somewhat toward long wavelength content.

Distress surveys: Almost no distress appeared within the wheelpaths of this section over the monitoring period. Nothing in the distress survey explains the bumps described above.

SECTION 040666

Roughness: The IRI of the left side increased somewhat erratically over the monitoring period from 37 to 47 inches/mi with a peak value of 49 inches/mi in visit 11. The IRI of the right side increased from 42 to 52 inches/mi over the monitoring period, with values ranging from 51 to 52 inches/mi in the last seven visits. The HRI was 15 percent to 20 percent below the MRI.

Elevation profile plots: The elevation profiles were fairly consistent on the left side throughout the monitoring period in the medium wavelength range and very consistent in the long wavelength range. The elevation profiles on the right side were very consistent in the last eight visits.

The left side profiles included bumps about 0.1 inch high from 185 to 191 ft from the start of the section and 233 to 237 ft from the start of the section. The right side profiles included a bump from 185 to 191 ft from the start of the section that was about 0.15 inch high.

The left side profiles also include very narrow (0.5 ft long) dips 344 and 395 ft from the start of the section. The dips first appear in visit 07, but do not appear in every repeat measurement in every visit until after visit 11.

Roughness profile plots: The roughness was not evenly distributed throughout the section, since some roughness was concentrated around the bumps described above. In visit 14 these caused peaks in the left side roughness profile of about 100 inches/mi and a peak in the right side roughness profile of up to 120 inches/mi. The progression in roughness in the left side profiles was distributed evenly across the section.

PSD plots: The spectral content is skewed somewhat toward long wavelength content. The PSD plots show a peak at a wavelength near 38 ft.

Distress surveys: Almost no distress appeared within the wheelpaths of this section over the monitoring period. Nothing in the distress surveys explain the bumps or the narrow dips described above.

SECTION 040667

Roughness: The IRI of the left side changed erratically over the monitoring period and had values between 63 and 72 inches/mi. However, initial and final values were nearly equal. The IRI of the right side held steady between 74 and 79 inches/mi. The HRI was 6 percent to 9 percent below the MRI. This is the lowest range of any section within this site.

Elevation profile plots: The elevation profiles were consistent throughout the monitoring period, particularly on the right side. A bump appeared in the profiles on both sides from 185 to 245 ft from the start of the section. The bump was about 0.8 inch high on the right side and came to a narrow peak with an unusually sharp change in slope 221 ft from the start of the section. The bump was about 0.5 to 0.6 inch high on the left side, but the change in slope at the peak was nearly as severe on the right side.

Roughness profile plots: The right side roughness profiles were very consistent with time, and the left side roughness profiles were fairly consistent with time. The section was roughest at the crest of a long bump 221 ft from the start of the section. The peak values in the roughness profiles at this location were high enough to qualify as localized roughness in about half of the repeat measurements. The severity of roughness at the bump did not progress with time, but the bump increased the IRI of the entire section by about 10 inches/mi on the left side and about 15 inches/mi on the right.

PSD plots: Content in the profile at wavelengths from 45 to 60 ft dominated the contributions to the IRI.

Distress surveys: Very little distress appeared within the wheelpaths of this section over the monitoring period. The exception was a small amount of longitudinal cracking in the left side of the lane noted in October 2002.

SECTION 040668

Roughness: The IRI of the left side increased erratically from 36 to 45 inches/mi over the monitoring period. The IRI of the right side increased erratically from 38 to 45 inches/mi over the monitoring period. The HRI was 13 percent to 15 percent below the MRI in visits 02 through 06 and 17 percent to 19 percent below the MRI in the rest.

Elevation profile plots: Very few features stood out in the elevation profiles. The exceptions were narrow (about 0.5 ft long) dips that were up to 0.25 inch deep 40 ft, 250 ft, and 475 ft from the start of the section on the left side. The dips did not appear, or were barely detectable, in visits 01 through 06, but were very obvious in all of the other visits. Companion dips appeared in the right side profiles about 1 ft downstream of each location starting in visit 08. (The 1 ft offset downstream on the right side is a consequence of the joint skew in the underlying pavement.)

Roughness profile plots: The overall level of roughness and much of the spatial distribution were fairly consistent with time, but the details of the plots were not. The three dips contributed to the roughness in some visits, but were not severe enough to cause localized roughness.

PSD plots: The left side PSD plots include a small peak at a wavelength of 15 ft. The right side profiles show a stronger peak at a wavelength of 15 ft and a companion peak at a wavelength of 7.5 ft.

Distress surveys: Very little distress appeared within the wheelpaths on this section over the monitoring period. Three transverse cracks appeared in all distress surveys that cut across the lane at an angle such that the intersection of the crack and the left lane edge was about 2 ft upstream of the intersection of the crack and the right lane edge. These were about 40, 250, and 475 ft from the start of the section. As described above, they did cause narrow dips in the elevation profiles, particularly in later visits. A patch of wheelpath cracking on the right side from 240 to 255 ft from the start of the section was recorded in October 2002, but it did not affect the profiles.

SECTION 040669

Roughness: The IRI of the left side increased erratically from 51 inches/mi to 59 inches/mi over the monitoring period. The IRI of the right side covered a range from 52 inches/mi in visit 02 to 59 inches/mi in visit 08, with a final value of 55 inches/mi. The HRI was 9 percent to 13 percent below the MRI.

Elevation profile plots: The profiles were very consistent over the entire monitoring period. An exception was some noise in the short wavelength plots for the left side in the early visits. No rough features stood out on the right side, but a sharp transition occurred between upward and downward slope at the apex of a long bump on the left side. This appeared 348 ft from the start of the section.

Roughness profile plots: The roughness profiles changed very little throughout the monitoring period. The roughness was not evenly distributed along the section on either side of the lane. The roughest area extended from 325 to 425 ft from the start of the section.

Localized roughness (or increased roughness severe enough to nearly qualify as localized roughness) appeared with a peak value 375 ft from the start of the section on the left side in all visits. This was caused by the sharp slope change described above. The peak value in the roughness profile occurred 25 ft downstream of the apex because it excited a transient in the IRI filter with a very long characteristic wavelength.

PSD plots: Content in the profile at wavelengths from 45 to 60 ft dominated the contributions to the IRI.

Distress surveys: Very little distress was recorded for this section. Nothing in the distress surveys explain the features described above.